Université de Montréal

Use of chemogenomic approaches to characterize *RUNX1*-mutated Acute Myeloid Leukemia and dissect sensitivity to glucocorticoids

By

Laura Simon

Programme de Biologie Moléculaire

Faculté de Médecine

Thèse présentée à la Faculté de médecine
en vue de l'obtention du grade de Docteur
en biologie moléculaire,
option biologie des systèmes

May 2020

Université de Montréal

Institut de recherche en immunologie et en cancerologie

Programme de biologie moléculaire

Faculté de médecine

Cette thèse intitulée:

Use of chemogenomic approaches to characterize *RUNX1*-mutated Acute Myeloid Leukemia and dissect sensitivity to glucocorticoids

Présentée par:

Laura Simon

A été évaluée par un jury composé des personnes suivantes :

Tarik Möröy

Président-rapporteur

Guy Sauvageau

Directeur de recherche

Dong-Er Zhang

Membre du jury

Lucy A. Godley

Examinateur externe

Résumé

RUNX1 est un facteur de transcription essentiel pour l'hématopoïèse et joue un rôle important dans la fonction immunitaire. Des mutations surviennent dans ce gène chez 5 à 13% des patients atteints de leucémie myéloïde aiguë (LMA) (*RUNX1*^{mut}) et définissent un sous-groupe particulier de LMA associé à un pronostic défavorable. En conséquence, il est nécessaire de procéder à une meilleure caractérisation génétique et de concevoir des stratégies thérapeutiques plus efficaces pour ce sous-groupe particulier de LMA. Bien que la plupart des mutations trouvées dans le gène *RUNX1* dans la LMA soient supposément acquises, des mutations germinales dans *RUNX1* sont observées chez les patients atteints du syndrome plaquettaire familial avec prédisposition aux hémopathies malignes (RUNX1-FPD, FPD/AML). En outre, 44 % des individus atteints évoluent vers le développement d'une LMA. Suite au séquençage du transcriptome (RNA-Seq) d'échantillons de la cohorte Leucégène, nous avons montré que le dosage allélique de *RUNX1* influence l'association avec des mutations coopérantes, le profil d'expression génique et la sensibilité aux médicaments dans les échantillons primaires de LMA *RUNX1*^{mut}. Aussi, la validation des mutations trouvées chez *RUNX1* a mené à la découverte que 30% des mutations identifiées dans notre cohorte de LMA étaient d'origine germinale, révélant une proportion plus élevée qu'attendue de cas de mutations *RUNX1* familiales. Un crible chimique a, quant à lui, révélé que la plupart des échantillons *RUNX1*^{mut} sont sensibles aux glucocorticoïdes (GCs) et nous avons confirmé que les GCs inhibent la prolifération des cellules de LMA et ce, via l'interaction avec le récepteur des glucocorticoïdes (Glucocorticoid Receptor, GR). De plus, nous avons observé que les échantillons contenant des mutations *RUNX1* censées entraîner une faible activité résiduelle étaient plus sensibles aux GCs. Nous avons aussi observé que la co-association de certaines mutations, *SRSF2*^{mut} par exemple, et les niveaux de GR contribuaient à la sensibilité aux GCs. Suite à cela, la sensibilité acquise aux GCs a été obtenue en régulant négativement l'expression de *RUNX1* dans des cellules LMA humaines, ce qui a été accompagné par une régulation positive de GR. L'analyse de transcriptome induit par GC a révélé que la différenciation des cellules de LMA induite par GCs pourrait être un mécanisme en jeu dans la réponse antiproliférative associée à ces médicaments. Plus important encore, un criblage génomique fonctionnel a identifié le répresseur transcriptionnel PLZF (*ZBTB16*) comme un modulateur spécifique de la réponse aux GCs dans les cellules LMA sensibles et résistantes. Ces observations fournissent une caractérisation supplémentaire de la LMA *RUNX1*^{mut}, soulignant l'importance de procéder à des tests germinaux pour les patients porteurs de mutations *RUNX1* délétères. Nos résultats ont également identifié un nouveau rôle pour *RUNX1* dans le réseau de signalisation de GR et montrent l'importance d'investiguer le repositionnement des GCs pour traiter la LMA *RUNX1*^{mut} dans des modèles précliniques. Enfin, nous avons fourni des indications sur le mécanisme d'action des GCs, en montrant que PLZF s'avère un facteur important favorisant la résistance aux GCs dans la LMA.

Mot-clés: Leucémie Myéloïde Aiguë, RUNX1, Glucocorticoïdes, chémogénomique, criblage CRISPR-Cas9, résistance aux Glucocorticoïdes

Abstract

RUNX1 is an essential transcription factor for definite hematopoiesis and plays important roles in immune function. Mutations in *RUNX1* occur in 5-13% of Acute Myeloid Leukemia (AML) patients (*RUNX1*^{mut}) and are associated with adverse outcome, thus highlighting the need for better genetic characterization and for the design of efficient therapeutic strategies for this particular AML subgroup. Although most *RUNX1* mutations in AML are believed to be acquired, germline *RUNX1* mutations are observed in the familial platelet disorder with predisposition to hematologic malignancies (RUNX1-FPD, FPD/AML) in which about 44% of affected individuals progress to AML. By performing RNA-sequencing of the Leucegene collection, we revealed that *RUNX1* allele dosage influences the association with cooperating mutations, gene expression profile, and drug sensitivity in *RUNX1*^{mut} primary AML specimens. Validation of *RUNX1* mutations led to the discovery that 30% of *RUNX1* mutations in our AML cohort are of germline origin, indicating a greater than expected proportion of cases with familial *RUNX1* mutations. Chemical screening showed that most *RUNX1*^{mut} specimens are sensitive to glucocorticoids (GC) and we confirmed that GCs inhibit AML cell proliferation via interaction with the Glucocorticoid Receptor (GR). We observed that specimens harboring *RUNX1* mutations expected to result in low residual RUNX1 activity were most sensitive to GCs, and that co-associating mutations, such as *SRSF2*^{mut}, as well as GR levels contribute to GC-sensitivity. Accordingly, acquired GC-sensitivity was achieved by negatively regulating *RUNX1* expression in human AML cells, which was accompanied by upregulation of the GR. GC-induced transcriptome analysis revealed that GC-induced differentiation of AML cells might be a mechanism at play in the antiproliferative response to these drugs. Most critically, functional genomic screening identified the transcriptional repressor PLZF (*ZBTB16*) as a specific modulator of the GC response in sensitive and resistant AML cells. These findings provide additional characterization of *RUNX1*^{mut} AML, further stressing the importance of germline testing for patients carrying deleterious *RUNX1* mutations. Our results also identified a novel role for RUNX1 in the GR signaling network and support the rationale of investigating GC repurposing for *RUNX1*^{mut} AML in preclinical models. Finally, we provided insights into the mechanism of action of GCs, which positions PLZF as an important factor promoting resistance to glucocorticoids in AML.

Keywords: Acute Myeloid Leukemia, RUNX1, Glucocorticoids, chemogenomics, CRISPR-Cas9 screening, Glucocorticoid-resistance

Table of contents

List of Figures

List of Tables

List of abbreviations

ACTH	Adrenocorticotropic Hormone
AL	Acute Leukemia
ALL	Acute Lymphoblastic Leukemia
AML	Acute Myeloid Leukemia
AML1	Acute Myeloid Leukemia 1
APC	Antigen-Presenting Cells
APL	Acute Promyelocytic Leukemia
BET	Bromodomain and Extra-terminal motif
BM	Bone marrow
CAR	Chimeric Antigen Receptor
CBF	Core Binding Factor
CDK	Cyclin-Dependent Kinase
CHIP	Clonal Hematopoiesis of Indeterminate Potential
CML	Chronic Myeloid Leukemia
CR	Complete Remission
CRH	Corticotropin-Releasing Hormone
CRISPR	Clustered Regularly Interspaced Short Palindromic Repeats
DBD	DNA Binding Domain
DCs	Dendritic Cells
DHS	DNase I Hypersensitive Sites
DMSO	Dimethyl Sulfoxide
DNA	Deoxyribonucleic acid
ELN	European LeukemiaNet
ERK	Extracellular Signal-Regulated Kinase
ESC	Embryonic Stem Cell
FAB	French-American-British classification
FDA	United States Food and Drug Administration
GEP	Gene Expression Profile
GCs	Glucocorticoids

GM-CSF	Granulocyte-Macrophage Colony-Stimulating Factor
GR	Glucocorticoid Receptor
GRE	Glucocorticoid Response Element
GBS	Glucocorticoid Binding Site
hESC	Human Embryonic Stem Cell
HPA	Hypothalamic–Pituitary–Adrenal
HSC	Hematopoietic Stem Cell
HSCT	Hematopoietic Stem Cell Transplantation
HSP	Heat Shock Protein
ID	Inhibitory Domain
KD	Knockdown
KO	Knockout
LBD	Ligand-Binding Domain
LSC	Leukemic Stem Cell
M-CSF	Macrophage Colony-Stimulating Factor
MDS	Myelodysplastic Syndromes
MEP	Megakaryocyte-Erythroid Progenitor
miRNA	Micro RNA
MK	Megakaryocyte
MM	Multiple Myeloma
MPN	Myeloproliferative Neoplasms
MPP	Multipotent Progenitor
MR	Mineralocorticoid Receptor
MRD	Measurable Residual Disease
mRNA	Messenger RNA
NES	Nuclear Export Signal
NLS	Nuclear Localization Signal
NMD	Nonsense-Mediated mRNA Decay
NMTS	Nuclear Matrix-Targeting Signal
NPC	Nuclear Pore Complex
NRH	Negative Regulatory Region for Heterodimerization

NRDB	Negative Regulatory Region for DNA Binding
NRS	Nuclear Retention Signal
OS	Overall Survival
PCR	Polymerase Chain Reaction
PTM	Posttranslational Modifications
qPCR	Real-Time Quantitative Polymerase Chain Reaction
RNA	Ribonucleic acid
RNAi	RNA Interference
sAML	Secondary AML
SCF	Stem Cell Factor
SEDIGRAM	Selective Dimerizing GR Agonists and Modulators
SEGRA	Selective GR Agonists
SEGRAM	Selective GR Agonists and Modulators
SEGRM	Selective GR Modulators
SEMOGRAM	Selective Monomer GR Agonists and Modulators
sgRNA	Guide RNA
shNT	Short Hairpin Non-Target
shRNA	Short Hairpin RNA
TA	Transactivation
TAD	Transactivation Domain
tAML	Therapy-related AML
TF	Transcription Factor
TKI	Tyrosine Kinase Inhibitor
TR	Transrepression
TRM	Treatment-related mortality
URE	Upstream Regulatory Element
VAF	Variant Allele Frequency
WBC	White Blood Cell count
WHO	World Health Organization

Acknowledgements

I would like to thank my supervisor, Dr. Guy Sauvageau, for the opportunity, the patient guidance, and endless support and encouragement he has provided throughout my time in my Ph.D. degree. His dedication, overwhelming passion and vision has made this thesis possible.

To present and past members of the Sauvageau lab, thank you for being exceptionally good scientists and colleagues, for teaching me so much and supporting me through this journey. Special thanks to Vincent-Philippe Lavallée, Chi-Yuan Yao and Jean-François Spinella for working with me in this project and providing bioinformatic support. I also want to thank Jalila Chagraoui, Bernhard Lehnertz, Tara MacRae, Jana Krosl, Simon Girard, Nadine Mayotte, Isabel Boivin, Céline Moison, Azadeh Hajmirza and Marie-Ève Bordeleau for their help with experiments, grant writing, and for all the chats about science, I am grateful for everything!

Very special thanks to Geneviève Boucher for being a knowledgeable source for everything related to data analysis and the French language, and for being a wonderful friend!

I would like to express my sincere thanks to Dr. Tarik Möröy, Dr. Dong-Er Zhang, and Dr. Lucy A. Godley for serving on my examination committee and accepting the task of critically analyzing this document. Additionally, I would like to thank Dr. Sylvie Mader for providing support and ideas that helped me in the development of this thesis.

Last but not least, my deepest gratitude to my family and friends for always being there to cheer me and support me through it all. To my wife and the new family she brought me, thank you for your unconditional love and for believing in me.

Chapter 1: Introduction

1.1 Acute Myeloid Leukemia (AML)

1.1.1 Overview

Acute Myeloid Leukemia (AML) is the most common form of acute leukemia in adults, with an incidence that increases with advanced age. The age-adjusted incidence of AML is 4.3 per 100,000 annually, with median age at diagnosis of 68 years in the United States (US) (Shallis et al., 2019). Estimated age-adjusted AML incidence rates in the United Kingdom, Canada and Australia mirror that of the US population (Alibhai et al., 2009; Gangatharan et al., 2013; Shallis et al., 2019; Shysh et al., 2017).

The disorder arises in a malignantly transformed multipotential hematopoietic stem/progenitor cell that acquires successive genomic alterations, ultimately evolving into clinically overt disease. AML is a remarkably complex malignancy, with considerable genetic, epigenetic, and phenotypic heterogeneity (Löwenberg and Rowe, 2015). Although it is usually of unknown etiology, AML can arise in patients with an underlying hematological disorder, or because of prior therapy (for example, exposure to topoisomerases II, alkylating agents or radiation). However, in the majority of cases, it appears as a *de novo* malignancy in previously healthy individuals (Kouchkovsky and Abdul-Hay, 2016).

AML is characterized by infiltration of the hematopoietic organs (bone marrow, blood, spleen, and other tissues) by abnormally differentiated and nonfunctional hematopoietic blasts. High and uncontrolled proliferation of leukemic cells causes the expulsion of the normal hematopoietic system and the loss of their functions, leading to life-threatening symptoms such as thrombocytopenia, anemia, and immunodeficiency (Estey, 2018).

1.1.2 Multistep process of leukemogenesis

The hematopoietic system provides the lifelong supply of blood cells, which are derived from a rare population of multipotent and self-renewing Hematopoietic Stem Cells (HSCs). Pioneering studies from Till and McCulloch and others used transplantation experiments to demonstrate the multipotent nature adult HSC, and they have indicated that most blood cells originate from very

few/single multipotent self-renewing HSCs (BECKER et al., 1963). Being at the top of the hematopoietic hierarchy, HSCs divide infrequently, giving rise to transient-amplifying multipotent (MPPs) and lineage restricted progenitors that proliferate extensively and differentiate toward mature blood cells (**Figure 1.1**) (Riether et al., 2015). The quiescent/dormant state of HSCs is believed to protect against introduction of oncogenic DNA mutations and exhaustion of HSC pool resulting from uncontrolled proliferation. Dormant HSCs are anchored to a specialized niche in the bone marrow in a hypoxic environment to protect them from oxidative damage by reactive oxygen species (Trumpp et al., 2010). However, HSCs can rapidly respond to external stimuli from mature immune cells and sense pathogens directly during inflammation or infection to adapt their cycling and differentiation behavior (Riether et al., 2015).

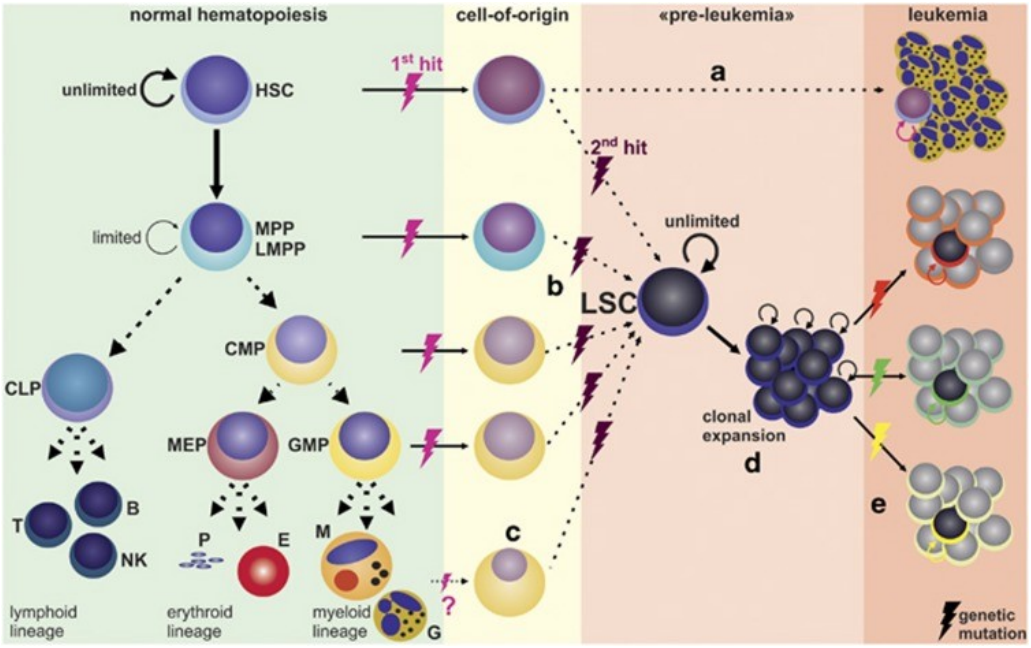

Figure 1.1: The leukemic stem cell model.

HSC, hematopoietic stem cell; MPP, multipotent progenitors; LMPP, lymphoid-primed MPPs; CLP, common lymphoid progenitor; CMP, common myeloid progenitors; MEP, megakaryocyte-erythrocyte progenitor; GMP, granulocyte-macrophage progenitors; B, B-cell; CML, chronic myeloid leukemia; E, erythrocyte; G, granulocyte; NK, natural killer cell; M, monocyte; P, platelet; T, T-cell; LSC, leukemic stem cell**.** Figure adapted from Riether et al., 2015 with permission.

The existence of a Leukemic Stem Cell (LSC) that shows characteristics of HSC, such as self-renewal and quiescence, was identified more than 25 years ago as an AML-initiating cell and responsible for propagating the disease (Lapidot et al., 1994). LSCs harbor genetic abnormalities that result in increased proliferation and resistance to apoptosis, and their functionality depend on similar interactions with niche cells as described for HSCs (Riether et al., 2015). The competitive growth advantage of LSC leads to clonal skewing and establishment of a pre-leukemic state (**Figure 1.1**). In a pre-leukemic disease phase, genetically unstable, self-renewing LSCs clonally expand, facilitating the acquisition of subsequent mutations, and once differentiation capacity is impaired leukemia emerges (Shlush and Minden, 2015). Sequencing studies have shown the presence of multiple clonal populations at overt leukemia or relapse (Ding et al., 2012). Clonal evolution within each AML patient appears to be a dynamic process consisting of continuous acquisition and loss of specific mutations, generating functionally divergent subclones with multiple defective intracellular processes and pathways (Gruszka et al., 2017).
Clonal hematopoiesis, however, is also documented in healthy individuals, in fact it occurs in a large segment of the aging population. Aging has been associated with a myeloid proliferation bias and myeloid-derived hematological cancers such as AML, myelodysplastic syndromes (MDS), and myeloproliferative neoplasms (MPN). Recently, acquired mutations conferring clonal growth advantage have been documented in aging healthy individuals with a normal hematopoietic phenotype, challenging the putative relationship between clonality and malignancy (Busque et al., 2018). In 2015, the term clonal hematopoiesis of indeterminate potential (CHIP) was proposed to describe individuals with a hematologic malignancy-associated somatic mutation in blood or marrow with variant allele frequency (VAF) >2%, but without other diagnostic criteria for a hematologic malignancy (Steensma et al., 2015). CHIP mutations occur commonly in genes encoding chromatin modifiers such as *DNMT3A*, *ASXL1*, and *TET2* (Busque et al., 2012; Genovese et al., 2014; Jaiswal et al., 2014; Shlush et al., 2014) and are believed to increase the risk of hematological malignancies.

1.1.3 Genomic landscape of AML

In 2002, Gilliland and Griffin suggested the “two-hit” model of leukemogenesis, in which AML onset requires the collaboration between two classes of mutations: Class 1) mutations leading to

constitutive activation of signaling pathways that increase cell proliferation and survival (typically observed in MPN); and Class 2) mutations and chromosomal translocations in transcription factors (TFs) that would lead to block in differentiation and consequently decreased apoptosis (typically observed in MDS) (Gilliland and Griffin, 2002). Even though this model correctly conceptualised AML as a disease where proliferation is increased and differentiation is blocked, many mutations recently discovered to synergistically reproduce the AML phenotype do not fit into one of the two classes (Grove and Vassiliou, 2014). The modern application of next-generation sequencing technology has uncovered marked heterogeneity and genomic complexity within AML (DiNardo and Cortes, 2016). The genomic interrogation of large patient cohorts has revealed patterns of cooperativity and mutual exclusivity of mutations and chromosomal rearrangements, the subclonal architecture and clonal evolution during the disease course, and the epigenetic landscape of the disease (Longo et al., 2015). Compared to other types of cancer, however, AML genomes have relatively fewer mutations, with an average of only 13 mutations per sample (Network, 2013; Tyner et al., 2018). Nonetheless, the number of driver mutations negatively influence overall survival in AML patients (Papaemmanuil et al., 2016). Genes that are significantly mutated in AML can be organized into several functional categories as shown in **Table 1.1**.

Table 1.1: Functional categories of genes recurrently mutated in AML

Functional category	**Genes**
Signal transduction genes	*FLT3*, *NRAS*, *KRAS*, *c-KIT*, *PTPN11*, *JAK2*
DNA modification genes	*DNMT3*, *IDH1*, *IDH2*, *TET2*
Chromatin modifiers	*MLL*-fusions, *ASXL1*, *EZH2*, *BCOR*, *DOT1L*, *MLL*-partial tandem duplication
Multi-function	*NPM1*
Chimeric or mutated TFs	PML/RARA, RUNX1/RUNX1T1, CBFB/ MYH11, *CEBPA*, *RUNX1*, *GATA2*
Tumor-suppressor genes	*TP53*, *PHF6*, *WT1*
Spliceosome genes	*SF3B1*, *SRSF2*, *U2AF1*, *ZRSR2*
Cohesin complex genes	*SMC1A*, *SMC3*, *RAD21*, *STAG2*

Genomic characterization of more than 1,500 AML patients showed that at least 1 driver mutation is identified in almost all patients (96%) and 2 or more driver mutations in 86% of patient samples (Papaemmanuil et al., 2016). Patterns of co-mutation and mutual exclusivity have been shown to be good indicators of disease subtype and prognosis. For example, the co-occurrence of mutations in *FLT3*, *DNMT3A*, and *NPM1*, frequently observed in AML cohorts,

was shown to be associated with a distinct clusters of mRNA and miRNA expression and DNA methylation, being suggested as a novel subtype of AML and to hold prognostic significance (Network, 2013; Papaemmanuil et al., 2016).

Despite point mutation and chromosomal translocations, large chromosomal gains or losses are commonly described in AML. Most frequently observed are deletion 5q, monosomy 7, and trisomies of chromosomes 8, 11 and 13 (Grove and Vassiliou, 2014). Evidence supports the idea that changes in the expression of deleted or amplified genes located in these large regions drive leukemogenesis and influence patient prognosis (Shlush et al., 2014).

1.1.4 Transcriptional signature in AML

Transcriptome of AML cells can be extensively altered and, like genetic aberrations, changes in gene expression contribute to leukemogenesis and may represent therapeutic targets. Several genes have been reported to date to be overexpressed in AML when compared to healthy control, including *KIT*, *BAALC*, *ERG*, *MN1*, *CDX2*, *WT1*, *PRAME*, and *HOX* genes (Handschuh, 2019). Microarray and RNA-sequencing technologies have been applied to derive gene expression profiles (GEP) in blast populations among AML patients, which may contribute to the identification of subsets of patients with differing outcomes. Some AML subgroups have a very distinct GEP, such as t(8;21), inv(16)/t(16;16), t(15;17), and *CEBPA*-mutated, whereas use of GEP is less successful in predicting other cytogenetic and molecular genetic subsets of AML (Mrózek et al., 2009). Overrepresented gene sets with stem cell-like properties, for example, can uncover the developmental state from which the AML emerged and are predictive of outcome (Eppert et al., 2011; Ng et al., 2016; Wiggers et al., 2019)

1.1.5 AML diagnosis and prognosis

Two systems currently exist to diagnose and classify AML: the French American British (FAB) and the World Health Organization (WHO) classifications. The FAB classification system was established in 1976 and defines eight subtypes of AML (M0 through M7 subtypes) based on morphological and cyto-chemical characteristics of the leukemic cells, from most undifferentiated (M0) to most differentiated (M7) (**Table 1.2**). In the FAB system, a minimum of 30% blast population in peripheral blood or bone marrow is required to diagnose AML. The

WHO classification first established in 2001 requires a minimum of 20% of blasts in bone marrow or blood to diagnose AML and classifies neoplasms based on morphologic, cytogenetic, clinical, and immunophenotypic criteria (Vardiman et al., 2002). The diagnosis of AML can also be established in the presence of an extramedullary tissue infiltrate, or in genetically defined subtypes of AML in which the diagnosis is independent of the blast percentage (Estey, 2018; Kouchkovsky and Abdul-Hay, 2016). The myeloid origin of these cells needs to be further confirmed through testing for myeloperoxidase activity, immunophenotyping or documenting the presence of Auer rods (Kouchkovsky and Abdul-Hay, 2016).

The WHO classification was last updated in 2016 and has moved toward a system based more on genetic information, incorporating recurrent structural cytogenetic abnormalities and specific gene mutations (Arber et al., 2016). The WHO classification defines six major disease entities: AML with recurrent genetic abnormalities; AML with myelodysplasia-related features; therapy-related AML; AML not otherwise specified; myeloid sarcoma; and myeloid proliferation related to Down syndrome (**Table 1.2**).

Table 1.2: FAB and WHO classification of AML

Acute myeloid leukemia (AML) and related neoplasms
AML with recurrent genetic abnormalities
AML with t(8;21)(q22;q22.1);*RUNX1-RUNX1T1*
AML with inv(16)(p13.1q22) or t(16;16)(p13.1;q22);*CBFB-MYH11*
APL with *PML-RARA* (M3)
AML with t(9;11)(p21.3;q23.3);*MLLT3-KMT2A*
AML with t(6;9)(p23;q34.1);*DEK-NUP214*
AML with inv(3)(q21.3q26.2) or t(3;3)(q21.3;q26.2);*RPN1-EVI1*
AML (megakaryoblastic) with t(1;22)(p13.3;q13.3);*RBM15-MKL1*
Provisional entity: AML with BCR-ABL1
AML with mutated *NPM1*
AML with biallelic mutations of *CEBPA*
Provisional entity: AML with mutated RUNX1
AML with myelodysplasia-related changes
Therapy-related myeloid neoplasms
AML, Not otherwise specified (NOS)
AML with minimal differentiation (M0)
AML without maturation (M1)
AML with maturation (M2)
Acute myelomonocytic leukemia (M4)
Acute monoblastic/monocytic leukemia (M5a, M5b)
Pure erythroid leukemia (M6)
Acute megakaryoblastic leukemia (M7)
Acute basophilic leukemia
Acute panmyelosis with myelofibrosis

Myeloid sarcoma
Myeloid proliferation related to Down syndrome

Table adapted from Arber et al., 2016 with permission

Newly-diagnosed AML classification and genetic testing is essential for optimal pretreatment risk stratification, which is central to the management of AML. Prognostic factors help guide the physician in deciding between standard or increased treatment intensity, consolidation chemotherapy or allogenic hematopoietic stem cell transplant (HSCT), conventional or investigational therapy (Kouchkovsky and Abdul-Hay, 2016). Prognostic factors can be subdivided into patient-associated factors and disease-associated factors. Patient-associated factors include age, coexisting conditions, and poor performance status and can predict treatment-related mortality (TRM). At the same time, disease-associated factors include white blood cell count, prior myelodysplastic syndrome or cytotoxic therapy for another disorder (therapy-related AML, tAML), and leukemic-cell genetic variations, and can predict resistance to current standard therapy (Longo et al., 2015).

The European LeukemiaNet (ELN) represents an international panel of experts to promote an integrative approach of the different fields of diagnostic expertise (morphology, karyotype, genomics and transcriptomics) in order to develop robust prognostic tools (Döhner et al., 2009). The ELN has proposed a risk scale based on karyotypes and the presence of certain gene mutations, which was last updated in 2017 (Döhner et al., 2017). This scale currently defines 3 risk categories ranging in prognosis from best to worst (**Table 1.3**). Analyses of specific gene mutations have suggested that patients carrying *MLL-PTD* and/or *RUNX1* mutation and/or *ASXL1* mutation have unfavorable prognosis, while patients carrying *TP53* mutation have a rather unfavorable prognosis (Grossmann et al., 2012). *TP53* mutations are significantly associated with AML with complex and monosomal karyotype, which are independent adverse prognosis markers (Döhner et al., 2017). More than the presence of gene mutations the level of mutated allele can be of prognostic value. *FLT3-ITD* mutations with VAF<0.5 (*FLT3-ITD*^{low}) shows more favorable prognosis than *FLT3-ITD*^{high} (VAF>0.5) (Gale et al., 2008; Ho et al., 2016).

Table 1.3: Prognostic-risk group based on cytogenetic and molecular profile

Prognostic-risk group	Cytogenetic profile and molecular abnormalities
Favorable	t(8;21)(q22;q22.1); *RUNX1-RUNX1T1*

	inv(16)(p13.1q22) or t(16;16)(p13.1;q22); *CBFB-MYH11* Mutated *NPM1* without *FLT3-ITD* or with *FLT3-ITD*^{low} Biallelic mutated *CEBPA*
Intermediate	Mutated *NPM1* and *FLT3-ITD*^{high} Wild-type *NPM1* without *FLT3-ITD* or with *FLT3-ITD*^{low} (without adverse-risk genetic lesions) t(9;11)(p21.3;q23.3); *MLLT3-KMT2A* Cytogenetic abnormalities not classified as favorable or adverse
Adverse	t(6;9)(p23;q34.1); *DEK-NUP214* t(v;11q23.3); *KMT2A* rearranged t(9;22)(q34.1;q11.2); *BCR-ABL1* inv(3)(q21.3q26.2) or t(3;3)(q21.3;q26.2); *GATA2,MECOM(EVI1)* -5 or del(5q); -7; -17/abn(17p) Complex karyotype, monosomal karyotype Wild-type *NPM1* and *FLT3-ITD*^{high} Mutated *RUNX1* Mutated *ASXL1* Mutated *TP53*

Table adapted from Döhner et al., 2017 with permission.

1.1.6 Conventional therapy

Initial assessment determines whether a patient is eligible for intensive induction chemotherapy, which is generally offered to patients with an intermediate to favorable prognosis and a low risk of TRM, and its goal is to induce complete remission (CR) . Induction therapy typically combines 3 days of an anthracycline (eg, daunorubicin, idarubicin, anthracenedione mitoxantrone) and 7 days of continuous infusion of cytarabine ("3 + 7") (Döhner et al., 2009). CR is achieved in 60 to 85% of adults who are 60 years of age or younger. In patients who are older than 60 years of age, CR rates are inferior (40 to 60%) (Longo et al., 2015). Hypomethylating agents such as decitabine and azacitidine have emerged as promising strategies to be used in the treatment of elderly patients (DiNardo and Cortes, 2016). Standard postremission strategies include conventional chemotherapy with repeated cycles of high-dose cytarabine as well as HSCT. Whether allogeneic transplantation is recommended depends on the leukemic genetic-risk profile, scores on established scales that predict the risk of TRM, and specific transplantation-associated factors in the patient (Longo et al., 2015).
Therapeutic failure in AML is caused by either TRM or resistance to therapy. TRM is typically defined as death within 28 days of treatment initiation (Buckley et al., 2015) and because of marked improvements in supportive care TRM appears to have decreased substantially in recent years, specially for older patients (Othus et al., 2014). Resistance to therapy is a result of either

failure to obtain CR despite living long enough to have done so or relapse from CR, and it is the most common cause of therapeutic failure in AML patients (Estey, 2018).
Although the great majority of adult AML patients attain CR with induction chemotherapy, more than 50% of patients relapse. The risk of relapse has been linked to the post chemotherapy persistence of "measurable residual disease" (MRD), which has been defined as leukemic cells at levels below morphologic detection (Ravandi et al., 2018). As reproducible and standardized methods of MRD monitoring continue to improve, this will be an important tool to guide treatment decisions for relapse/refractory disease. Immunophenotypic assessment using multiparameter flow cytometry can be applied to track aberrant AML blasts populations. Molecular MRD utilizes real-time quantitative polymerase chain reaction (qPCR) for detection of common cytogenetic abnormalities, and newer technologies, including digital PCR and next-generation sequencing (NGS) for detection of point mutations (Schuurhuis et al., 2018).

1.1.7 Targeted therapy for AML

Conventional chemotherapy works by inducing DNA damage in replicating cells, thus targeting AML blasts more than normal cells because of their high replicative rate and low DNA repair capabilities. However, quiescent LSCs can evade treatment and survive to propagate the disease. Chemotherapeutic agents' high cytotoxicity can cause genetic damage to surviving leukemia cells, which contributes to relapse via the selection of resistant clones (Gao and Estey, 2015). Moreover, some patients are unfit for standard induction chemotherapy, especially older adults who account for the majority of patients. Targeted therapy uses drugs directed against specific genetic or other abnormalities related to the leukemic cell clone, and it is thought to diminish toxicity in healthy tissues and to increase the specificity of the target malignant cells (Yang and Wang, 2018). Successful examples of targeted therapy in leukemia treatment are the use of all-trans retinoic acid and arsenic trioxide for Acute Promyelocytic Leukemia (APL) by targeting the promyelocytic leukemia/retinoic acid receptor-alpha (PML-RARA) protein (Wang and Chen, 2008), and tyrosine kinase inhibitors (TKIs) targeting the Philadelphia chromosome (BCR-ABL) in Chronic Myeloid Leukemia (CML) and Acute Lymphoblastic Leukemia (ALL) (Labarthe et al., 2006; Smith and Shah, 2011).

Due to the biological complexity of AML, it is unlikely that single targeted agents would be successful in inducing long term remission. Combination of multiple targeted agents or with standard chemotherapeutic drugs are being investigated to circumvent this issue. Currently, numerous combination regimens are under investigation at preclinical or clinical level (Winer and Stone, 2019). Furthermore, data integration of genomic and transcriptomic analyses, and *ex vivo* drug sensitivity studies will be helpful in assigning specific AML subgroups to targeted therapies (Lavallée et al., 2015, 2016; Tyner et al., 2018).

Novel targeted drugs for AML include checkpoint inhibitors (targeting CTLA-4, PD-1, PD-L1), mutationally targeted inhibitors (targeting mutant FLT3, IDH1, IDH2), pro-apoptotic agents (inhibitor of anti-apoptotic BCL2), and immunotherapy (monoclonal antibodies and chimeric antigen receptor (CAR) T cells). We may expect that only a small fraction of these trials will be paradigm changing but will almost surely serve as the basis for new breakthroughs in patient care (Winer and Stone, 2019). For example, encouraging results from the use of Venetoclax, an oral BCL2 protein inhibitor, prompted its approval by the United States Food and Drug Administration (FDA) for use in combination with a hypomethylating agent or low-dose cytarabine, and may be becoming the standard of care for treatment of AML in older patients or those unfit for induction chemotherapy (Jonas and Pollyea, 2019).

1.2 The RUNX1 gene

1.2.1 Core-binding factor, *RUNX1*

The TF RUNX1 (RUNT-related TF 1) is the DNA-binding subunit of a heterodimeric TF known as the core binding factor (CBF). CBF is composed of an alpha subunit (RUNX1, RUNX2, RUNX3) and a beta subunit (Core binding factor B, CBFB) (Bruijn and Speck, 2004). In humans, the *RUNX1* gene spans ~261 kb on the long arm of chromosome 21. It was first discovered by Miyoshi et al. (Miyoshi et al., 1991) based on its location at the breakpoint of the 8;21 translocation in AML and was initially named acute myeloid leukemia gene 1 (*AML1*). CBFB is a non-DNA-binding regulatory protein that allosterically enhances the sequence-specific DNA-binding capacity of RUNX1. Shortly after cloning of *RUNX1*, *CBFB* was cloned and identified as one of the genes disrupted by the inv(16) in AML (Liu et al., 1993). Interestingly, the two types of AMLs in which inv(16) and t(8;21) take place are different: inv(16) is a marker

for the M4Eo subtype of AML, which shows both granulocytic and monocytic differentiation, and is characterized by abnormal eosinophilia; in contrast, t(8;21) is highly predictive for the M2 subtype of AML, which is characterized by granulocyte maturation (Liu et al., 1993). Nonetheless, these findings show a dependency on CBF activity for proper hematopoiesis and the role of CBF fusion proteins in the development of AML.

1.2.2 RUNX1 structure

Transcription of *RUNX1* generates three major isoforms by use of two promoters and alternative splicing (**Figure 1.2**). Proximal promoter P2 controls the expression of RUNX1b (453 amino acids) and the less abundant isoform RUNX1a (250 amino acids). Distal promoter P1 controls expression of RUNX1c (483 amino acids), which is identical to isoform 1B except for 32 amino acids encoded by alternative exons at its amino terminus (Sood et al., 2017). The RUNX1 gene contains 9 exons, exons 1 and 2 are present only in the RUNX1c isoform. The RUNT domain is encoded by exons 3 to 6, while the transactivation domain spans exons 7A, 7B and 8 (Marshall et al., 2008).

At the N-terminus, RUNX1 contains a conserved 128 amino acid RUNT homology domain (RHD) which is responsible for DNA binding and is also relevant for nuclear localization and protein–protein interactions, including interaction with the heterodimer CBFB and lineage-specific co-factors. RUNX1 recognizes the core consensus binding sequence 5'-YGYGGTY-3' (where Y= C or T) via the RUNT domain (Sood et al., 2017). The C-terminal part is less conserved, and contains an activation domain, an inhibitory domain, a region rich in proline (PY). Nuclear localization signal (NLS) is found in the C-terminal portion of the RUNT domain and a nuclear matrix-targeting signal (NMTS) present at the C-terminal portion of the RUNX1 protein to enhance nuclear matrix interaction for functional organization of the nucleus (**Figure 1.3**) (Koh et al., 2013; Zeng et al., 1997). Although DNA binding and heterodimerization with CBFB occur through the RUNT domain, negative regulatory regions for CBFB heterodimerization are found N-terminus and C-terminus to the RUNT domain (NRHn and NRHc, respectively). Similarly, negative regulatory regions for DNA binding are found in the N-terminus and C-terminus to the RUNT domain (NRDBn and NRDBc, respectively). The transcriptional activator domain (TAD) and the inhibitory domain (ID or RUNXI) are responsible

for binding to a number of activating and repressor proteins. Moreover, the evolutionarily conserved VWRPY penta-peptide sequences has been shown to be responsible for repressive function as a platform to recruit Groucho/TLE transcriptional corepressors (Imai et al., 1998) (**Figure 1.3**). The RUNT domain is conserved in all 3 isoforms of RUNX1 (**Figure 1.2**), suggesting that they can all bind to DNA. The TAD, ID and VWRPY sequence, however, are only present in RUNX1b and RUNX1c.

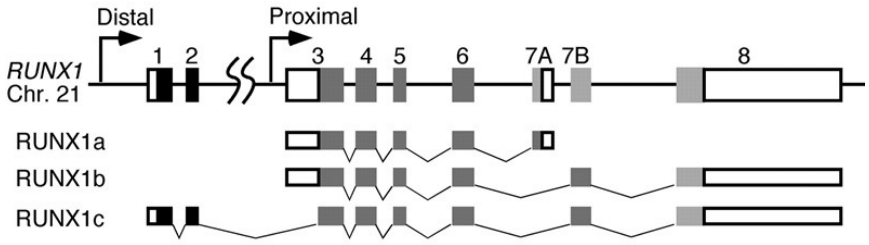

Figure 1.2: Schematic representation of the human RUNX1 gene

Open boxes represent noncoding exons, and shaded boxes indicate coding exons. The three major splice variants of RUNX1 are indicated. Figure was adapted from Marshall LJ et al., 2008 with permission.

1.2.3 RUNX1 mechanism of action

RUNX1 acts as an epigenetic regulator and as an activator or repressor of transcriptional programs (Bruijn and Dzierzak, 2017). RUNX1 control of hematopoietic development involves activation of key TFs, cytokine production, and control of growth factor signaling. An important role of RUNX1 at the onset of hematopoiesis is the activation of transcription of the master TF SPI-1 (PU.1) (Lichtinger et al., 2012) by binding to three RUNX1 sites in the upstream regulatory element (URE) of the *SPI-1* gene (Huang et al., 2008).

Curiously, the transcription activation of several hematopoietic genes by RUNX1 requires adjacent binding sites for other TFs such as C/EBP-alpha, SPI-1, c-MYB, ETS, GATA1, and TCF/LEF (**Figure 1.3**) (Mikhail et al., 2006). Well described examples include several genes involved in hematopoietic growth and myeloid-specification, such as interleukin-3 (IL-3) (Cameron et al., 1994), the colony-stimulating factor-1 receptor (*CSF1R*) (or macrophage colony-stimulating factor (M-CSF) receptor) (Zhang et al., 1994, 1996), the colony-stimulating factor-2

(*CSF2*) (or granulocyte-macrophage colony-stimulating factor (GM-CSF)) (Takahashi et al., 1995), the myeloperoxidase (*MPO*), and neutrophil elastase (*NE*) genes (Nuchprayoon et al., 1994). In addition to regulating hematopoiesis-specific genes, RUNX1 also regulates cell-cycle-related genes, including repression of the promoter of $p21^{CDKN1A}$ (also known as WAF1/CIP1), which encodes a cyclin-dependent kinase inhibitor important for checkpoint controls and terminal differentiation (Lutterbach et al., 2000).

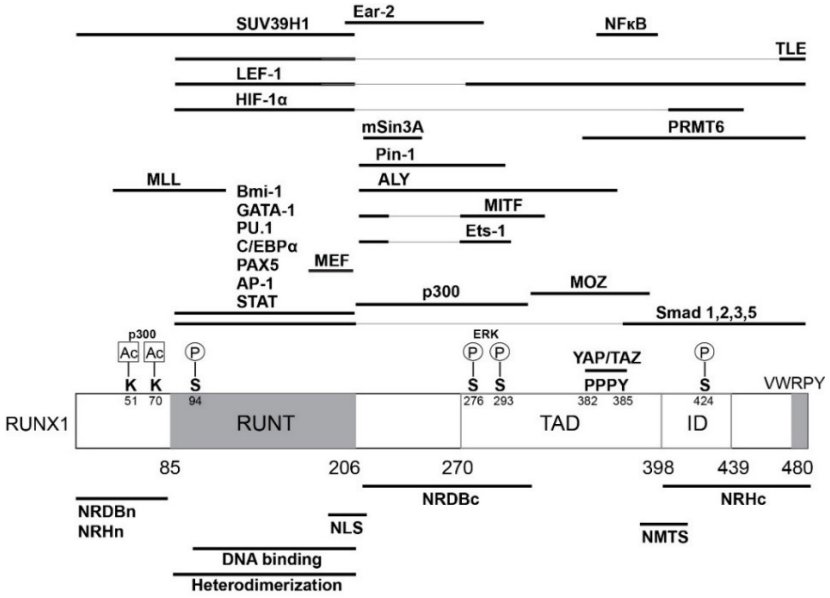

Figure 1.3: Schematic diagram of RUNX1 structure

A diagram of the RUNX1 protein (RUNX1c isoform, NP_001745.2) shows functional domains, sites of phosphorylation and acetylation, and portions interacting with other indicated proteins. TAD, transactivation domain; ID, inhibitory domain; NRH, negative regulatory region for CBFB heterodimerization; NRDB, negative regulatory region for DNA binding; NLS, nuclear localization signal; NMTS, nuclear matrix. Figure adapted from Koh CP et al., 2013 with permission.

Depending on cell type and genomic context, RUNX1 can interact with a multitude of chromatin modifiers that support both a transcription activating and repressive role of RUNX1 (Obier and Bonifer, 2016). Histone acetyltransferases, such as monocytic leukemia zinc finger protein (MOZ) and p300/CBP are found to be associated with RUNX1 transcriptional complex and to

strongly stimulate RUNX1 transcriptional activity during differentiation of myeloid cells (Kitabayashi et al., 1998, 2001). RUNX1 can also interact with core components of the chromatin-remodeling switch/sucrose-nonfermentable (SWI/SNF) complex, which is associated with active RUNX1 target gene promoters in hematopoietic cells (Bakshi et al., 2010). Transcriptional repression by RUNX1 occurs through the recruitment of repressive complexes like Suv39H1 (Durst and Hiebert, 2004), mSin3A (Imai et al., 2004), polycomb repressive complex 1 (PRC1) (Yu et al., 2012), Groucho/TLE (Levanon et al., 1998), arginine methyltransferase PRMT6, as well as HDACs (Herglotz et al., 2013).

1.2.4 RUNX1 in hematopoietic development

RUNX1 activity is indispensable for the establishment of definitive hematopoiesis. *Runx1*-deficient mice die during embryonic development between E11.5–E12.5 due to extensive hemorrhaging and embryos lack hematopoietic progenitors in both the yolk sac and fetal liver (North et al., 1999; Okuda et al., 1995; Wang et al., 1996). Similar to what was observed in mice, RUNX1 is essential for the initial specification of definitive HSCs in humans (Challen and Goodell, 2010; Ditadi et al., 2015) and is highly expressed in human ESC (hESC) during *in vitro* formation of the hemogenic endothelium (Angelos et al., 2017). Even though RUNX1 is expressed in virtually all hematopoietic stem and progenitor cells and in most cells differentiating into the monocyte/granulocyte lineages and the lymphoid compartment, it is not essential for maintenance of adult HSC (North et al., 2004). Deletion of *Runx1* from adult hematopoietic stem cells in mice revealed pronounced defects in T and B cell development, inefficient platelet formation due to a block in megakaryocyte development, and establishment of a myeloproliferative phenotype (Growney et al., 2005; Ichikawa et al., 2004).
RUNX1 dosage has been extensively characterized in ontogeny and shows great similarities between mice and human studies. Although total *Runx1* knock-out (KO) is embryonic lethal, heterozygous mice appeared unaffected. Thorough investigation showed that reduction of RUNX1 through haploinsufficiency expedites HSC emergence in *in vivo* and *in vitro* models (Cai et al., 2000; Lacaud et al., 2004). Moreover, RUNX1 haploinsufficiency affects HSC migration and maintenance in the embryo (Cai et al., 2000). Conversely, forced overexpression in hESC of either RUNX1b or RUNX1c isoforms, but not of RUNX1a, completely blocks the emergence of

early hemogenic endothelium and consequently drastically reduce the production of hematopoietic stem/progenitor cells (Chen et al., 2017). Thus, it is clear that a tight spatial-temporal control of RUNX1 levels is necessary for the proper development of the hematopoietic system.

1.2.5 RUNX1 in adult hematopoiesis

Even though RUNX1 is dispensable for HSC commitment to myeloid lineages and to double-negative CD4/CD8 thymocytes, it is essential for terminal differentiation of the megakaryocytes (MK) and T-lymphoid lineages. The absence of RUNX1 greatly affects MK polyploidization and terminal maturation resulting in thrombocytopenia (Growney et al., 2005; Ichikawa et al., 2004; Putz et al., 2005). RUNX1 activate the transcription of megakaryocyte specific genes while blocking the erythrocyte program at the branch point of megakaryocyte versus erythroid differentiation in the megakaryocyte-erythroid progenitor cells (MEPs) (Kuvardina et al., 2015). During differentiation of T cell lymphocytes in the thymus, immature thymocytes lacking CD4 and CD8 coreceptors differentiate into double-positive cells (CD4+CD8+), which are selected to become either CD4+CD8− helper cells or CD4−CD8+ cytotoxic cells (Taniuchi et al., 2002). RUNX1 is required for CD4 silencing in the double-negative stage and for activating the expression of CD8 gene as cells differentiate to the double-positive stage (Taniuchi et al., 2002). RUNX1 activity also supports the survival and proliferation of B-cell progenitors and regulates the expression of several genes involved in pre-B-cell transition, therefore supporting B-cell development (Niebuhr et al., 2013). Not surprisingly RUNX1 malfunctioning is linked to a diverse array of blood disorders and malignancies.

1.2.6 Regulation of RUNX1 activity

Numerous studies have shown that RUNX1 activity is regulated by posttranslational modification (PTMs), including phosphorylation, acetylation, methylation and ubiquitination. These PTMs regulate RUNX1 activity either positively or negatively by altering RUNX1-mediated transcription, promoting protein degradation and affecting protein-protein interactions (Goyama et al., 2014).

Extracellular signal-regulated kinase (ERK), which is activated by hematopoietic cytokines and growth factors, phosphorylates RUNX1 in five serine (S) and threonine (T) residues located in the C-terminal region of RUNX1 (S276, S293, S303, S462 and T300) (Tanaka et al., 1996). Phosphorylation by ERK and homeodomain-interacting protein kinase 2 (HIPK2) result in subsequent transcriptional activation by RUNX1 (Imai et al., 2004; Aikawa et al., 2006). Additionally, RUNX1 can be phosphorylated by cyclin-dependent kinases (CDKs) which affects the overall stability of RUNX1 as well as the ability of certain ubiquitin ligase complexes, such as Cdc20-anaphase-promoting complex (APC), to target RUNX1 for degradation (Biggs et al., 2006). On the other hand, Tyrosine (Y) residues in RUNX1 were shown to be phosphorylated by Src family kinases, which negatively regulates RUNX1 activity (Huang et al., 2012). Acetylation and methylation of conserved residues in RUNX1 have been reported to increase transactivation potential of RUNX1 (Kitabayashi et al., 2001; Yamaguchi et al., 2004; Zhao et al., 2008). Finally, RUNX1 is susceptible to proteolytic degradation by the ubiquitin– proteasome system and multiple lysine residues in RUNX1 are putative targets of ubiquitination (Goyama et al., 2014). RUNX1 is an unstable protein with a half-life of ~60 min in its free form. The half-life of RUNX1 was demonstrated to increase to up to ~200 min when bound to CBFB. Since heterodimerization of RUNX1 with CBFB occurs through the RUNT domain, and the lysine residues of RUNX1 cluster within or around the RUNT domain, it is believed that CBFB-RUNX1 physical interaction protects RUNX1 from degradation (Huang et al., 2001). Apart from APC and SCF ubiquitin ligase complexes (Biggs et al., 2006), the E-3 ligase CHIP has also been shown to promote ubiquitination and proteasome degradation of RUNX1 (Shang et al., 2009). Although the physiologic relevance of RUNX1 PTMs and the crosstalk among various modifications remains largely unknown, they represent interesting druggable targets to be explored in order to modulate RUNX1 activity.

1.3 RUNX1 involvement in hematological malignancies

1.3.1 Chromosomal translocations involving *RUNX1*

AML with t(8;21)(q22;q22) or with inv(16)(p13;q22) or t(16)(p13;q22), which disrupt RUNX1 or CBFB respectively, are included under the category of "AML with recurrent genetic abnormalities" in the 2016 WHO classification scheme (Arber et al., 2016) and together are often

referred to as “core-binding factor acute myeloid leukemia” (CBF-AML) (Bellissimo and Speck, 2017). To date, over 50 different chromosomal translocations involving RUNX1 have been identified in patients with AML, T-cell ALL, B-cell ALL, CML, and MDS. Most recurrent examples include RUNX1-RUNX1T1, RUNX1-EVI1, and ETV6-RUNX1, respectively the products of t(8;21)(q22;q22), t(3;21)(q26.2;q22), and t(12;21)(p13;q22) translocations (Kouwe and Staber, 2019).

1.3.1.1 t(8;21) AML

The t(8;21) translocation is found in 4-7% of adult AML, being more prevalent in younger adults and frequently observed in AML of the subtype M2 (Grimwade et al., 2010; Sanderson et al., 2006). The resulting fusion protein RUNX1-RUNX1T1 (also known as RUNX1-ETO or RUNX1-MTG8) consists of the N-terminus of RUNX1, including the conserved RUNT domain, fused to almost the entire RUNX1T1 protein (Miyoshi et al., 1993). RUNX1T1 is a nuclear protein and exerts its activity by associating with several corepressors like nuclear receptor co-repressor 1 (NCOR), silencing mediator of retinoic acid and thyroid hormone receptor (SMRT), mSin3A and histone deacetylases (HDACs) (Goyama and Mulloy, 2011). RUNX1-RUNX1T1 retains the ability to bind to the RUNX1 DNA consensus sequence, and because RUNX1T1 interacts with and recruits a wide range of repressors, it is thus commonly understood to suppress native RUNX1 activity (Kouwe and Staber, 2019). Using mice heterozygous for RUNX1-RUNX1T1 allele, this was first evidenced by the similarity of early embryonic lethality and hematopoietic defects to that observed in RUNX1 null mice (Yergeau et al., 1997). Nonetheless, yolk sac progenitors in RUNX1-RUNX1T1 embryos can undergo differentiation and give rise exclusively to macrophages, which differs from RUNX1 null or RUNX1 wild-type embryos, as determined by *in vitro* colony assays (Yergeau et al., 1997), suggesting that a more complex relationship between RUNX1-RUNX1T1 and native RUNX1 might be at play. While RUNX1-RUNX1T1 has been shown to block RUNX1 activity in the promoter of RUNX1 target genes such as the *CSF2* (GM-CSF) (Frank et al., 1995), it synergizes with RUNX1 to activate transcription from the *CSF1R* promoter (M-CSF receptor) (Rhoades et al., 1996). RUNX1-RUNX1T1 can form a complex with native RUNX1 on chromatin through interaction between their RUNT domains, and recruitment of coregulators determines if the target gene is activated or

repressed (Li et al., 2016). It is understood that t(8;21) cells have a dependency on wild type RUNX1 for the establishment of leukemogenesis by RUNX1-RUNX1T1, which is further supported by clinical data showing absence of inactivating mutations in *RUNX1* in t(8;21) AML (Lin et al., 2017).

1.3.2 *RUNX1* mutations in hematological malignancies

RUNX1 mutations have been reported in 18% of patients with T-cell ALL, 3.8% of patients with B-cell ALL, 10-20% of patients with MDS, and near 15% of patients with Chronic Myelomonocytic Leukemia (CMML) (Grossmann et al., 2011; Mangan and Speck, 2011; Patnaik and Tefferi, 2016). Even though mutations found in *RUNX1* in CMML, AML and MDS patients are similar, the types of cooperating mutations are different with mutations that confer a proliferation advantage being predominantly found in AML (Mangan and Speck, 2011).

1.3.2.1 *RUNX1*-mutated AML

According to the most recent WHO classification of AML, AML with mutated *RUNX1* constitutes a new provisional entity for cases of *de novo* AML with this mutation (Arber et al., 2016). *RUNX1* mutations are also observed in secondary AML (sAML) evolving from a previous myeloid disorder or resulting from prior treatment with chemotherapy or radiation (therapy-related AML, t-AML). Mutations in *RUNX1* are reported in 5–13% of *de novo* AML, showing adverse prognostic impact on overall survival (OS) and disease progression (Gaidzik et al., 2016, 2011; Mendler et al., 2012; Network, 2013; Tang et al., 2009). *RUNX1*-mutated AML are generally associated with older age and show a distinct pattern of cytogenetic abnormalities with a high frequency of trisomy 8 or 13. In general, *RUNX1* mutations occur more frequently in patients with intermediate-risk cytogenetics, particularly those with a normal karyotype, as compared to those with complex cytogenetic abnormalities (Khan et al., 2017; Schnittger et al., 2011). Morphologically, AML with *RUNX1* mutations are predominantly undifferentiated. They are found at particularly high frequency in AML M0, and at high proportion in AML M1, AML M2, and observed in AML M4 (Gaidzik et al., 2016; Preudhomme et al., 2000; Roumier et al., 2003; Schnittger et al., 2011).

RUNX1-mutated AML are almost always mutually exclusive of AML with recurrent chromosome abnormalities (CBF-AML), *NPM1* and *CEBPA* mutations. On the other hand, they co-occur with a wide variety of gene mutations, including in epigenetic modifiers (*ASXL1*, *IDH2*, *KMT2A*, *EZH2*, *DNMT3A*, *BCOR*), components of the spliceosome complex (*SRSF2*, *SF3B1*), signaling pathways (*RAS, FLT3-ITD*) and *STAG2*, *PHF6* (Gaidzik et al., 2016; Haferlach et al., 2014; Khan et al., 2017). Prognostic effect of mutation co-associations has shown that *RUNX1*/*ASXL1* and *RUNX1*/*SRSF2* seem to have particularly worse overall survival (Gaidzik et al., 2016). *RUNX1* co-mutations in *FLT3-ITD* and MLL-PTD, both unfavorable subgroups, do not confer an additional unfavorable effect (Schnittger et al., 2011).

1.3.2.2 *RUNX1* germline mutations in Familial Platelet Disorder with predisposition to hematologic malignancies

The work by Song et al. (Song et al., 1999) first determined that point mutations in *RUNX1* are implicated in familial platelet disorder with predisposition to hematologic malignancies (RUNX1-FPD, FPD/AML, FPDMM), an autosomal dominant disorder characterized by moderate thrombocytopenia that often progresses to progressive pancytopenia, hematopoietic dysplasia, and acute leukemia (AL). The lifetime risk of myeloid malignancy in mutation carriers varies greatly (range, 11%-100%; median, 44%), with an average age of onset of 33 years (range 6–76 years) (Godley and Shimamura, 2017; West et al., 2014).

The numerous RUNX1-FPD pedigrees annotated to date have either germline monoallelic nonsense, frameshift and missense mutations in *RUNX1*, large intragenic deletions, or complete deletion of one allele and, except for a few recurrent mutations, the great majority of mutations is unique to a single pedigree (Latger-Cannard et al., 2016). Hematological malignancies observed are most frequently found to be AML, MDS, CMML and ALL. In some cases, AML develops in patients that presented T-cell ALL first (Latger-Cannard et al., 2016).

Diagnosis of patients with germline predisposition to hematological neoplasms is of clinical relevance, as they should be closely monitored to optimize the time of intervention and be offered genetic counseling (Duployez et al., 2019). The classic phenotypic presentation of RUNX1-FPD includes both quantitative and qualitative platelet defects. However, some patients do not demonstrate thrombocytopenia or the aspirin-like platelet dysfunction and, thus, the absence of these findings does not rule out the diagnosis (West et al., 2014). Platelet dysfunction in RUNX1-

FPD patients often causes clinical bleeding with minor trauma or surgical procedures as well as poor wound healing (Godley, 2014). A few patients do not present any symptoms and remain undiagnosed until the development of MDS/acute leukemia (Galera et al., 2019).
The precise mechanism by which *RUNX1* haploinsufficiency induces thrombocytopenia is not completely understood. Thrombocytopenia is caused by abnormal megakaryocyte maturation and impaired proplatelet formation. In a recent report, bone marrow aspirates from 14 patients with RUNX1-FPD showed that all patients had abnormal megakaryocytes with loss of polyploidy (Chisholm et al., 2019). Patient's platelets abnormally express several proteins linked to platelet function, and reduced expression of RUNX1 target genes include thrombopoietin receptor (MPL), non-muscle myosin IIA/myosin heavy chain 9 (*MYH9*) and its regulatory chain *MLC2*, myosin heavy chain 10 (*MYH10*), arachidonate 12-lipoxygenase (*ALOX12*), platelet factor 4 (*PF4*) and nuclear factor erythroid 2 (*NFE2*) (Bluteau et al., 2012; Lordier et al., 2012; Schlegelberger and Heller, 2017; Sun et al., 2004; SUN et al., 2006).

1.3.3 Biochemical effects of RUNX1 mutations

Mutations in *RUNX1* include large deletions, missense, splicing, frameshift, and nonsense mutations. The majority of RUNX1 mutations will fall into one of following categories based on their potential impact on the protein function: 1) large deletions (null allele); 2) mutations resulting in truncation within the Runt domain; 3) missense mutations in the RUNT domain at the DNA interface that affect DNA but not CBFB binding; 4) missense mutations in the RUNT domain at the CBFB interface that affect CBFB but not DNA binding; 5) missense mutations in the RUNT domain that affect both DNA and CBFB binding through destabilizing the RUNT domain fold; 6) mutations that truncate RUNX1 C-terminal to the RUNT domain and remove all or part of the transactivation domain; and 7) missense mutations that are C-terminal to the RUNT domain (rare) (Mangan and Speck, 2011).
These mutations in *RUNX1* are thought to lead to at least three types of allele function: haploinsufficient (loss-of-function), hypomorphic or dominant-negative (Matheny et al., 2007). Nonsense or frameshift mutations that truncate the RUNX1 protein N-terminal to or within the DNA-binding domain typically generate a loss-of-function allele. Nonsense and frameshift alterations occurring C-terminal to the RUNT domain may produce loss-of-function alleles for

eliminating the transactivation or inhibitory domains, and/or inducing nonsense-mediated mRNA decay (NMD). NMD is predicted if the premature termination codon occurs upstream of the 3′-most 50 nucleotides of the penultimate exon (Luo et al., 2019). Frameshift mutations that disrupt the C-terminal TAD and do not undergo NMD can act as dominant-negative alleles. That is believed to be due to the ability of mutant RUNX1 to occupy its target sites through their intact RUNT domain and consequently block occupancy and transactivation by wild type RUNX1 proteins (Bellissimo and Speck, 2017).

Biochemical studies revealed a diverse phenotypic effect of RUNX1 missense mutations. It was demonstrated by Matheny et al., that mutations involving DNA-contacting residues severely inactivate RUNX1 function, whereas mutations that affect CBFB binding but not DNA binding result in hypomorphic alleles (Matheny et al., 2007). It has also been observed that mutations in DNA-contacting residues that disrupt DNA binding without perturbing the structure of the DNA-binding domain behave as weakly dominant-negative mutations, which might be due to sequestering of the heterologous partner CBFB that serve as a limiting protein for proper activity of wild type RUNX1 proteins (Bellissimo and Speck, 2017).

1.3.4 Gene expression signature of *RUNX1*-mutated AML

Gene expression signature of *RUNX1*-mutated AML was first derived from microarray data comparing *RUNX1*-mutated versus *RUNX1*-wild type primary AML samples. Genes highly expressed in early hematopoietic progenitor/stem cells (HSPCs) were overexpressed in *RUNX1*-mutated compared to *RUNX1*-wild type and included *BAALC*, *CD109*, *P2RY14*, *HGF*, *SETBP1*, as well as several genes normally expressed in early lymphoid precursors, such as *DNTT*, *BLNK*, *IRF8*, *FOXO1*, *FLT3*. Conversely, *CEBPA*, a key promoter of granulopoiesis, and *AZU1*, *MPO*, and *CTSG*, components of neutrophil granules, were downregulated in *RUNX1*-mutated AML (Mendler et al., 2012). The gene expression profile is consistent with previous observations demonstrating that *RUNX1* mutations occur more frequently in minimally differentiated (M0) AML. Moreover, RUNX1 has been implicated in the inhibition of self-renewal programs in early HSPCs (Behrens et al., 2016; Ross et al., 2012). Introduction of a C-terminal *RUNX1* mutation (S291fs300X) in hematopoietic stem/progenitor cells leads to differentiation block at the granulocyte-macrophage progenitor (GMP) stage. RNA-seq data comparing *RUNX1* mutant and

RUNX1 wild-type cells revealed an enrichment of stem cell genes (e.g. *MEIS1*, *TCF4*, *ERG*, *CD34* and *HMGA2*) and a loss of genes involved in granulocytic differentiation (e.g. *ELANE*, *CEBPE*, *MPO*, *CTSG*, and *CEBPA*)(Gerritsen et al., 2019). These observations provide insights into the mechanisms by which RUNX1 defects impact AML development.

1.4 Glucocorticoids

1.4.1 Glucocorticoid biology and therapeutic use

Glucocorticoids (GCs) or corticosteroid hormones are produced under the control of the hypothalamic–pituitary–adrenal (HPA) axis, the major neuroendocrine axis regulating homeostasis in mammals (Gjerstad et al., 2018). GCs are synthetized from cholesterol by the adrenal cortex under the control of adrenocorticotropic hormone (ACTH). The production of ACTH in turn is controlled by corticotropin-releasing hormone (CRH) released by endocrine hypothalamus (HPA axis) (Dallman et al., 1994). The main glucocorticoid hormone released by the human adrenal cortex is cortisol (hydrocortisone). Cortisol is known as a stress hormone involved in the response to physical/emotional stress. By regulating the metabolism of carbohydrates, proteins and lipids, cortisol acts in homeostatic maintenance and preserves normal function of the cardiovascular system, the immune system, the kidney, skeletal muscle, the endocrine system, and the nervous system (Parente, 2001).

The first reported use of glucocorticoids for therapeutic purposes dates to 1949, when Hench and colleagues administered an adrenal cortical steroid extract to fourteen patients with severe or moderately severe rheumatoid arthritis and, in each case, improvement in clinical features was observed within a few days (Hench et al., 1949). Since these pivotal observations several synthetic glucocorticoids have been synthetized by the pharmaceutical industry and are widely prescribed for the treatment of acute and chronic inflammatory diseases, autoimmune diseases, organ transplant rejection, and malignancies (Oakley and Cidlowski, 2010).

GCs mediate their effects via activation of the glucocorticoid receptor (GR) and the mineralocorticoid receptor (MR). In physiological conditions, GRs are activated with high plasma corticosteroid levels, reached after a stressor, and have an established function in the response to and recovery from stress. The affinity for corticosteroids is higher for MR than for GR, therefore MRs are heavily occupied even with low plasma corticosteroid concentrations. The

activation of MR by GCs was suggested to have a proactive role in setting the threshold for stress responsiveness (Groeneweg et al., 2012). The therapeutic effects of GR are indeed mainly associated with GR activity; therefore, synthetic GCs are designed to have higher affinity for GR than MR.

1.4.2 Glucocorticoid Receptor gene and protein structure

GR is a ligand activated TF that is ubiquitously expressed throughout the body (Gjerstad et al., 2018). The GR is a member of the nuclear receptor family and is encoded by the *NR3C1* gene (Nuclear Receptor Subfamily 3 Group C Member 1) located on chromosome 5 (5q31). The *NR3C1* gene consists of nine exons of which exon 1 forms the 5′ untranslated region (UTR) and exons 2–9 encode the GR protein. GR exon 1 contains multiple promoter regions (A1–3, B, C1–3, D–F, H–J) and differential use of these promoters causes varying expression levels of GR protein isoforms (**Figure 1.4A**). Moreover, alternative splicing of *NR3C1* gene and the use of alternative translation initiation sites give rise to multiple GR variants (Timmermans et al., 2019). Research has mainly focused on the most abundantly expressed isoforms, glucocorticoid receptor α (GRα) and glucocorticoid receptor β (GRβ), which are isoforms derived from alternative splicing of exon 9 (Hollenberg et al., 1985). Due to differences in the C-terminus, GRβ is unable to bind ligands (Quax et al., 2013). Despite this, GRβ is constitutively found in the nucleus where it performs several functions, including to be an antagonist to the GRα isoform (Timmermans et al., 2019).

GR contains an N-terminal transactivation domain (NTD), a central DNA binding domain (DBD), a hinge region (H), and a C-terminal ligand-binding domain (LBD). The NTD, encoded by exon 2, contains the ligand independent activation function 1 (AF1) that serves as a platform to bind cofactors, chromatin modulators, and the transcription machinery. The GR DBD is encoded by exons 3 and 4 and is important for DNA binding and GR dimerization. Exons 5–9 of the *NR3C1* gene encode the GR's hinge region and LBD. The former provides both flexibility between the DBD and LBD as well as a regulatory interface (Timmermans et al., 2019).

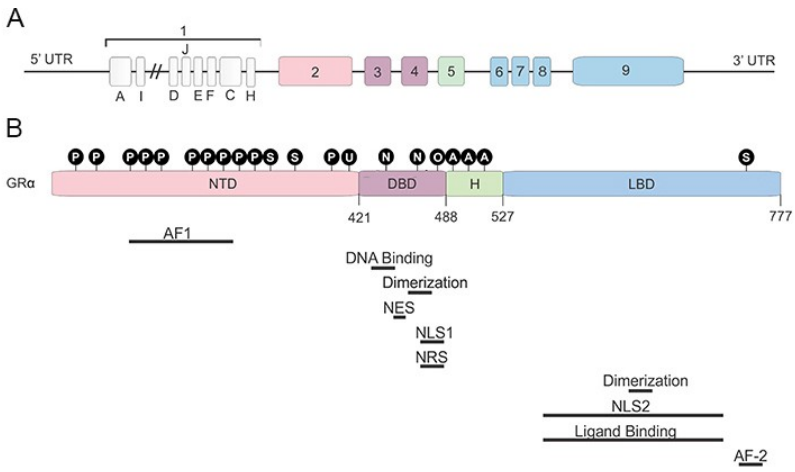

Figure 1.4: Schematic representation of the GR gene and protein

(A) Genomic structure of the GR gene *NR3C1*. **(B)** Primary structure of the GRα protein consisting of an N-terminal domain (NTD), DNA-binding domain (DBD), a hinge region (H), and a ligand-binding domain (LBD). Figure was adapted from Timmermans et al., 2019 with permission.

1.4.3 Nucleocytoplasmic shuttling of the GR

GCs are lipophilic molecules and therefore can rapidly cross the cell membrane and bind the GR in the cytosol. In the absence of ligands, GR is predominantly found in the cytoplasm complexed with accessory proteins (HSP90, HSP70, p23, and immunophilins). That is achieved because HSPs bound to the LBD of GR mask/inactivate the two nuclear translocation signals (NLS) found in GR, NLS-1 and NLS-2 (**Figure 1.4B**), thereby maintaining GR in the cytoplasm in a conformation of high-binding affinity to GC (Oakley and Cidlowski, 2010). Binding to ligand results in conformational changes that exposes NLS-1 and NLS-2 and leads to nuclear translocation of the receptor. The dynamic nucleocytoplasmic shuttling of the GR takes place through the nuclear pore complex (NPC), a macromolecular multimeric structure embedded in the nuclear envelope, mediated by adapter receptors Importin α and β. Importin α binds the NLS of the GR and forms a trimeric complex with Importin β, the transport receptor that favors the passage of cargoes through the nuclear pore (Echeverria and Picard, 2010). The retrograde movement of the GR toward the nucleus also involves association to molecular motor protein cytoplasmic dynein, which can move cellular cargo along microtubules in the cells. Immunophilins present in the GR-HSP90 heterocomplexes have been shown to be responsible for

coadsorption of cytoplasmic dynein and is better characterized for FKBP52, one of the major immunophilins in GR-HSP90 heterocomplexes (Galigniana et al., 2001).
Nuclear recycling is also recognised as an important process for signaling through GR and involves intranuclear unloading and reloading of the ligand to receptor complexes, allowing them to bind chromatin intermittently (Stavreva et al., 2009). After ligand withdrawal and release of GR from chromatin-binding sites, GR is complexed with HSP90 and p23, which facilitates export of GR from nucleus and consequent inhibition of GR transcriptional activity. A nuclear export signal (NES) is located in the DBD of GR (**Figure 1.4B**) and have been shown to be bound by exportins, such as XPO1, and by the nuclear export receptor calreticulin in the transport of GR from nucleus to cytoplasm (Vandevyver et al., 2012). Additionally, a nuclear retention signal (NRS) has been identified in the GR (**Figure 1.4B**) and its presence contributes to a delay in the nuclear export (Carrigan et al., 2007).

1.4.4 Non-genomic actions of GR

Several mechanisms of nongenomic glucocorticoid signaling have been postulated. GC effects detected within 5–15 min are usually nongenomic, whereas genomic effects require at least 15-30 min to be detectable. The nongenomic actions of GCs are typically attributed to interaction with the cytosolic GR, interactions with membrane-bound glucocorticoid receptors (mGR), and nonspecific interactions with cellular membranes (Buttgereit and Scheffold, 2002).
Rapid effects of glucocorticoids observed in several tissues are suggestive of a mechanism that is independent of protein synthesis, but requires binding to GR (Croxtall et al., 2000). It has been postulated that the nongenomic effect observed through the cytosolic GR could be due to the action of other proteins that are released from the GR-HSP90 complex after binding of GC (Croxtall et al., 2000). Alternatively, several reports have shown indications that a distinct membrane glucocorticoid receptor (mGR) mediates nongenomic effects of glucocorticoids (Quax et al., 2013). Presence of mGR isoforms have been described in several mouse and human tissues and correlates with the effectiveness of glucocorticoid-induced cell death (Bartholome et al., 2004; Chen et al., 1999; Galera et al., 2019; Sackey and Watson, 1997).
Finally, nonspecific interactions with cellular membranes has been observed in high-dose glucocorticoid therapy. Evidence suggests that the rapid effects on cell metabolism in

lymphocytes are due to inhibition of calcium and sodium cycling across the plasma membrane (Buttgereit and Scheffold, 2002).

1.4.5 Genomic actions of GR

In the nucleus, the GR acts as a TF that can activate (transactivation) or inhibit (transrepression) gene expression as well as modulate the function of other TFs (tethering). Depending on the experimental model used and the type of cell studied, ~1–20% of all genes are estimated to be positively or negatively regulated by GC, illustrating the diversity of GC action (Quax et al., 2013). GR interacts with DNA through glucocorticoid binding sites (GBS) containing a Glucocorticoid Response Element (GRE). GREs are 15 bp long sequence motifs of two imperfect inverted palindromic repeats of 6 bp separated by a 3 bp spacer. The generally accepted GRE consensus sequence is AGAACAnnnTGTTCT (Timmermans et al., 2019). The GR binds the GRE as a homodimer in a head-to-head fashion (**Figure 1.5**). Recent evidence suggested that DNA binding triggers an interdomain allosteric regulation within the GR, leading to tetramerization (Presman et al., 2016). However, the importance of this GR tetramer in transcriptional regulation is not well-understood and needs further investigation.

The interaction of GR with GREs is dynamic, with the GR binding to and dissociating from GREs in the order of seconds (McNally et al., 2000). In living cells, GR can bind to GREs where chromatin remodelling is already ongoing prior to GR activation ("pre-programmed") or to GREs where GR itself initiates the remodeled state ("de novo") (John et al., 2008). Genome-scale analyses of GBS showed that the majority of receptor binding sites occurs distally from promoters in intergenic and intronic regions, which posits that nuclear receptors frequently act as long-range enhancers rather than classic TFs (Biddie et al., 2010). *In vivo*, the vast majority of GBS are mapped to DNase I hypersensitive sites (DHS), which represent active chromatin regions conducive to initiation of transcription (Love et al., 2017). Interestingly, DHS mapping and the associated GBS are radically different between cell types, indicating that active GBS are cell type-specific, which is dictated by the pre-existing chromatin landscape (Franco et al., 2019; John et al., 2011).

Not all genes modulated by GR contain the canonical GRE consensus site. Alternatively, GR is capable of binding as a monomer to GRE-half sites *in vivo* (**Figure 1.5**), resulting in regulation of

target genes (Schiller et al., 2014). If a binding site for another TF is nearby the GRE-half site, both elements may act as a composite site where there is an interaction (positive or negative) between the monomeric GR and the other TF (**Figure 1.5**) (Timmermans et al., 2019).
A third mechanism for GR interaction with DNA was described to be associated with negative regulation of transcription. It involves inverted-repeat GREs (IR-GREs) that have the consensus CTCC$(N)_{0–2}$GGAGA sequence. These elements prompt the binding of two GR monomers on the opposite sides of DNA in a head-to-tail fashion. In this orientation, the dimerization loop of each GR monomer (located in the DBD) is directed away from the other monomer and rotated by 180° around the DNA axis (**Figure 1.5**), impeding GR dimerization. These unique negative GREs alter the conformation of GR residues critical for transcriptional activation, illustrating the importance of DNA as an allosteric modulator of receptor activity (Hudson et al., 2012).
The gene regulatory regions of many inflammatory mediators inhibited by GCs do not contain GREs, GRE-half sites or IR-GREs, which indicates that additional indirect mechanisms are very important (Goulding and Flower, 2001). This is achieved through tethering, a mechanism in which GR is recruited to heterologous TF complexes through direct protein-protein interaction. Thus ligand-bound GR can alter the capacity of the TF to bind DNA, recruit cofactors, and activate/repress gene transcription (**Figure 1.5**). The ability to recruit GR has been attributed to AP-1, STAT, and NF-κB families of TFs (Louw, 2019).

1.4.5.1 Transactivation and transrepression

Gene transactivation by GR is triggered mainly by the dimeric form of the receptor when bound to canonical GREs. DNA binding induces conformational changes in the dimerization interface that expose otherwise silent transcriptional activation surfaces (Tilborg et al., 2000). Although GR can interact with many co-activators, it has been better characterized for the p160 family including steroid receptor co-activators SRC1, SRC2, and SRC3, coded by *NCOA1-3* genes. One of the best studied GR-interacting factors is the GR-interacting protein 1 (GRIP1, SRC2, *NCOA2*). This protein has a dual action upon binding to GR: it can act as both an activator and a repressor, in a gene-dependent context, ultimately serving to enhance the anti-inflammatory properties of GR.

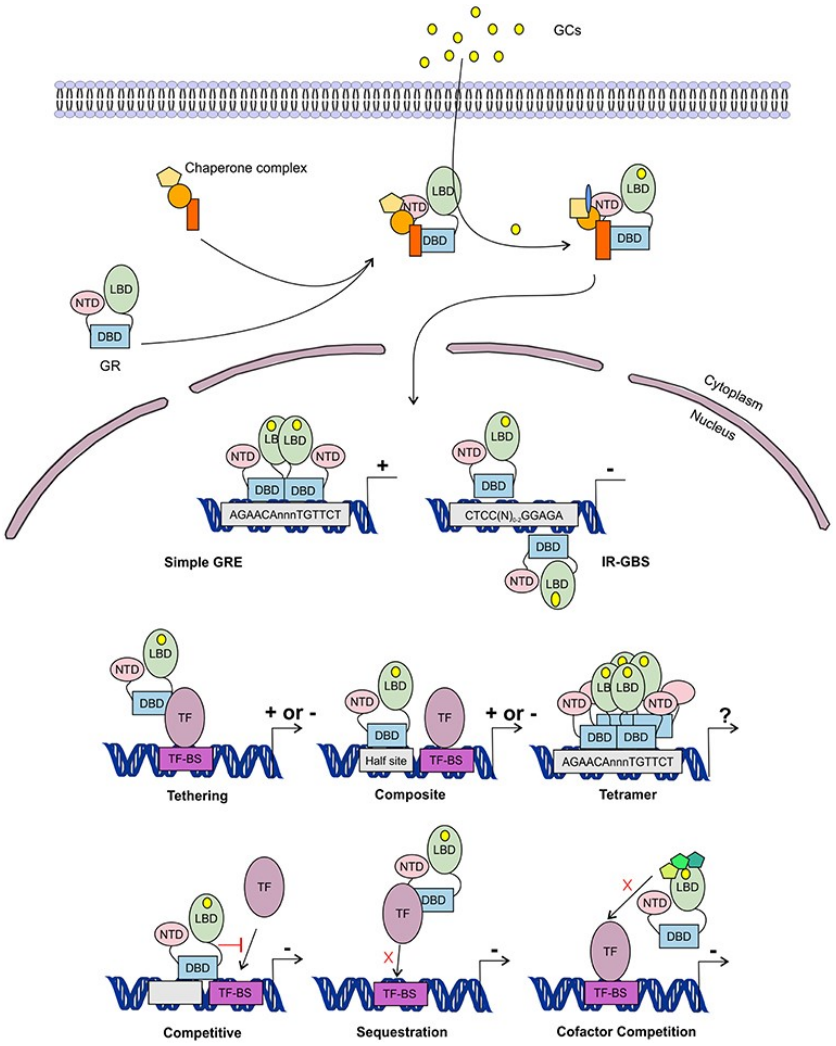

Figure 1.5: GR activation and function

Lipophilic glucocorticoids (GCs) diffuse through the cell membrane and bind the glucocorticoid receptor (GR) in the cytoplasm. This induces a change in the chaperone complex bound to GR, after which it translocates to the nucleus to transactivate (+) or transrepress (-) gene transcription. The GR can transactivate genes by binding to Glucocorticoid Responsive Elements (GREs) as a dimer, but also as a monomer by binding to other TFs through tethering or by binding to composite-elements. The GR can further transrepress gene-expression by binding to inverted repeat GR-binding sequences (IR-GBS), by tethering, by composite-elements, by competing for DNA binding-sites (BS), by sequestrating TFs and by competing for cofactors with other TFs. Figure adapted from Timmermans et al., 2019 with permission.

GR has also been demonstrated to interact with the SWI/SNF family of proteins that also enhance transcription by alleviating the repressive effects of histone-DNA contacts. BRG1 (*SMARCA4*), BRG1-associated factor 250 (BAF250), BAF60a, and BAF57 associate with GR and enable the receptor to remodel the chromatin and induce transcriptional enhancement (Cain and Cidlowski, 2017; Petta et al., 2016).

GR monomers, by contrast, can bind negative GREs (nGREs, also known as IR-GREs), and recruit the co-repressors NCOR (*NCOR1*) and SMRT (*NCOR2*) to inhibit gene transcription (Cain and Cidlowski, 2017). NCOR and SMRT function as macromolecular docking platforms for nuclear receptors and many TFs and repress the transcriptional activity by attracting HDAC/Sin3 complexes (Petta et al., 2016).

Molecular dissection of the mechanism of action of GR initially led to the postulation of the Transactivation-Transrepression (TA-TR) hypothesis for dissociated activity of GR. It posits that GCs exert immunosuppressive effects primarily through GR tethering of TFs such as NF-κB and AP-1, which reduces the expression of pro-inflammatory genes (transrepression, TR), whereas adverse side effects occur through gene activation via direct binding of the GR to GREs (transactivation, TA) (Cain and Cidlowski, 2017). However, compelling evidence has shown that this model is too simplistic. Some side effects are indeed predominantly mediated via transactivation (e.g. hyperglycemia and muscle wasting), yet other side effects arise from transrepression (e.g. hypothalamic-pituitary-adrenal axis suppression) or are mediated by both transactivation and transrepression (e.g. osteoporosis)(Sundahl et al., 2015).

1.4.6 Selective agonists or modulators of the GR

Compounds that can activate specific GR mechanisms and thus alter GR-mediated gene expression profiles are referred to as dissociated compounds. These compounds are classified as selective GR agonists (SEGRAs) or selective GR modulators (SEGRMs). SEGRMs are non-steroidal molecules able to modulate the activity of a GR agonist allosterically and may or may not bind to the GR ligand-binding pocket (Sundahl et al., 2015). SEGRAs and SEGRMs are collectively denominated SEGRAMs (selective GR agonists and modulators). It is believed that the development of SEGRAMs could give rise to safer drugs and/or provide drugs tailored to specific disease phenotypes (Louw, 2019; Sundahl et al., 2015).

Historically, the main focus of research has been on the development of SEGRAMs that have potent anti-inflammatory properties and decreased side effects. Since TA is the mechanism of action generally linked to unwanted side effects of GC-therapy, compounds were designed to favor TR by GR monomer over TA of GRE-regulated genes by GR dimer (Barnes, 2011). It has been theorized that, especially in chronic inflammatory diseases that require long-term GC therapy and where unwanted side effects are particularly threatening, the use of "Selective Monomer GR Agonists and Modulators" (SEMOGRAMs) would be beneficial (Timmermans et al., 2019). On the other hand, GR dimers also contribute to a full resolution of inflammation thus treatment with compounds that induce TA of anti-inflammatory genes is advantageous for acute inflammatory situations. Molecules that favor GR dimerization have been named "Selective Dimerizing GR Agonists and Modulators" (SEDIGRAM) (Souffriau et al., 2018). Other SEGRAMs may induce a ratio of both TA and TR phenotypes, with a bias in one or other direction (Bosscher et al., 2016).

More than two decades of research has shown that dissociating the side effects and immunomodulatory effects of GCs only on the basis of the TA-TR hypothesis is unrealistic (Vandewalle et al., 2018). Limitations to the development of dissociated compounds lie on our incomplete understanding of the GR dimerization process, the role of post-translational modifications on GR conformational change and the impact of DNA as an allosteric modulator of GR activity (Bosscher et al., 2016). Additionally, transcription-based screens for GR modulators usually measure GR activation at a single GRE-containing promoter, which does not allow efficient identification of molecules that produce promoter-specific responses. Despite initial enthusiasm in finding dissociated molecules, it remains virtually impossible to predict GR gene regulation based on ligand design and to produce therapeutically relevant transcriptional selectivity (Gerber and Diamond, 2009).

1.4.7 Glucocorticoid activity in immune cells

Glucocorticoids exert multiple functions in the immune system. Endogenous GCs link the endocrine and immune systems and ensure the correct function of inflammatory events during tissue repair, regeneration, and pathogen elimination (Strehl et al., 2019). The potent immunosuppressive and anti-inflammatory effects of GCs result primarily from the inhibition of

T-lymphocytes and antigen-presenting cells (APCs) and downregulation of proinflammatory cytokines (Diehl et al., 2016). GCs inhibit B and T lymphocytes by activation of apoptosis (Gruver-Yates et al., 2014). Among APCs, GCs can regulate the maturation, survival, and migration of dendritic cells (DCs), and reduce the ability of DCs to stimulate T cells (Liberman et al., 2018). GCs promote an anti-inflammatory state on both monocytes and macrophages by inhibiting the liberation of pro-inflammatory mediators by both types of cells (Liberman et al., 2018). GCs at low levels stimulate macrophage activity, whereas at high levels they inhibit. The exposure of peripheral blood monocytes to GCs has been shown to induce a highly phagocytic monocyte-derived macrophage (MDMφ) or alternatively activated M2c macrophage phenotype, re-programming monocyte differentiation towards an 'anti-inflammatory' phenotype (Giles et al., 2001; MANTOVANI et al., 2004; Zen et al., 2011). Moreover, GCs reduce the number of basophils and stimulate the apoptosis of neutrophils and eosinophils (Zen et al., 2011). GCs inhibit leukocyte extravasation, which is the movement of leukocytes out of the circulation and toward the site of tissue damage or infection during an inflammatory reaction. GCs can reduce rolling, adhesion, activation, and transmigration capabilities of leukocytes, therefore controlling the inflammatory reaction and contributing to the increase of circulating leukocytes (Liberman et al., 2018).

1.4.8 GC therapy in cancer

GCs are a primary therapeutic choice in cancer treatment for either their pro-apoptotic effects or their use as an adjuvant therapy, in combination with chemotherapeutic agents, to reduce symptoms such as inflammation, allergic reactions, pain and nausea (Wilkinson et al., 2018). Depending on the therapeutically affected cell type, GCs actions strongly vary (Strehl et al., 2019). GCs are among the first drug classes used in the treatment of patients with ALL and are essential components of treatment (Inaba and Pui, 2010). GCs such as dexamethasone and prednisone play crucial roles as part of the CHOP regimen (Cyclophosphamide-Hydroxyldaunorubicin-Oncovin(Vincristine)-Prednisone) to treat non-Hodgkin lymphoma as well as in multiple myeloma (MM) therapy (Strehl et al., 2019). The heterogeneous character of AML has limited the use of GCs as targeted therapy, as the treatment largely relies on the use of aggressive chemotherapy. Beneficial effects of GCs have been demonstrated in children with

AML, which was partially explained by the induction of differentiation and apoptosis of leukemic cells (Hiçsönmez, 2006). Furthermore, the addition of high-dose GC therapy to chemotherapy of adult AML patients led to increased remission rates and improved patient outcome (Hiçsönmez, 2006). More recently, a retrospective clinical study showed that adding dexamethasone to chemotherapy in a European cohort of AML patients with high WBC improved relapse incidence, disease-free survival, event-free survival, and overall survival (Bertoli et al., 2018). The beneficial effects of dexamethasone could be attributed to the modulation of inflammation in leukemic cells, and evidences showed that dexamethasone reduced the frequency of leukemic long-term culture initiating cells by 38% and enhanced the cytotoxicity of doxorubicin and cytarabine (Bertoli et al., 2018). It was also revealed that cytarabine-resistant AML cell lines displayed increased expression of the GR and increased *in vitro* sensitivity to GCs (Malani et al., 2017). Pre-clinical studies demonstrated that GCs can induce terminal differentiation of premature CD34+ AML cells *in vitro* towards monocytic/myeloid lineages (Laverdière et al., 2018) and induce apoptosis in t(8;21)-positive AML cell lines and primary AML specimens, potentially through proteasomal degradation of the RUNX1-RUNX1T1 fusion protein (Corsello et al., 2009). However, high rates of GC resistance in AML patients have been reported. Additionally, GC-induced proliferation of the leukemic cells was observed for a proportion of cases, with AML-M5 subtype and *FLT3*-mutated samples being especially prone to this phenomenon (Klein et al., 2016).
With the growing trend of combining therapeutics that target different pathways, it becomes imperative to identify which downstream targets of GR elicit the therapeutic properties of GCs in AML, which will provide the basis for the development of novel therapeutic approaches that induce cell death in the face of GC resistance (Thomas et al., 2015).

1.4.9 Glucocorticoid resistance

GCs are one of the most widely prescribed drugs in the world with estimated 1% of the population in developed countries using them (Overman et al., 2013). Although effective agents, it is believed that approximately 30% of all patients receiving treatment show a degree of GC insensitivity (Quax et al., 2013), and 10-30% of ALL patients are GC resistant (Haarman et al., 2003).

GC resistance is characterized by impaired sensitivity to GC treatment and may be divided into two major groups: generalized (systemic/primary) or acquired (localized/secondary) (Wilkinson et al., 2018). One of the main drivers of acquired glucocorticoid resistance is homologous down-regulation of the GR (Louw, 2019). Drug tolerance is primarily controlled by the cytosolic free receptor density, which is modulated by *de novo* receptor synthesis and receptor degradation via the ubiquitin-proteasome pathway. When in a dynamic state of equilibrium and unperturbed, the synthesis of GR is roughly equivalent to receptor turnover and the level of the GR pool remains constant (Wilkinson et al., 2018).

Several reports indicate that the GR gene (*NR3C1*) expression is repressed following exposure to its own ligand thus decreasing the GR pool. Elucidation of this mechanism revealed a regulatory element for ligand-induced downregulation of the GR gene (nGRE) at exon 6 of *NR3C1* (Ramamoorthy and Cidlowski, 2013a). While hormone-induced downregulation of GR represents a mechanism for maintaining GC homeostasis in normal cells, it also has the potential to limit therapeutic responses to GCs under inflammatory and malignant conditions (Ramamoorthy and Cidlowski, 2013b). In patients with MM, it was demonstrated that baseline GR expression level directly correlates with the clinical outcome in patients who received GC-containing regimens. *In vitro* analysis of GC-resistant and GC-sensitive MM cell lines revealed a novel mechanism of *NR3C1* downregulation that involves a block on the transcriptional elongation in the second intron of *NR3C1* in GC-resistant cell lines (Sánchez-Vega and Gandhi, 2009). Moreover, repressive epigenetic regulation of the *NR3C1* promoter, such as DNA methylation, decreases the GR pool and is a direct cause of GC resistance (McGowan et al., 2009).

Another possible mechanism of GC resistance arises from the altered expression of GR isoforms. It has been shown that the ability of GC to induce apoptosis in ALL cells is inversely correlated with GRβ levels (Koga et al., 2005). However, other groups have not seen a correlation between GRβ and GC resistance in ALL (Haarman et al., 2004; Tissing et al., 2005), and the functional significance of GRβ levels in hematological malignancies remains controversial. Even though mutations in *NR3C1* have been reported to positively or negatively impact GR transcriptional activity, they are largely absent in cancer patients that undergo GC therapy and therefore have not been linked to GC resistance (Smith and Cidlowski, 2010). In hematological malignancies, limitations to GC chemotherapy involve the emergence of GC-resistant clonal populations during

prolonged GC therapy, GC-resistant disease upon relapse or the existence of inherently resistant leukemic cells. Leukemias of the myelogenous lineage are often innately resistant to GC therapy, which can not be explained by GR levels or mutations (Smith and Cidlowski, 2010). Resistance to GC may also be determined by sequestration of transcriptional cofactors by other TFs thus precluding accessibility to the GR (Dendoncker et al., 2019). Downstream of GR, the epigenetic landscape has been proposed to play a determinant role in GR-mediated gene regulation by controlling DNA accessibility and potentiating GR chromatin binding in a cell type-specific fashion (Wang et al., 2019). In ALL, dysregulation of expression of several chromatin modifiers have been shown to influence GC response and patient prognosis (Gruhn et al., 2013; Jones et al., 2014; Moreno et al., 2010). Furthermore, crosstalk between GR signaling and various kinase pathways play important roles in the GC response in hematological malignancies and modulation of the kinome represents an attractive avenue in the development of alternatives to ameliorate GC resistance (Smith and Cidlowski, 2010).

1.5 Dissecting chemogenomic interactions for targeted therapy

The promise of precision medicine relies on the concept that causative mutations in a patient's cancer drive its biology and therefore informs on therapeutic responses (Padma, 2015). For targeted therapy to result in significant clinical improvement the target must be both rate-limiting in terms of tumour growth and be present in most or all of the tumour cells (Schmitt et al., 2015). The development of ultra high-throughput sequencing technologies known as 'next-generation' or 'massively parallel' DNA sequencing have achieved remarkable advances in capacity, read length and accuracy since their initial introduction in the mid-2000s (Mardis, 2012), and their application for molecular characterization in AML can enhance diagnostic and prognostic accuracy. The biological heterogeneity of AML became apparent over the last 15 years, but translation of this knowledge into more efficient therapies has just recently begun with approval by the FDA of Midostaurin, an inhibitor of FLT3 tyrosine kinase activity for treatment of *FLT3*-mutated AML (Stone et al., 2017), as well as Enasidenib for relapsed/refractory AML with *IDH2* mutations (Stein et al., 2017). However, the ever-growing genomic information collected from AML patients across the world has shown that several aspects of the disease pose challenges to the development of targeted therapy: only a few cancer genes are straightforward therapeutic

targets; many cancer genes are only rarely mutated in a given tumor type; each patient's tumor typically has several driver mutations; multiple combinations of different driver mutations are observed across patients; AML is characterized by high clonal diversity, which is believed to contribute to treatment resistance (Gerstung et al., 2017). Nonetheless, large knowledge banks of clinical-genomic data have been used to generate a model to improve patient prognostic stratification and predict the best therapy regimen for each patient based on the tumor's mutational landscape, which has been proven successful in identifying patients that are resistant to conventional chemotherapy and/or should receive HSCT (Gerstung et al., 2017; Huet et al., 2018). Integration of clinical-genomic information with *ex vivo* chemical screening of primary patient samples has been successful in identifying tumor vulnerabilities in AML (Baccelli et al., 2017, 2019; Tyner et al., 2018). It is expected that long-term treatment for AML would require combinatorial targeted therapies; therefore, use of chemogenomic studies is crucial for unrevealing novel therapeutic targets that will efficiently kill founder AML LSC clones (Baccelli et al., 2017).

1.5.1 Cell line as a model

The establishment of continuous hematopoietic cell lines started in the early 1960s with the development of several lines derived from Burkitt's lymphoma patients (Pulvertaft, 1964). The advent of cell culture technology and the use of continuous cell lines have opened new possibilities to examine hematopoietic cell biology. Major advantages are the unlimited supply of cellular material, easy storage in liquid nitrogen and recovery without any detrimental loss of cellular features or cell viability (Drexler et al., 2000).

Cancer cell lines are valuable *in vitro* systems that are widely used in cancer research and drug development. Importantly, genomic, transcriptomic and proteomic characterization of most available cancer cell lines have been published and made available through online datasets, which facilitates the exploration of detailed molecular and cellular alterations, such as mutations, copy number variations, and gene and protein expression profiles (Mirabelli et al., 2019). Among historically important models for drug discovery, K562 cell line carrying the BCR-ABL fusion protein has been critical in the development of STI-751 (Imatinib), the first tyrosine kinase inhibitor that is able to specifically block the catalytic site of the BCR-ABL fusion protein, which

rapidly led to the development of an oral Imatinib formulation for the treatment of CML patients carrying BCR-ABL fusion protein (Druker et al., 1996; Wood et al., 2002). Large-scale genetic and pharmacological characterization of human cancer cell lines have been published in the past decade and confirmed that many human cell lines capture the genomic diversity of their respective cancers and, consequently, can be used as *in vitro* model systems of the diseases from which they were derived ((Barretina et al., 2012; Garnett et al., 2012; Mirabelli et al., 2019). Under optimal culture conditions, the genetic features of a cell line will remain stable in long-term culture. However, *in vitro* artifacts may arise from deliberate experimental manipulations and intentional or accidental suboptimal culture conditions. For example, contamination with mycoplasma, cell line cross-contamination, use of inappropriate culture media or supplements and over-dilution leading to 'bottle-necking' may exert selection pressures that, in turn, result in phenotypic and genotypic shifts (Drexler et al., 2000). Additionally, gene expression profiles of tumor cells change dramatically when cells are grown *in vitro*, specially because cell lines grown in culture do not have interactions with other cell types, their growth is not under the influence of cytokines and other cell signaling molecules, and the native tissue architecture is lost. Moreover, the effects of *in vivo* drug distribution and metabolism are not easily matched *in vitro* (Mirabelli et al., 2019; Uhlen et al., 2019). It is important to notice that even though patient-derived leukemic cell lines are largely used in cell-based assays for identification of novel therapeutic approaches, these cells do not reflect the hierarchical organization of the ancestral primary disease and do not represent a functionally relevant LSC population (Pabst et al., 2014).

1.5.2 Primary cells as a model

AML is initiated and sustained by a small, self-renewing population of LSC, which are predominantly in a quiescent state and, thus, are insensitive to the effects of most chemotherapeutic agents (Mayani et al., 2009; Burnett et al., 2011; Hope et al., 2004). Many strategies to study the biology of leukemia cells have been developed, which include semisolid colony assays, Dexter-type long-term bone marrow cultures and liquid suspension cultures (Mayani et al., 2009).

Semisolid colony assays constitute the first system for study of hematopoietic progenitors, in which cells are grown in a matrix of agar or methylcellulose in the presence of hematopoietic

stimulators, which can be added as soluble recombinant factors or as part of conditioned media (Metcalf, 2008). It has been used as an *in vitro* system to test the effects of chemotherapeutic agents on leukemic cells (Récher et al., 2005), however, colony-forming assays do not support the growth of early progenitor cells with self-renewal capabilities, which is an important characteristic of chemoresistant LSC (Mayani et al., 2009). Long-term bone marrow culture (LTMC), also known as Dexter-type LTMC, is more appropriate for *in vitro* analysis of primitive hematopoietic progenitors for reproducing many aspects of the marrow microenvironment (Dexter et al., 1977; Klug et al., 2001). This is due to the development of an adherent cell layer, consisting of marrow stromal cells (mainly fibroblasts, macrophages and adipocytes), which provide the microenvironment that stem/progenitor cells need in order to proliferate and differentiate (Greenberger, 1991; Mayani et al., 2009). In recent years, it has become clear that the bone marrow microenvironment influences leukemic cells' morphology and proliferation rate and promotes the evasion of leukemic cells from treatment (Wolf and Langhans, 2019). That is achieved by secretion of soluble factors and/or cell adhesion-mediated mechanisms through which stromal cells activate several pathways that protect AML cells (Hazlehurst et al., 2007; Kojima et al., 2011; Matsunaga et al., 2003). In order to better mimic the role of the niche in leukemia cell survival, stromal cell lines have been routinely used for long-term support of primary hematopoietic cells and are a suitable model for high-throughput drug screening to identify effective strategies targeting stroma-regulated AML (Zeng et al., 2017). Growing cells in 3-dimensional (3D) format is considered to more closely resemble phenotypic characteristics of the originating tumor, as the bone marrow niche is itself a 3D structure, therefore constituting an ideal model for identifying potential therapeutics (Wolf and Langhans, 2019). Generation of patient-specific 3D spheroid co-cultures using both primary mesenchymal stromal cells and primary AML cells from the same patient might represent the best option for the development of targeted therapy, given that stromal cells may also undergo genomic alterations in AML patients and contribute to the disease phenotype (Salman et al., 2015).

While expansion and differentiation of normal HSPC can be achieved in liquid cultures in serum- and stroma-free conditions in the presence of a cytokine cocktail of hematopoietic stimulators, the long-term growth of AML progenitors in suspension cultures is extremely defective (Dorantes-Acosta et al., 2008; Mayani et al., 2009). That is because optimized systems to grow normal HSPC do not promote self-renewal of LSC in the majority of primary AML specimens,

and long-term AML cultures show selective generation of myeloid cells, predominantly macrophages (Mayani et al., 2009). Nonetheless, liquid suspension cultures of primary AML cells have been widely used to test the *in vitro* effect of therapeutic drugs on leukemic cells. Studies that explored the relationship between stroma and AML cells led to the discovery of important pathways that are activated in LSC to maintain self-renewal and therefore can be targeted with small molecules to control cell fate. Similarly to what was shown for normal HSPC (Boitano et al., 2010), our group has demonstrated that suppressors of the aryl hydrocarbon receptor (AhR) signaling pathway, such as SR1, promote the *ex vivo* expansion of undifferentiated AML cells and partially rescue their capacity to engraft immunocompromised mice (Pabst et al., 2014). Moreover, chemical screening of AML specimens identified a new pyrimido-indole, UM729, which lacks AhR suppressor activity, and has an additive effect with AhR antagonists in preventing differentiation in most AML specimens, indicating that at least two different pathways contribute to the maintenance of LSC activity *ex vivo*. Use of optimized conditions on serum-free medium supplemented with the small molecules SR1 and UM729 yields improved relative and absolute numbers of phenotypically undifferentiated CD34+ AML cells that are otherwise rapidly lost in culture, which enables cell-based assays for primary human AML cells for the identification of new antileukemic drugs that target LSC (Pabst et al., 2014).

1.5.3 Xenograft models

Although today there are some *ex vivo* alternatives, the xenograft model remains the gold standard technique to study cancer stem cells (Griessinger and Andreeff, 2018; Bonnet and Dick, 1997). Up to date, several mice models have been developed from the immunodeficient NOD/SCID mice (non-obese diabetic/severe combined immunodeficiency mice), which are suitable models of leukemia. The NSG (NOD-SCID-IL-2Rγcnull) mouse, for example, is a robust recipient for human AML xenotransplantation samples, allowing a better understanding and characterization of AML biology, especially in the context of drug therapy studies (Sanchez et al., 2009). Despite major advances in human to mouse xenografts, a good proportion of the human AML samples fail to adequately engraft available strains of mice, which has been linked to intrinsic properties of the AML cells injected. There is also evidence for strong clonal selection of the primary AML specimens in these models. Engraftment failure is common for good

prognosis AML and, inversely, xenograft potential is high for more aggressive poor prognosis AML (Pearce et al., 2006; Monaco et al., 2004). Apart from AML intrinsic characteristics, engraftment is affected by elements of homing, survival in a foreign niche, expansion in the absence of specific human growth factors and supporting stromal cells, escape from immune surveillance and residual innate immunity in the mice (Wunderlich et al., 2010). Mouse strains expressing various human cytokines have been generated in the past two decades. Knock-in for human stem cell factor (SCF), granulocyte-macrophage colony-stimulating factor (GM-CSF), and interleukin 3 (IL-3) in the background of the NSG recipient presented significant improvement in human AML engraftment compared to the parental strain (Krevvata et al., 2018; Wunderlich et al., 2010; Feuring-Buske et al., 2003). Nonetheless, development of xenograft models is a long and costly process, which usually requires a 10 to 12 weeks period after injection to demonstrate signs of human engraftment. Conditional knock-in mice models that express potent oncogenic proteins or transplantation of normal human HSPC transduced with oncogenic proteins can be generated to model leukemias. In contrast with models of solid tumors that typically require several different oncogenes to transform primary human cells, high penetrance leukemia is achieved by introduction of a single fusion protein such as *MLL-AF9* and *MLL-AF4*, which is compatible with the aggressive disease seen in patients with such abnormalities (Barabe et al., 2007; Krivtsov et al., 2006).

1.5.4 Chemogenomic studies

1.5.4.1 Chemical screening

The term 'chemogenomics' emerged in the early 2000s to describe the use of chemical libraries directed to a specific target (gene) or target-families (gene family or pathway) as a means to accelerate drug discovery research. Over time, the area of chemogenomics came to represent the study of all gene products using pharmacological modulation (Jones and Bunnage, 2017). Chemogenomic screening libraries contain small molecules that have well-annotated pharmacology and are suitable for phenotypic screens. Our ability to maintain patient-derived cell lines and primary cells *ex vivo* has enabled disease-relevant phenotypic screening in AML using chemogenomic libraries that contain hundreds to thousands of compounds (Fares et al., 2014; Pabst et al., 2014; Baccelli et al., 2017; Tyner et al., 2018). Identifying a hit in a screen using

primary patient cells is extremely valuable because it suggests that the target is amenable to functional pharmacological modulation inside the patient's cells and thus provides opportunities to accelerate small-molecule drug discovery. Small-molecule pharmacological agents also enable the interrogation of modalities that cannot be investigated using genetic perturbation, such as the modulation of specific protein–protein interactions and allosterism (Jones and Bunnage, 2017). Screening of existing drugs in primary patient cells may also reveal hits that represent direct repurposing opportunities for the relevant patient population and can be readily tested in clinical trials. Application of chemogenomic screens have enabled biological targets and molecular mechanisms to be linked to certain phenotypes in a variety of cell types (Eriksson et al., 2015). Parallel screening of normal and cancerous primary cells has helped uncover tumor vulnerabilities and deconvolute targets that are particularly relevant in cancers but are inactive in normal cells (Eriksson et al., 2015; Tyner et al., 2018; Baccelli et al., 2019).

1.5.4.2 Functional genomic screening

Understanding how drugs act is particularly important for precision medicine efforts, in which therapies are precisely targeted at the genetic and environmental background of a patient and which therefore require drugs with high specificity for well-defined targets (Jost and Weissman, 2018). Recent advances in functional genetics and genome-scale screening provide powerful new technologies for identifying drug targets and understanding drug mechanism of action and resistance, such as RNA interference (RNAi) and CRISPR-based methods (Cheung-Ong et al., 2013). Briefly, RNAi relies on short RNAs (shRNA) complementary to target mRNAs that are introduced into cells to mediate degradation or interfere with translation of these mRNAs and thereby reduce target expression (Hannon, 2002; Jost and Weissman, 2018). The primary advantages to using RNAi for functional genomics are that shRNA molecules can be easily introduced, either transiently or stably, into cells and screens can be done in arrayed (well-by-well) or pooled formats (Cheung-Ong et al., 2013). Major technical limitations of shRNA include off-target effects and limited knockdown efficiency (Kaelin, 2012), which limits sensitivity and increases background noise, thus hampering their widespread application in large scale screens (Jost and Weissman, 2018). Another off-target activity of RNAi is elicited by the introduction of RNA molecules thus causing upregulation of interferon-regulated genes and alteration in protein

expression (Bridge et al., 2003). Nevertheless, knockdown with RNAi produces a hypomorphic phenotype in contrast to the true null knockout possible with CRISPR-Cas9, which in some cases could be advantageous. For example, knockout of essential genes is cell lethal, making effects on these difficult to study. Knockdown rather than knockout can also better mimic the inhibition of a target by a drug or a hypomorphic allele introduced by mutation.

In CRISPR-based approaches, an effector protein such as Cas9 is programmed with a short-guide RNA (sgRNA) that directs the effector to a DNA locus of interest via sequence complementarity (Haurwitz et al., 2010; Jinek et al., 2012). Cas9 then introduces a double-strand break, which triggers DNA repair mechanisms that in protein coding regions frequently result in frameshift mutations and consequently inactivate that gene product (Wright et al., 2016; Jost and Weissman, 2018). CRISPR-Cas9-based genome editing provides high specificity and produces penetrant phenotypes as null alleles can be generated (Behan et al., 2019). Other CRISPR-based approaches rely on a catalytically inactivated mutant of Cas9 (dCas9) that is essentially a highly programmable DNA-binding protein and can be used to deliver TFs to target loci to mediate knockdown (CRISPRi) or overexpression (CRISPRa) without DNA cutting (Konermann et al., 2014; Joung et al., 2017; Jost and Weissman, 2018). Loss-of-function approaches, for example, may fail in cases of redundancy or pleiotropy, whereas overexpression of a drug target may not provide resistance if the target functions as part of a multiprotein complex. Combining knockdown and overexpression profiling has provided particular utility, as both the direct target and modifiers of sensitivity can be identified with high precision (Gilbert et al., 2014; Jost et al., 2017).

For the application of genome-wide CRISPR screening approaches, a model system amenable to genetic manipulation is required to implement the CRISPR effectors, and the compound of interest must generate a selectable phenotype, such as impact on cell proliferation (Jost and Weissman, 2018). Several groups have focused on improving the accuracy and scalability of CRISPR screens, which led to the development of multiple CRISPR libraries used in large-scale genetic analysis of lethal phenotypes (Hart et al., 2015; Wang et al., 2015; Tzelepis et al., 2016; Bertomeu et al., 2017). Even though most early pooled-library approaches needed large numbers of sgRNAs per gene (>10 sgRNAs/gene) to overcome the unknown sources of variation in sgRNA targeting efficiency, smaller libraries using sequence-optimized sgRNAs with 4 shRNAs/gene have been shown to perform with similar sensitivity, and are expected to reduce

the scale of such experiments and facilitate its applications (Hart et al., 2017). Altogether, the aforementioned functional genomics tools have revolutionized our ability to interfere in all human genes, thus allowing the analysis of how drug-gene interactions vary across different tissue types, genetic backgrounds, and epigenetic states, and identify pre-emptively possible mechanisms of acquired resistance or pre-existent sources of resistance within a tumor population or a disease phenotype (Colic et al., 2019).

1.6 References

Aikawa, Y., Nguyen, L., Isono, K., Takakura, N., Tagata, Y., Schmitz, M., … Kitabayashi, I. (2006). Roles of HIPK1 and HIPK2 in AML1- and p300-dependent transcription, hematopoiesis and blood vessel formation. *The EMBO Journal*, *25*(17), 3955-3965. doi:10.1038/sj.emboj.7601273

Alibhai, S. M. H., Leach, M., Minden, M. D. and Brandwein, J. (2009). Outcomes and quality of care in acute myeloid leukemia over 40 years. *Cancer*, *115*(13), 2903-2911. doi:10.1002/cncr.24373

Angelos, M., Abrahante, J., Blum, R. and Kaufman, D. (2018). Single Cell Resolution of Human Hematoendothelial Cells Defines Transcriptional Signatures of Hemogenic Endothelium. *STEM CELLS*, *36*(2), 206-217. doi:10.1002/stem.2739

Arber, D., Orazi, A., Hasserjian, R., Thiele, J., Borowitz, M., Beau, M., … Vardiman, J. (2016). The 2016 revision to the World Health Organization classification of myeloid neoplasms and acute leukemia. *Blood*, *127*(20), 2391-2405. doi:10.1182/blood-2016-03-643544

Baccelli, I., Gareau, Y., Lehnertz, B., Gingras, S., Spinella, J., Corneau, S., … Sauvageau, G. (2019). Mubritinib Targets the Electron Transport Chain Complex I and Reveals the Landscape of OXPHOS Dependency in Acute Myeloid Leukemia. *Cancer Cell*, *36*(1), 84-99.e8. doi:10.1016/j.ccell.2019.06.003

Baccelli, I., Krosl, J., Boucher, G., Boivin, I., Lavallée, V.-P., Hébert, J., … Sauvageau, G. (2017). A novel approach for the identification of efficient combination therapies in primary human acute myeloid leukemia specimens. *Blood cancer journal*, *7*(2), e529. doi:10.1038/bcj.2017.10

Bakshi, R., Hassan, M. Q., Pratap, J., Lian, J. B., Montecino, M. A., Wijnen, A. J. van, … Stein, G. S. (2010). The human SWI/SNF complex associates with RUNX1 to control transcription of hematopoietic target genes. *Journal of Cellular Physiology*, *225*(2), 569-576. doi:10.1002/jcp.22240

Barabe, F., Kennedy, J. A., Hope, K. J. and Dick, J. E. (2007). Modeling the Initiation and Progression of Human Acute Leukemia in Mice. *Science*, *316*(5824), 600-604. doi:10.1126/science.1139851

Barnes, P. (2011). Glucocorticosteroids: current and future directions. *British Journal of Pharmacology*, *163*(1), 29-43. doi:10.1111/j.1476-5381.2010.01199.x

Barretina, J., Caponigro, G., Stransky, N., Venkatesan, K., Margolin, A. A., Kim, S., … Garraway, L. A. (2012). The Cancer Cell Line Encyclopedia enables predictive modelling of anticancer drug sensitivity. *Nature*, *483*(7391), 603-607. doi:10.1038/nature11003

Barthe, C., Cony-Makhoul, P., Melo, J. and Mahon, J. (2001). Roots of Clinical Resistance to STI-571 Cancer Therapy. *Science*, *293*(5538), 2163-2163. doi:10.1126/science.293.5538.2163a

Bartholome, B., Spies, C., Gaber, T., Schuchmann, S., Berki, T., Kunkel, D., … Buttgereit, F. (2004). Membrane glucocorticoid receptors (mGCR) are expressed in normal human peripheral blood mononuclear cells and up-regulated after in vitro stimulation and in patients with rheumatoid arthritis. *The FASEB Journal*, *18*(1), 70-80. doi:10.1096/fj.03-0328com

BECKER, A., McCULLOCH, E. and TILL, J. (1963). Cytological Demonstration of the Clonal Nature of Spleen Colonies Derived from Transplanted Mouse Marrow Cells. *Nature*, *197*(4866), 452-454. doi:10.1038/197452a0

Behan, F., Iorio, F., Picco, G., Gonçalves, E., Beaver, C., Migliardi, G., … Garnett, M. (2019). Prioritization of cancer therapeutic targets using CRISPR–Cas9 screens. *Nature*, *568*(7753), 511-516. doi:10.1038/s41586-019-1103-9

Behrens, K., Triviai, I., Schwieger, M., Tekin, N., Alawi, M., Spohn, M., … Stocking, C. (2016). Runx1 downregulates stem cell and megakaryocytic transcription programs that support niche interactions. *Blood*, *127*(26), 3369-3381. doi:10.1182/blood-2015-09-668129

Bellissimo, D. and Speck, N. (2017). RUNX1 Mutations in Inherited and Sporadic Leukemia. *Frontiers in Cell and Developmental Biology*, *5*, 111. doi:10.3389/fcell.2017.00111

Bertoli, S., Picard, M., Bérard, E., Griessinger, E., Larrue, C., Mouchel, P., … Récher, C. (2018). Dexamethasone in hyperleukocytic acute myeloid leukemia. *Haematologica*, *103*(6), haematol.2017.184267. doi:10.3324/haematol.2017.184267

Bertomeu, T., Coulombe-Huntington, J., Chatr-aryamontri, A., Bourdages, K., Coyaud, E., Raught, B., … Tyers, M. (2017). A High-Resolution Genome-Wide CRISPR/Cas9 Viability Screen Reveals Structural Features and Contextual Diversity of the Human Cell-Essential Proteome. *Molecular and Cellular Biology*, *38*(1), e00302-17. doi:10.1128/mcb.00302-17

Biddie, S. C., John, S. and Hager, G. L. (2010). Genome-wide mechanisms of nuclear receptor action. *Trends in Endocrinology & Metabolism*, *21*(1), 3-9. doi:10.1016/j.tem.2009.08.006

Biggs, J., Peterson, L., Zhang, Y., Kraft, A. and Zhang, D. (2006). AML1/RUNX1 Phosphorylation by Cyclin-Dependent Kinases Regulates the Degradation of AML1/RUNX1 by the Anaphase-Promoting Complex‡. *Molecular and Cellular Biology*, *26*(20), 7420-7429. doi:10.1128/mcb.00597-06

Bluteau, D., Glembotsky, A. C., Raimbault, A., Balayn, N., Gilles, L., Rameau, P., … Raslova, H. (2012). Dysmegakaryopoiesis of FPD/AML pedigrees with constitutional RUNX1 mutations is linked to myosin II deregulated expression. *Blood*, *120*(13), 2708-2718. doi:10.1182/blood-2012-04-422337

Boitano, A., Wang, J., Romeo, R., Bouchez, L., Parker, A., Sutton, S., … Cooke, M. (2010). Aryl Hydrocarbon Receptor Antagonists Promote the Expansion of Human Hematopoietic Stem Cells. *Science*, *329*(5997), 1345-1348. doi:10.1126/science.1191536

Bonnet, D. and Dick, J. (1997). Human acute myeloid leukemia is organized as a hierarchy that originates from a primitive hematopoietic cell. *Nature Medicine*, *3*(7), 730-737. doi:10.1038/nm0797-730

Bosscher, K., Beck, I., Ratman, D., Berghe, W. and Libert, C. (2016). Activation of the Glucocorticoid Receptor in Acute Inflammation: the SEDIGRAM Concept. *Trends in Pharmacological Sciences*, *37*(1), 4-16. doi:10.1016/j.tips.2015.09.002

Bridge, A., Pebernard, S., Ducraux, A., Nicoulaz, A. and Iggo, R. (2003). Induction of an interferon response by RNAi vectors in mammalian cells. *Nature Genetics*, *34*(3), 263-264. doi:10.1038/ng1173

Bruijn, M. and Dzierzak, E. (2017). Runx transcription factors in the development and function of the definitive hematopoietic system. *Blood*, *129*(15), 2061-2069. doi:10.1182/blood-2016-12-689109

Bruijn, Mf. and Speck, N. (2004). Core-binding factors in hematopoiesis and immune function. *Oncogene*, *23*(24), 4238-4248. doi:10.1038/sj.onc.1207763

Buckley, S., Estey, E. and Walter, R. (2015). The treatment-related mortality score is associated with non-fatal adverse events following intensive AML induction chemotherapy. *Blood Cancer Journal*, *5*(1), e276-e276. doi:10.1038/bcj.2014.97

Burnett, A., Wetzler, M. and Löwenberg, B. (2011). Therapeutic Advances in Acute Myeloid Leukemia. *Journal of Clinical Oncology*, *29*(5), 487-494. doi:10.1200/jco.2010.30.1820

Busque, L, Patel, J., Figueroa, M., Vasanthakumar, A., Provost, S., Hamilou, Z., … Levine, R. (2012). Recurrent somatic TET2 mutations in normal elderly individuals with clonal hematopoiesis. *Nature Genetics*, *44*(11), 1179-1181. doi:10.1038/ng.2413

Busque, Lambert, Buscarlet, M., Mollica, L. and Levine, R. L. (2018). Concise Review: Age-Related Clonal Hematopoiesis: Stem Cells Tempting the Devil: Age-Related Clonal Hematopoiesis. *STEM CELLS*, *36*(9), 1287-1294. doi:10.1002/stem.2845

Buttgereit, F. and Scheffold, A. (2002). Rapid glucocorticoid effects on immune cells. *Steroids*, *67*(6), 529-534. doi:10.1016/s0039-128x(01)00171-4

Cai, Z., Bruijn, M. de, Ma, X., Dortland, B., Luteijn, T., Downing, J. R. and Dzierzak, E. (2000). Haploinsufficiency of AML1 Affects the Temporal and Spatial Generation of Hematopoietic Stem Cells in the Mouse Embryo. *Immunity*, *13*(4), 423-431. doi:10.1016/s1074-7613(00)00042-x

Cain, D. and Cidlowski, J. (2017). Immune regulation by glucocorticoids. *Nature Reviews Immunology*, *17*(4), 233-247. doi:10.1038/nri.2017.1

Cameron, S., Taylor, D., TePas, E., Speck, N. and Mathey-Prevot, B. (1994). Identification of a critical regulatory site in the human interleukin-3 promoter by in vivo footprinting. *Blood*, *83*(10), 2851-2859. doi:10.1182/blood.v83.10.2851.2851

Carrigan, A., Walther, R., Salem, H., Wu, D., Atlas, E., Lefebvre, Y. and Haché, R. (2007). An Active Nuclear Retention Signal in the Glucocorticoid Receptor Functions as a Strong Inducer of Transcriptional Activation. *Journal of Biological Chemistry*, *282*(15), 10963-10971. doi:10.1074/jbc.m602931200

Challen, G. A. and Goodell, M. A. (2010). Runx1 isoforms show differential expression patterns during hematopoietic development but have similar functional effects in adult hematopoietic stem cells. *Experimental hematology*, *38*(5), 403-16. doi:10.1016/j.exphem.2010.02.011

Chen, F., Watson, C. and Gametchu, B. (1999). Multiple glucocorticoid receptor transcripts in membrane glucocorticoid receptor-enriched S-49 mouse lymphoma cells. *Journal of Cellular Biochemistry*, *74*(3), 418-429. doi:10.1002/(sici)1097-4644(19990901)74:3<418::aid-jcb10>3.0.co;2-6

Chen, B., Teng, J., Liu, H., Pan, X., Zhou, Y., Huang, S., … Ma, F. (2017). Inducible overexpression of RUNX1b/c in human embryonic stem cells blocks early hematopoiesis from mesoderm. *Journal of Molecular Cell Biology*, *9*(4), 262-273. doi:10.1093/jmcb/mjx032

Cheung-Ong, K., Giaever, G. and Nislow, C. (2013). DNA-Damaging Agents in Cancer Chemotherapy: Serendipity and Chemical Biology. *Chemistry & Biology*, *20*(5), 648-659. doi:10.1016/j.chembiol.2013.04.007

Chisholm, K. M., Denton, C., Keel, S., Geddis, A. E., Xu, M., Appel, B. E., … Shimamura, A. (2019). Bone Marrow Morphology Associated With Germline RUNX1 Mutations in Patients With Familial Platelet Disorder With Associated Myeloid Malignancy. *Pediatric and Developmental Pathology*, *22*(4), 315-328. doi:10.1177/1093526618822108

Colic, M., Wang, G., Zimmermann, M., Mascall, K., McLaughlin, M., Bertolet, L., … Hart, T. (2019). Identifying chemogenetic interactions from CRISPR screens with drugZ. *Genome Medicine*, *11*(1), 52. doi:10.1186/s13073-019-0665-3

Corsello, S. M., Roti, G., Ross, K. N., Chow, K. T., Galinsky, I., DeAngelo, D. J., … Stegmaier, K. (2009). Identification of AML1-ETO modulators by chemical genomics. *Blood*, *113*(24), 6193-205. doi:10.1182/blood-2008-07-166090

Croxtall, J., Choudhury, Q. and Flower, R. (2000). Glucocorticoids act within minutes to inhibit recruitment of signalling factors to activated EGF receptors through a receptor-dependent, transcription-independent mechanism. *British Journal of Pharmacology*, *130*(2), 289-298. doi:10.1038/sj.bjp.0703272

Cunningham, L., Finckbeiner, S., Hyde, R., Southall, N., Marugan, J., Yedavalli, V., … Liu, P. (2012). Identification of benzodiazepine Ro5-3335 as an inhibitor of CBF leukemia through quantitative high throughput screen against RUNX1–CBFβ interaction. *Proceedings of the National Academy of Sciences*, *109*(36), 14592-14597. doi:10.1073/pnas.1200037109

Dallman, M., Akana, S., Walker, C., Bradbury, M. and Scribner, K. (1994). Corticosteroids and the control of function in the hypothalamo-pituitary-adrenal (HPA) axis. *Annals of the New York Academy of Sciences*, *746*, 22-31; discussion 31-2, 64-7. doi:10.1111/j.1749-6632.1994.tb39206.x

Dendoncker, K., Timmermans, S., Vandewalle, J., Eggermont, M., Lempiäinen, J., Paakinaho, V., … Libert, C. (2019). TNF-α inhibits glucocorticoid receptor-induced gene expression by reshaping the GR nuclear cofactor profile. *Proceedings of the National Academy of Sciences*, *116*(26), 12942-12951. doi:10.1073/pnas.1821565116

Dexter, T., Allen, T. and Lajtha, L. (1977). Conditions controlling the proliferation of haemopoietic stem cells in vitro. *Journal of Cellular Physiology*, *91*(3), 335-344. doi:10.1002/jcp.1040910303

Diehl, R., Ferrara, F., Müller, C., Dreyer, A., McLeod, D., Fricke, S. and Boltze, J. (2016). Immunosuppression for in vivo research: state-of-the-art protocols and experimental approaches. *Cellular & Molecular Immunology*, *14*(2), 146-179. doi:10.1038/cmi.2016.39

DiNardo, C. D. and Cortes, J. E. (2016). Mutations in AML: prognostic and therapeutic implications. *Hematology*, *2016*(1), 348-355. doi:10.1182/asheducation-2016.1.348

Ding, L., Ley, T., Larson, D., Miller, C., Koboldt, D., Welch, J., … DiPersio, J. (2012). Clonal evolution in relapsed acute myeloid leukaemia revealed by whole-genome sequencing. *Nature*, *481*(7382), 506-510. doi:10.1038/nature10738

Ditadi, A., Sturgeon, C. M., Tober, J., Awong, G., Kennedy, M., Yzaguirre, A. D., … Keller, G. (2015). Human definitive haemogenic endothelium and arterial vascular endothelium represent distinct lineages. *Nature Cell Biology*, *17*(5), 580-591. doi:10.1038/ncb3161

Döhner, H., Estey, E., Grimwade, D., Amadori, S., Appelbaum, F. R., Büchner, T., … Bloomfield, C. D. (2017). Diagnosis and management of AML in adults: 2017 ELN recommendations from an international expert panel. *Blood*, *129*(4), 424-447. doi:10.1182/blood-2016-08-733196

Döhner, H., Estey, E. H., Amadori, S., Appelbaum, F. R., Büchner, T., Burnett, A. K., … LeukemiaNet, E. (2009). Diagnosis and management of acute myeloid leukemia in adults: recommendations from an international expert panel, on behalf of the European LeukemiaNet. *Blood*, *115*(3), 453-74. doi:10.1182/blood-2009-07-235358

Dorantes-Acosta, E., Chávez-González, A., Santos, J., Medina-Sanson, A. and Mayani, H. (2008). Defective in vitro growth of primitive hematopoietic cells from pediatric patients with acute myeloid leukemia. *Pediatric Blood & Cancer*, *51*(6), 741-746. doi:10.1002/pbc.21706

Drexler, H., Matsuo, Y. and MacLeod, R. (2000). Continuous hematopoietic cell lines as model systems for leukemia–lymphoma research. *Leukemia Research*, *24*(11), 881-911. doi:10.1016/s0145-2126(00)00070-9

Druker, B., Tamura, S., Buchdunger, E., Ohno, S., Segal, G., Fanning, S., … Lydon, N. (1996). Effects of a selective inhibitor of the Abl tyrosine kinase on the growth of Bcr–Abl positive cells. *Nature Medicine*, *2*(5), 561-566. doi:10.1038/nm0596-561

Duployez, N., Martin, J.-E., Khalife-Hachem, S., Benkhelil, R., Saada, V., Marzac, C., … Antony-Debré, I. (2019). Germline RUNX1 Intragenic Deletion: Implications for Accurate Diagnosis of FPD/AML. *HemaSphere*, *3*(3), e203. doi:10.1097/hs9.0000000000000203

Durst, K. L. and Hiebert, S. W. (2004). Role of RUNX family members in transcriptional repression and gene silencing. *Oncogene*, *23*(24), 4220-4224. doi:10.1038/sj.onc.1207122

Echeverria, P. and Picard, D. (2010). Molecular chaperones, essential partners of steroid hormone receptors for activity and mobility. *Biochimica et Biophysica Acta (BBA) - Molecular Cell Research*, *1803*(6), 641-649. doi:10.1016/j.bbamcr.2009.11.012

Eppert, K., Takenaka, K., Lechman, E. R., Waldron, L., Nilsson, B., Galen, P. van, … Dick, J. E. (2011). Stem cell gene expression programs influence clinical outcome in human leukemia. *Nature Medicine*, *17*(9), 1086-1093. doi:10.1038/nm.2415

Eriksson, A., Österroos, A., Hassan, S., Gullbo, J., Rickardson, L., Jarvius, M., … Larsson, R. (2015). Drug screen in patient cells suggests quinacrine to be repositioned for treatment of acute myeloid leukemia. *Blood Cancer Journal*, *5*(4), e307-e307. doi:10.1038/bcj.2015.31

Estey, E. H. (2018). Acute myeloid leukemia: 2019 update on risk-stratification and management. *American Journal of Hematology*, *93*(10), 1267-1291. doi:10.1002/ajh.25214

Fares, I., Chagraoui, J., Gareau, Y., Gingras, S., Ruel, R., Mayotte, N., … Sauvageau, G. (2014). Pyrimidoindole derivatives are agonists of human hematopoietic stem cell self-renewal. *Science*, *345*(6203), 1509-1512. doi:10.1126/science.1256337

Feuring-Buske, M., Gerhard, B., Cashman, J., Humphries, R. K., Eaves, C. J. and Hogge, D. E. (2003). Improved engraftment of human acute myeloid leukemia progenitor cells in beta 2-microglobulin-deficient NOD/SCID mice and in NOD/SCID mice transgenic for human growth factors. *Leukemia*, *17*(4), 760-763. doi:10.1038/sj.leu.2402882

Franco, L. M., Gadkari, M., Howe, K. N., Sun, J., Kardava, L., Kumar, P., … Germain, R. N. (2019). Immune regulation by glucocorticoids can be linked to cell type–dependent transcriptional responses. *Journal of Experimental Medicine*, *216*(2), 384-406. doi:10.1084/jem.20180595

Frank, R., Zhang, J., Uchida, H., Meyers, S., Hiebert, S. W. and Nimer, S. D. (1995). The AML1/ETO fusion protein blocks transactivation of the GM-CSF promoter by AML1B. *Oncogene*, *11*(12), 2667-74.

Gaidzik, V. I., Bullinger, L., Schlenk, R. F., Zimmermann, A. S., Röck, J., Paschka, P., … Döhner, K. (2011). RUNX1 Mutations in Acute Myeloid Leukemia: Results From a Comprehensive Genetic and Clinical Analysis From the AML Study Group. *Journal of Clinical Oncology*, *29*(10), 1364-1372. doi:10.1200/JCO.2010.30.7926

Gaidzik, V., Teleanu, V., Papaemmanuil, E., Weber, D., Paschka, P., Hahn, J., … Döhner, H. (2016). RUNX1 mutations in acute myeloid leukemia are associated with distinct clinico-pathologic and genetic features. *Leukemia*. doi:10.1038/leu.2016.126

Gale, R., Green, C., Allen, C., Mead, A., Burnett, A., Hills, R., … Party, M. (2008). The impact of FLT3 internal tandem duplication mutant level, number, size, and interaction with NPM1 mutations in a large cohort of young adult patients with acute myeloid leukemia. *Blood*, *111*(5), 2776-2784. doi:10.1182/blood-2007-08-109090

Galera, P., Dulau-Florea, A. and Calvo, K. R. (2019). Inherited thrombocytopenia and platelet disorders with germline predisposition to myeloid neoplasia. *International Journal of Laboratory Hematology*, *41*(S1), 131-141. doi:10.1111/ijlh.12999

Galigniana, M., Radanyi, C., Renoir, J., Housley, P. and Pratt, W. (2001). Evidence That the Peptidylprolyl Isomerase Domain of the hsp90-binding Immunophilin FKBP52 Is Involved in Both Dynein Interaction and Glucocorticoid Receptor Movement to the Nucleus. *Journal of Biological Chemistry*, *276*(18), 14884-14889. doi:10.1074/jbc.m010809200

Gangatharan, S., Grove, C., Leahy, M. and Wright, M. (2013). Acute myeloid leukaemia in Western Australia 1991-2005: a retrospective population-based study of 898 patients regarding epidemiology, cytogenetics, treatment and outcome. *Internal medicine journal*, *43*(8), 903-11. doi:10.1111/imj.12169

Gao, W. and Estey, E. (2015). Moving toward targeted therapies in acute myeloid leukemia. *Clinical advances in hematology & oncology : H&O*, *13*(11), 748-54.

Garnett, M. J., Edelman, E. J., Heidorn, S. J., Greenman, C. D., Dastur, A., Lau, K., … Benes, C. H. (2012). Systematic identification of genomic markers of drug sensitivity in cancer cells. *Nature*, *483*(7391), 570-5. doi:10.1038/nature11005

Genovese, G., Kähler, A. K., Handsaker, R. E., Lindberg, J., Rose, S. A., Bakhoum, S. F., … McCarroll, S. A. (2014). Clonal Hematopoiesis and Blood-Cancer Risk Inferred from Blood DNA Sequence. *The New England Journal of Medicine*, *371*(26), 2477-2487. doi:10.1056/nejmoa1409405

Gerber, A. and Diamond, M. (2009). Discovery of selective glucocorticoid receptor modulators by multiplexed reporter screening. *Proceedings of the National Academy of Sciences*, *106*(12), 4929-4934. doi:10.1073/pnas.0812308106

Gerritsen, M., Yi, G., Tijchon, E., Kuster, J., Schuringa, J., Martens, J. and Vellenga, E. (2019). RUNX1 mutations enhance self-renewal and block granulocytic differentiation in human in vitro models and primary AMLs. *Blood advances*, *3*(3), 320-332. doi:10.1182/bloodadvances.2018024422

Gerstung, M., Papaemmanuil, E., Martincorena, I., Bullinger, L., Gaidzik, V., Paschka, P., … Campbell, P. (2017). Precision oncology for acute myeloid leukemia using a knowledge bank approach. *Nature Genetics*, *49*(3), 332-340. doi:10.1038/ng.3756

Gilbert, L., Horlbeck, M., Adamson, B., Villalta, J., Chen, Y., Whitehead, E., … Weissman, J. (2014). Genome-Scale CRISPR-Mediated Control of Gene Repression and Activation. *Cell*, *159*(3), 647-661. doi:10.1016/j.cell.2014.09.029

Giles, K., Ross, K., Rossi, A., Hotchin, N., Haslett, C. and Dransfield, I. (2001). Glucocorticoid Augmentation of Macrophage Capacity for Phagocytosis of Apoptotic Cells Is Associated with Reduced p130Cas Expression, Loss of Paxillin/pyk2 Phosphorylation, and High Levels of Active Rac. *The Journal of Immunology*, *167*(2), 976-986. doi:10.4049/jimmunol.167.2.976

Gilliland, D. G. and Griffin, J. D. (2002). The roles of FLT3 in hematopoiesis and leukemia. *Blood*, *100*(5), 1532-1542. doi:10.1182/blood-2002-02-0492

Gjerstad, J., Lightman, S. and Spiga, F. (2018). Role of glucocorticoid negative feedback in the regulation of HPA axis pulsatility. *Stress*, *21*(5), 1-14. doi:10.1080/10253890.2018.1470238

Godley, L. A. (2014). Inherited predisposition to acute myeloid leukemia. *Seminars in hematology*, *51*(4), 306-21. doi:10.1053/j.seminhematol.2014.08.001

Godley, L. A. and Shimamura, A. (2017). Genetic predisposition to hematologic malignancies: management and surveillance. *Blood*, *130*(4), 424-432. doi:10.1182/blood-2017-02-735290

Gorczynski, M., Grembecka, J., Zhou, Y., Kong, Y., Roudaia, L., Douvas, M., … Bushweller, J. (2007). Allosteric Inhibition of the Protein-Protein Interaction between the Leukemia-Associated Proteins Runx1 and CBFβ. *Chemistry & Biology*, *14*(10), 1186-1197. doi:10.1016/j.chembiol.2007.09.006

Gorre, M., Mohammed, M., Ellwood, K., Hsu, N., Paquette, R., Rao, P. and Sawyers, C. (2001). Clinical Resistance to STI-571 Cancer Therapy Caused by BCR-ABL Gene Mutation or Amplification. *Science*, *293*(5531), 876-880. doi:10.1126/science.1062538

Goulding, N. and Flower, R. (2001). Glucocorticoids, 3-15. doi:10.1007/978-3-0348-8348-1_1

Goyama, S, Huang, G., Kurokawa, M. and Mulloy, J. (2014). Posttranslational modifications of RUNX1 as potential anticancer targets. *Oncogene*, *34*(27), 3483-92. doi:10.1038/onc.2014.305

Goyama, S, Schibler, J., Cunningham, L., Zhang, Y., Rao, Y., Nishimoto, N., … Mulloy, J. (2013). Transcription factor RUNX1 promotes survival of acute myeloid leukemia cells. *Journal of Clinical Investigation*, *123*(9), 3876-3888. doi:10.1172/jci68557

Goyama, Susumu and Mulloy, J. C. (2011). Molecular pathogenesis of core binding factor leukemia: current knowledge and future prospects. *International Journal of Hematology*, *94*(2), 126-133. doi:10.1007/s12185-011-0858-z

Greenberger, J. (1991). The hematopoietic microenvironment. *Critical Reviews in Oncology/Hematology*, *11*(1), 65-84. doi:10.1016/1040-8428(91)90018-8

Griessinger, E. and Andreeff, M. (2018). NSG-S mice for acute myeloid leukemia, yes. For myelodysplastic syndrome, no. *Haematologica*, *103*(6), 921-923. doi:10.3324/haematol.2018.193847

Grimwade, D., Hills, R. K., Moorman, A. V., Walker, H., Chatters, S., Goldstone, A. H., … Group, on behalf of the N. C. R. I. A. L. W. (2010). Refinement of cytogenetic classification in acute myeloid leukemia: determination of prognostic significance of rare recurring chromosomal abnormalities among 5876 younger adult patients treated in the United Kingdom Medical Research Council trials. *Blood*, *116*(3), 354-365. doi:10.1182/blood-2009-11-254441

Groeneweg, F., Karst, H., Kloet, Er. and Joëls, M. (2012). Mineralocorticoid and glucocorticoid receptors at the neuronal membrane, regulators of nongenomic corticosteroid signalling. *Molecular and Cellular Endocrinology*, *350*(2), 299-309. doi:10.1016/j.mce.2011.06.020

Grossmann, V., Kern, W., Harbich, S., Alpermann, T., Jeromin, S., Schnittger, S., … Kohlmann, A. (2011). Prognostic relevance of RUNX1 mutations in T-cell acute lymphoblastic leukemia. *Haematologica*, *96*(12), 1874-1877. doi:10.3324/haematol.2011.043919

Grossmann, V., Schnittger, S., Kohlmann, A., Eder, C., Roller, A., Dicker, F., … Haferlach, C. (2012). A novel hierarchical prognostic model of AML solely based on molecular mutations. *Blood*, *120*(15), 2963-2972. doi:10.1182/blood-2012-03-419622

Grove, C. S. and Vassiliou, G. S. (2014). Acute myeloid leukaemia: a paradigm for the clonal evolution of cancer? *Disease Models & Mechanisms*, *7*(8), 941-951. doi:10.1242/dmm.015974

Growney, J. D., Shigematsu, H., Li, Z., Lee, B. H., Adelsperger, J., Rowan, R., … Gilliland, D. G. (2005). Loss of Runx1 perturbs adult hematopoiesis and is associated with a myeloproliferative phenotype. *Blood*, *106*(2), 494-504. doi:10.1182/blood-2004-08-3280

Gruhn, B., Naumann, T., Gruner, D., Walther, M., Wittig, S., Becker, S., … Sonnemann, J. (2013). The expression of histone deacetylase 4 is associated with prednisone poor-response in childhood acute lymphoblastic leukemia. *Leukemia Research*, *37*(10), 1200-1207. doi:10.1016/j.leukres.2013.07.016

Gruszka, A. M., Valli, D. and Alcalay, M. (2017). Understanding the molecular basis of acute myeloid leukemias: where are we now? *International Journal of Hematologic Oncology*, *6*(2), 43-53. doi:10.2217/ijh-2017-0002

Gruver-Yates, A., Quinn, M. and Cidlowski, J. (2014). Analysis of Glucocorticoid Receptors and Their Apoptotic Response to Dexamethasone in Male Murine B Cells During Development. *Endocrinology*, *155*(2), 463-474. doi:10.1210/en.2013-1473

Haarman, E. G., Kaspers, G. L. and Veerman, A. J. P. (2003). Glucocorticoid resistance in childhood leukaemia: mechanisms and modulation. *British Journal of Haematology*, *120*(6), 919-929. doi:10.1046/j.1365-2141.2003.04189.x

Haarman, E., Kaspers, G., Rottier, M. and Veerman, A. (2004). Glucocorticoid receptor alpha, beta and gamma expression vs in vitro glucocorticod resistance in childhood leukemia. *Leukemia*, *18*(3), 530-537. doi:10.1038/sj.leu.2403225

Haferlach, T., Nagata, Y., Grossmann, V., Okuno, Y., Bacher, U., Nagae, G., … Ogawa, S. (2014). Landscape of genetic lesions in 944 patients with myelodysplastic syndromes. *Leukemia*, *28*(2), 241-247. doi:10.1038/leu.2013.336

Handschuh, L. (2019). Not Only Mutations Matter: Molecular Picture of Acute Myeloid Leukemia Emerging from Transcriptome Studies. *Journal of Oncology*, *2019*, 1-36. doi:10.1155/2019/7239206

Hannon, G. (2002). RNA interference. *Nature*, *418*(6894), 244-251. doi:10.1038/418244a

Hart, T., Chandrashekhar, M., Aregger, M., Steinhart, Z., Brown, K., MacLeod, G., … Moffat, J. (2015). High-Resolution CRISPR Screens Reveal Fitness Genes and Genotype-Specific Cancer Liabilities. *Cell*, *163*(6), 1515-1526. doi:10.1016/j.cell.2015.11.015

Hart, T., Tong, A., Chan, K., Leeuwen, J., Seetharaman, A., Aregger, M., … Moffat, J. (2017). Evaluation and Design of Genome-Wide CRISPR/SpCas9 Knockout Screens. *G3: Genes|Genomes|Genetics*, *7*(8), 2719-2727. doi:10.1534/g3.117.041277

Haurwitz, R., Jinek, M., Wiedenheft, B., Zhou, K. and Doudna, J. (2010). Sequence- and Structure-Specific RNA Processing by a CRISPR Endonuclease. *Science*, *329*(5997), 1355-1358. doi:10.1126/science.1192272

Hazlehurst, L., Argilagos, R. and Dalton, W. (2007). Beta-1 integrin mediated adhesion increases Bim protein degradation and contributes to drug resistance in leukaemia cells. *British Journal of Haematology*, *136*(2), 269-275. doi:10.1111/j.1365-2141.2006.06435.x

Hench, P., Kendall, E., Slocumb, C. and Polley, H. (1949). Adrenocortical Hormone in Arthritis : Preliminary Report. *Annals of the Rheumatic Diseases*, *8*(2), 97-104. doi:10.1136/ard.8.2.97

Herglotz, J., Kuvardina, O. N., Kolodziej, S., Kumar, A., Hussong, H., Grez, M. and Lausen, J. (2013). Histone arginine methylation keeps RUNX1 target genes in an intermediate state. *Oncogene*, *32*(20), 2565-2575. doi:10.1038/onc.2012.274

Hiçsönmez, G. (2006). The effect of steroid on myeloid leukemic cells: The potential of short-course high-dose methylprednisolone treatment in inducing differentiation, apoptosis and in stimulating myelopoiesis. *Leukemia Research*, *30*(1), 60-68. doi:10.1016/j.leukres.2005.05.015

Ho, A. D., Schetelig, J., Bochtler, T., Schaich, M., Schäfer-Eckart, K., Hänel, M., … Leukemia, S. A. (2016). Allogeneic Stem Cell Transplantation Improves Survival in Patients with Acute Myeloid Leukemia Characterized by a High Allelic Ratio of Mutant FLT3-ITD. *Biology of Blood and Marrow Transplantation*, *22*(3), 462-469. doi:10.1016/j.bbmt.2015.10.023

Hollenberg, S., Weinberger, C., Ong, E., Cerelli, G., Oro, A., Lebo, R., … Evans, R. (1985). Primary structure and expression of a functional human glucocorticoid receptor cDNA. *Nature*, *318*(6047), 635-641. doi:10.1038/318635a0

Hope, K., Jin, L. and Dick, J. (2004). Acute myeloid leukemia originates from a hierarchy of leukemic stem cell classes that differ in self-renewal capacity. *Nature Immunology*, *5*(7), 738-743. doi:10.1038/ni1080

Huang, G, Shigesada, K., Ito, K., Wee, H., Yokomizo, T. and Ito, Y. (2001). Dimerization with PEBP2β protects RUNX1/AML1 from ubiquitin–proteasome-mediated degradation. *The EMBO Journal*, *20*(4), 723-733. doi:10.1093/emboj/20.4.723

Huang, Gang, Zhang, P., Hirai, H., Elf, S., Yan, X., Chen, Z., … Tenen, D. G. (2008). PU.1 is a major downstream target of AML1 (RUNX1) in adult mouse hematopoiesis. *Nature Genetics*, *40*(1), 51-60. doi:10.1038/ng.2007.7

Huang, H., Woo, A., Waldon, Z., Schindler, Y., Moran, T., Zhu, H., … Cantor, A. (2012). A Src family kinase–Shp2 axis controls RUNX1 activity in megakaryocyte and T-lymphocyte differentiation. *Genes & Development*, *26*(14), 1587-1601. doi:10.1101/gad.192054.112

Hudson, W. H., Youn, C. and Ortlund, E. A. (2012). The structural basis of direct glucocorticoid-mediated transrepression. *Nature Structural & Molecular Biology*, *20*(1), 53-58. doi:10.1038/nsmb.2456

Huet, S., Paubelle, E., Lours, C., Grange, B., Courtois, L., Chabane, K., … Sujobert, P. (2018). Validation of the prognostic value of the knowledge bank approach to determine AML prognosis in real life. *Blood*, *132*(8), 865-867. doi:10.1182/blood-2018-03-840348

Ichikawa, M., Asai, T., Saito, T., Yamamoto, G., Seo, S., Yamazaki, I., … Kurokawa, M. (2004). AML-1 is required for megakaryocytic maturation and lymphocytic differentiation, but not for maintenance of hematopoietic stem cells in adult hematopoiesis. *Nature Medicine*, *10*(3), 299-304. doi:10.1038/nm997

Illendula, A., Pulikkan, J., Zong, H., Grembecka, J., Xue, L., Sen, S., … Bushweller, J. (2015). A small-molecule inhibitor of the aberrant transcription factor CBFβ-SMMHC delays leukemia in mice. *Science*, *347*(6223), 779-784. doi:10.1126/science.aaa0314

Imai, Y, Kurokawa, M., Yamaguchi, Y., Izutsu, K., Nitta, E., Mitani, K., … Hirai, H. (2004). The Corepressor mSin3A Regulates Phosphorylation-Induced Activation, Intranuclear Location, and Stability of AML1. *Molecular and Cellular Biology*, *24*(3), 1033-1043. doi:10.1128/mcb.24.3.1033-1043.2004

Imai, Yoichi, Kurokawa, M., Tanaka, K., Friedman, A. D., Ogawa, S., Mitani, K., … Hirai, H. (1998). TLE, the Human Homolog of Groucho, Interacts with AML1 and Acts as a Repressor of AML1-Induced Transactivation. *Biochemical and Biophysical Research Communications*, *252*(3), 582-589. doi:10.1006/bbrc.1998.9705

Inaba, H. and Pui, C. (2010). Glucocorticoid use in acute lymphoblastic leukaemia. *The Lancet Oncology*, *11*(11), 1096-1106. doi:10.1016/s1470-2045(10)70114-5

Jaiswal, S., Fontanillas, P., Flannick, J., Manning, A., Grauman, P. V., Mar, B. G., … Ebert, B. L. (2014). Age-Related Clonal Hematopoiesis Associated with Adverse Outcomes. *The New England Journal of Medicine*, *371*(26), 2488-2498. doi:10.1056/nejmoa1408617

Jinek, M., Chylinski, K., Fonfara, I., Hauer, M., Doudna, J. A. and Charpentier, E. (2012). A programmable dual-RNA-guided DNA endonuclease in adaptive bacterial immunity. *Science (New York, N.Y.)*, *337*(6096), 816-21. doi:10.1126/science.1225829

John, S, Sabo, P., Johnson, T., Sung, M., Biddie, S., Lightman, S., … Hager, G. (2008). Interaction of the Glucocorticoid Receptor with the Chromatin Landscape. *Molecular Cell*, *29*(5), 611-624. doi:10.1016/j.molcel.2008.02.010

John, Sam, Sabo, P. J., Thurman, R. E., Sung, M.-H., Biddie, S. C., Johnson, T. A., … Stamatoyannopoulos, J. A. (2011). Chromatin accessibility pre-determines glucocorticoid receptor binding patterns. *Nature Genetics*, *43*(3), 264-268. doi:10.1038/ng.759

Jonas, B. A. and Pollyea, D. A. (2019). How we use venetoclax with hypomethylating agents for the treatment of newly diagnosed patients with acute myeloid leukemia. *Leukemia*, *33*(12), 2795-2804. doi:10.1038/s41375-019-0612-8

Jones, C., Bhatla, T., Blum, R., Wang, J., Paugh, S., Wen, X., … Carroll, W. (2014). Loss of TBL1XR1 Disrupts Glucocorticoid Receptor Recruitment to Chromatin and Results in Glucocorticoid Resistance in a B-Lymphoblastic Leukemia Model. *Journal of Biological Chemistry*, *289*(30), 20502-20515. doi:10.1074/jbc.m114.569889

Jones, L. and Bunnage, M. (2017). Applications of chemogenomic library screening in drug discovery. *Nature Reviews Drug Discovery*, *16*(4), 285-296. doi:10.1038/nrd.2016.244

Jost, M., Chen, Y., Gilbert, L., Horlbeck, M., Krenning, L., Menchon, G., … Weissman, J. (2017). Combined CRISPRi/a-Based Chemical Genetic Screens Reveal that Rigosertib Is a Microtubule-Destabilizing Agent. *Molecular Cell*, *68*(1), 210-223.e6. doi:10.1016/j.molcel.2017.09.012

Jost, M. and Weissman, J. (2018). CRISPR Approaches to Small Molecule Target Identification. *ACS Chemical Biology*, *13*(2), 366-375. doi:10.1021/acschembio.7b00965

Joung, J., Konermann, S., Gootenberg, J. S., Abudayyeh, O. O., Platt, R. J., Brigham, M. D., … Zhang, F. (2017). Genome-scale CRISPR-Cas9 knockout and transcriptional activation screening. *Nature Protocols*, *12*(4), 828-863. doi:10.1038/nprot.2017.016

Kaelin, W. (2012). Use and Abuse of RNAi to Study Mammalian Gene Function. *Science*, *337*(6093), 421-422. doi:10.1126/science.1225787

Khan, M., Cortes, J., Kadia, T., Naqvi, K., Brandt, M., Pierce, S., … DiNardo, C. D. (2017). Clinical Outcomes and Co-Occurring Mutations in Patients with RUNX1-Mutated Acute Myeloid Leukemia. *International Journal of Molecular Sciences*, *18*(8), 1618. doi:10.3390/ijms18081618

Kitabayashi, I., Aikawa, Y., Nguyen, L. A., Yokoyama, A. and Ohki, M. (2001). Activation of AML1-mediated transcription by MOZ and inhibition by the MOZ–CBP fusion protein. *The EMBO Journal*, *20*(24), 7184-7196. doi:10.1093/emboj/20.24.7184

Kitabayashi, I., Yokoyama, A., Shimizu, K. and Ohki, M. (1998). Interaction and functional cooperation of the leukemia-associated factors AML1 and p300 in myeloid cell differentiation. *The EMBO Journal*, *17*(11), 2994-3004. doi:10.1093/emboj/17.11.2994

Klein, K., Haarman, E., Haas, V., Zwaan, C., Creutzig, U. and Kaspers, G. (2016). Glucocorticoid-Induced Proliferation in Untreated Pediatric Acute Myeloid Leukemic Blasts: A Short Report on Glucocorticoid Response in Pediatric AML. *Pediatric Blood & Cancer*, *63*(8), 1457-1460. doi:10.1002/pbc.26011

Klug, C., Jordan, C., Miller, C. and Eaves, C. (2001). Hematopoietic Stem Cell Protocols. *Methods in molecular medicine*, *63*, 123-141. doi:10.1385/1-59259-140-x:123

Koga, Y., Matsuzaki, A., Suminoe, A., Hattori, H., Kanemitsu, S. and Hara, T. (2005). Differential mRNA expression of glucocorticoid receptor α and β is associated with glucocorticoid sensitivity of acute lymphoblastic leukemia in children. *Pediatric Blood & Cancer*, *45*(2), 121-127. doi:10.1002/pbc.20308

Koh, C., Wang, C., Ng, C., Ito, Y., Araki, M., Tergaonkar, V., … Osato, M. (2013). RUNX1 meets MLL: epigenetic regulation of hematopoiesis by two leukemia genes. *Leukemia*, *27*(9), 1793-1802. doi:10.1038/leu.2013.200

Kojima, K., McQueen, T., Chen, Y., Jacamo, R., Konopleva, M., Shinojima, N., … Andreeff, M. (2011). p53 activation of mesenchymal stromal cells partially abrogates microenvironment-mediated resistance to FLT3 inhibition in AML through HIF-1α–mediated down-regulation of CXCL12. *Blood*, *118*(16), 4431-4439. doi:10.1182/blood-2011-02-334136

Konermann, S., Brigham, M., Trevino, A., Joung, J., Abudayyeh, O., Barcena, C., … Zhang, F. (2014). Genome-scale transcriptional activation by an engineered CRISPR-Cas9 complex. *Nature*, *517*(7536), 583-588. doi:10.1038/nature14136

Kouchkovsky, I. D. and Abdul-Hay, M. (2016). Acute Myeloid Leukemia: a comprehensive review and 2016 update. *Blood Cancer Journal*, *6*(7), e441-e441. doi:10.1038/bcj.2016.50

Kouwe, E. van der et Staber, P. B. (2019). RUNX1-ETO: Attacking the Epigenome for Genomic Instable Leukemia. *International Journal of Molecular Sciences*, *20*(2), 350. doi:10.3390/ijms20020350

Krevvata, M., Shan, X., Zhou, C., Santos, C., Ndikuyeze, G., Secreto, A., … Carroll, M. (2018). Cytokines increase engraftment of human acute myeloid leukemia cells in immunocompromised mice but not engraftment of human myelodysplastic syndrome cells. *Haematologica*, *103*(6), 959-971. doi:10.3324/haematol.2017.183202

Krivtsov, A., Twomey, D., Feng, Z., Stubbs, M., Wang, Y., Faber, J., … Armstrong, S. (2006). Transformation from committed progenitor to leukaemia stem cell initiated by MLL–AF9. *Nature*, *442*(7104), 818-822. doi:10.1038/nature04980

Kuvardina, O., Herglotz, J., Kolodziej, S., Kohrs, N., Herkt, S., Wojcik, B., … Lausen, J. (2015). RUNX1 represses the erythroid gene expression program during megakaryocytic differentiation. *Blood*, *125*(23), 3570-3579. doi:10.1182/blood-2014-11-610519

Labarthe, A. de, Rousselot, P., Huguet-Rigal, F., Delabesse, E., Witz, F., Maury, S., … (GRAALL), G. for R. on A. A. L. L. (2006). Imatinib combined with induction or consolidation chemotherapy in patients with de novo Philadelphia chromosome–positive acute lymphoblastic leukemia: results of the GRAAPH-2003 study. *Blood*, *109*(4), 1408-1413. doi:10.1182/blood-2006-03-011908

Lacaud, G., Kouskoff, V., Trumble, A., Schwantz, S. and Keller, G. (2004). Haploinsufficiency of Runx1 results in the acceleration of mesodermal development and hemangioblast specification upon in vitro differentiation of ES cells. *Blood*, *103*(3), 886-889. doi:10.1182/blood-2003-06-2149

Lapidot, T., Sirard, C., Vormoor, J., Murdoch, B., Hoang, T., Caceres-Cortes, J., … Dick, J. E. (1994). A cell initiating human acute myeloid leukaemia after transplantation into SCID mice. *Nature*, *367*(6464), 645-648. doi:10.1038/367645a0

Latger-Cannard, V., Philippe, C., Bouquet, A., Baccini, V., Alessi, M.-C., Ankri, A., … Favier, R. (2016). Haematological spectrum and genotype-phenotype correlations in nine unrelated families with RUNX1 mutations from the French network on inherited platelet disorders. *Orphanet Journal of Rare Diseases*, *11*(1), 49. doi:10.1186/s13023-016-0432-0

Lavallée, V.-P., Baccelli, I., Krosl, J., Wilhelm, B., Barabé, F., Gendron, P., … Sauvageau, G. (2015). The transcriptomic landscape and directed chemical interrogation of MLL-rearranged acute myeloid leukemias. *Nature Genetics*, *47*(9), 1030-1037. doi:10.1038/ng.3371

Lavallée, V.-P., Krosl, J., Lemieux, S., Boucher, G., Gendron, P., Pabst, C., … Sauvageau, G. (2016). Chemo-genomic interrogation of CEBPA mutated AML reveals recurrent CSF3R mutations and subgroup sensitivity to JAK inhibitors. *Blood*, *127*(24), 3054-61. doi:10.1182/blood-2016-03-705053

Laverdière, I., Boileau, M., Neumann, A. L., Frison, H., Mitchell, A., Ng, S. W. K., … Eppert, K. (2018). Leukemic stem cell signatures identify novel therapeutics targeting acute myeloid leukemia. *Blood Cancer Journal*, *8*(6), 52. doi:10.1038/s41408-018-0087-2

Levanon, D., Goldstein, R. E., Bernstein, Y., Tang, H., Goldenberg, D., Stifani, S., … Groner, Y. (1998). Transcriptional repression by AML1 and LEF-1 is mediated by the TLE/Groucho corepressors. *Proceedings of the National Academy of Sciences*, *95*(20), 11590-11595. doi:10.1073/pnas.95.20.11590

Li, Y., Wang, H., Wang, X., Jin, W., Tan, Y., Fang, H., … Wang, K. (2016). Genome-wide studies identify a novel interplay between AML1 and AML1/ETO in t(8;21) acute myeloid leukemia. *Blood*, *127*(2), 233-242. doi:10.1182/blood-2015-03-626671

Liberman, A., Budziñski, M., Sokn, C., Gobbini, R., Steininger, A. and Arzt, E. (2018). Regulatory and Mechanistic Actions of Glucocorticoids on T and Inflammatory Cells. *Frontiers in Endocrinology*, *9*, 235. doi:10.3389/fendo.2018.00235

Lichtinger, M., Ingram, R., Hannah, R., Müller, D., Clarke, D., Assi, S. A., … Bonifer, C. (2012). RUNX1 reshapes the epigenetic landscape at the onset of haematopoiesis. *The EMBO Journal*, *31*(22), 4318-4333. doi:10.1038/emboj.2012.275

Lin, S., Mulloy, J. C. and Goyama, S. (2017). RUNX1-ETO Leukemia. *Advances in experimental medicine and biology*, *962*, 151-173. doi:10.1007/978-981-10-3233-2_11

Liu, P., Tarle, S., Hajra, A., Claxton, D., Marlton, P., Freedman, M., … Collins, F. (1993). Fusion between transcription factor CBF beta/PEBP2 beta and a myosin heavy chain in acute myeloid leukemia. *Science*, *261*(5124), 1041-1044. doi:10.1126/science.8351518

Longo, D. L., Döhner, H., Weisdorf, D. J. and Bloomfield, C. D. (2015). Acute Myeloid Leukemia. *The New England Journal of Medicine*, *373*(12), 1136-1152. doi:10.1056/nejmra1406184

Lordier, L., Bluteau, D., Jalil, A., Legrand, C., Pan, J., Rameau, P., … Chang, Y. (2012). RUNX1-induced silencing of non-muscle myosin heavy chain IIB contributes to megakaryocyte polyploidization. *Nature communications*, *3*(1), 717. doi:10.1038/ncomms1704

Louw, A. (2019). GR Dimerization and the Impact of GR Dimerization on GR Protein Stability and Half-Life. *Frontiers in Immunology*, *10*, 1693. doi:10.3389/fimmu.2019.01693

Love, M. I., Huska, M. R., Jurk, M., Schöpflin, R., Starick, S. R., Schwahn, K., … Meijsing, S. H. (2017). Role of the chromatin landscape and sequence in determining cell type-specific genomic glucocorticoid receptor binding and gene regulation. *Nucleic Acids Research*, *45*(4), 1805-1819. doi:10.1093/nar/gkw1163

Löwenberg, B. and Rowe, J. M. (2015). Introduction to the review series on advances in acute myeloid leukemia (AML). *Blood*, *127*(1), 1. doi:10.1182/blood-2015-10-662684

Luo, X., Feurstein, S., Mohan, S., Porter, C. C., Jackson, S. A., Keel, S., … Godley, L. A. (2019). ClinGen Myeloid Malignancy Variant Curation Expert Panel recommendations for germline RUNX1 variants. *Blood Advances*, *3*(20), 2962-2979. doi:10.1182/bloodadvances.2019000644

Lutterbach, B., Westendorf, J. J., Linggi, B., Isaac, S., Seto, E. and Hiebert, S. W. (2000). A Mechanism of Repression by Acute Myeloid Leukemia-1, the Target of Multiple Chromosomal Translocations in Acute Leukemia. *Journal of Biological Chemistry*, *275*(1), 651-656. doi:10.1074/jbc.275.1.651

Malani, D., Murumägi, A., Yadav, B., Kontro, M., Eldfors, S., Kumar, A., … Kallioniemi, O. (2017). Enhanced sensitivity to glucocorticoids in cytarabine-resistant AML. *Leukemia*, *31*(5), 1187-1195. doi:10.1038/leu.2016.314

Mangan, J. K. and Speck, N. A. (2011). RUNX1 mutations in clonal myeloid disorders: from conventional cytogenetics to next generation sequencing, a story 40 years in the making. *Critical reviews in oncogenesis*, *16*(1-2), 77-91. doi:10.1615/CritRevOncog.v16.i1-2.80

MANTOVANI, A., SICA, A., SOZZANI, S., ALLAVENA, P., VECCHI, A. and LOCATI, M. (2004). The chemokine system in diverse forms of macrophage activation and polarization. *Trends in Immunology*, *25*(12), 677-686. doi:10.1016/j.it.2004.09.015

Marshall, L. J., Moore, A. C., Ohki, M., Kitabayashi, I., Patterson, D. and Ornelles, D. A. (2008). RUNX1 permits E4orf6-directed nuclear localization of the adenovirus E1B-55K protein and associates with centers of viral DNA and RNA synthesis. *Journal of virology*, *82*(13), 6395-408. doi:10.1128/jvi.00043-08

Matheny, C. J., Speck, M. E., Cushing, P. R., Zhou, Y., Corpora, T., Regan, M., … Speck, N. A. (2007). Disease mutations in RUNX1 and RUNX2 create nonfunctional, dominant-negative, or hypomorphic alleles. *The EMBO Journal*, *26*(4), 1163-1175. doi:10.1038/sj.emboj.7601568

Matsunaga, T., Takemoto, N., Sato, T., Takimoto, R., Tanaka, I., Fujimi, A., … Niitsu, Y. (2003). Interaction between leukemic-cell VLA-4 and stromal fibronectin is a decisive factor for minimal residual disease of acute myelogenous leukemia. *Nature Medicine*, *9*(9), 1158-1165. doi:10.1038/nm909

Mardis, E. (2012). Genome sequencing and cancer. *Current Opinion in Genetics & Development*, *22*(3), 245-250. doi:10.1016/j.gde.2012.03.005

Mayani, H., Flores-Figueroa, E. and Chávez-González, A. (2009). In vitro biology of human myeloid leukemia. *Leukemia Research*, *33*(5), 624-637. doi:10.1016/j.leukres.2008.11.011
McGowan, P., Sasaki, A., D'Alessio, A., Dymov, S., Labonté, B., Szyf, M., … Meaney, M. (2009). Epigenetic regulation of the glucocorticoid receptor in human brain associates with childhood abuse. *Nature Neuroscience*, *12*(3), 342-348. doi:10.1038/nn.2270
McNally, J., Müller, W., Walker, D., Wolford, R. and Hager, G. (2000). The Glucocorticoid Receptor: Rapid Exchange with Regulatory Sites in Living Cells. *Science*, *287*(5456), 1262-1265. doi:10.1126/science.287.5456.1262
Mendler, J. H., Maharry, K., Radmacher, M. D., Mrózek, K., Becker, H., Metzeler, K. H., … Bloomfield, C. D. (2012). RUNX1 Mutations Are Associated With Poor Outcome in Younger and Older Patients With Cytogenetically Normal Acute Myeloid Leukemia and With Distinct Gene and MicroRNA Expression Signatures. *Journal of Clinical Oncology*, *30*(25), 3109-3118. doi:10.1200/JCO.2011.40.6652
Metcalf, D. (2008). Hematopoietic cytokines. *Blood*, *111*(2), 485-491. doi:10.1182/blood-2007-03-079681
Mikhail, F. M., Sinha, K. K., Saunthararajah, Y. and Nucifora, G. (2006). Normal and transforming functions of RUNX1: A perspective. *Journal of Cellular Physiology*, *207*(3), 582-593. doi:10.1002/jcp.20538
Mirabelli, P., Coppola, L. and Salvatore, M. (2019). Cancer Cell Lines Are Useful Model Systems for Medical Research. *Cancers*, *11*(8), 1098. doi:10.3390/cancers11081098
Miyoshi, H., Kozu, T., Shimizu, K., Enomoto, K., Maseki, N., Kaneko, Y., … Ohki, M. (1993). The t(8;21) translocation in acute myeloid leukemia results in production of an AML1-MTG8 fusion transcript. *The EMBO Journal*, *12*(7), 2715-2721. doi:10.1002/j.1460-2075.1993.tb05933.x
Miyoshi, H., Shimizu, K., Kozu, T., Maseki, N., Kaneko, Y. and Ohki, M. (1991). t(8;21) breakpoints on chromosome 21 in acute myeloid leukemia are clustered within a limited region of a single gene, AML1. *Proceedings of the National Academy of Sciences*, *88*(23), 10431-10434. doi:10.1073/pnas.88.23.10431
Monaco, G., Konopleva, M., Munsell, M., Leysath, C., Wang, R., Jackson, C., … Andreeff, M. (2004). Engraftment of Acute Myeloid Leukemia in NOD/SCID Mice Is Independent of CXCR4 and Predicts Poor Patient Survival. *Stem Cells*, *22*(2), 188-201. doi:10.1634/stemcells.22-2-188
Moreno, D., Scrideli, C., Cortez, M., Queiroz, R., Valera, E., Silveira, V., … Tone, L. (2010). research paper: Differential expression of HDAC3, HDAC7 and HDAC9 is associated with prognosis and survival in childhood acute lymphoblastic leukaemia: HDAC Expression in Paediatric ALL. *British Journal of Haematology*, *150*(6), 665-673. doi:10.1111/j.1365-2141.2010.08301.x
Mrózek, K., Radmacher, M. D., Bloomfield, C. D. and Marcucci, G. (2009). Molecular signatures in acute myeloid leukemia. *Current Opinion in Hematology*, *16*(2), 64-69. doi:10.1097/moh.0b013e3283257b42
Network, C. (2013). Genomic and Epigenomic Landscapes of Adult De Novo Acute Myeloid Leukemia. *The New England Journal of Medicine*, *368*(22), 2059-2074. doi:10.1056/NEJMoa1301689
Ng, S. W. K., Mitchell, A., Kennedy, J. A., Chen, W. C., McLeod, J., Ibrahimova, N., … Wang, J. C. Y. (2016). A 17-gene stemness score for rapid determination of risk in acute leukaemia. *Nature*, *540*(7633), 433-437. doi:10.1038/nature20598
Niebuhr, B., Kriebitzsch, N., Fischer, M., Behrens, K., Günther, T., Alawi, M., … Stocking, C. (2013). Runx1 is essential at two stages of early murine B-cell development. *Blood*, *122*(3), 413-423. doi:10.1182/blood-2013-01-480244
North, T. E., Stacy, T., Matheny, C. J., Speck, N. A. and Bruijn, M. F. T. R. de. (2004). Runx1 Is Expressed in Adult Mouse Hematopoietic Stem Cells and Differentiating Myeloid and Lymphoid Cells, But Not in Maturing Erythroid Cells. *Stem Cells*, *22*(2), 158-168. doi:10.1634/stemcells.22-2-158
North, T., Gu, T. L., Stacy, T., Wang, Q., Howard, L., Binder, M., … Speck, N. A. (1999). Cbfa2 is required for the formation of intra-aortic hematopoietic clusters. *Development (Cambridge, England)*, *126*(11), 2563-75.
Nuchprayoon, I., Meyers, S., Scott, L. M., Suzow, J., Hiebert, S. and Friedman, A. D. (1994). PEBP2/CBF, the murine homolog of the human myeloid AML1 and PEBP2 beta/CBF beta proto-oncoproteins, regulates the murine myeloperoxidase and neutrophil elastase genes in immature myeloid cells. *Molecular and Cellular Biology*, *14*(8), 5558-5568. doi:10.1128/mcb.14.8.5558
Oakley, R. and Cidlowski, J. (2010). Cellular Processing of the Glucocorticoid Receptor Gene and Protein: New Mechanisms for Generating Tissue-specific Actions of Glucocorticoids. *Journal of Biological Chemistry*, *286*(5), 3177-3184. doi:10.1074/jbc.r110.179325
Obier, N. and Bonifer, C. (2016). Chromatin programming by developmentally regulated transcription factors: lessons from the study of haematopoietic stem cell specification and differentiation. *FEBS Letters*, *590*(22), 4105-4115. doi:10.1002/1873-3468.12343

Okuda, T., Deursen, J. van, Hiebert, S. W., Grosveld, G. and Downing, J. R. (1995). AML1, the Target of Multiple Chromosomal Translocations in Human Leukemia, Is Essential for Normal Fetal Liver Hematopoiesis. *Cell*, *84*(2), 321-330. doi:10.1016/S0092-8674(00)80986-1

Othus, M., Kantarjian, H., Petersdorf, S., Ravandi, F., Godwin, J., Cortes, J., … Estey, E. (2014). Declining rates of treatment-related mortality in patients with newly diagnosed AML given 'intense' induction regimens: a report from SWOG and MD Anderson. *Leukemia*, *28*(2), 289-292. doi:10.1038/leu.2013.176

Overman, R. A., Yeh, J. and Deal, C. L. (2013). Prevalence of oral glucocorticoid usage in the United States: A general population perspective. *Arthritis Care & Research*, *65*(2), 294-298. doi:10.1002/acr.21796

Pabst, C., Krosl, J., Fares, I., Boucher, G., Ruel, R., Marinier, A., … Sauvageau, G. (2014). Identification of small molecules that support human leukemia stem cell activity ex vivo. *Nature methods*, *11*(4), 436-42. doi:10.1038/nmeth.2847

Padma, V. (2015). An overview of targeted cancer therapy. *BioMedicine*, *5*(4), 19. doi:10.7603/s40681-015-0019-4

Papaemmanuil, E., Gerstung, M., Bullinger, L., Gaidzik, V. I., Paschka, P., Roberts, N. D., … Campbell, P. J. (2016). Genomic Classification and Prognosis in Acute Myeloid Leukemia. *The New England Journal of Medicine*, *374*(23), 2209-2221. doi:10.1056/NEJMoa1516192

Parente, L. (2001). Glucocorticoids, 35-51. doi:10.1007/978-3-0348-8348-1_3

Patnaik, M. M. and Tefferi, A. (2016). Cytogenetic and molecular abnormalities in chronic myelomonocytic leukemia. *Blood Cancer Journal*, *6*(2), e393-e393. doi:10.1038/bcj.2016.5

Pearce, D., Taussig, D., Zibara, K., Smith, L., Ridler, C., Preudhomme, C., … Bonnet, D. (2006). AML engraftment in the NOD/SCID assay reflects the outcome of AML: implications for our understanding of the heterogeneity of AML. *Blood*, *107*(3), 1166-1173. doi:10.1182/blood-2005-06-2325

Petta, I., Dejager, L., Ballegeer, M., Lievens, S., Tavernier, J., Bosscher, K. and Libert, C. (2016). The Interactome of the Glucocorticoid Receptor and Its Influence on the Actions of Glucocorticoids in Combatting Inflammatory and Infectious Diseases. *Microbiology and Molecular Biology Reviews*, *80*(2), 495-522. doi:10.1128/mmbr.00064-15

Presman, D. M., Ganguly, S., Schiltz, R. L., Johnson, T. A., Karpova, T. S. and Hager, G. L. (2016). DNA binding triggers tetramerization of the glucocorticoid receptor in live cells. *Proceedings of the National Academy of Sciences*, *113*(29), 8236-8241. doi:10.1073/pnas.1606774113

Preudhomme, C., Warot-Loze, D., Roumier, C., Grardel-Duflos, N., Garand, R., Lai, J., … Fenaux, P. (2000). High incidence of biallelic point mutations in the Runt domain of the AML1/PEBP2 alpha B gene in Mo acute myeloid leukemia and in myeloid malignancies with acquired trisomy 21. *Blood*, *96*(8), 2862-9.

Pulvertaft, R. (1964). CYTOLOGY OF BURKITT'S TUMOUR (AFRICAN LYMPHOMA). *The Lancet*, *283*(7327), 238-240. doi:10.1016/s0140-6736(64)92345-1

Putz, G., Rosner, A., Nuesslein, I., Schmitz, N. and Buchholz, F. (2005). AML1 deletion in adult mice causes splenomegaly and lymphomas. *Oncogene*, *25*(6), 929-939. doi:10.1038/sj.onc.1209136

Quax, R. A., Manenschijn, L., Koper, J. W., Hazes, J. M., Lamberts, S. W., Rossum, E. F. van and Feelders, R. A. (2013). Glucocorticoid sensitivity in health and disease. *Nature Reviews Endocrinology*, *9*(11), 670-686. doi:10.1038/nrendo.2013.183

Ramamoorthy, S and Cidlowski, J. (2013). Ligand-Induced Repression of the Glucocorticoid Receptor Gene Is Mediated by an NCoR1 Repression Complex Formed by Long-Range Chromatin Interactions with Intragenic Glucocorticoid Response Elements. *Molecular and Cellular Biology*, *33*(9), 1711-1722. doi:10.1128/mcb.01151-12

Ramamoorthy, Sivapriya and Cidlowski, J. A. (2013). Exploring the Molecular Mechanisms of Glucocorticoid Receptor Action from Sensitivity to Resistance. *Endocrine Development*, *24*, 41-56. doi:10.1159/000342502

Ravandi, F., Walter, R. B. et Freeman, S. D. (2018). Evaluating measurable residual disease in acute myeloid leukemia. *Blood Advances*, *2*(11), 1356-1366. doi:10.1182/bloodadvances.2018016378

Récher, C., Beyne-Rauzy, O., Demur, C., Chicanne, G., Santos, C., Mas, V., … Payrastre, B. (2005). Antileukemic activity of rapamycin in acute myeloid leukemia. *Blood*, *105*(6), 2527-2534. doi:10.1182/blood-2004-06-2494

Rhoades, K. L., Hetherington, C. J., Rowley, J. D., Hiebert, S. W., Nucifora, G., Tenen, D. G. and Zhang, D. E. (1996). Synergistic up-regulation of the myeloid-specific promoter for the macrophage colony-stimulating factor receptor by AML1 and the t(8;21) fusion protein may contribute to leukemogenesis. *Proceedings of the National Academy of Sciences*, *93*(21), 11895-11900. doi:10.1073/pnas.93.21.11895

Riether, C., Schürch, C. M. and Ochsenbein, A. F. (2015). Regulation of hematopoietic and leukemic stem cells by the immune system. *Cell Death & Differentiation*, *22*(2), 187-198. doi:10.1038/cdd.2014.89

Ross, K., Sedello, A., Todd, G., Paszkowski-Rogacz, M., Bird, A., Ding, L., … Buchholz, F. (2012). Polycomb group ring finger 1 cooperates with Runx1 in regulating differentiation and self-renewal of hematopoietic cells. *Blood*, *119*(18), 4152-4161. doi:10.1182/blood-2011-09-382390

Roumier, C., Eclache, V., Imbert, M., Davi, F., MacIntyre, E., Garand, R., … Preudhomme, C. (2003). M0 AML, clinical and biologic features of the disease, includingAML1 gene mutations: a report of 59 cases by the Groupe Français d'Hématologie Cellulaire (GFHC) and the Groupe Français de Cytogénétique Hématologique (GFCH). *Blood*, *101*(4), 1277-1283. doi:10.1182/blood-2002-05-1474

Sackey, F. and Watson, C. (1997). Cell cycle regulation of membrane glucocorticoid receptor in CCRF-CEM human ALL cells: correlation to apoptosis. *The American journal of physiology*, *273*(3 Pt 1), E571-83. doi:10.1152/ajpendo.1997.273.3.e571

Salman, Z., Balandrán-Juárez, J., Pelayo, R. and Guzman, M. (2015). A Novel Three-Dimensional Co-Culture System to Study Leukemia in the Bone Marrow Microenvironment. *Blood*, *126*(23), 1864-1864. doi:10.1182/blood.v126.23.1864.1864

Sanchez, P., Perry, R., Sarry, J., Perl, A., Swider, C., Choi, J. and Biegel, J. (2009). A robust xenotransplantation model for acute myeloid leukemia. *Leukemia*, *23*(11), 2109-2117. doi:10.1038/leu.2009.143

Sánchez-Vega, B. and Gandhi, V. (2009). Glucocorticoid resistance in a multiple myeloma cell line is regulated by a transcription elongation block in the glucocorticoid receptor gene (NR3C1). *British Journal of Haematology*, *144*(6), 856-864. doi:10.1111/j.1365-2141.2008.07549.x

Sanderson, R. N., Johnson, P. R. E., Moorman, A. V., Roman, E., Willett, E., Taylor, P. R., … Bowen, D. T. (2006). Population-based demographic study of karyotypes in 1709 patients with adult Acute Myeloid Leukemia. *Leukemia*, *20*(3), 444-450. doi:10.1038/sj.leu.2404055

Schlegelberger, B. and Heller, P. G. (2017). RUNX1 deficiency (familial platelet disorder with predisposition to myeloid leukemia, FPDMM). *Seminars in Hematology*, *54*(2), 75-80. doi:10.1053/j.seminhematol.2017.04.006

Schiller, B. J., Chodankar, R., Watson, L. C., Stallcup, M. R. and Yamamoto, K. R. (2014). Glucocorticoid receptor binds half sites as a monomer and regulates specific target genes. *Genome biology*, *15*(7), 418. doi:10.1186/s13059-014-0418-y

Schmitt, M., Loeb, L. and Salk, J. (2015). The influence of subclonal resistance mutations on targeted cancer therapy. *Nature Reviews Clinical Oncology*, *13*(6), 335-347. doi:10.1038/nrclinonc.2015.175

Schnittger, S., Dicker, F., Kern, W., Wendland, N., Sundermann, J., Alpermann, T., … Haferlach, T. (2011). RUNX1 mutations are frequent in de novo AML with noncomplex karyotype and confer an unfavorable prognosis. *Blood*, *117*(8), 2348-2357. doi:10.1182/blood-2009-11-255976

Schuurhuis, G. J., Heuser, M., Freeman, S., Béné, M.-C., Buccisano, F., Cloos, J., … Ossenkoppele, G. J. (2018). Minimal/measurable residual disease in AML: a consensus document from the European LeukemiaNet MRD Working Party. *Blood*, *131*(12), 1275-1291. doi:10.1182/blood-2017-09-801498

Shallis, R. M., Wang, R., Davidoff, A., Ma, X. and Zeidan, A. M. (2019). Epidemiology of acute myeloid leukemia: Recent progress and enduring challenges. *Blood Reviews*, *36*, 70-87. doi:10.1016/j.blre.2019.04.005

Shang, Y., Zhao, X., Xu, X., Xin, H., Li, X., Zhai, Y., … Chang, Z. (2009). CHIP functions an E3 ubiquitin ligase of Runx1. *Biochemical and Biophysical Research Communications*, *386*(1), 242-246. doi:10.1016/j.bbrc.2009.06.043

Shlush, L. I. and Minden, M. D. (2015). Preleukemia. *Current Opinion in Hematology*, *22*(2), 77-84. doi:10.1097/moh.0000000000000111

Shlush, L. I., Zandi, S., Mitchell, A., Chen, W. C., Brandwein, J. M., Gupta, V., … Dick, J. E. (2014). Identification of pre-leukaemic haematopoietic stem cells in acute leukaemia. *Nature*, *506*(7488), 328-333. doi:10.1038/nature13038

Shysh, A. C., Nguyen, L. T., Guo, M., Vaska, M., Naugler, C. and Rashid-Kolvear, F. (2017). The incidence of acute myeloid leukemia in Calgary, Alberta, Canada: a retrospective cohort study. *BMC Public Health*, *18*(1), 94. doi:10.1186/s12889-017-4644-6

Smith, C. C. and Shah, N. P. (2011). Tyrosine Kinase Inhibitor Therapy for Chronic Myeloid Leukemia: Approach to Patients with Treatment-Naive or Refractory Chronic-Phase Disease. *Hematology*, *2011*(1), 121-127. doi:10.1182/asheducation-2011.1.121

Smith, L. and Cidlowski, J. (2010). Progress in Brain Research. *Progress in Brain Research*, *182*, 1-30. doi:10.1016/s0079-6123(10)82001-1

Song, W., Sullivan, M., Legare, R., Hutchings, S., Tan, X., Kufrin, D., … Gilliland, D. (1999). Haploinsufficiency of CBFA2 causes familial thrombocytopenia with propensity to develop acute myelogenous leukaemia. *Nature genetics*, *23*(2), 166-75. doi:10.1038/13793

Sood, R., Kamikubo, Y. and Liu, P. (2017). Role of RUNX1 in hematological malignancies. *Blood*, *129*(15), 2070-2082. doi:10.1182/blood-2016-10-687830

Souffriau, J., Eggermont, M., Ryckeghem, S., Looveren, K., Wyngene, L., Hamme, E., … Libert, C. (2018). A screening assay for Selective Dimerizing Glucocorticoid Receptor Agonists and Modulators (SEDIGRAM) that are effective against acute inflammation. *Scientific Reports*, *8*(1), 12894. doi:10.1038/s41598-018-31150-w

Stavreva, D., Wiench, M., John, S., Conway-Campbell, B., McKenna, M., Pooley, J., … Hager, G. (2009). Ultradian hormone stimulation induces glucocorticoid receptor-mediated pulses of gene transcription. *Nature Cell Biology*, *11*(9), 1093-1102. doi:10.1038/ncb1922

Steensma, D. P., Bejar, R., Jaiswal, S., Lindsley, R. C., Sekeres, M. A., Hasserjian, R. P. and Ebert, B. L. (2015). Clonal hematopoiesis of indeterminate potential and its distinction from myelodysplastic syndromes. *Blood*, *126*(1), 9-16. doi:10.1182/blood-2015-03-631747

Stein, E., DiNardo, C., Pollyea, D., Fathi, A., Roboz, G., Altman, J., … Tallman, M. (2017). Enasidenib in mutant IDH2 relapsed or refractory acute myeloid leukemia. *Blood*, *130*(6), 722-731. doi:10.1182/blood-2017-04-779405

Strehl, C., Ehlers, L., Gaber, T. and Buttgereit, F. (2019). Glucocorticoids—All-Rounders Tackling the Versatile Players of the Immune System. *Frontiers in Immunology*, *10*, 1744. doi:10.3389/fimmu.2019.01744

Stone, R., Mandrekar, S., Sanford, B., Laumann, K., Geyer, S., Bloomfield, C., … Döhner, H. (2017). Midostaurin plus Chemotherapy for Acute Myeloid Leukemia with a FLT3 Mutation. *The New England Journal of Medicine*, *377*(5), 454-464. doi:10.1056/nejmoa1614359

SUN, L., GOROSPE, J. R., HOFFMAN, E. P. and RAO, A. K. (2006). Decreased platelet expression of myosin regulatory light chain polypeptide (MYL9) and other genes with platelet dysfunction and CBFA2/RUNX1 mutation: insights from platelet expression profiling: Platelet profiling in CBFA2/RUNX1 haplodeficiency. *Journal of Thrombosis and Haemostasis*, *5*(1), 146-154. doi:10.1111/j.1538-7836.2006.02271.x

Sun, L., Mao, G. and Rao, A. K. (2004). Association of CBFA2 mutation with decreased platelet PKC-θ and impaired receptor-mediated activation of GPIIb-IIIa and pleckstrin phosphorylation: proteins regulated by CBFA2 play a role in GPIIb-IIIa activation. *Blood*, *103*(3), 948-954. doi:10.1182/blood-2003-07-2299

Sundahl, N., Bridelance, J., Libert, C., Bosscher, K. and Beck, I. (2015). Selective glucocorticoid receptor modulation: New directions with non-steroidal scaffolds. *Pharmacology & Therapeutics*, *152*, 28-41. doi:10.1016/j.pharmthera.2015.05.001

Takahashi, A., Satake, M., Yamaguchi-Iwai, Y., Bae, S., Lu, J., Maruyama, M., … Arai, K. (1995). Positive and negative regulation of granulocyte-macrophage colony- stimulating factor promoter activity by AML1-related transcription factor, PEBP2. *Blood*, *86*(2), 607-616. doi:10.1182/blood.v86.2.607.bloodjournal862607

Tanaka, T., Kurokawa, M., Ueki, K., Tanaka, K., Imai, Y., Mitani, K., … Hirai, H. (1996). The extracellular signal-regulated kinase pathway phosphorylates AML1, an acute myeloid leukemia gene product, and potentially regulates its transactivation ability. *Molecular and Cellular Biology*, *16*(7), 3967-3979. doi:10.1128/mcb.16.7.3967

Tang, J.-L., Hou, H.-A., Chen, C.-Y., Liu, C.-Y., Chou, W.-C., Tseng, M.-H., … Tien, H.-F. (2009). AML1/RUNX1 mutations in 470 adult patients with de novo acute myeloid leukemia: prognostic implication and interaction with other gene alterations. *Blood*, *114*(26), 5352-5361. doi:10.1182/blood-2009-05-223784

Taniuchi, I., Osato, M., Egawa, T., Sunshine, M. J., Bae, S.-C., Komori, T., … Littman, D. R. (2002). Differential Requirements for Runx Proteins in CD4 Repression and Epigenetic Silencing during T Lymphocyte Development. *Cell*, *111*(5), 621-633. doi:10.1016/s0092-8674(02)01111-x

Thomas, A. L., Coarfa, C., Qian, J., Wilkerson, J. J., Rajapakshe, K., Krett, N. L., … Rosen, S. T. (2015). Identification of Potential Glucocorticoid Receptor Therapeutic Targets in Multiple Myeloma. *Nuclear Receptor Signaling*, *13*(1), nrs.13006. doi:10.1621/nrs.13006

Tilborg, Maa., Lefstin, J., Teuben, J.- and Yamamoto, K. (2000). Mutations in the glucocorticoid receptor DNA-binding domain mimic an allosteric effect of DNA 1 1Edited by P. E. Wright. *Journal of Molecular Biology*, *301*(4), 947-958. doi:10.1006/jmbi.2000.4001

Timmermans, S., Souffriau, J. and Libert, C. (2019). A General Introduction to Glucocorticoid Biology. *Frontiers in Immunology*, *10*, 1545. doi:10.3389/fimmu.2019.01545

Tissing, W., Lauten, M., Meijerink, J., Boer, Ml., Koper, J., Sonneveld, P. and Pieters, R. (2005). Expression of the glucocorticoid receptor and its isoforms in relation to glucocorticoid resistance in childhood acute lymphocytic leukemia. *Haematologica*, *90*(9), 1279-81.

Trumpp, A., Essers, M. and Wilson, A. (2010). Awakening dormant haematopoietic stem cells. *Nature Reviews Immunology*, *10*(3), 201-209. doi:10.1038/nri2726

Tyner, J. W., Tognon, C. E., Bottomly, D., Wilmot, B., Kurtz, S. E., Savage, S. L., … Druker, B. J. (2018). Functional genomic landscape of acute myeloid leukaemia. *Nature*, *562*(7728), 526-531. doi:10.1038/s41586-018-0623-z

Tzelepis, K., Koike-Yusa, H., De Braekeleer, E., Li, Y., Metzakopian, E., Dovey, O., … Yusa, K. (2016). A CRISPR Dropout Screen Identifies Genetic Vulnerabilities and Therapeutic Targets in Acute Myeloid Leukemia. *Cell Reports*, *17*(4), 1193-1205. doi:10.1016/j.celrep.2016.09.079

Uhlen, M., Karlsson, M., Zhong, W., Tebani, A., Pou, C., Mikes, J., … Brodin, P. (2019). A genome-wide transcriptomic analysis of protein-coding genes in human blood cells. *Science*, *366*(6472), eaax9198. doi:10.1126/science.aax9198

Vandevyver, S., Dejager, L. and Libert, C. (2012). On the Trail of the Glucocorticoid Receptor: Into the Nucleus and Back. *Traffic*, *13*(3), 364-374. doi:10.1111/j.1600-0854.2011.01288.x

Vandewalle, J., Luypaert, A., Bosscher, K. and Libert, C. (2018). Therapeutic Mechanisms of Glucocorticoids. *Trends in Endocrinology & Metabolism*, *29*(1), 42-54. doi:10.1016/j.tem.2017.10.010

Vardiman, J. W., Harris, N. L. and Brunning, R. D. (2002). The World Health Organization (WHO) classification of the myeloid neoplasms. *Blood*, *100*(7), 2292-2302. doi:10.1182/blood-2002-04-1199

Wang, C., Nanni, L., Novakovic, B., Megchelenbrink, W., Kuznetsova, T., Stunnenberg, H. G., … Logie, C. (2019). Extensive epigenomic integration of the glucocorticoid response in primary human monocytes and in vitro derived macrophages. *Scientific Reports*, *9*(1), 2772. doi:10.1038/s41598-019-39395-9

Wang, Q., Stacy, T., Binder, M., Marin-Padilla, M., Sharpe, A. and Speck, N. (1996). Disruption of the Cbfa2 gene causes necrosis and hemorrhaging in the central nervous system and blocks definitive hematopoiesis. *Proceedings of the National Academy of Sciences of the United States of America*, *93*(8), 3444-9. doi:10.1073/pnas.93.8.3444

Wang, T., Birsoy, K., Hughes, N. W., Krupczak, K. M., Post, Y., Wei, J. J., … Sabatini, D. M. (2015). Identification and characterization of essential genes in the human genome. *Science*, *350*(6264), 1096-1101. doi:10.1126/science.aac7041

Wang, Z.-Y. and Chen, Z. (2008). Acute promyelocytic leukemia: from highly fatal to highly curable. *Blood*, *111*(5), 2505-2515. doi:10.1182/blood-2007-07-102798

West, A. H., Godley, L. A. and Churpek, J. E. (2014). Familial myelodysplastic syndrome/acute leukemia syndromes: a review and utility for translational investigations. *Annals of the New York Academy of Sciences*, *1310*(1), 111-8. doi:10.1111/nyas.12346

Wiggers, C. R. M., Baak, M. L., Sonneveld, E., Nieuwenhuis, E. E. S., Bartels, M. and Creyghton, M. P. (2019). AML Subtype Is a Major Determinant of the Association between Prognostic Gene Expression Signatures and Their Clinical Significance. *Cell Reports*, *28*(11), 2866-2877.e5. doi:10.1016/j.celrep.2019.08.012

Wilkinson, L., Verhoog, N. and Louw, A. (2018). Disease- and treatment-associated acquired glucocorticoid resistance. *Endocrine Connections*, *7*(12), R328-R349. doi:10.1530/ec-18-0421

Winer, E. S. and Stone, R. M. (2019). Novel therapy in Acute myeloid leukemia (AML): moving toward targeted approaches. *Therapeutic Advances in Hematology*, *10*, 204062071986064. doi:10.1177/2040620719860645

Wolf, D. and Langhans, S. (2019). Moving Myeloid Leukemia Drug Discovery Into the Third Dimension. *Frontiers in Pediatrics*, *7*, 314. doi:10.3389/fped.2019.00314

Wood, A., Savage, D. and Antman, K. (2002). Imatinib Mesylate — A New Oral Targeted Therapy. *New England Journal of Medicine*, *346*(9), 683-693. doi:10.1056/nejmra013339

Wright, A., Nuñez, J. and Doudna, J. (2016). Biology and Applications of CRISPR Systems: Harnessing Nature's Toolbox for Genome Engineering. *Cell*, *164*(1-2), 29-44. doi:10.1016/j.cell.2015.12.035

Wunderlich, M., Chou, F.-S., Link, K. A., Mizukawa, B., Perry, R. L., Carroll, M. and Mulloy, J. C. (2010). AML xenograft efficiency is significantly improved in NOD/SCID-IL2RG mice constitutively expressing human SCF, GM-CSF and IL-3. *Leukemia*, *24*(10), 1785-8. doi:10.1038/leu.2010.158

Yamaguchi, Y., Kurokawa, M., Imai, Y., Izutsu, K., Asai, T., Ichikawa, M., … Hirai, H. (2004). AML1 Is Functionally Regulated through p300-mediated Acetylation on Specific Lysine Residues. *Journal of Biological Chemistry*, *279*(15), 15630-15638. doi:10.1074/jbc.m400355200

Yang, X. and Wang, J. (2018). Precision therapy for acute myeloid leukemia. *Journal of Hematology & Oncology*, *11*(1), 3. doi:10.1186/s13045-017-0543-7

Yergeau, D. A., Hetherington, C. J., Wang, Q., Zhang, P., Sharpe, A. H., Binder, M., … Zhang, D.-E. (1997). Embryonic lethality and impairment of haematopoiesis in mice heterozygous for an AML1-ETO fusion gene. *Nature Genetics*, *15*(3), 303-306. doi:10.1038/ng0397-303

Yu, M., Mazor, T., Huang, H., Huang, H.-T., Kathrein, K. L., Woo, A. J., … Cantor, A. B. (2012). Direct Recruitment of Polycomb Repressive Complex 1 to Chromatin by Core Binding Transcription Factors. *Molecular Cell*, *45*(3), 330-343. doi:10.1016/j.molcel.2011.11.032

Zen, M., Canova, M., Campana, C., Bettio, S., Nalotto, L., Rampudda, M., … Doria, A. (2011). The kaleidoscope of glucorticoid effects on immune system. *Autoimmunity Reviews*, *10*(6), 305-310. doi:10.1016/j.autrev.2010.11.009

Zeng, C., Wijnen, A. J. van, Stein, J. L., Meyers, S., Sun, W., Shopland, L., … Hiebert, S. W. (1997). Identification of a nuclear matrix targeting signal in the leukemia and bone-related AML/CBF- transcription factors. *Proceedings of the National Academy of Sciences*, *94*(13), 6746-6751. doi:10.1073/pnas.94.13.6746

Zeng, Z., Liu, W., Tsao, T., Qiu, Y., Zhao, Y., Samudio, I., … Andreeff, M. (2017). High-throughput profiling of signaling networks identifies mechanism-based combination therapy to eliminate microenvironmental resistance in acute myeloid leukemia. *Haematologica*, *102*(9), 1537-1548. doi:10.3324/haematol.2016.162230

Zhang, D. E., Fujioka, K., Hetherington, C. J., Shapiro, L. H., Chen, H. M., Look, A. T. and Tenen, D. G. (1994). Identification of a region which directs the monocytic activity of the colony-stimulating factor 1 (macrophage colony-stimulating factor) receptor promoter and binds PEBP2/CBF (AML1). *Molecular and Cellular Biology*, *14*(12), 8085-8095. doi:10.1128/mcb.14.12.8085

Zhang, D. E., Hetherington, C. J., Meyers, S., Rhoades, K. L., Larson, C. J., Chen, H. M., … Tenen, D. G. (1996). CCAAT enhancer-binding protein (C/EBP) and AML1 (CBF alpha2) synergistically activate the macrophage colony-stimulating factor receptor promoter. *Molecular and Cellular Biology*, *16*(3), 1231-1240. doi:10.1128/mcb.16.3.1231

Zhao, X., Jankovic, V., Gural, A., Huang, G., Pardanani, A., Menendez, S., … Nimer, S. (2008). Methylation of RUNX1 by PRMT1 abrogates SIN3A binding and potentiates its transcriptional activity. *Genes & Development*, *22*(5), 640-653. doi:10.1101/gad.1632608

Chapter 2: Chemogenomic landscape of *RUNX1*-mutated AML reveals importance of *RUNX1* allele dosage in genetics and glucocorticoid sensitivity

Laura Simon[1], Vincent-Philippe Lavallée[1,2], Marie-Eve Bordeleau[1], Jana Krosl[1], Irène Baccelli[1], Geneviève Boucher[1], Bernhard Lehnertz[1], Jalila Chagraoui[1], Tara MacRae[1], Réjean Ruel[1], Yves Chantigny[1], Sébastien Lemieux[1,3], Anne Marinier[1,4], Josée Hébert[1,2,5,6,*] and Guy Sauvageau[1,2,5,6,*].

[1] The Leucegene Project at Institute for Research in Immunology and Cancer, Université de Montréal. [2] Division of Hematology, Maisonneuve-Rosemont Hospital. [3] Department of Computer Science and Operations Research, Université de Montréal. [4] Department of Chemistry, Université de Montréal. [5] Leukemia Cell Bank of Quebec, Maisonneuve-Rosemont Hospital. [6] Department of Medicine, Faculty of Medicine, Université de Montréal, Montréal, Canada.

*Corresponding Authors
Corresponding Authors: Guy Sauvageau, Institute for Research in Immunology and Cancer (IRIC), P.O. Box 6128, Downtown Station, Montreal, Quebec H3C 3J7, Canada. Phone: 514-343-7134; Fax: 514-343-5839; E-mail: guy.sauvageau@umontreal.ca; and Josée Hébert, josee.hebert@umontreal.ca

Running title: ***RUNX1* dosage in genetics and GC sensitivity of *RUNX1*^{mut} AML**

Keywords: Acute Myeloid Leukemia; RUNX1; RNA-sequencing; chemical screening; glucocorticoids.

Manuscript published in ***Clinical Cancer Research*** 2017 Nov 15;23(22):6969-6981.

doi: 10.1158/1078-0432.CCR-17-1259.

2.1 Author contributions

L.S., V.-P.L., M.-E.B., J.H. and G.S. designed the experiments and wrote the manuscript. L.S. performed chemical screens, conducted functional experiments and analyzed the results. V.-P.L. performed mutation and transcriptomic characterization and contributed to chemical screens analyses. M.-E.B. spearheaded the data analysis and manuscript redaction. J.K. and I.B. performed original chemical screen. G.B. and S.L. assisted with data analysis. B.L. and J.C. contributed to experiment design, data analysis, and figure editing. B.L. and T.M. constructed lentivirus vectors used in this study. R.R., Y.C. and A.M., provided chemistry expertise regarding experiments involving GCs.

Contribution:

Data in Figures 2.4(b),(c),(d), 2.5(a),(b), 2.6, S2.4, S2.5, S2.6, S2.7, and S2.8 were generated by Laura Simon (100%).

Data in Figures 2.3(a),(b),(d) were generated by Jana Krosl and Irène Baccelli.

Data in Figures S2.2(a),(b) and S2.3 were generated by Irène Baccelli.

Data in Figure 2.3(c) was generated by Laura Simon and Jana Krosl.

Data in Figure 2.5(c) was generated by Laura Simon and analysis and figure generated by Vincent-Philippe Lavallée.

Data analysis and figure generation for Figures 2.1, 2.2, S2.1 and tables S2.1, S2.2, S2.3, S2.4, S2.5, and S2.6 were done by Vincent-Philippe Lavallée (100%).

2.2 Statement of translational relevance

This study characterized the effect of *RUNX1* allele dosage on the gene expression profile and glucocorticoid sensitivity of primary *RUNX1*^{mut} AML specimens. Our findings suggest a new role for *RUNX1* in the glucocorticoid response and support the rationale to evaluate the addition of glucocorticoids in preclinical models of *RUNX1*^{mut} AML.

2.3 Abstract

Purpose: *RUNX1*-mutated (*RUNX1*^{mut}) Acute Myeloid Leukemia (AML) is associated with adverse outcome, highlighting the urgent need for a better genetic characterization of this AML subgroup and for the design of efficient therapeutic strategies for this disease. Towards this goal, we further dissected the mutational spectrum and gene expression profile of *RUNX1*^{mut} AML and correlated these results to drug sensitivity to identify novel compounds targeting this AML subgroup.

Experimental design: RNA-sequencing of 47 *RUNX1*^{mut} primary AML specimens was performed and sequencing results were compared to those of *RUNX1* wild-type samples. Chemical screens were also conducted using *RUNX1*^{mut} specimens to identify compounds selectively affecting the viability of *RUNX1*^{mut} AML.

Results: We show that samples with no remaining *RUNX1* wild-type allele are clinically and genetically distinct and display a more homogeneous gene expression profile. Chemical screening revealed that most *RUNX1*^{mut} specimens are sensitive to glucocorticoids (GCs) and we confirmed that GCs inhibit AML cell proliferation through their interaction with the Glucocorticoid Receptor (GR). We observed that specimens harboring *RUNX1* mutations expected to result in low residual RUNX1 activity are most sensitive to GCs, and that co-associating mutations as well as that GR levels contribute to GC sensitivity. Accordingly, acquired glucocorticoid sensitivity was achieved by negatively regulating *RUNX1* expression in human AML cells.

Conclusion: Our findings show the profound impact of *RUNX1* allele dosage on gene expression profile and glucocorticoid sensitivity in AML, thereby opening opportunities for preclinical testing which may lead to drug repurposing and improved disease characterization.

2.4 Introduction

RUNX1 is a master regulator of definitive hematopoiesis where it regulates the differentiation of myeloid, megakaryocytic and lymphocytic lineage progenitors (1,2). RUNX1 is part of the core binding factor (CBF) transcriptional complex, and its transcriptional activity is dependent on the recruitment of its heterodimeric partner, CBFB. RUNX1 contains a RUNT domain at its N-terminus that is responsible for both DNA binding and protein heterodimerization (3). The C-terminal region of the protein encompasses domains for nuclear localization and regulation of DNA binding (4), as well as for the interaction with lineage specific transcription factors, transcriptional coactivators and corepressors.

Anomalies involving the *RUNX1* gene or its partner *CBFB* have been implicated in the pathogenesis of subsets of human myeloid and lymphoblastic leukemias (5). The *RUNX1* and *CBFB* genes are involved in the t(8;21)(q22;q22) and inv(16)(p13.1q22) chromosomal rearrangements, respectively, and these entities constitute the CBF Acute Myeloid Leukemia (AML) subgroup (6,7). Prognosis is favorable for patients carrying these cytogenetic anomalies when compared with other AML subtypes (8). In addition to chromosomal rearrangements, mutations in the *RUNX1* gene are also found in myelodysplastic syndrome (MDS) and in 10-21% of AMLs where they are associated with French-American-British (FAB) M0 morphology (9–11). In contrast to CBF AMLs, *RUNX1*^{mut} AMLs are associated with adverse outcome (11–17). In a large proportion of cases, *RUNX1*^{mut} AMLs harbor normal karyotype or non-complex chromosomal imbalances, with a frequent association with trisomy 13 (12–15). *RUNX1* mutations are also generally mutually exclusive of recurrent translocations in AML, and mutational analyses using targeted approaches revealed that *RUNX1* mutations co-occur with mutations in epigenetic modifiers, such as *ASXL1*, splicing factors, *STAG2*, *BCOR* and *PHF6* (14,17). Microarray analysis has been used to derive a *RUNX1* mutation-associated gene expression signature (17), however a complete assessment of the mutational and gene expression landscape of *RUNX1*^{mut} AML is lacking.

Two types of mutations in *RUNX1* have been described in AML: missense mutations found in the RUNT domain, and nonsense or frameshift mutations distributed throughout the entire gene. Some frameshift mutations located in the C-terminal region produce elongated versions of the protein with intact DNA binding activity that retain the ability to heterodimerize with CBFB and that are believed to act as dominant negatives (10,12,15,18). Approximately 30% of *RUNX1* mutations

occur in combination (i.e. double heterozygosity) or are associated with a loss of heterozygosity, both of which lead to a complete loss of wild-type *RUNX1* in these leukemias (15). In line with this, it has been proposed that the greater the extent of *RUNX1* inactivation in hematopoietic cells, the higher the propensity to develop leukemia, suggesting a dependence on RUNX1 protein dosage for disease onset (19,20).

The unique genetic, biological and clinical features of *de novo* AMLs with mutated *RUNX1* prompted its suggestion as a distinct entity in the 2016 revision of the World Health Organization (WHO) classification of myeloid neoplasms (21). The poor outcome of patients suffering from *RUNX1*^{mut} leukemias highlights the need to better understand the genetics of this disease and to develop more specific and efficient therapeutic strategies. In this study, we further dissected the mutational spectrum and gene expression profile of *RUNX1*^{mut} AML and correlated these results to drug sensitivity. This was accomplished by RNA sequencing of the 47 *RUNX1*^{mut} specimens included in the Leucegene cohort and by testing the sensitivity of these specimens to a collection of small molecules. This effort represents the first chemogenomic assessment of *RUNX1*^{mut} AML.

2.5 Materials and Methods

2.5.1 Primary AML specimens

The Leucegene project is an initiative approved by the Research Ethics Boards of Université de Montréal and Maisonneuve-Rosemont Hospital. As part of this project, RNA sequencing of 415 primary AML specimens from various cytogenetic groups was performed as previously described (22). All leukemia samples were collected and characterized by the Quebec Leukemia Cell Bank (BCLQ). RNA sequencing data is available at GEO or through the Leucegene web page: leucegene.ca/research/resources/.

2.5.2 Next-generation sequencing and mutation validations

Sequencing was performed as previously described (22). Sequenced data were mapped to the reference genome hg19 according to RefSeq annotations (UCSC, April 16th 2014). Variants were all identified using CASAVA 1.8.2 or km (https://bitbucket.org/iric-soft/km) approaches according to the previously reported pipeline (23). All variants present in 97 genes mutated in myeloid cancers or in acute leukemias were investigated (**Table S2.1**). Genes and positions from **Table S2.5** were also investigated by km approach previously described, using a 5% VAF cutoff for missense and nonsense mutations as well as for indels confirmed by another approach, of 10% for other indels. *RUNX1* longest isoform (NM_001754/NP_001745.2) was used for representations.

2.5.3 Primary AML cell culture and chemical screens

Freshly thawed primary AML specimens were used for chemical screens. Cryopreserved cells were thawed at 37°C in Iscove's modified Dulbecco's medium (IMDM) containing 20% FBS and DNase I (100 µg/ml). Cells were resuspended in IMDM supplemented with 15% BIT (bovine serum albumin, insulin, transferrin; Stem Cell Technologies), 100 ng/ml SCF (Shenandoah 100-04), 50 ng/ml FLT3L (Shenandoah), 20 ng/ml IL-3 (Shenandoah), 20 ng/ml G-CSF (Shenandoah), 10^{-4} M β-mercaptoethanol, gentamicin (50 µg/ml), ciprofloxacin (10 µg/ml), SR1 (500 nM, Alichem) and UM729 (500 nM, IRIC) and 5000 cells were plated per well of 384 well white plates in 50µl. Compounds were dissolved in DMSO and diluted in media immediately before use. Compounds were added to plated cells by Biomek automatic pipettor at a final DMSO concentration of 0.1%. Glucocorticoids were tested in the exploratory screen at single doses of 2.5 µM as described (24). In the confirmatory screen, compounds were added in serial dilutions (ranging from 10,000 nM to

4.5 nM). Cells were grown in culture in the presence of compounds for 6 days before determining cell viability using luminescent CellTiter Glo assay (Promega). Absolute IC_{50} values were calculated using ActivityBase SARview Suite. For cases where compounds failed to inhibit AML cell survival/proliferation, IC_{50} values were reported as the highest concentration tested (10,000 nM). Compounds that showed more than 50% inhibition at the lowest concentration tested had IC_{50} assigned as the lowest dose tested (4.5 nM). Dose response curves were generated using GraphPad Prism 5.0. Heat map representations of IC_{50} values were created using GENE-E software (http://www.broadinstitute.org/cancer/software/GENE-E).

2.5.4 AML cell lines and chemical screen

AML cell lines were purchased from the DSMZ German collection of Microorganisms and cell culture (Leibniz Institute), the ATCC, the University Health Network, or otherwise donated from collaborators. Cell lines were obtained from January to October 2015, and no authentication test was done by the authors. Cells were cultured according to manufacturer's or collaborator's instructions. The chemical screen performed with AML cell lines was carried out as described for primary AML cells with a few modifications. Compounds were added at concentrations ranging from 20,000 nM to 1 nM. Cell viability was evaluated after 7 days of culture in the presence of compounds using the CellTiter Glo assay (Promega).

2.5.5 Knockdown experiments

Lentiviral vectors carrying shRNAs targeting the *RUNX1* and *NR3C1* genes were generated by cloning appropriate shRNA sequences as described in (25) into MNDU vectors comprising miR-E sequences as well as GFP or YFP. Control vector (shNT) contained shRNA targeting renilla luciferase. Lentiviruses were produced in HEK-293 cells and AML cell lines were infected with lentiviruses in media supplemented with 10 ng/mL polybrene for 48 hrs. Infection efficiency, as determined by the percentage of GFP or YFP positive cells, was monitored by flow cytometry using a BD FACSCantoII flow cytometer. Infected cells were sorted using a BD Aria II cell sorter and knockdown efficiency was determined by quantitative RT-PCR and western botting using standard methods.

2.5.6 Immunofluorescence

AML cell lines treated or not with Dexamethasone were applied to 0.01% poly-L-lysine-coated (Sigma) iBIDI chambers and were fixed with 4% paraformaldehyde (PFA) in PBS for 10 minutes at room temperature. Cells were incubated with permeabilization/blocking solution (0.25% Triton-X, 1% BSA in PBS) for 40 minutes and incubated with primary antibodies against GR (1:50, Cell Signaling 12041) and CD44-FITC (1:400) (eBioscience 11-0441-85) for one hour at room temperature. GR signal was revealed using Cy3-conjugated anti-rabbit secondary antibody (1:2000) which was incubated with cells for 40 minutes at room temperature. Images were acquired on a Zeiss LSM 700 confocal laser scanning microscope.

2.5.7 Statistical Analysis

Mutations and transcriptome:

Statistical tests for mutation and gene expression analyses were performed using R version 3.2.3. Fisher's exact test was used in the analysis of contingency tables. Analysis of continuous variables and differential gene expression was performed using the Wilcoxon rank-sum test. False discovery rate (FDR) method was applied for global gene analysis.

Chemical screens and functional studies:

Figure 3b shows the Spearman correlation between the inhibitory responses of compounds of the GC cluster. Growth inhibition is presented as rank transformed percentage of inhibition. (100 – (100 x (Number of cells (compound)/Mean number of cells (DMSO controls)). In Figure 5b, Fisher's exact test was used to test the association of the type of *RUNX1* mutation and GC sensitivity in GraphPad Prism 5.0. In Figure 5c, the difference in response to compounds between mutation groups was calculated based on IC_{50} values using Wilcoxon rank-sum test in R. The highest dose tested (10,000 nM) was arbitrarily assigned to samples when the compounds failed to inhibit 50% of cell proliferation. Similarly, the lowest dose tested (4.5 nM) was reported in cases where the inhibitory response was higher than 50% at the lowest dose. Determination of differentially active compounds in mutation subgroups was performed using Wilcoxon rank sum test on IC_{50} values in R. In Figure 6c, the differences in IC_{50} values between OCI-AML5 cells expressing shNT and OCI-AML5 cells expressing sh*RUNX1* were calculated using Wilcoxon rank-sum test in R. In Figure 5c, Figure 6b, 6d, Supplementary Figure 8d, and 8e p values were calculated using two-tailed Student's *t* test in GraphPad Prism 5.0.

2.6 Results

RNA sequencing data of 47 *RUNX1*^{mut} primary AML specimens was compared to that of 368 control *RUNX1* wild-type (*RUNX1*^{wt}) samples, which were sequenced as part of the Leucegene project (22) (**Table S2.1**). *RUNX1*^{mut} specimens were associated with older age, FAB M0 morphology, intermediate-risk cytogenetics with abnormal karyotype (**Figure 2.1a)** and poor patient survival (**Figure 2.1b**) compared to *RUNX1*^{wt} specimens, in accordance with published characteristics (14,26). Twenty-seven specimens (57%) carried a nonsense or frameshift mutation (*RUNX1*$^{ns/fs}$), whereas twenty specimens (43%) were characterized by missense mutations only (*RUNX1*^{mis}) (**Table S2.2**). As previously reported, most missense mutations were located in the RUNT domain whereas nonsense/frameshift mutations were more widely distributed (**Figure 2.1c**) (18). No significant differences in clinical and laboratory characteristics were observed between *RUNX1*$^{ns/fs}$ and *RUNX1*^{mis} AML samples (data not shown). Fourteen samples (30%) were characterized by either homozygous *RUNX1* mutations, defined by a variant allele frequency (VAF) greater than 75%, or by double heterozygous mutations (*RUNX1*$^{-/-}$ in **Figure 2.1d**, on the left), suggesting that an important percentage of *RUNX1*^{mut} cases have very little remaining RUNX1 activity.

2.6.1 *RUNX1*^{mut} AMLs are genetically distinct

Specimens of our *RUNX1*^{mut} cohort harbored mutations in 39 different genes (**Figure 2.1d** and **Table S2.3**). These included: *ASXL1* (18/47, 38%), *SRSF2* (13/47, 28%), *TET2* (10/47, 21%), *FLT3* (9/47, 19%), *BCOR* and *NRAS* (8/47 each, 17%), *DNMT3A* (7/47, 15%), *KMT2A*/*MLL* and *STAG2* (6/47 each, 13%), *CEBPA*, *EZH2*, *IDH1* and *IDH2* (5/47 each, 11%), *JAK2*, *TP53* and *U2AF1* (4/47 each, 9%) as well as *KRAS* and *NF1* (3/47 each, 6%) (**Figure 2.1d** and **Table S2.3**). Statistical analysis revealed that *ASXL1*, *SRSF2*, *BCOR*, *EZH2*, *JAK2, STAG2* and *PHF6* mutations significantly associated with *RUNX1* mutations, whereas an anti-association was found between *RUNX1* and *NPM1* or *FLT3* mutations (**Figure 2.1d**). Mutations in components of the spliceosome such as *SRSF2* and *SF3B1* have been previously reported in *RUNX1*^{mut} AML (27), however when comparing *RUNX1*$^{ns/fs}$ and *RUNX1*^{mis} specimens, we observed an association between *SRSF2* and *RUNX1*$^{ns/fs}$ mutations (12/27 for *RUNX1*$^{ns/fs}$ vs 1/20 for *RUNX1*^{mis}, p = 0.003, **Figure 2.1d**). This

association between splicing genes and *RUNX1* mutations remained highly significant (p = 0.009) when all splicing genes (*SRSF*2, *U2AF1*, *SF3B1*) were considered, suggesting a possible link between loss of *RUNX1* function and altered splicing activity in AML. Moreover, FAB M0 morphology and trisomy 13, which are 2 characteristic features of *RUNX1*^{mut} AMLs, were significantly associated to samples with no remaining *RUNX1* wild-type allele (*RUNX1*$^{-/-}$), compared to samples carrying *RUNX1* heterozygous mutations (*RUNX1*$^{-/+}$) (36% vs 9% for trisomy 13 and 57% vs 9% for M0, **Figure 2.1d,** right panel). Furthermore, *RUNX1*$^{-/-}$ samples harboring either nonsense or frameshift mutations were also significantly associated with *ASXL1* mutations (86% vs 30%, **Figure 2.1d**, right panel). On the other end of the spectrum, RUNX1$^{-/+}$ AML samples, especially those with heterozygous missense mutations, are enriched for mutations in *EZH2* and in *CEBPA*. Altogether, these data suggest that *RUNX1*^{mut} samples lacking a wild-type *RUNX1* allele display distinct genetic features (e.g. trisomy 13 and M0 in RUNX1$^{-/-}$ versus EZH2 and CEBPA in RUNX1$^{-/+}$).

2.6.2 *RUNX1* allele dosage determines gene expression signature

Comparative transcriptomic analysis of *RUNX1*^{mut} and *RUNX1*^{wt} specimens revealed a list of 100 differentially expressed candidate genes (**Figure 2.2a** and **Table S2.4**). Projecting *RUNX1*^{mut} specimens on a PCA representation constructed with these 100 genes predictably identified most *RUNX1*^{mut} specimens, but lacked the specificity previously reported for other AML subgroups (28,29). Indeed, several *RUNX1*^{mut} specimens were in the vicinity of control *RUNX1*^{wt} AML specimens (**Figure 2.2b**). Interestingly, we observed a correlation between *RUNX1* allele dosage and the expression levels of the most specific transcripts of the *RUNX1*^{mut} signature such as *BAALC* and *DNTT* (**Figure 2.2a, c** and **Figure S2.1**). These 2 genes are expressed at much higher levels in specimens homozygous for nonsense/frameshift *RUNX1* mutations than in those with heterozygous missense mutations (**Figure 2.2c**). This highlights the importance of considering the degree of wild-type *RUNX1* loss to accurately reveal the gene expression profile of this AML subgroup.
Following the hypothesis that mutation type and allelic burden are determinant in *RUNX1*^{mut} AML, we derived a model which identified transcripts whose expression is determined by *RUNX1* allele dosage (**Figure 2.2d** and **Table S2.6**). Consistent with the ability of RUNX1 to regulate its own expression (30) the *RUNX1* transcript was among the most positively correlated ones (**Figure 2.2d**). Interestingly, *TCF4* was the 2nd top candidate (**Figure 2.2d**). TCF4 recognizes the CANNTG

binding site, an E-box found to be enriched in the promoter of genes identified by our model ($q = 1.17 \times 10^{-4}$), suggesting that it may play a role in establishing the *RUNX1*^{mut} signature as recently suggested for Blastic Plasmacytoid Dendritic Cell Neoplasms (BPDCNs) (31).

2.6.3 *RUNX1* mutations are associated with glucocorticoid sensitivity

To identify small molecules selectively affecting the survival of *RUNX1*^{mut} AML cells we screened a panel of primary AML specimens, which included *RUNX1*^{mut} and *RUNX1*^{wt} samples, selected to represent the genetic heterogeneity of the disease, with a library of compounds enriched for clinically approved drugs. This strategy was rendered possible by our advanced cell culture conditions which transiently support the *ex vivo* activity of leukemia progenitor/stem cells (32). This initial screen revealed groups of compounds exhibiting similar patterns of inhibition across specimens, which we named "compound correlation clusters" (CCCs) (24). One such cluster identified in the screen was the glucocorticoid (GC) cluster, which comprises 34 compounds sharing structural similarities (**Figure 2.3a** and **Figure S2.2**). Interestingly, primary AML specimens found to be sensitive to GCs in the screen were enriched in samples harboring *RUNX1* mutations (4/6 GC sensitive specimens were mutated for *RUNX1*, p=0.003, and **Figure 2.3b**). To further explore the link between GC sensitivity and *RUNX1* status, we interrogated a cohort of *RUNX1*^{mut} specimens and of specimens carrying a t(8;21) translocation resulting in the *RUNX1-RUNX1T1* fusion with compounds of the glucocorticoid cluster (**Figure 2.3c**). We observed that *RUNX1*^{mut} specimens and those presenting *RUNX1-RUNX1T1* fusions were more frequently sensitive to GCs than *RUNX1*^{wt} samples (**Figure 2.3c**). Primary AML specimens responded similarly to all compounds of the GC cluster, indicating that these compounds most likely share a common target and operate via the same mechanism (**Figure 2.3b and 2.3c**). Notably, an impressive difference in GC IC_{50} was observed between sensitive and resistant specimens, ranging from single digit nM for sensitive samples to >10,000 nM for resistant ones, with few cases of intermediate sensitivity (**Figure 2.3d** and **Figure S2.3**). These results suggest that *RUNX1* loss of function confers sensitivity to GCs in AML.

2.6.4 Glucocorticoid receptor mediates the GC response in AML

GCs are glucocorticoid receptor (GR) agonists that cause its translocation into the nucleus to modulate transcription of specific genes (33). The possibility that GR is the target through which GC affect AML cell behavior was first evaluated using a panel of AML-derived cell lines (**Figure S2.4**). The ability of GCs to induce translocation of the GR from the cytoplasm to the nucleus was intact in the different AML cell lines tested (**Figure 2.4a** and data not shown for other cell lines due to space limitation). We observed that treatment of GC sensitive Kasumi-1 and OCI-AML3 cell lines with increasing concentrations of the GR antagonist RU486 progressively decreases their GC sensitivity (**Figure 2.4b** for Dexamethasone and **Figure S2.5** for Mometasone furoate), demonstrating that GR inhibition prevents GCs from exerting their effect on cell viability. To validate this hypothesis, we designed shRNAs targeting the GR gene, *NR3C1*, producing 75 to 90% gene knockdown and a corresponding decrease in GR protein levels in OCI-AML3 cells (**Figure 2.4c**), and observed that GR knock-down abrogates the antiproliferative effect of GCs, and enables proliferation of sh*NR3C1*-expressing cells in GC-supplemented media (**Figure 2.4d** for Dexamethasone and **Figure S2.6** for other GCs). Altogether, these results suggest that GCs inhibit AML cell proliferation through their interaction with the GR.

2.6.5 *RUNX1* allele dosage and co-associated mutations contribute to GC sensitivity

About one third of *RUNX1*^{mut} specimens did not respond to GC treatment (**Figure 2.3c**). To gain further insight into the impact of *RUNX1* mutations on GC response, we determined the IC_{50} values of at least one GC (dexamethasone, hydrocortisone, and/or flumethasone) in an enlarged cohort of 33 *RUNX1*^{mut} primary AML samples. We observed that *RUNX1*$^{fs/ns}$ specimens showed increased sensitivity to GCs when compared to *RUNX1*^{mis} specimens (**Figure 2.5a**), suggesting a strong impact of *RUNX1* allele dosage on GC sensitivity. In support of this, we observed that missense mutations reported to have no impact on RUNX1 function were enriched among GC-resistant specimens, whereas frameshift mutations predicted to produce elongated versions of RUNX1 with dominant negative activity (10,12,18) were more frequent in the GC-sensitive group (p=0.03, compare distribution of *RUNX1*^{mis} (blue triangles) to that of dominant negatives (red diamonds) in **Figure 2.5b**). Nonetheless, 10-18% of *RUNX1*^{mis} specimens were sensitive to GCs, and similarly, 14-18% of *RUNX1*$^{ns/fs}$ were resistant (**Figure 2.5a**). To identify genetic lesions that may contribute to modulation of GC responsiveness, we analyzed GC sensitivity of various defined genetic groups of AML. We found that *CEBPA*^{bi} and *SRSF2*-mutated specimens were significantly more sensitive

to GCs than other leukemias (**Figure 2.5c**), and GC-sensitive *RUNX1*^{mut} specimens were enriched for these two mutations (**Figure 2.5b**).

Given that Acute Lymphoblastic Leukemias (ALL) are known to respond to GCs, we examined the expression of lymphoid markers in specimens of the Leucegene collection. t(8;21) specimens exhibited elevated expression of these markers (**Figure S2.7**), however *RUNX1*^{mut} specimens did not, thereby suggesting that lymphoid lineage associated genes do not contribute to the GC response of *RUNX1*^{mut} specimens. Interestingly, we observed that samples expressing the highest levels of *NR3C1* were enriched with specimens harboring *SRSF2* and *RUNX1* mutations (**Figure S2.7**), suggesting that GR levels influence GC sensitivity for these mutation groups. However, the resistance of *RUNX1*^{mut} specimens to GCs could not be explained by altered expression levels of wild-type *RUNX1, NR3C1, CEBPA* or *SRSF2* (**Figure S2.7**). These observations suggest that inactivation of *RUNX1* is associated with *NR3C1* upregulation and sensitivity to GCs, and that interference with the function of the splicing machinery (*SRSF2*) or of other transcription factors (*CEBPA*), and possibly other yet to be identified processes, also appears to be involved in the GC response in AML cells.

2.6.6 *RUNX1* silencing sensitizes AML cells to GCs

To validate our model predicting that *RUNX1* dosage and the resulting RUNX1 protein availability modulate GC responsiveness, we evaluated how *RUNX1* silencing affects survival of GC-resistant AML cell lines in GC-supplemented media. We designed shRNAs targeting *RUNX1* for which gene knockdown and reduction of RUNX1 protein levels were validated in OCI-AML5 cells (**Figure 2.6a**). We observed that *RUNX1* silencing was able to sensitize 5 of the 8 AML cell lines tested to Dexamethasone (**Figure 2.6b**). A *RUNX1* level-dependent shift in Dexamethasone sensitivity as revealed by a decrease in IC_{50} values for sh*RUNX1*-expressing cells compared to controls, reaching 2 digit nanomolar range in these engineered cells, was observed in OCI-AML5 (**Figure 2.6c**) and OCI-AML1 cells (**Figure S2.8**). Interestingly, a concomitant increase in *NR3C1* expression was noted in these cells, further strengthening the idea that GR levels impact on the GC response (**Figure 2.6d** and **Figure S2.8**). In accordance with the increased GC sensitivity observed for sh*RUNX1*-expressing cells, Dexamethasone induced pronounced apoptosis in OCI-AML5 cells upon *RUNX1* knockdown (**Figure 2.6e**). The GC-sensitizing effect of *RUNX1* dosage was also observed for other GCs, such as Flumethasone and Budesonide (**Figure S2.8**), and appeared to be

specific to the GC response, as it was not observed with other cytotoxic agents such as cytarabine and 6-thioguanine (**Figure 2.6f and Figure S2.8**). In summary, our data provide functional evidence that RUNX1 dosage influences GC sensitivity, suggesting a novel role for RUNX1 in the response to GCs in AML cells.

2.7 Discussion

In this study we used a chemogenomic approach to characterize *RUNX1*^{mut} AML. RNA sequencing confirmed most mutations in other genes previously reported for this subgroup. Interestingly, *RUNX1* allele dosage appears to identify a clinically and genetically distinct subgroup of AML patients lacking a wild-type *RUNX1* allele (*RUNX1*$^{-/-}$), as demonstrated by their frequent association with M0 morphology and trisomy 13, as well as with *ASXL1* mutations in nonsense or frameshift cases. Our observations complement a recent report associating *RUNX1*$^{-/-}$ samples to adverse clinical outcome (34). Altogether, these data suggest that *RUNX1*^{mut} AML, which has been recently added as a provisional entity in the WHO classification, may be more heterogeneous than previously believed. This *RUNX1* allele dosage effect also revealed the complexity of the *RUNX1* AML gene signature and appears to predispose AML cells to GC sensitivity or resistance. To the best of our knowledge, this is the first study linking *RUNX1* mutations to GC sensitivity in AML.
In our study, primary AML specimens carrying *RUNX1* C-terminal mutations showed increased sensitivity to GCs when compared to samples harboring N-terminal mutations (C-terminal mutations: 7/8 in GC sensitive group vs 10/29 for N-terminal mutations, p=0.014). All insertions located in the C-terminal region are predicted to lead to elongated RUNX1 proteins, which are known to act as dominant-negative inhibitors of RUNX1 (10,12,18), and these mutations were enriched in the GC sensitive group. Interestingly, *RUNX1* C-terminal mutations have been shown to affect protein function and leukemogenesis differently than N-terminal mutations involving the RUNT domain (10,18,35). Among the GC sensitive specimens in our cohort, one specimen presenting a MLL-PTD fusion was later found to carry a novel translocation involving *RUNX1* and *SON*, which results in a chimeric transcript comprising a truncated version of *RUNX1* RUNT domain expected to result in *RUNX1* loss of function, in accordance with our model (**Figure S2.2**). We also show that primary AML specimens carrying a t(8;21) translocation involving the *RUNX1* gene are more frequently sensitive to GCs than *RUNX1*^{wt} specimens (**Figure 2.3c**), further supporting our model. In line with these results, Corsello *et al.* identified GCs as modulators of the

gene expression signature associated with the AML1-ETO fusion in Kasumi-1 cells (36). They demonstrated that ectopic expression of the fusion in U937 cells sensitizes them to GCs, and that GC treatment decreases AML1-ETO fusion protein levels in a proteasome-dependent manner, suggesting that a similar mechanism might be at play in t(8;21) primary AML specimens. We also show that AML cell lines are susceptible to the modulation of *RUNX1* dosage as *RUNX1* silencing dramatically increased the sensitivity of various AML cell lines to GCs. Similarly, residual RUNX1 activity in primary AML specimens carrying heterozygous mutations or hypomorphic alleles could contribute to the resistance of these specimens to GCs. Overall, these results further support our theory that *RUNX1* dosage dictates GC response in AML.

The mechanism by which *RUNX1* loss of function mediates GC sensitivity is not immediately clear. We observed that elevated *NR3C1* expression identifies primary AML specimens carrying *RUNX1* mutations (**Figure S2.7**), suggesting an involvement of GR levels in GC sensitivity of *RUNX1*^{mut} specimens. This finding is in line with a recent study by Malani *et al.* (37) which showed that acquired cytarabine resistance and GC sensitivity in AML cells is associated with increased expression of *NR3C1*. *NR3C1* levels could not account for differences in GC response within the *RUNX1* mutated group however (**Figure S2.7**), implying that other factors are involved. This is supported by the observation that additional mutations (*SRSF2* and *CEBPA*^{bi}) are associated with GC sensitivity. One hypothesis to explain the interplay between RUNX1 and the GR in the GC response could be that RUNX1 negatively modulates the transcription of the *NR3C1* gene. In accordance with this, we identified *NR3C1* as one of the transcripts whose expression is determined by *RUNX1* allele dosage in primary AML specimens (**Figure 2.2d** and **Figure S2.7**) and we showed that *RUNX1* silencing results in the upregulation of *NR3C1* in AML cell lines (**Figure 2.6c** and **Figure S2.8**). Moreover, RUNX1 has been shown to modulate *NR3C1* expression (38) and to exert a protective effect against GC-induced apoptosis in lymphoma cells (39). Evidence for RUNX1 occupancy in the promoter region of the *NR3C1* gene in normal hematopoietic stem/progenitor cells and AML cells also suggests that RUNX1 can directly regulate the expression of the *NR3C1* (40). Interestingly, in ALL, activation of the GR by synthetic GCs, such as dexamethasone, leads to an apoptotic response by negative regulation of *BCL2* expression and upregulation of proapoptotic *BIM* genes (41). We show that OCI-AML5 cells undergo apoptosis following GC treatment, therefore one can envision that a similar mechanism exists in AML. It

therefore appears that elucidation of the precise mechanism by which *RUNX1* loss of function confers GC sensitivity in AML will require further investigation.

Considering that *RUNX1* sequencing is now included in the initial prognostic assessment of AML patients, our study supports the rationale to evaluate the addition of GC therapy for a subset of patients, for example those with dominant negative or *RUNX1*$^{-/-}$ mutations. GCs are largely used in the treatment of ALL, and correlation of *in vitro* prednisolone sensitivity of primary pediatric ALL specimens to clinical characteristics revealed that low IC_{50} values for this compound *in vitro* are associated with good short-term response and long-term clinical outcome (42). Similarly to what is observed for prednisolone, clinical trials for ALL have shown that Dexamethasone treatment improves relapse free survival for these patients (43,44). Interestingly, patients with *ETV6-RUNX1*-positive B-cell precursor ALL were amongst the best responders to GC treatment in this study (45). Results from these clinical trials and case reports support the idea that as for ALL, *in vitro* sensitivity to GCs might correlate with good GC treatment outcome for AML patients. In support of this, effective clinical doses of dexamethasone and prednisolone have been reported for ALL (44,46) and circulating plasma levels as well as disposition for these GCs have been determined after i.v. or p.o. administration in several clinical trials (47–49). The IC_{50} values determined for inhibition of primary AML cells viability by GCs in our study systematically fall well below the dexamethasone and prednisolone plasma levels that can be inferred from the above, suggesting that clinically relevant GC concentrations could be achieved in patients for the treatment of *RUNX1*^{mut} AML.

In conclusion, our data suggests that *RUNX1*^{mut} AMLs have distinct genetic and transcriptomic features, possibly impacting on their sensitivity to drugs such as glucocorticoids. Our data also indicates that *SRSF2* loss of function contributes to the GC response, suggesting that GC treatment could be beneficial for AML patients carrying both *SRSF2* and *RUNX1* mutations. Of interest, such patients were recently reported to have particularly poor outcome (14). Collectively, our results reveal a potentially easy clinical intervention that may rapidly impact the outcome of patients suffering from *RUNX1*^{mut} AML. Adequately designed preclinical studies will help determine the nature of these interventions.

2.8 Figures

a

	RUNX1^{mut} (n=47)	*RUNX1*^{wt} (n=368)	p-value
Age	63 (27 - 83)	57.5 (17-87)	0.003
WBC (x 10^9/L)	33.3 (0.9 - 200.8)	32.1 (0.8 - 447)	
T-related	4 (8.5%)	25 (6.8%)	
Myelodysplasia	15 (31.9%)	85 (23.1%)	
Gender			
Male	28 (59.6%)	207 (56.3%)	
Female	19 (40.4%)	161 (43.8%)	
Cytogenetic risk			
Favorable	0 (0%)	63 (17.1%)	0.0004
Intermediate	35 (74.5%)	192 (52.2%)	0.0047
NK	11 (23.4%)	119 (32.3%)	
Inter (others)	24 (51.1%)	73 (19.8%)	< 0.0001
Adverse	12 (25.5%)	113 (30.7%)	
FAB			
M0	11 (23.4%)	16 (4.3%)	< 0.0001
M1	13 (27.7%)	103 (28.0%)	
M2	8 (17.0%)	44 (12.0%)	
M3	0 (0%)	15 (4.1%)	
M4	3 (6.4%)	53 (14.4%)	
M5	3 (6.4%)	63 (17.1%)	
M6	0 (0%)	10 (2.7%)	
M7	0 (0%)	3 (0.8%)	
NC	8 (17%)	61 (16.6%)	
Other	1 (2.1%)	0 (0%)	

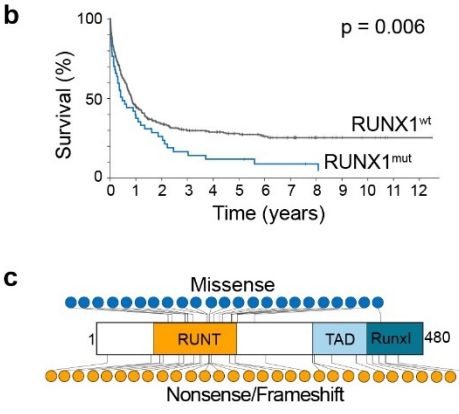

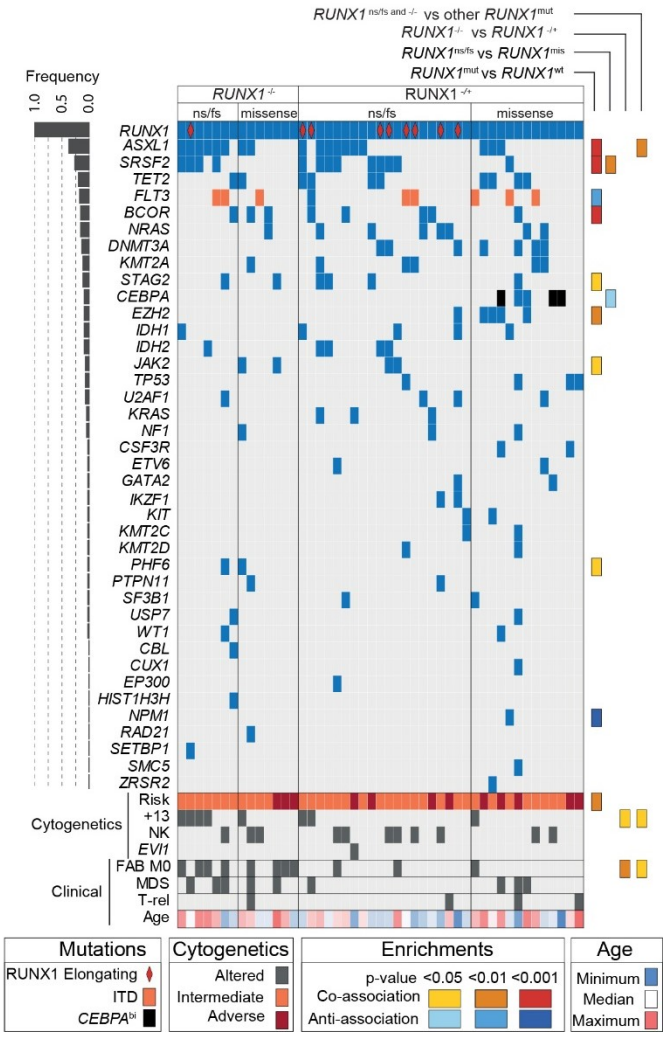

Figure 2.1: Mutational landscape of *RUNX1*^{mut} primary AML specimens

(**a**) Characteristics of *RUNX1*^{mut} and *RUNX1*^{wt} cohorts. p values are based on two-tailed Fisher's exact test or Wilcoxon rank-sum test. (**b**) Patient survival according to *RUNX1* mutation status. p value was calculated using the log rank test. (**c**) Primary structure and position of mutations on RUNX1 protein (NP_001745.2). RUNT: 85-206, TAD: 318-398, RUNXI: 389-480. (**d**) Mutational profile of *RUNX1*^{mut} primary AML specimens. Samples are grouped according to their *RUNX1* mutation type, with samples carrying mutations at variant allele frequency (VAF) ≥ 75% and double heterozygous mutations on the left (*RUNX1*$^{-/-}$) and *RUNX1* heterozygous mutations on the right (*RUNX1*$^{-/+}$). Each column represents a patient sample. Cytogenetic and other clinical information is provided in the last rows, whereas mutation frequency within *RUNX1*^{mut} cohort and enrichment between indicated comparison groups are shown in left and right panels, respectively.

Enrichments were calculated using Fisher's exact test. WBC: white blood cell, T-related: therapy-related, myelodysplasia: myelodysplasia-related changes, NK: normal karyotype, Inter: intermediate, FAB: French-American-British, TAD: transcriptional activation domain, RunxI: Runx1 inhibition domain, ITD: internal tandem duplications, *CEBPA*^{bi}: biallelic *CEBPA* mutations.

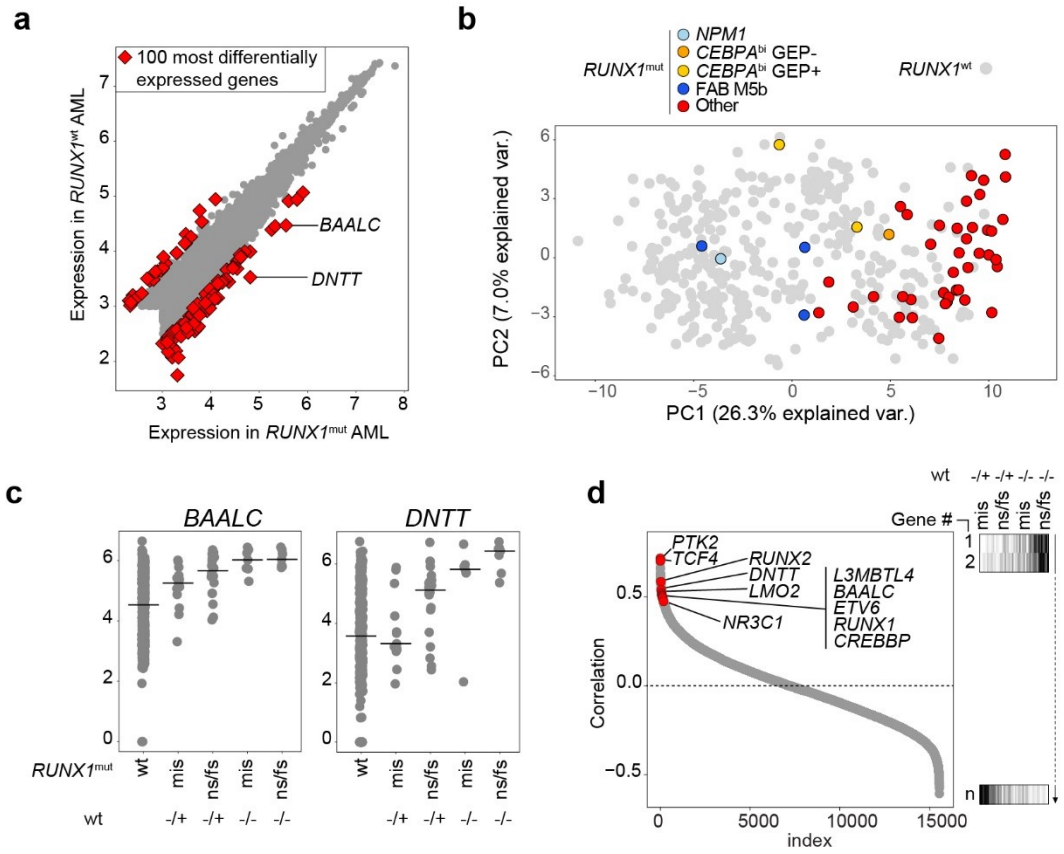

Figure 2.2: *RUNX1* allele dosage determines *RUNX1* mutation-associated gene expression signature

(a) Differentially expressed genes in *RUNX1*^{mut} specimens as revealed by RNA sequencing. The 100 most differentially expressed genes are indicated by red diamonds. Scale: average($\log_{10}$((RPKM + 0.0001) * 10,000)). Genes with a value < 3 in both groups, corresponding to approximately 0.1 RPKM, were not included in this analysis. RPKM of 1 is equivalent to approximately 4 on the scale. **(b)** Principal component analysis (PCA) performed using sequencing data from 415 primary AML specimens using the *RUNX1* 100-gene signature. **(c)** Expression levels of the *BAALC* and *DNTT* genes according to mutation type (ns/fs = nonsense/frameshift; mis = missense) and load (variant allele frequency) using scale defined in panel **a**. Double heterozygous cases with missense and nonsense/frameshift mutations were classified as nonsense/frameshift. VAF ≥ 75% for homozygous mutation, or sum of VAF ≥ 75% for double heterozygous mutations was used to label a sample *RUNX1*$^{-/-}$. All *RUNX1*^{mut} subgroup comparisons to *RUNX1*^{wt} specimens were significant, except *RUNX1*^{mis} vs *RUNX1*^{wt} for *DNTT*. p values were calculated using Wilcoxon test. **(d)** Correlation of the 100 most differentially expressed genes identified in **a** according to model based on mutational pattern identified in **c**. Correlations were performed in the

RUNX1^{mut} cohort only (n=47), using the following template: 1 (missense$^{-/+}$), 2 (nonsense/frameshift$^{-/+}$), 3 (missense$^{-/-}$), 4 (nonsense/frameshift$^{-/-}$). Genes are ordered according to their correlation to this template. Genes with maximum expression levels in *RUNX1*^{mut} specimens < 1 RPKM were not included in this analysis. A selection of the most correlated genes known to be related to leukemia is labeled, as well as the Glucocorticoid receptor gene, *NR3C1*.

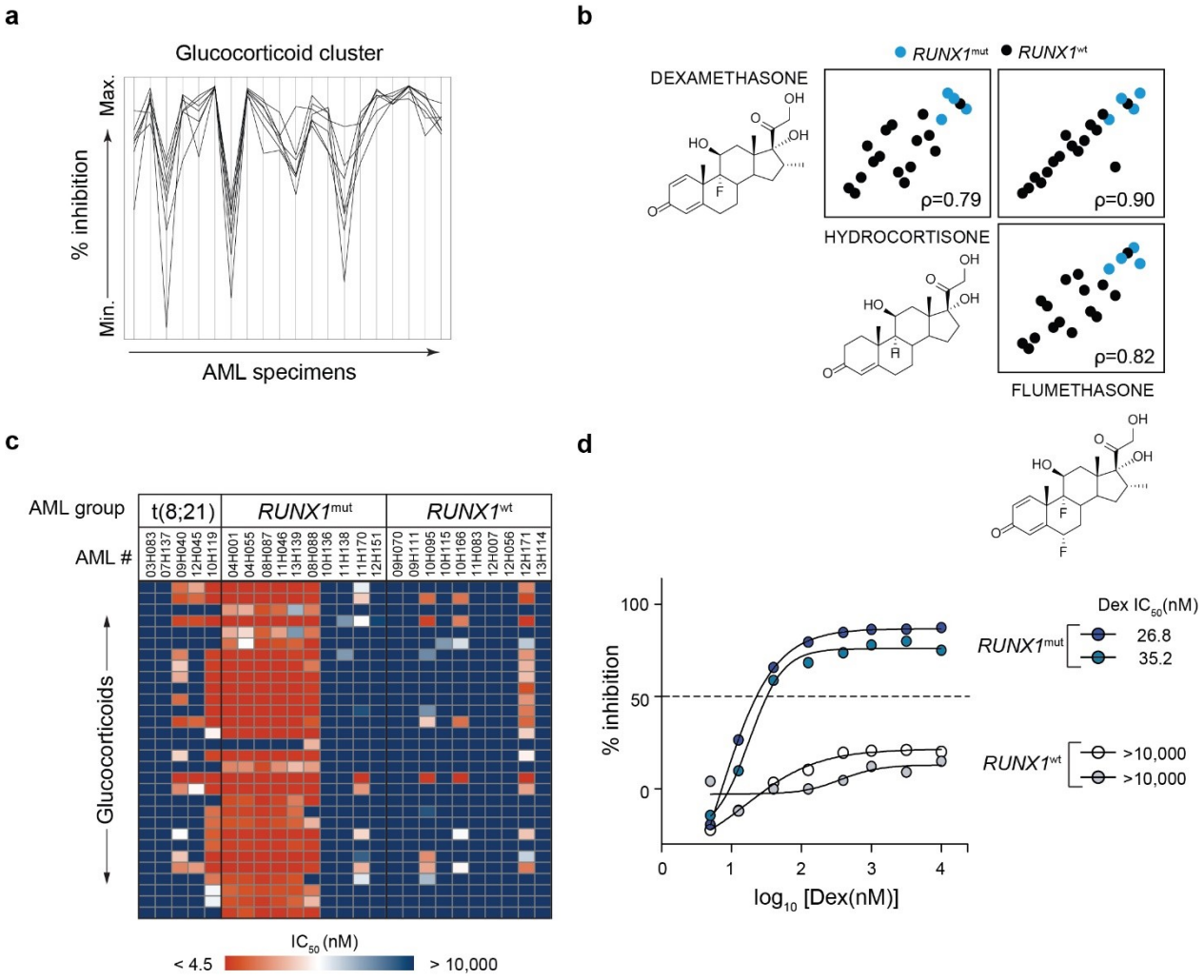

Figure 2.3: *RUNX1*^{mut} primary AML specimens are sensitive to glucocorticoid treatment

(**a**) Response of 20 primary AML specimens (1 AML per vertical line on x axis) to different compounds of the glucocorticoid cluster (each compound represented by 1 line in graph) as indicated by % inhibition of cell viability (y axis). (**b**) Correlation of inhibitory response of 20 primary AML specimens to three representatives of the glucocorticoid cluster with decreasing potency (flumethasone > dexamethasone > hydrocortisone). Black dots: *RUNX1*^{wt} specimens; blue dots: *RUNX1*^{mut} specimens. ρ: Spearman's rank correlation coefficient. (**c**) Heat map showing IC_{50} values for validation screen carried out on 25 additional primary AML specimens and 30 GCs. Drugs were tested in 8 serial dilutions ranging from 4.5 to 10,000 nM. (**d**) Dose response curves for Dexamethasone and associated IC_{50} values for two representative *RUNX1*^{mut} and two *RUNX1*^{wt} specimens.

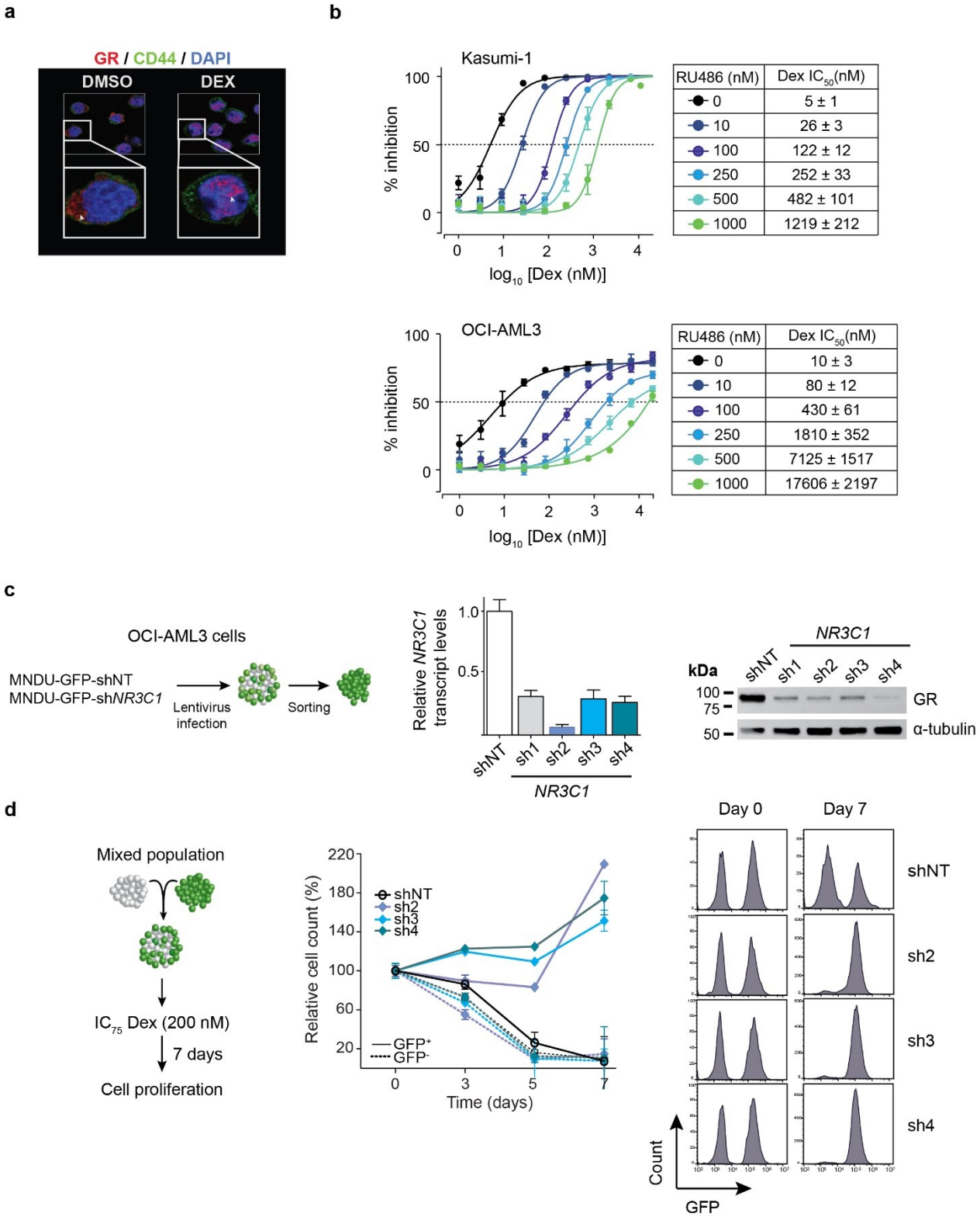

Figure 2.4: Inhibitory response to GCs in AML cells is dependent on Glucocorticoid Receptor activity

(**a**) Evaluation of subcellular localisation of the GR following Dexamethasone treatment (1 μM for 1h) by immunofluorescence in HL-60 cells. Representative of 3 independent experiments. (**b**) Dose response curves and associated IC_{50} values for Dexamethasone in Kasumi-1 and OCI-AML3 cells with increasing concentrations of GR full antagonist, RU486. Data is shown as mean ± SEM for 3 independent experiments. (**c**) Assessment of GR knockdown efficiency by shRNAs targeting *NR3C1* (sh1 to sh4) in shRNA expressing OCI-AML3 cells (GFP^+) by qRT-PCR (middle panel, results are shown for 2 independent infections and expressed as mean ± SEM) western blotting (right panel, representative of 2 independent infections). (**d**) Determination of the impact of GR knockdown on inhibition of OCI-AML3 cell proliferation by Dexamethasone. GFP^+ cells were sorted, mixed with uninfected cells and treated with a single dose of Dexamethasone (IC_{75} = 200 nM). Cell proliferation was evaluated at the indicated times after treatment by cell counting of the live GFP^+ and GFP^- populations, and expressed relative to DMSO controls. Line graph shows mean ± SEM of 3 independent experiments. Histograms are representatives of 3 replicates after 7 days of exposure to Dexamethasone.

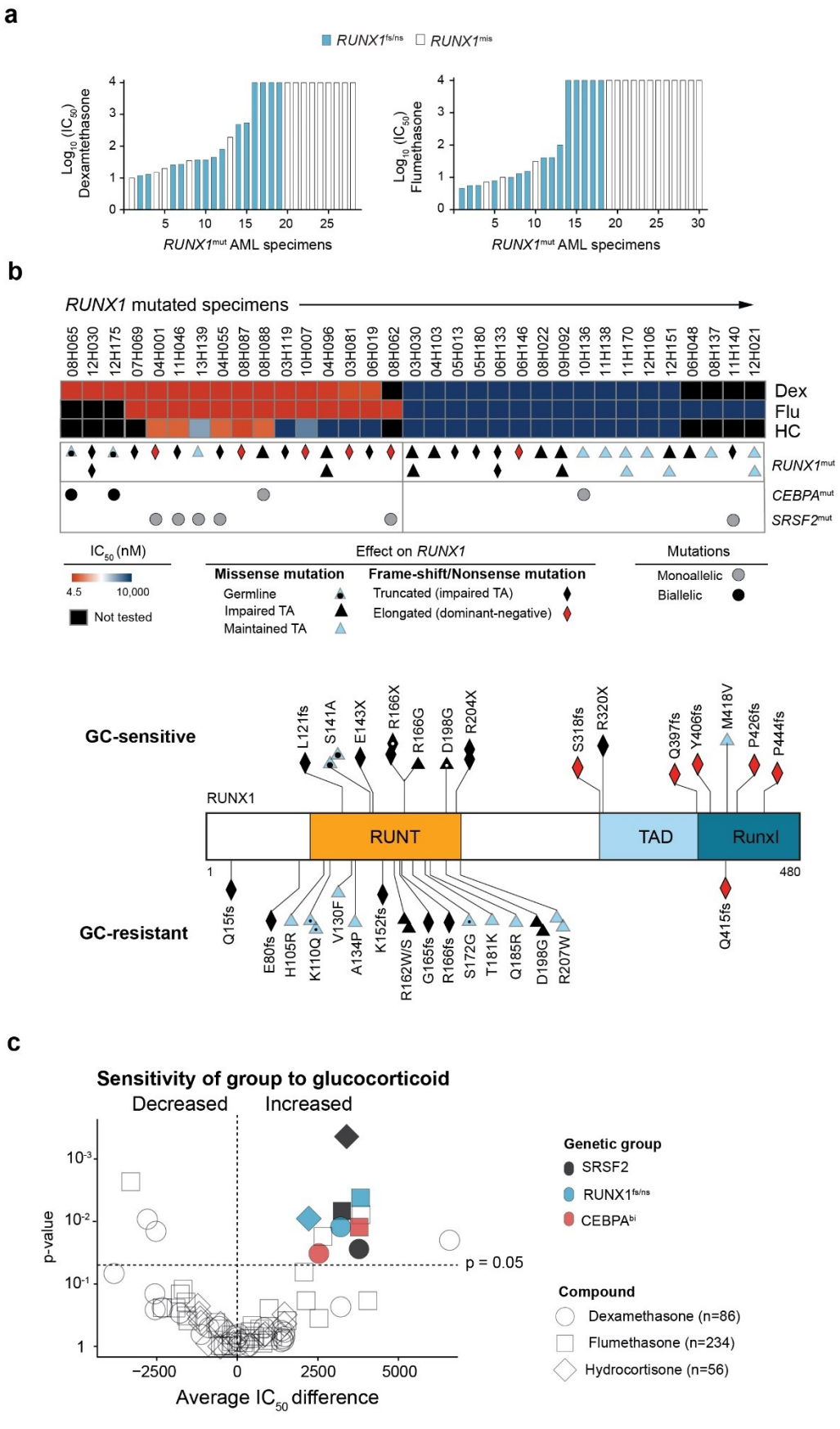
a
RUNX1fs/ns
RUNX1mis
Log10 (IC50) Dexamethasone
Log10 (IC50) Flumethasone
RUNX1mut AML specimens
RUNX1mut AML specimens
b
RUNX1 mutated specimens
08H065 12H030 12H175 07H069 04H001 11H046 13H139 04H055 08H087 08H088 03H119 10H007 04H096 03H081 06H019 08H062 03H030 04H103 05H013 05H180 06H133 06H146 08H022 09H092 10H136 11H138 11H170 12H106 12H151 06H048 08H137 11H140 12H021
Dex
Flu
HC
RUNX1mut
CEBPAmut
SRSF2mut
IC50 (nM)
4.5
10,000
Not tested
Effect on RUNX1
Missense mutation
Germline
Impaired TA
Maintained TA
Frame-shift/Nonsense mutation
Truncated (impaired TA)
Elongated (dominant-negative)
Mutations
Monoallelic
Biallelic
GC-sensitive
L121fs S141A E143X R166X R166G D198G R204X S318fs R320X Q397fs Y406fs M418V P426fs P444fs
RUNX1
RUNT
TAD
RunxI
1
480
GC-resistant
Q15fs E80fs H105R K110Q V130F A134P K152fs R162W/S G165fs R166fs S172G T181K Q185R D198G R207W Q415fs
c
Sensitivity of group to glucocorticoid
Decreased
Increased
p-value
p = 0.05
Average IC50 difference
Genetic group
SRSF2
RUNX1fs/ns
CEBPAbi
Compound
Dexamethasone (n=86)
Flumethasone (n=234)
Hydrocortisone (n=56)

Figure 2.5: *RUNX1* allele dosage dictates GC response in *RUNX1*^{mut} AML

(**a**) IC_{50} values of 28 *RUNX1*^{mut} specimens in response to Dexamethasone (left) and of 30 *RUNX1*^{mut} specimens in response to Flumethasone (right). Double-heterozygous samples were labeled as missense when both alleles had missense mutations or as frame-shift/nonsense when at least one mutated allele had a frameshift or nonsense mutation. (**b**) Heat map showing IC_{50} values for Dexamethasone (Dex), Flumethasone (Flu) and Hydrocortisone (HC) for 33 *RUNX1*^{mut} specimens. The effect of mutations on RUNX1 function was determined based on previously published functional studies. (**c**) Volcano plot showing integrative analysis of chemical screens using primary AML specimens from various genetic groups and GCs (flumethasone, dexamethasone and hydrocortisone). Specimens from genetic groups significantly more sensitive to at least 2 GCs than wild-type specimens are represented as filled symbols.

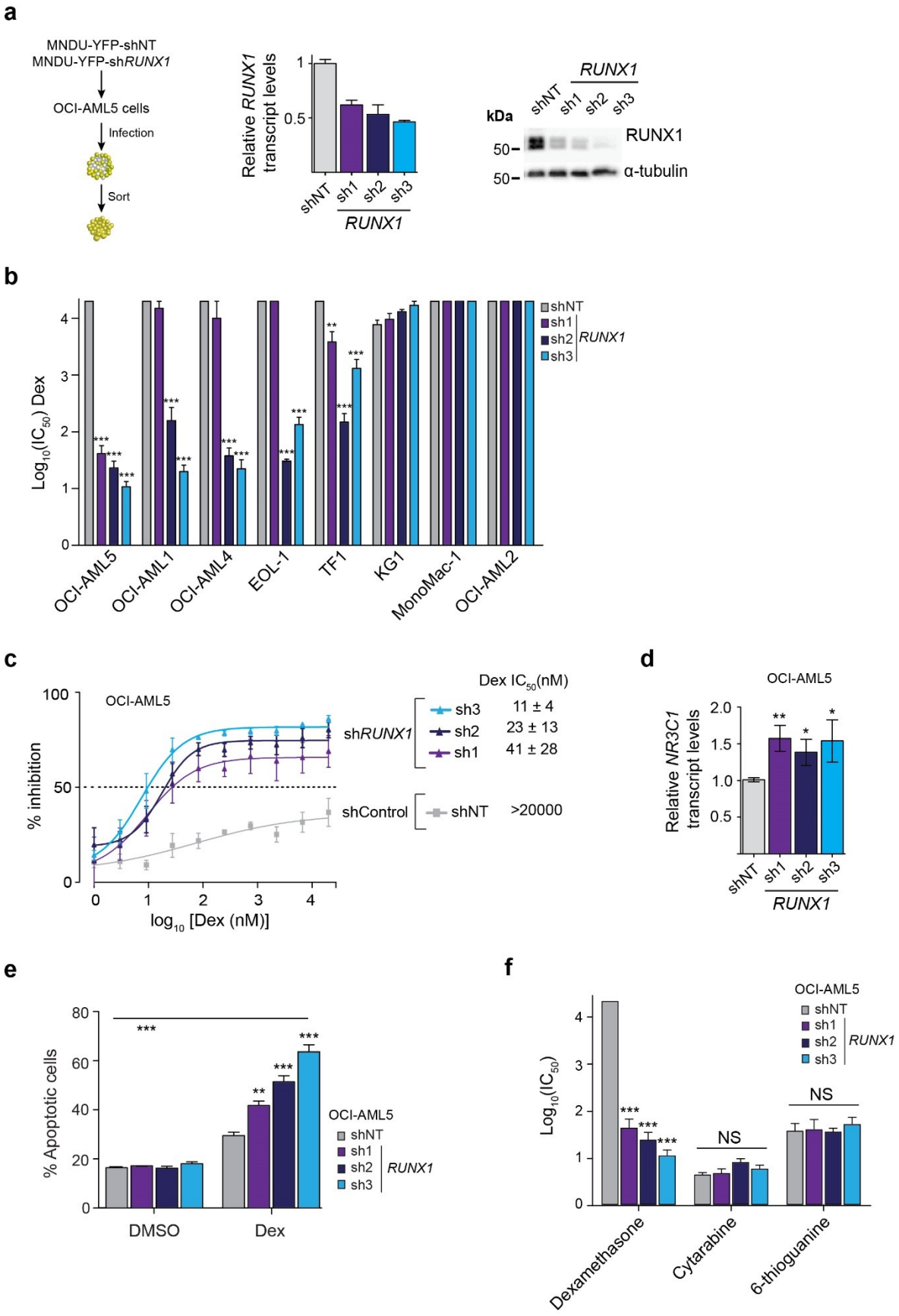
a
MNDU-YFP-shNT
MNDU-YFP-shRUNX1
OCI-AML5 cells
Infection
Sort
Relative RUNX1 transcript levels
shNT
sh1
sh2
sh3
RUNX1
kDa
RUNX1
α-tubulin
50
50
b
Log10(IC50) Dex
shNT
sh1
sh2
sh3
RUNX1
OCI-AML5
OCI-AML1
OCI-AML4
EOL-1
TF1
KG1
MonoMac-1
OCI-AML2
c
OCI-AML5
% inhibition
log10 [Dex (nM)]
Dex IC50(nM)
shRUNX1
sh3 11 ± 4
sh2 23 ± 13
sh1 41 ± 28
shControl
shNT >20000
d
OCI-AML5
Relative NR3C1 transcript levels
e
% Apoptotic cells
DMSO
Dex
OCI-AML5
f
Log10(IC50)
NS
Dexamethasone
Cytarabine
6-thioguanine

Figure 2.6: *RUNX1* silencing in AML cells increases sensitivity to GCs

(**a**) Assessment of *RUNX1* knockdown efficiency by shRNAs (sh1 to sh3) in YFP^+ sorted OCI-AML5 cells by qRT-PCR (middle panel, results are shown for 2 independent infections and expressed as mean ± SEM) and western blotting (right panel, representative of 2 independent infections). (**b**) IC_{50} values for Dexamethasone in eight AML cell lines expressing sh*RUNX1* or shNT (control). Cells were treated with increasing concentrations of Dexamethasone (1 to 20,000 nM) and the effect on cell viability was monitored. Results from 3 independent experiments are shown with SEM. p values were determined by two-tailed unpaired t-test. *p<0.05; **p<0.01; ***p<0.001. (**c**) Dose response curves and associated IC_{50}s for Dexamethasone in OCI-AML5 cells expressing sh*RUNX1* or shNT. Results from 3 independent experiments are shown with SEM. (**d**) *NR3C1* transcript levels in OCI-AML5 cells expressing sh*RUNX1* or shNT. Results from 3 independent experiments are shown with SEM. p values were determined by two-tailed unpaired t-test. **p<0.01; ***p<0.001. (**e**) Proportion of apoptotic cells determined by Annexin-V staining 24 hours after treatment of OCI-AML5 with 100 nM Dexamethasone or DMSO as control. Results from 3 independent experiments are shown with SEM. p values were determined by two-tailed unpaired t-test. Comparisons between DMSO and Dexamethasone for each shRNA are represented by connecting line with ***. **p<0.01 ***p<0.001 (**f**) IC_{50}s for Dexamethasone, Cytarabine and 6-thioguanine in OCI-AML5 cells expressing sh*RUNX1* or shNT. Cells obtained from two independent infections were used for drug treatment, values are expressed with SEM. p values were calculated using two-tailed unpaired t-test. ***p<0.001, NS, not significant.

2.9 Acknowledgments

The authors wish to thank Muriel Draoui for project coordination, Sophie Corneau and Nadine Mayotte for sample coordination, Isabel Boivin for mutation validation and chemical screens assistance, and Simon Girard for assistance with protein analysis. The authors acknowledge Marianne Arteau and Raphaëlle Lambert at the IRIC genomics platform for RNA sequencing; Jean Duchaine, Dominic Salois and Sébastien Guiral at the IRIC high-throughput screening platform for assay optimization and chemical screens supervision; Danièle Gagné and Gaël Dulude at the IRIC flow cytometry platform for assistance with flow cytometry acquisition, analysis, and cell sorting; and Christian Charbonneau at the IRIC bio-imaging platform for guidance with confocal analysis. The authors thank Dr. Trang Hoang, Dr. Brian Wilhelm, Dr. Toshio Kitamura, Dr. Kathy Borden, and Dr. Oliver Herault for the generous donation of cell lines used in this study. The authors also acknowledge the Banque de cellules leucémiques du Québec (BCLQ) team who characterized and provided all AML samples of the Leucegene cohort with special thanks to G. D'Angelo, C. Rondeau and S. Lavallée. J.H. analyzed cytogenetic studies and provided the clinical expertise.

Financial support:

L.S. is supported by the IRIC Members Ph.D. Awards and the Faculté de Médecine recruitment scholarship (Université de Montréal), and the Cole Foundation. V.-P.L. is supported by a fellowship from the Cole Foundation. This work was supported in part by the Government of Canada through Genome Canada and the Ministère de l'économie, de l'innovation et des exportations du Québec through Génome Québec and the Fonds de partenariat pour un Québec innovant et en santé, with supplementary funds from AmorChem and, through grants awarded to G.S., J.H., A.M. and S.L. The work was also supported by a CCSRI impact grant to G.S. G.S. and J.H. are recipients of research chairs from the Canada Research Chair program and Industrielle-Alliance (Université de Montréal), respectively. The BCLQ is supported by grants from the Cancer Research Network of the Fonds de recherche du Québec-Santé (FRQS).

Conflict of interest: The authors declare no competing financial interests.

2.10 References

1. Ichikawa M, Asai T, Saito T, Yamamoto G, Seo S, Yamazaki I, et al. AML-1 is required for megakaryocytic maturation and lymphocytic differentiation, but not for maintenance of hematopoietic stem cells in adult hematopoiesis. *Nat Med.* 2004;10:299–304.
2. Mangan J, Speck N. RUNX1 mutations in clonal myeloid disorders: from conventional cytogenetics to next generation sequencing, a story 40 years in the making. *Crit Rev Oncogenesis.* 2011;16:77–91.
3. Kagoshima H, Shigesada K, Satake M, Ito Y, Miyoshi H, Ohki M, et al. The runt domain identifies a new family of heteromeric transcriptional regulators. *Trends Genet* 1993;9:338-341.
4. Mikhail F, Sinha K, Saunthararajah Y, Nucifora G. Normal and transforming functions of RUNX1: A perspective. *J Cell Physiol.* 2006;207:582–593.
5. Speck NA, Stacy T, Wang Q, North T, Gu TL, Miller J, et al. Core-binding factor: a central player in hematopoiesis and leukemia. *Cancer Res.* 1999;59:1789s–1793s.
6. Speck NA, Gilliland D. Core-binding factors in haematopoiesis and leukaemia. *Nat Rev Cancer.* 2002;2:502–513.
7. Blyth K, Cameron E, Neil J. The runx genes: gain or loss of function in cancer. *Nat Rev Cancer.* 2005;5:376–387.
8. Grimwade D, Hills R, Moorman A, Walker H, Chatters S, Goldstone A, et al. Refinement of cytogenetic classification in acute myeloid leukemia: determination of prognostic significance of rare recurring chromosomal abnormalities among 5876 younger adult patients treated in the United Kingdom Medical Research Council trials. *Blood.* 2010;116:354–365.
9. Osato M, Asou N, Abdalla E, Hoshino K, Yamasaki H, Okubo T, et al. Biallelic and heterozygous point mutations in the runt domain of the AML1/PEBP2alphaB gene associated with myeloblastic leukemias. *Blood.* 1999;93:1817–24.
10. Harada H, Harada Y, Niimi H, Kyo T, Kimura A, Inaba T. High incidence of somatic mutations in the AML1/RUNX1 gene in myelodysplastic syndrome and low blast percentage myeloid leukemia with myelodysplasia. *Blood.* 2004;103:2316–24.
11. Greif P, Konstandin N, Metzeler K, Herold T, Pasalic Z, Ksienzyk B, et al. RUNX1 mutations in cytogenetically normal acute myeloid leukemia are associated with a poor prognosis and up-regulation of lymphoid genes. *Haematologica.* 2012;97:1909–1915.
12. Tang J, Hou H, Chen C, Liu C, Chou W, Tseng M, et al. AML1/RUNX1 mutations in 470 adult patients with de novo acute myeloid leukemia: prognostic implication and interaction with other gene alterations. *Blood.* 2009;114:5352–5361.
13. Gaidzik V, Bullinger L, Schlenk R, Zimmermann A, Röck J, Paschka P, et al. RUNX1 Mutations in Acute Myeloid Leukemia: Results From a Comprehensive Genetic and Clinical Analysis From the AML Study Group. *J Clin Oncol.* 2011;29:1364–1372.
14. Gaidzik V, Teleanu V, Papaemmanuil E, Weber D, Paschka P, Hahn J, et al. RUNX1 mutations in acute myeloid leukemia are associated with distinct clinico-pathologic and genetic features. *Leukemia.* 2016;30:2160–2168.
15. Schnittger S, Dicker F, Kern W, Wendland N, Sundermann J, Alpermann T, et al. RUNX1 mutations are frequent in de novo AML with noncomplex karyotype and confer an unfavorable prognosis. *Blood* 2011;117:2348–2357.
16. Grossmann V, Schnittger S, Kohlmann A, Eder C, Roller A, Dicker F, et al. A novel hierarchical prognostic model of AML solely based on molecular mutations. *Blood.* 2012;120:2963–2972.
17. Mendler J, Maharry K, Radmacher M, Mrózek K, Becker H, Metzeler K, et al. RUNX1 Mutations Are Associated With Poor Outcome in Younger and Older Patients With Cytogenetically Normal Acute Myeloid Leukemia and With Distinct Gene and MicroRNA Expression Signatures. *J Clin Oncol.* 2012;30:3109–3118.
18. Kuo M-C, Liang D-C, Huang C-F, Shih Y-S, Wu J-H, Lin T-L, et al. RUNX1 mutations are frequent in chronic myelomonocytic leukemia and mutations at the C-terminal region might predict acute myeloid leukemia transformation. *Leukemia.* 2009;23:1426–1431.
19. Michaud J, Wu F, Osato M, Cottles G, Yanagida M, Asou N, et al. In vitro analyses of known and novel RUNX1/AML1 mutations in dominant familial platelet disorder with predisposition to acute myelogenous leukemia: implications for mechanisms of pathogenesis. *Blood.* 2002;99:1364–72.
20. Antony-Debre I, Manchev VT, Balayn N, Bluteau D, Tomowiak C, Legrand C, et al. Level of RUNX1 activity is critical for leukemic predisposition but not for thrombocytopenia. *Blood* 2015;125:930–940.
21. Arber DA, Orazi A, Hasserjian R, Thiele J, Borowitz MJ, Le Beau MM, et al. The 2016 revision to the World Health Organization classification of myeloid neoplasms and acute leukemia. *Blood* 2016;127:2391–2405.
22. Lavallée V-P, Baccelli I, Krosl J, Wilhelm B, Barabé F, Gendron P, et al. The transcriptomic landscape and directed chemical interrogation of MLL-rearranged acute myeloid leukemias. *Nature Genetics.* 2015;47:1030–1037.

23. Lavallée V-P, Lemieux S, Boucher G, Gendron P, Boivin I, Girard S, et al. Identification of MYC mutations in acute myeloid leukemias with NUP98–NSD1 translocations. *Leukemia.* 2016;30:1621–1624.
24. Baccelli I, Krosl J, Boucher G, Boivin I, Lavallée V-P, Hébert J, et al. A novel approach for the identification of efficient combination therapies in primary human acute myeloid leukemia specimens. *Blood Cancer J.* 2017;7:e529.
25. Fellmann C, Hoffmann T, Sridhar V, Hopfgartner B, Muhar M, Roth M, et al. An Optimized microRNA Backbone for Effective Single-Copy RNAi. *Cell Reports.* 2013;5:1704–1713.
26. Rose D, Haferlach T, Schnittger S, Perglerová K, Kern W, Haferlach C. Subtype-specific patterns of molecular mutations in acute myeloid leukemia. *Leukemia.* 2016;31:11–17.
27. Larsson C, Cote G, Quintás-Cardama A. The Changing Mutational Landscape of Acute Myeloid Leukemia and Myelodysplastic Syndrome. *Mol Cancer Res.* 2013;11:815–827.
28. Lavallée V-P, Gendron P, Lemieux S, D'Angelo G, Hébert J, Sauvageau G. EVI1-rearranged acute myeloid leukemias are characterized by distinct molecular alterations. *Blood.* 2015;125:140–143.
29. Lavallée V-P, Krosl J, Lemieux S, Boucher G, Gendron P, Pabst C, et al. Chemo-genomic interrogation of CEBPA mutated AML reveals recurrent CSF3R mutations and subgroup sensitivity to JAK inhibitors. *Blood.* 2016;127:3054–61.
30. Martinez M, Hinojosa M, Trombly D, Morin V, Stein J, Stein G, et al. Transcriptional Auto-Regulation of RUNX1 P1 Promoter. *Plos One.* 2016;11:e0149119.
31. Ceribelli M, Hou ZE, Kelly PN, Huang DW, Wright G, Ganapathi K, et al. A Druggable TCF4- and BRD4-Dependent Transcriptional Network Sustains Malignancy in Blastic Plasmacytoid Dendritic Cell Neoplasm. *Cancer Cell.* 2016;30:764–778.
32. Pabst C, Krosl J, Fares I, Boucher G, Ruel R, Marinier A, et al. Identification of small molecules that support human leukemia stem cell activity ex vivo. *Nat Methods.* 2014;11:436–42.
33. Quax RA, Manenschijn L, Koper JW, Hazes JM, Lamberts SW, Rossum EF van, et al. Glucocorticoid sensitivity in health and disease. *Nat Rev Endocrinol.* 2013;9:670–86.
34. Stengel A, Kern W, Meggendorfer M, Perglerová K, Haferlach T, Haferlach C. The Number of RUNX1 Mutations and the Presence of One Intact RUNX1 Allele Influence Cytogenetic Abnormalities, Additional Molecular Mutations and Prognosis in RUNX1 Mutated AML. *Blood.* 2016;128:284.
35. Watanabe-Okochi N, Kitaura J, Ono R, Harada H, Harada Y, Komeno Y, et al. AML1 mutations induced MDS and MDS/AML in a mouse BMT model. *Blood*. 2008;111:4297–4308.
36. Corsello S, Roti G, Ross K, Chow K, Galinsky I, DeAngelo D, et al. Identification of AML1-ETO modulators by chemical genomics. *Blood*. 2009;113:6193–6205.
37. Malani D, Murumägi A, Yadav B, Kontro M, Eldfors S, Kumar A, et al. Enhanced sensitivity to glucocorticoids in cytarabine-resistant AML. *Leukemia*. 2016;31:1187–1195.
38. Wotton S, Terry A, Kilbey A, Jenkins A, Herzyk P, Cameron E, et al. Gene array analysis reveals a common Runx transcriptional programme controlling cell adhesion and survival. *Oncogene.* 2008;27:5856-5866.
39. Kilbey A, Terry A, Wotton S, Borland G, Zhang Q, Mackay N, et al. Runx1 Orchestrates Sphingolipid Metabolism and Glucocorticoid Resistance in Lymphomagenesis. *J Cell Biochem*. 2017;118:1432–1441.
40. Chacon D, Beck D, Perera D, Wong J, Pimanda J. BloodChIP: a database of comparative genome-wide transcription factor binding profiles in human blood cells. *Nucleic Acids Res.* 2014;42:D172–D177.
41. Jing D, Bhadri VA, Beck D, Thoms JAI, Yakob NA, Wong JWH, et al. Opposing regulation of BIM and BCL2 controls glucocorticoid-induced apoptosis of pediatric acute lymphoblastic leukemia cells. *Blood* 2015;125:273–283.
42. Kaspers GJ, Pieters R, Van Zantwijk CH, Van Wering ER, Van Der Does-Van Den Berg A, Veerman AJ. Prednisolone resistance in childhood Acute Lymphoblastic Leukemia: Vitro-Vivo correlations and cross-resistance to other drugs. *Blood* 1998;92:259-266.
43. Bostrom B, Sensel M, Sather H, Gaynon P, La M, Johnston K, et al. Dexamethasone versus prednisone and daily oral versus weekly intravenous mercaptopurine for patients with standard-risk acute lymphoblastic leukemia: a report from the Children's Cancer Group. *Blood.* 2003;101:3809–3817.
44. Inaba H, Pui C-H. Glucocorticoid use in acute lymphoblastic leukaemia. *Lancet Oncol.* 2010;11:1096–106.
45. Schrappe M, Zimmermann M, Möricke A, Mann G, Valsecchi MG, Bartram CR, et al. Dexamethasone in Induction Can Eliminate One Third of All Relapses in Childhood Acute Lymphoblastic Leukemia (ALL): Results of An International Randomized Trial in 3655 Patients (Trial AIEOP-BFM ALL 2000). *Blood* 2008;112:7.
46. Domenech C, Suciu S, Moerloose B, Mazingue F, Plat G, Ferster A, et al. Dexamethasone (6 mg/m2/day) and prednisolone (60 mg/m2/day) were equally effective as induction therapy for childhood acute lymphoblastic leukemia in the EORTC CLG 58951 randomized trial. *Haematologica.* 2014;99:1220–1227.

47. O'Sullivan B, Cutler D, Hunt G, Walters C, Johnson G, Caterson I. Pharmacokinetics of dexamethasone and its relationship to dexamethasone suppression test outcome in depressed patients and healthy control subjects. *Biol Psychiat.* 1997;41:574–584.
48. Groll A, Desai A, Han D, Howieson C, Kato K, Akhtar S, et al. Pharmacokinetic Assessment of Drug-Drug Interactions of Isavuconazole With the Immunosuppressants Cyclosporine, Mycophenolic Acid, Prednisolone, Sirolimus, and Tacrolimus in Healthy Adults. *Clin Pharmacol Drug Dev.* 2017;6:76–85.
49. Buttgereit F, Straub R, Wehling M, Burmester G. Glucocorticoids in the treatment of rheumatic diseases: An update on the mechanisms of action. *Arthritis Rheumatism.* 2004;50:3408–3417.

2.11 Supplemental Figures and Tables

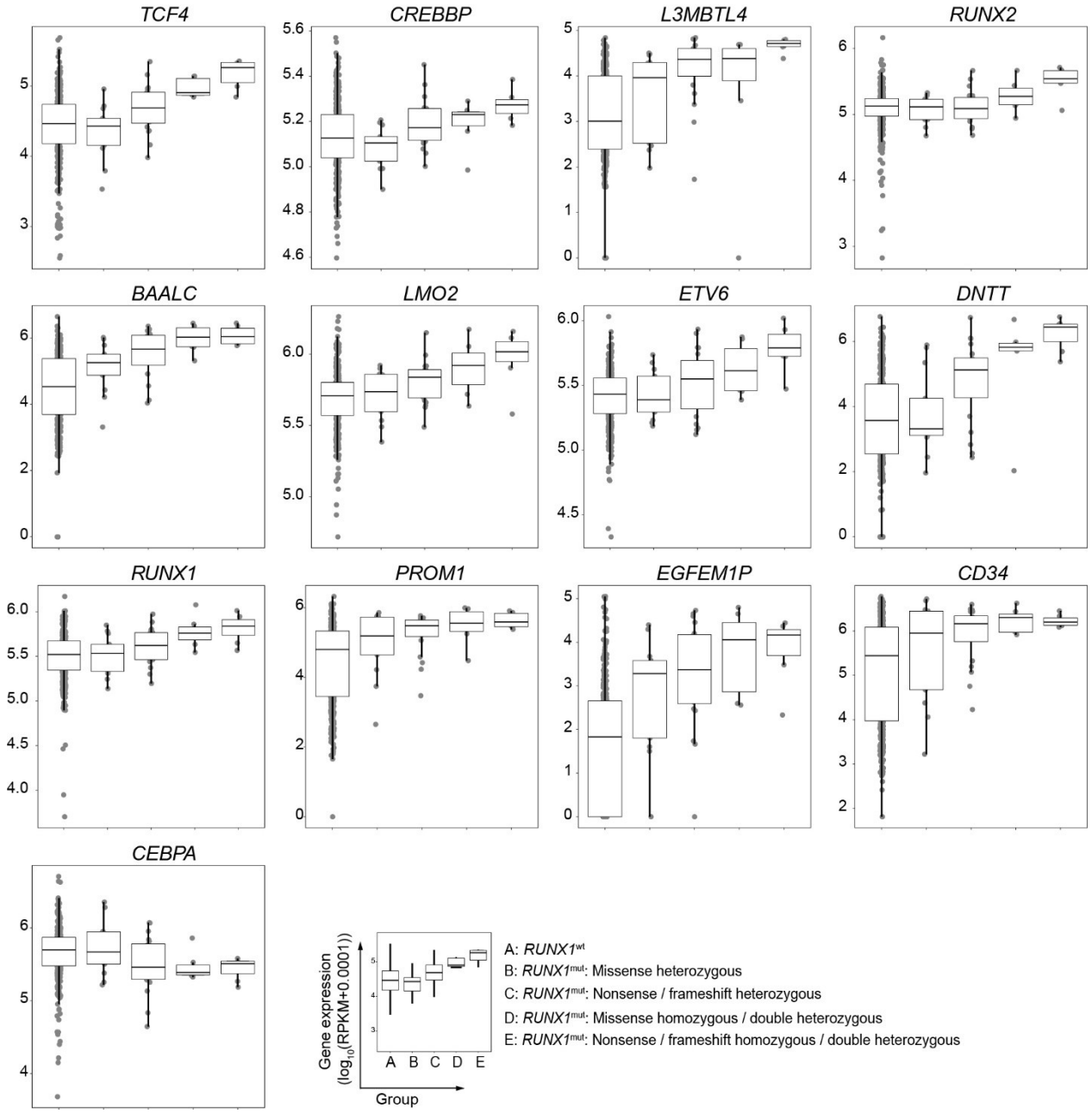

Figure S2.1: Subgroup expression of genes modulated by *RUNX1* dosage

Additional examples of genes most correlated (> 0.50 or <-0.50) to *RUNX1* mutation type and VAF, as described in Figure 2C.

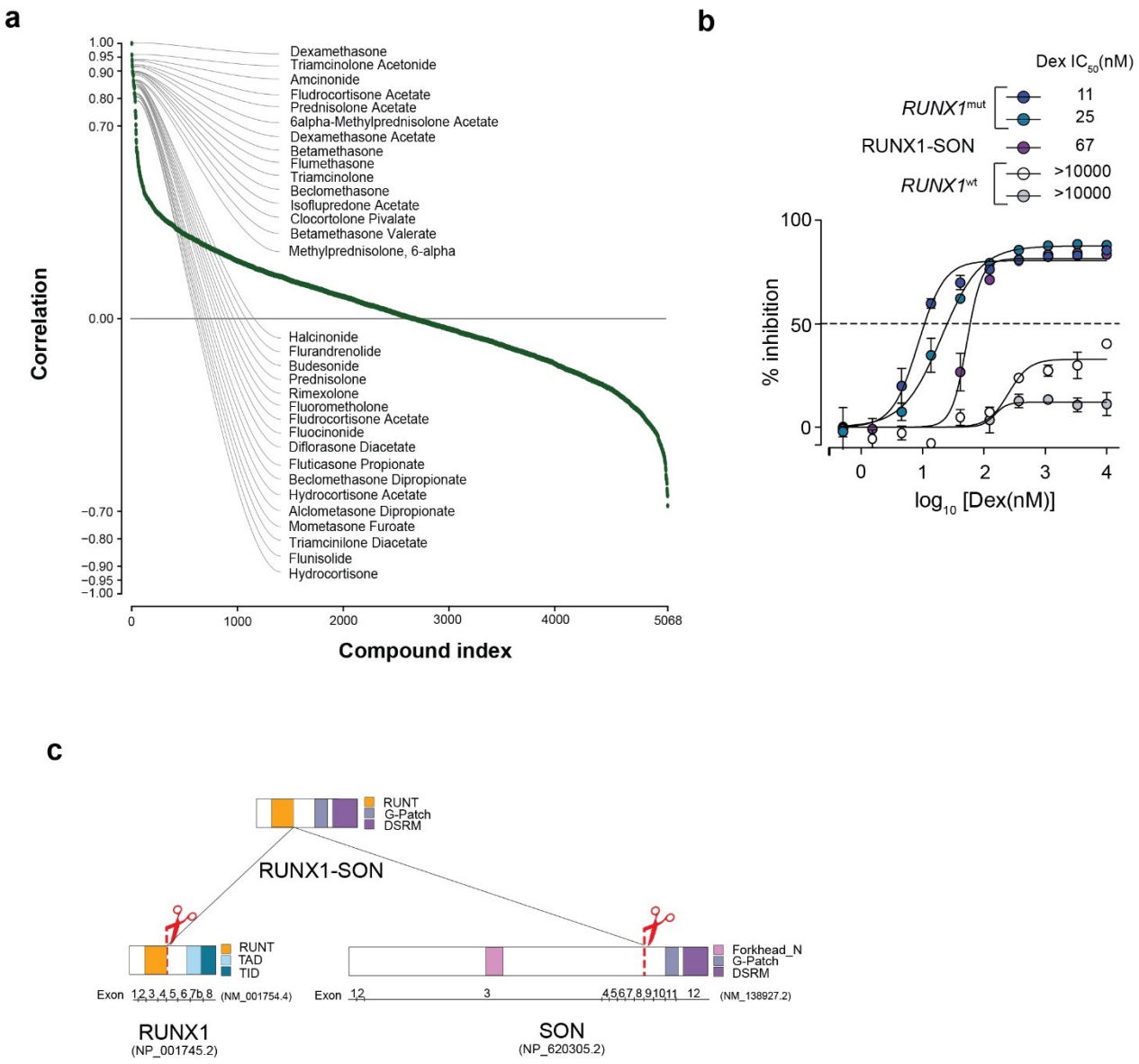

Figure S2.2: Identification of the Glucocorticoid cluster and chemical interrogation of primary *RUNX1*^{mut} specimens

(a) Waterfall plot showing Pearson correlation coefficients calculated between all compounds tested in viability screen (n=5,068) and Dexamethasone. The top 31 compounds correlating with Dexamethasone are GCs (identified as the Glucocorticoid cluster), except for 2 compounds, Naproxol and Karanjin, that could not be validated in independent experiments. (b) Validation of hits from viability screen. Dose-response curves and associated IC50s for Dexamethasone (6 days exposure) for *RUNX1*^{mut} (n=2), RUNX1-SON (n=1) and *RUNX1*^{wt} (n=2) AML specimens. Results

are shown for experimental duplicates with SEM. (c) Schematic representation of the novel gene fusion involving the RUNT domain of RUNX1 and the C-terminal domain of SON.

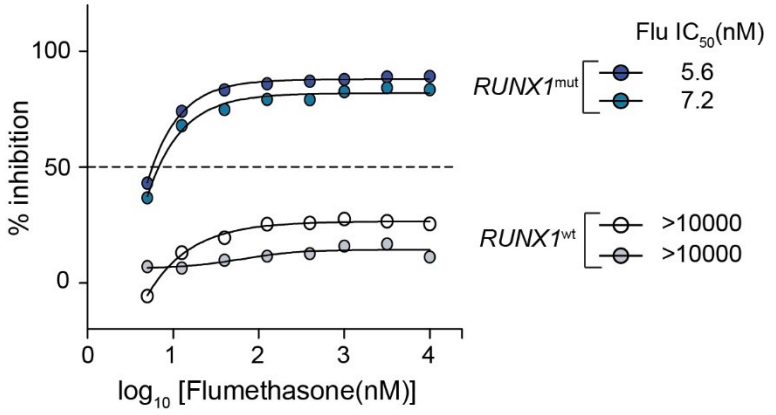

Figure S2.3: Dose response curves for Flumethasone (Flu), representative of the GC cluster, for *RUNX1*^{mut} and *RUNX1*^{wt} specimens

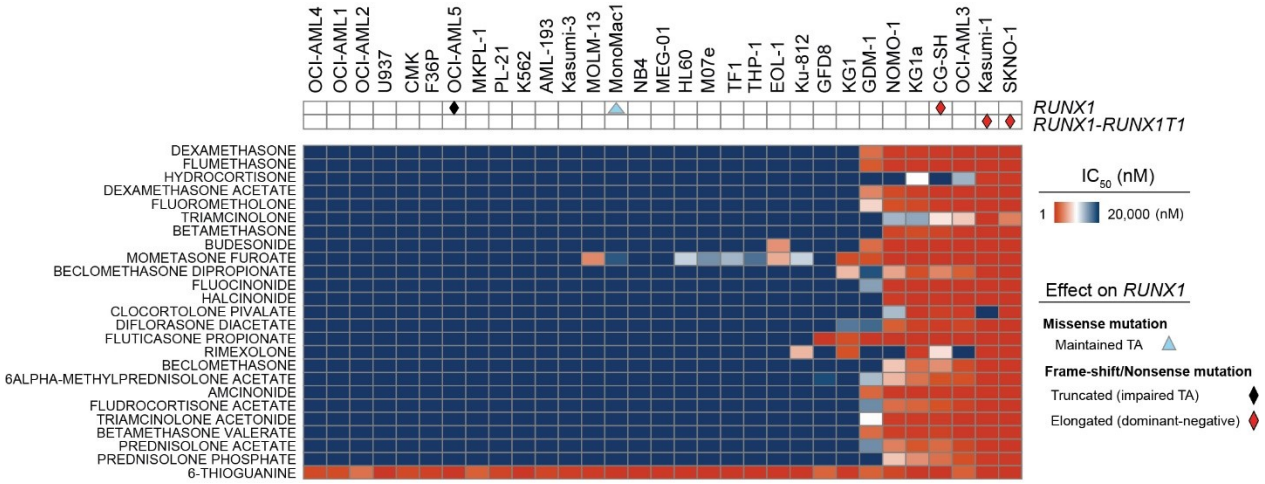

Figure S2.4: Heat map showing response profile of 32 AML cell lines to compounds of the GC cluster (n=24) and 6-thioguanine

Cells were exposed to compounds for 7 days. *RUNX1* lesions and predicted effect on RUNX1 protein function are shown. OCI-AML5 cell line has a frame-shift insertion in *RUNX1*, confirmed by RNA-sequencing, which is predicted to result in a truncated protein (T148fsX153; VAF ~40%). MonoMac-1 is reported to have a missense mutation in the RUNT domain of RUNX1 (A134V). CG-SH, an AML cell line with normal karyotype, carries double heterozygous *RUNX1* mutations, L56S and L405PfsX601, the latter predicted to generate an elongated mutant protein. Kasumi-1 and SKNO-1 are t(8;21) AML cell lines and express RUNX1-RUNX1T1 fusion protein.

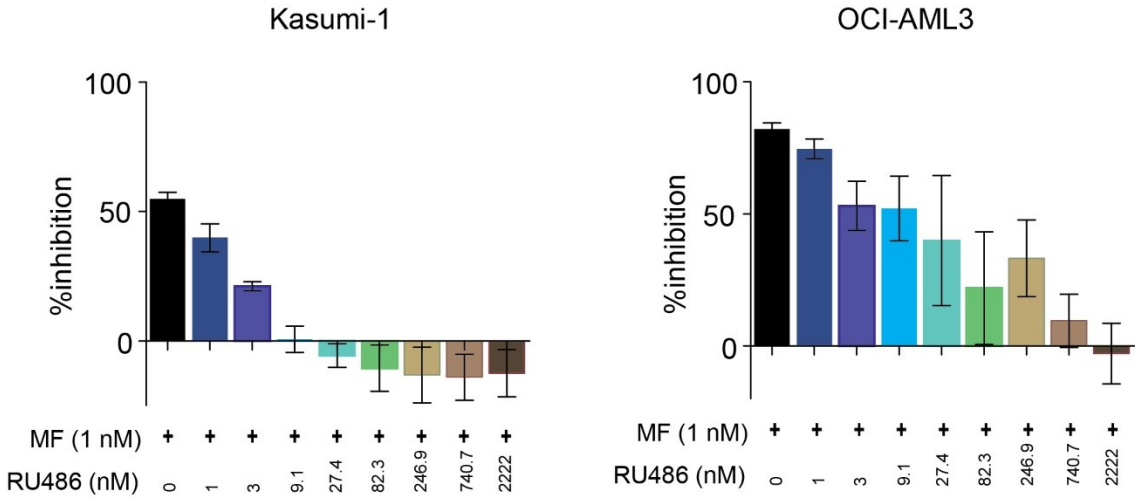

Figure S2.5: Response to GC Mometasone Furoate (MF) observed in Kasumi-1 and OCI-AML3 cells in the presence of increasing concentrations of GR full antagonist RU486

Results are shown as mean ± SD for a single experiment with 4 replicates for each dose tested.

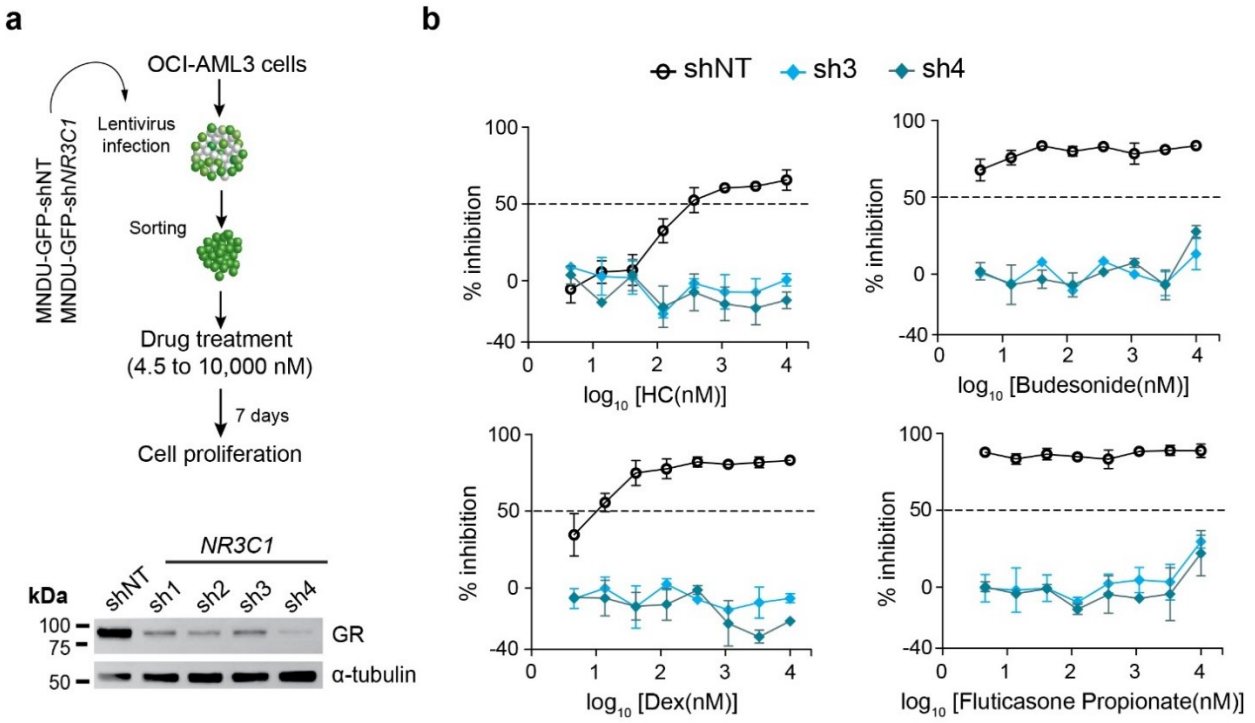

Figure S2.6: Validation of *NR3C1* knockdown and response to GCs

(a) Infection of OCI-AML3 cells with shRNAs targeting *NR3C1* (sh1 to sh4) and assessment of GR knockdown efficiency in GFP+ sorted cells by western blotting. Representative of 2 independent experiments. (b) Response of OCI-AML3 cells expressing shNT (control) or sh*NR3C1* (sh3 and sh4) to Hydrocortisone (HC), Dexamethasone (Dex), Budesonide and Fluticasone Propionate. Results are shown for 2 independent experiments with SEM.

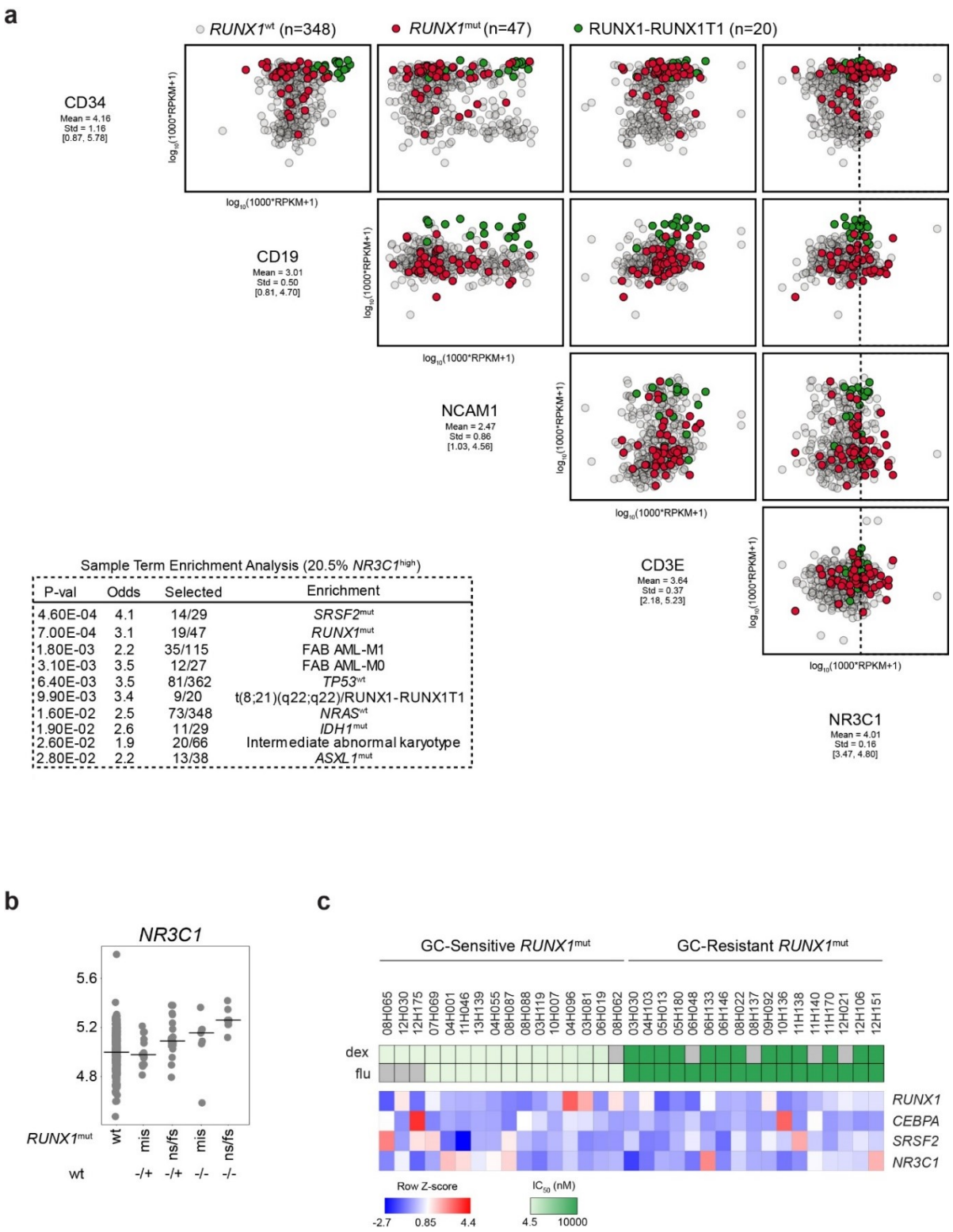

Figure S2.7: Expression profile of lymphoid markers and of the *NR3C1* gene

(a) *Top* Expression profile of lymphoid markers and of the *NR3C1* gene (encoding the GR) in AML specimens of the Leucegene cohort. Dotted line represents the threshold to identify

specimens expressing high levels of *NR3C1* (representing approximately 20% of specimens). *Bottom* Enrichment analysis using the top 20% *NR3C1* expressers. (b) Expression levels of the *NR3C1* gene according to *RUNX1* mutation type (ns/fs = nonsense/frameshift; mis = missense) and load (variant allele frequency). All *RUNX1*^{mut} subgroup comparisons to *RUNX1*^{wt} specimens were significant, except *RUNX1*$^{mis\ (-/+)}$ vs *RUNX1*^{wt}. p values were calculated using one-sided Wilcoxon rank sum test. (c) Gene expression levels of *RUNX1*, *CEBPA*, *SRSF2*, and *NR3C1* (GR), in primary GC-resistant and GC-sensitive *RUNX1*^{mut} AML specimens. Sensitivity to GCs was determined based on IC50 values for Dexamethasone (dex) and/or Flumethasone (flu) (light green, GC-sensitive; dark green, GC-resistant). Heat map shows the row Z-score of the gene expression values.

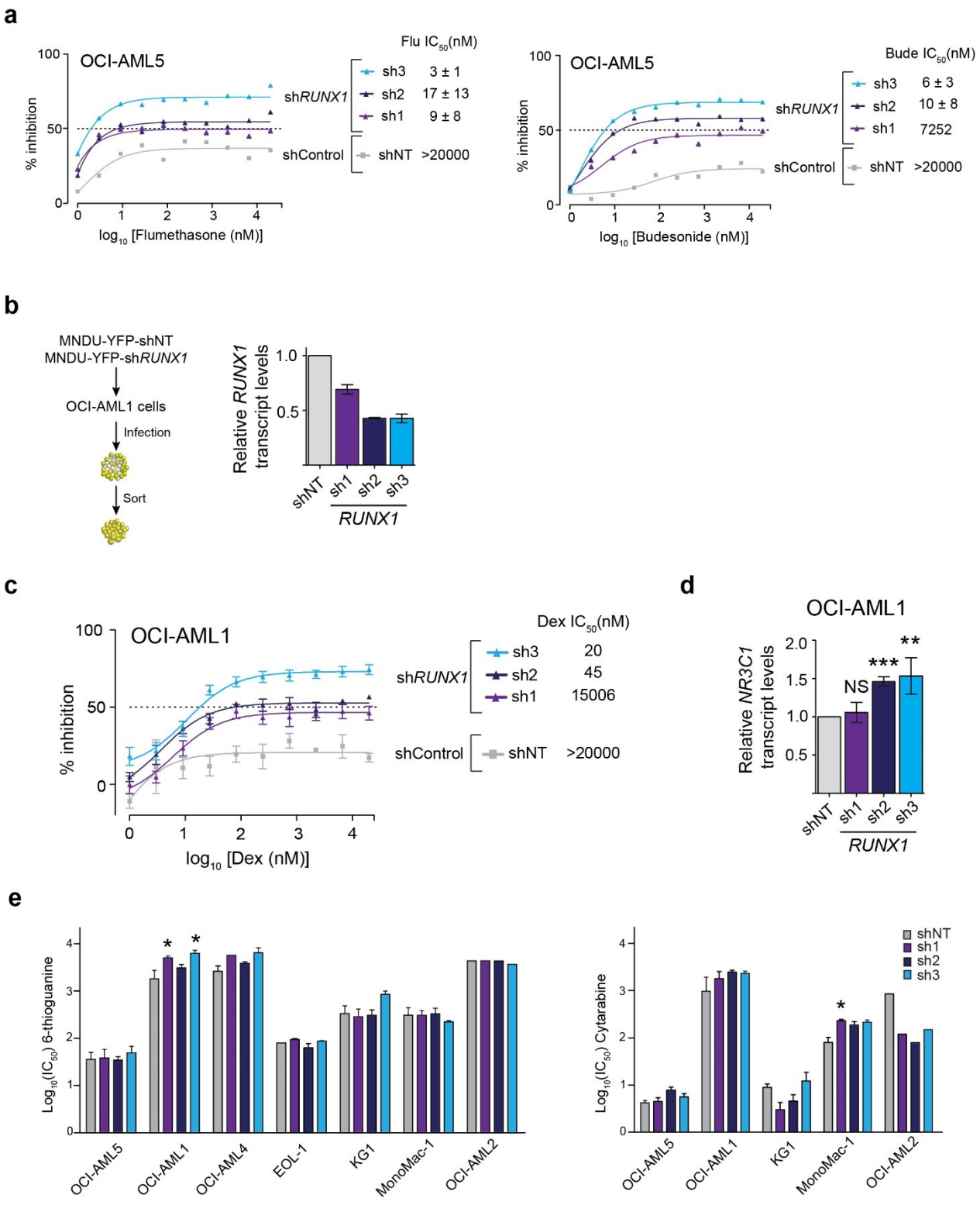

Figure S2.8: Validation of *RUNX1* knockdown and response to GCs

(a) Dose response curves and associated IC_{50}s for Flumethasone (Flu) and Budesonide (Bude) upon *RUNX1* knockdown in OCI-AML5 cells. Results are shown for 3 independent experiments. (b)

Infection of OCI-AML1 cells with sh*RUNX1* (sh1 to sh3) and assessment of *RUNX1* knockdown by qRT-PCR. Results are shown for 3 independent experiments with SEM. (c) Dose response curves and associated IC_{50}s for Dexamethasone (Dex) upon *RUNX1* knockdown in OCI-AML1 cells. Results are shown for 3 independent experiments with SEM. (d) Expression levels of the Glucocorticoid receptor gene, *NR3C1*, in OCI-AML1 cells expressing sh*RUNX1* as determined by qRT-PCR. Results are shown for 3 independent experiments with SEM. p values were determined by two-tailed unpaired t-test. **p<0.01; ***p<0.001. (e) IC_{50} values for 6-thioguanine and Cytarabine in AML cell lines expressing sh*RUNX1* or shNT (Control). Results are shown for 3 independent experiments with SEM. *p.<0.05.

Table S2.1: List of 97 gene mutations and fusions systematically included in mutational analysis

Due to size constraints, this table is not presented in the document.
The file is available as an Excel file online at
https://clincancerres.aacrjournals.org/content/23/22/6969

Table S2.2: *RUNX1* mutations identified in the Leucegene cohort

Position of mutations are indicated using NM_001754 and NM_001001890, coding for RUNX1 proteins of 480 and 453 AA respectively. VAF: variant allele frequency.

Gene	Sample	Position	VAF	NM_001754	NM_001001890
RUNX1	11H140	chr21:36421151	0.477	p.Q15fsX	
RUNX1	05H013	chr21:36259252	0.341	p.E80fsX	p.E53fsX
RUNX1	14H027	chr21:36259213	0.311	p.D93fsX	p.D66fsX
RUNX1	04H138	chr21:36259198	0.833	p.L98fsX	p.L71fsX
RUNX1	08H137	chr21:36259177	0.396	p.H105R	p.H78R
RUNX1	03H030	chr21:36259163	0.986	p.K110Q	p.K83Q
RUNX1	09H092	chr21:36259163	0.991	p.K110Q	p.K83Q
RUNX1	03H119	chr21:36252999	0.455	p.L12fsX	p.L94fsX
RUNX1	03H024	chr21:36252979	0.117	p.T128fsX	p.T101fsX
RUNX1	11H170	chr21:36252974	0.54	p.V130F	p.V103F
RUNX1	12H151	chr21:36252962	0.475	p.A134P	p.A107P
RUNX1	08H065	chr21:36252941	0.459	p.S141A	p.S114A
RUNX1	12H175	chr21:36252941	0.497	p.S141A	p.S114A
RUNX1	06H019	chr21:36252935	0.371	p.E143X	p.E116X
RUNX1	06H133	chr21:36252906	0.384	p.K152fsX	p.K125fsX
RUNX1	11H232	chr21:36252902	0.396	p.Q154X	p.Q127X
RUNX1	04H103	chr21:36252878	0.521	p.R162W	p.R135W
RUNX1	08H022	chr21:36252876	0.53	p.R162S	p.R135S
RUNX1	09H106	chr21:36252871	0.493	p.V164D	p.V137D
RUNX1	06H133	chr21:36252867	0.449	p.G165fsX	p.G138fsX
RUNX1	04H055	chr21:36252866	0.996	p.R166X	p.R139X
RUNX1	08H088	chr21:36252866	0.476	p.R166G	p.R139G
RUNX1	10H063	chr21:36252866	0.349	p.R166X	p.R139X
RUNX1	12H030	chr21:36252866	0.486	p.R166X	p.R139X
RUNX1	13H039	chr21:36252865	0.415	p.R166Q	p.R139Q
RUNX1	05H180	chr21:36252864	0.482	p.R166fsX	p.R139fsX
RUNX1	09H079	chr21:36252856	0.098	p.R169fsX	p.R142fsX
RUNX1	12H021	chr21:36231870	0.996	p.S172G	p.S145G
RUNX1	12H106	chr21:36231842	0.488	p.T181K	p.T154K
RUNX1	10H136	chr21:36231830	0.475	p.Q185R	p.Q158R
RUNX1	07H155	chr21:36231797	0.34	p.T196fsX	p.T169fsX
RUNX1	04H096	chr21:36231791	0.994	p.D198G	p.D171G
RUNX1	06H048	chr21:36231791	0.521	p.D198G	p.D171G
RUNX1	12H151	chr21:36231791	0.527	p.D198G	p.D171G
RUNX1	09H046	chr21:36231789	0.314	p.G199W	p.G172W
RUNX1	11H046	chr21:36231774	0.471	p.R204X	p.R177X
RUNX1	12H030	chr21:36231774	0.476	p.R204X	p.R177X
RUNX1	11H138	chr21:36206893	0.5	p.R207W	p.R180W
RUNX1	11H170	chr21:36206893	0.432	p.R207W	p.R180W
RUNX1	13H048	chr21:36206818	0.926	p.R232W	p.R205W
RUNX1	14H027	chr21:36206765	0.517	p.P249fsX	p.P222fsX
RUNX1	08H087	chr21:36171612	0.403	p.S318fsX	p.S291fsX
RUNX1	07H069	chr21:36171607	0.551	p.R320X	p.R293X
RUNX1	13H039	chr21:36171607	0.555	p.R320X	p.R293X
RUNX1	09H015	chr21:36164838	0.41	p.R346fsX	p.R319fsX
RUNX1	07H124	chr21:36164728	0.368	p.P382fsX	p.P355fsX
RUNX1	08H062	chr21:36164685	0.636	p.Q397fsX	p.Q370fsX
RUNX1	10H007	chr21:36164657	0.316	p.Y406fsX	p.Y379fsX
RUNX1	06H146	chr21:36164631	0.447	p.Q415fsX	p.Q388fsX
RUNX1	13H139	chr21:36164623	0.484	p.M418V	p.M391V
RUNX1	05H149	chr21:36164600	0.713	p.P425fsX	p.P398fsX
RUNX1	04H001	chr21:36164597	0.785	p.P426fsX	p.P399fsX
RUNX1	03H081	chr21:36164544	0.437	p.P444fsX	p.P417fsX

Table S2.3: Additional mutations in *RUNX1*^{mut} specimens

VAF: variant allele frequency, ITD: internal tandem duplication, PTD: partial tandem duplication.

Due to size constraints, this table is not presented in the document.
The file is available as an Excel file online at
https://clincancerres.aacrjournals.org/content/23/22/6969

Table S2.4: List of 100 most differentially expressed genes in *RUNX1*^{mut} AML (n=47) compared to *RUNX1*^{wt} AML (n=368)

Due to size constraints, this table is not presented in the document.
The file is available as an Excel file online at
https://clincancerres.aacrjournals.org/content/23/22/6969

Table S2.5: Genes and positions investigated using km approach

Gene	Location
ASXL1	exon 12
BRAF	exon 15
CALR	whole transcript
CSF3R	exons 13-15
DNMT3A	exon 23
FLT3	exons 13-15
FLT3	exon 20
GATA2	exons 2-6
IDH1	exons 3-5
IDH2	exons 3-5
JAK2	exons 13-15
KIT	exons 17-18
KIT	exons 7-9
KMT2A	exons 8+2
KRAS	exons 2-3
NPM1	exons 10-11
NRAS	exons-2-3
PTPN11	exon 3
SF3B1	exons 12-16
SRSF2	whole transcript
TP53	whole transcript
WT1	exons 5-6

Table S2.6: List of the genes that showed best positive and negative correlation according to our model based on mutational pattern

Correlations were performed in the *RUNX1*^{mut} cohort only (n=47), using the following template: 1 (missense-/+), 2 (nonsense/frameshift-/+), 3 (missense-/-), 4 (nonsense/frameshift-/-). Genes are ordered according to their correlation to this template. Genes with maximum expression levels in *RUNX1*^{mut} specimens < 1 RPKM were not included in this analysis.

Due to size constraints, this table is not presented in the document.
The file is available as an Excel file online at
https://clincancerres.aacrjournals.org/content/23/22/6969

Chapter 3: High frequency of germline *RUNX1* mutations in patients with *RUNX1*-mutated AML

Laura Simon[1], Jean-François Spinella[1], Chi-Yuan Yao[1], Vincent-Philippe Lavallée[1], Isabel Boivin[1], Geneviève Boucher[1], Eric Audemard[1], Marie-Eve Bordeleau[1], Sébastien Lemieux[1,2], Josée Hébert[1,3,4,5]* and Guy Sauvageau[1,3,5]*.

[1] The Leucegene Project at Institute for Research in Immunology and Cancer, Université de Montréal, Montréal, Québec, Canada. [2] Department of Biochemistry, Université de Montréal, Montréal, Canada. [3] Division of Hematology-Oncology, Maisonneuve-Rosemont Hospital, Montréal, Québec, Canada. [4] Leukemia Cell Bank of Quebec, Maisonneuve-Rosemont Hospital, Montréal, Canada. [5] Department of Medicine, Faculty of Medicine, Université de Montréal, Montréal, Canada.

*Corresponding Authors:
Guy Sauvageau, Institute for Research in Immunology and Cancer (IRIC), P.O. Box 6128, Downtown Station, Montreal, Quebec H3C 3J7, Canada. Phone: 514-343-7134; Fax: 514-343-5839; E-mail: guy.sauvageau@umontreal.ca; and Josée Hébert, josee.hebert@umontreal.ca

Manuscript published in ***Blood*** 2020 May 21;135(21):1882–1886.

doi:10.1182/blood.2019003357

3.1 Author contributions

L.S., J-F.S., J.H. and G.S. designed the experiments and wrote the manuscript. L.S., V-P.L., and I.B. performed validation of mutations. L.S., J-F.S. and C-Y.Y. performed mutation, copy number variation and transcriptomic characterization, and generated all the figures. G.S. and M.-E.B. spearheaded the data analysis and manuscript redaction. V-P.L., G.B., E.A., and S.L. assisted with data analysis.

Contribution:

All figures and tables were generated by Laura Simon (100%), with the exception of the figures listed below :

Figure S3.3 was generated by Jean-François Spinella (100%)

Figures 3.1(c), 3.2(a), S3.1, S3.2, S3.7 were generated by Laura Simon and Chi-Yuan Yao with supervision of Jean-François Spinella

Figure S3.4 was generated by Geneviève Boucher with assistance from Laura Simon

Figure S3.6 was generated by Eric Audemard with assistance from Laura Simon

3.2 Abstract

RUNX1 is mutated in approximately 10% of adult AML. Although most *RUNX1* mutations in this disease are believed to be acquired, they can also be germline. Indeed, germline *RUNX1* mutations result in the well-described autosomal dominant familial platelet disorder with predisposition to hematologic malignancies (RUNX1-FPD, FPD/AML, FPDMM) in which about 44% of affected individuals progress to AML or myelodysplastic syndromes. Using the Leucegene *RUNX1* AML patient group, we sought to investigate the proportion of germline versus acquired *RUNX1* mutations in this cohort. Our results showed that 30% of *RUNX1* mutations in our AML cohort are germline. Molecular profiling revealed higher frequencies of *NRAS* mutations and other mutations known to activate various signaling pathways in these *RUNX1* germline mutated AML. Moreover, two patients (mother and son) had co-occurrence of *RUNX1* and *CEBPA* germline mutations with variable AML disease onset at 59 and 27 years, respectively. Together this data suggests a higher than anticipated frequency of germline *RUNX1* mutations in the Leucegene cohort and further highlights the importance of testing for *RUNX1* mutations in instances where allogeneic stem cell transplantation with related donor is envisioned.

Key points:

1/ Up to 30% of *RUNX1* mutations in the Leucegene AML cohort were confirmed to be germline.

2/ *RUNX1* germline-mutated AML shows a high frequency of *NRAS* mutations and other mutations known to activate various signaling pathways.

3.3 Introduction

Many acute leukemia predisposition syndromes (LPS) have been identified over the years (1). The revised WHO classification categorizes myeloid neoplasms with germline predisposition as a distinct entity (2). The most frequently mutated genes in these syndromes are: *GATA2*, *ETV6*, *CEBPA*, and *RUNX1* (3). Inherited mutations in *RUNX1* lead to familial platelet disorder with predisposition to hematologic malignancies or RUNX1-FPD. In this disease alterations in *RUNX1* include heterozygous missense, frameshift and nonsense mutations, as well as large intragenic and chromosomal deletions involving chr21q22.12 (4,5). It is estimated that approximately 44% of individuals with RUNX1-FPD will develop AML or myelodysplastic syndromes throughout their lives, with a median age of onset of 33 years (6,7). Identifying these patients is crucial for genetic counselling and for carefully monitoring patients at risk of malignant transformation to optimize the timing of treatment intervention and, if an allogeneic transplantation is indicated, ensure that an affected family member is not a donor (1,3).

3.4 Materials and Methods

Material and methods are detailed in supplemental Methods. Primary AML specimens were collected between 2001 and 2015 according to Quebec Leukemia Cell Bank (BCLQ) procedures. Genetic variants were identified by RNA-sequencing as described in (8) and validated in tumor DNA. Copy number variations (CNVs) were identified using whole genome sequencing (depth coverage ~5X). Forty four *RUNX1* and 12 non-*RUNX1* mutations were validated as somatic or germline based on PCR and bi-directional Sanger sequencing of patient normal DNA obtained from buccal swabs or saliva harvested at diagnosis (oligo sets described in **Table S3.1** and **Table S3.2**). Differential gene expression analysis and screening of acquired mutations in 80 AML-related genes was performed and used to compare groups of patients carrying germline and somatic *RUNX1* mutations.

3.5 Results and Discussion

3.5.1 High frequency of *RUNX1* germline mutations in adult AML

The algorithm for somatic (newly acquired) versus germline status of *RUNX1* mutations in our 430 specimens of the Leucegene collection is shown in **Figure 3.1(A)**. In brief, 67 specimens were found with *RUNX1* mutations. Of these 23 were excluded for 3 main reasons: i) the identified *RUNX1* mutated allele was considered polymorphic in the general population, (>1E-02; n=19; **Table S3.3**); ii) insufficient specimen material for confirmation studies (n=2) and iii) Variant Allele Frequency (VAF) below 30% (n=2) (**Figure 3.1(A)**; **Table S3.4**). Comparison of *RUNX1* allele status was next determined for each of the 44 remaining specimens using normal and tumor DNA (**Figure 3.1(A)**). Chromatogram examination was performed and individually analyzed to identify germline candidate specimens as detailed in **Figure 3.1(B)** and **Figures S3.1 and S3.2**.
To rule out leukemia contamination of non-leukemic tissue as the likely explanation resulting in false positive, we evaluated normal DNA/AML cDNA pairs of each patient for the presence of an additional genetic marker (e.g. *NRAS*, *FLT3*, etc.), which, for germline *RUNX1* mutations, should only be detectable in the leukemic DNA and not in the normal counterpart (**Figure 3.1(B)**). Additionally, heterozygous germline mutations should show the expected mutant/normal allele ratio in buccal DNA of near 50% VAF. Four specimens were considered false positives and excluded from analysis. To control *RUNX1* copy number status, CNVs and ploidy were determined using low-pass WGS data (**Supplemental Methods** and **Figure S3.3**) and/or cytogenetics information. With this approach we could confidently validate 12 candidate specimens as positive for the presence of germline *RUNX1* mutations (**Figure 3.1(A)** and **Figure S3.2**). This shows, at least in our cohort, that up to 30% of *RUNX1* mutations are germline. If our VAF filter is not taken into consideration (as per certain clinical laboratories), this frequency would be 28.6% (12/42).

3.5.2 *RUNX1* germline mutation characteristics

Germline *RUNX1* mutations comprised missense (n=5/12), nonsense (n=4/12) and frameshift (n=3/12) mutations (**Figure 3.1(C**)). Among these, only 4 germline *RUNX1* variants have been previously reported in RUNX1-FPD (p.A60V, p.S141A, p.R166X and p.R204X) (9–12) . Of the 10 distinct germline *RUNX1* mutations identified in this study, eight are predicted to be deleterious

to RUNX1 function (based on published functional studies or prediction tools) and six to be pathogenic/likely pathogenic based on MM-VCEP rules (13) (**Tables S3.6 and S3.7**). Functional predictions for *RUNX1* mutations are in agreement with abnormal expression levels of several transcripts associated with *RUNX1*^{mut} signature (**Figure S3.4**).

3.5.3 Clinical and molecular characteristics of germline and somatic *RUNX1*-mutated patients

Germline *RUNX1*-mutated patients showed a tendency to develop leukemia at a younger age (median = 56.5 yo) than somatic *RUNX1* AML patients (median = 63.5 yo) and to have higher white blood cell (WBC) counts (**Figure 3.1(D)**), as reported by others (14–16). Most notably, four out of 12 patients in the germline *RUNX1* group developed leukemia under the age of 50 (33.3%), compared to only 2 patients from the somatic *RUNX1* group (7.1%; **Figure S3.5(A)**). No major difference in French-American-British (FAB) or genetic subtype frequency was observed between the two groups. Two germline mutations were recurrent in more than one patient, p.S141A and p.R204X. Patient data confirmed that patients P3 and P4 carrying p.S141A were related (see below). On the other hand, family history for patients carrying p.R204X (P9 and P10) was not available and pairwise comparison of genetic alterations in common between each specimen of the Leucegene cohort could not differentiate them from random unrelated pairs (**Figure S3.6**).

Somatic mutations in *RUNX1* are frequently observed in leukemic progression of individuals with germline *RUNX1* mutation (17). This was indeed found in two of our patients (**Figure 3.2(A)**, **Figure S3.5(A)**). We observed a trend for higher frequency of acquired *NRAS* mutations in germline *RUNX1* specimens (p=0.055) than somatic *RUNX1* specimens. Mutations in *NRAS* have been observed in malignant transformation of RUNX1-FPD patients (18). Interestingly, we observed a higher frequency of activating mutations, notably in the RAS pathway, for the germline subgroup (41.7%) when compared to the somatic one (21.4%; p=0.254) (**Figures 3.2(B) and (C)**). *ASXL1* was more frequently mutated in somatic *RUNX1* mutated specimens (39.3% in the somatic vs 25% in the germline; p=0.484). Another group has identified that co-occurring mutations in *RUNX1*-mutated AML patients were primarily *ASXL1* mutations in older patients and *RAS* mutations in younger patients (19). This dichotomy in *RUNX1* co-occurring mutations indicates that several mechanisms of malignant progression may be at play for different groups of *RUNX1* mutated patients.

Differential gene expression analysis identified a list of 10 genes that were significantly upregulated in the germline subgroup (FDR<0.01, **Figure S3.7**, **Table S3.8**). Interestingly, *IL11,* which plays important roles in the differentiation and maturation of megakaryocytes, was among top candidates overexpressed in germline *RUNX1* group compared to somatic *RUNX1*.

3.5.4 Germline mutations in *GATA2* and *CEPBA* observed in AML patients with early onset

Remarkably, the youngest patients to develop leukemia in our cohort at age 27 (P3) carried a germline *CEBPA* mutation (p.R297L). The p.R297L mutation has been previously reported as germline in familial AML with mutated *CEBPA* (20) . Of interest, his mother carrying the same germline mutation load developed AML at 59, and acquired a *GATA2* mutation not found in the son's specimen (**Table S3.9**, **Figure S3.5(B) and (D)**). This suggests that *RUNX1* and *CEBPA* are not sufficient to induce full transformation of hematopoietic stem/progenitor cells, and that additional events, such as *GATA2*, are involved. Conversely and interestingly, a patient with germline *GATA2* mutation developed AML at age 31 (P42) in which acquired *RUNX1* mutation was found (**Figures S3.5(A) and (C**)).

3.6 Conclusion

Using rigorous criteria, we could identify a high incidence of 30% germline *RUNX1* mutations in *RUNX1* mutated AML of the Leucegene cohort. RNA-sequencing at the time of AML diagnosis revealed that these leukemias show high frequency of *NRAS* mutations and of other mutations known to activate various signaling pathways. Identification of germline mutations in other driver genes such as *CEBPA* and *GATA2* further highlight the notion that germline mutations might be underestimated and importantly impact leukemia predisposition. Overall, and at least this study suggests that testing for donor *RUNX1* mutation status may be important in families where RUNX1-FPD cases have been identified and where familial stem cell transplantation is considered. These data merit confirmation in larger population cohorts.

3.7 Figures

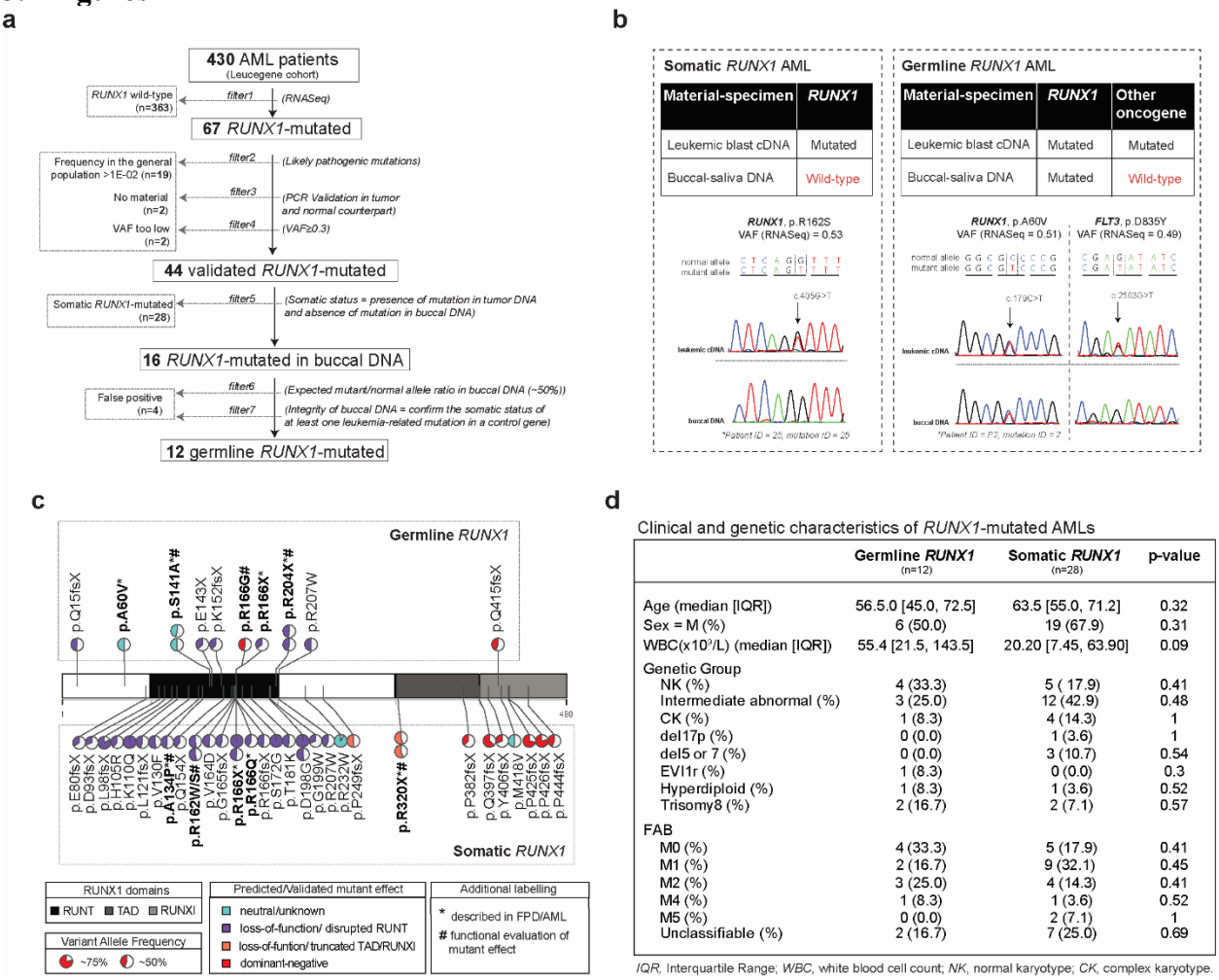

Figure 3.1: AML patients from the Leucegene cohort carrying germline and somatic *RUNX1* mutations

(a) Diagram showing the pipeline used for the identification of germline and somatic *RUNX1* mutations. (b) Sequencing chromatograms of leukemic cDNA/normal DNA pairs covering mutation sites for *RUNX1* and control oncogene. Refer to Supplementary Figure 1 and 2 for complete analysis of leukemic/normal DNA pairs (c) Diagram depicting primary structure of RUNX1 protein with identified germline mutations (top) and somatic mutations (bottom). Pie charts show variant allele frequency (VAF) for each mutation as revealed by RNA-sequencing. Predicted effect of mutation on protein function was determined by prediction tools when not previously described in functional studies and it is depicted by color scheme. Mutations that have been validated in functional studies are highlighted in bold and marked with #. Mutations that have been described in RUNX1-FPD pedigrees are highlighted in bold and marked with *. Refer to

Supplementary Table 5 for references to such studies. Protein domains and mutation positions are based on isoform NP_001745.2. RUNT: 85-206, TAD: 318-398, RUNXI: 389-480. (d) Clinical and genetic characteristics of AML patients with germline and somatic *RUNX1* mutations.

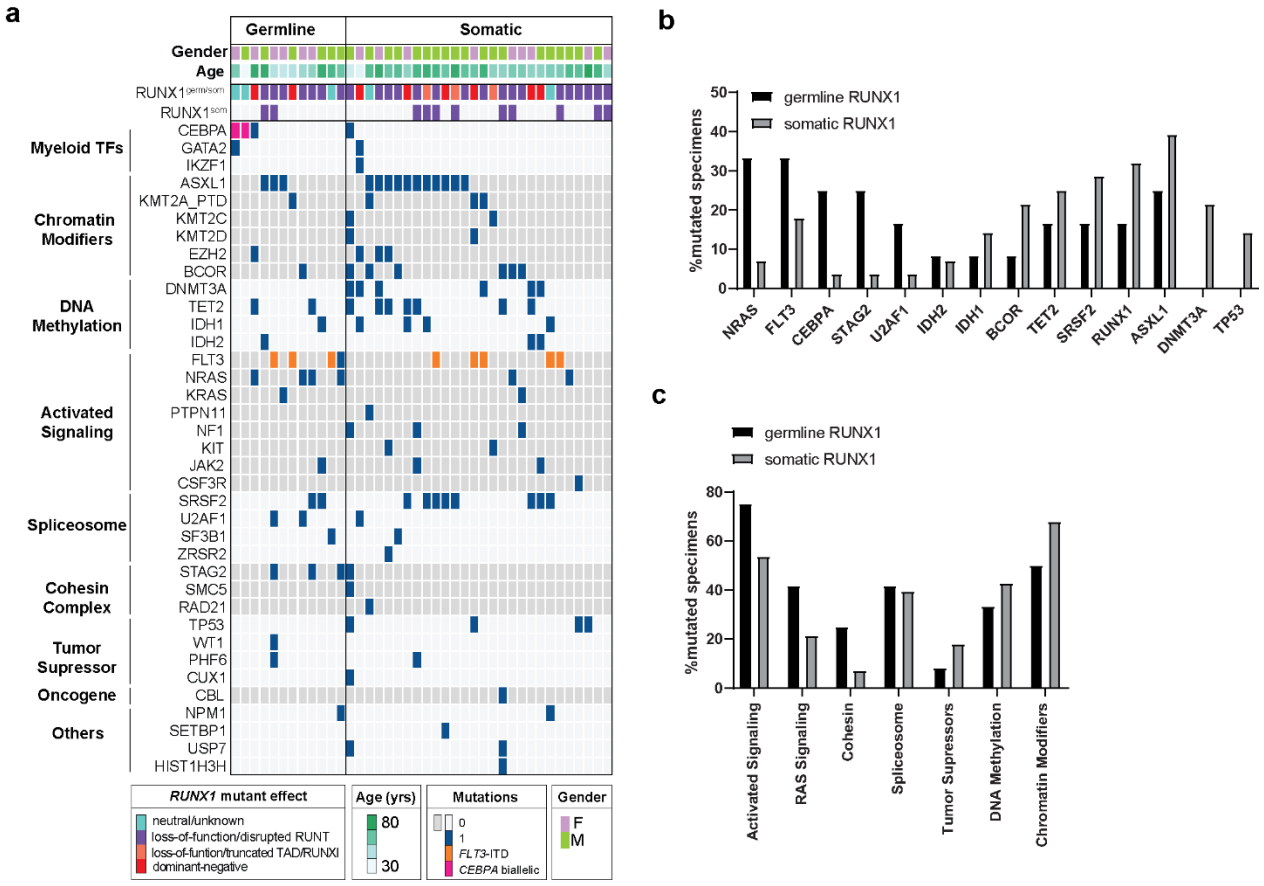

Figure 3.2: Mutational profile of primary AML cells with germline *RUNX1*^{mut} shows enrichment of activated signaling pathway

(a) Mutation grid of *RUNX1*-mutated primary AML specimens presenting one patient sample per column. Samples are grouped according to their *RUNX1* mutation germinal status. Co-occurring mutated genes are shown in each row and are grouped by gene ontology. Enrichment between comparison groups was calculated using Fisher's exact test. (b) Distribution of most frequent mutated genes (c) and mutated groups in germline and somatic *RUNX1* patient cohorts.

3.8 Acknowledgments

We thank Katrin Ericson for helpful discussions and critical reading of the manuscript. We thank Muriel Draoui for project coordination, Sophie Corneau and Nadine Mayotte for sample coordination. We acknowledge Raphaëlle Lambert and Jennifer Huber at the IRIC genomics platform for RNA sequencing. We also acknowledge the Banque de cellules leucémiques du Québec (BCLQ) team who characterized and provided all AML samples of the Leucegene cohort with special thanks to G. D'Angelo, C. Rondeau and S. Lavallée. The research was supported by the Leukemia and Lymphoma Society and the Babich Family Foundation Runx1 Research Program (grant #6553-18), by the Government of Canada through Genome Canada and the Ministère de l'Économie et de l'Innovation du Québec through Génome Québec (grant #13528). J Hébert is recipient of the Industrielle-Alliance research chair in leukemia at Université de Montréal. BCLQ is supported by grants from the Cancer Research Network of the Fonds de Recherche du Québec – Santé (FRQS). L Simon received graduate scholarships from the Cole Foundation and the FRQS. V-P Lavallée is recipient of a Vanier Canada Graduate Scholarship. JF Spinella is supported by a postdoctoral fellowship from the Canadian Institutes of Health Research (#158159).
Disclosure of Conflicts of Interest: No conflict of interest for any of the authors.

3.9 References

1. Porter CC. Germ line mutations associated with leukemias. *Hematology Am Soc Hematol Educ Program.* 2016;2016(1):302-308.
2. Arber DA, Orazi A, Hasserjian R, et al. The 2016 revision to the World Health Organization classification of myeloid neoplasms and acute leukemia. *Blood*. 2016;127:2391–2405.
3. Godley L, Shimamura A. Genetic predisposition to hematologic malignancies: management and surveillance. *Blood*. 2017;130:424–432.
4. Béri-Dexheimer M, Latger-Cannard V, Philippe C, et al. Clinical phenotype of germline RUNX1 haploinsufficiency: from point mutations to large genomic deletions. *Eur J Hum Genet.* 2008;16:ejhg200889.
5. Morgan NV, Daly ME. Gene of the issue: RUNX1 mutations and inherited bleeding. *Platelets.* 2017; 28(2): 208–210.
6. Godley L. Inherited Predisposition to Acute Myeloid Leukemia. *Semin Hematol*. 2014;51(4):306–321.
7. Brown A, Churpek J, Malcovati L, Döhner H, Godley L. Recognition of familial myeloid neoplasia in adults. *Semin Hematol.* 2017; 54(2):60-68.
8. Simon L, Lavallée V-P, Bordeleau M-E, et al. Chemogenomic Landscape of RUNX1-mutated AML Reveals Importance of RUNX1 Allele Dosage in Genetics and Glucocorticoid Sensitivity. *Clin Cancer Res*. 2017; 23(22):6969-6981.
9. Lorente NP. Molecular characterization of patients with hereditary myeloid neoplasms by next-generation sequencing [thesis]. https://riunet.upv.es. Acessed 7 September 2019.
10. Song W-J, Sullivan M, Legare R, et al. Haploinsufficiency of CBFA2 causes familial thrombocytopenia withpropensity to develop acute myelogenous leukaemia. *Nat Genet.* 1999; 23(2):166-175.
11. Bluteau D, Gilles L, Hilpert M, et al. Down-regulation of the RUNX1-target gene NR4A3 contributes to hematopoiesis deregulation in familial platelet disorder/acute myelogenous leukemia. *Blood.* 2011; 118(24):6310-6320.
12. The RUNX1 Research Program. https://runx1db.runx1.com. Accessed 7 September 2019.
13. Luo X, Feurstein S, Mohan S, et al. ClinGen Myeloid Malignancy Variant Curation Expert Panel recommendations for germline RUNX1 variants. *Blood Adv.* 2019;3:2962–2979.
14. Babushok D, Bessler M, Olson T. Genetic predisposition to myelodysplastic syndrome and acute myeloid leukemia in children and young adults. *Leuk Lymphoma.* 2016;57(3):520-536.
15. Kanagal-Shamanna R, Loghavi S, DiNardo C, et al. Bone marrow pathologic abnormalities in familial platelet disorder with propensity for myeloid malignancy and germline RUNX1 mutation. *Haematologica.* 2017; 102(10):1661-1670.
16. Owen C, Toze C, Koochin A, et al. Five new pedigrees with inherited RUNX1 mutations causing familial platelet disorder with propensity to myeloid malignancy. *Blood.* 2008;112(12):4639-45.
17. Preudhomme C, Renneville A, Bourdon V, et al. High frequency of RUNX1 biallelic alteration in acute myeloid leukemia secondary to familial platelet disorder. *Blood* 2009;113:5583–5587.
18. Duarte B, Yamaguti-Hayakawa G, Medina S, et al. Longitudinal sequencing of RUNX1 familial platelet disorder: new insights into genetic mechanisms of transformation to myeloid malignancies. *Br J Haematol*. 2019;186(5):724-734.
19. Khan M, Cortes J, Kadia T, et al. Clinical outcomes and co-occurring mutations in patients with RUNX1-mutated acute myeloid leukemia. *Int J Mol Sci.* 2017;18(8):1618.
20. Nickels EM, Soodalter J, Churpek JE, Godley LA. Recognizing familial myeloid leukemia in adults. *Ther Adv Hematol*. 2013;4(4):254–269.

3.10 Supplemental material and methods

3.10.1 Human leukemia samples

This study is part of the Leucegene project (http://leucegene.ca), an initiative approved by the Research Ethics Boards of the University of Montreal and Maisonneuve-Rosemont Hospital. The Leucegene cohort of primary human AML specimens originating from the Quebec Leukemia Cell Bank (BCLQ) was collected between 2001 and 2015 at 5 university and 4 regional hospitals in the Province of Quebec, Canada, according to the BCLQ procedures. These specimens are collected and cryopreserved in accordance with the Standard Operating Procedures of the Canadian Tissue Repository Network (CTRNet). Tumor DNA was obtained from patient's mononuclear cells separated using Ficoll-Paque gradient centrifugation of blood or bone marrow aspirates collected at the time of diagnosis. Normal DNA was extracted from buccal swabs or saliva collected at the time of diagnosis.

3.10.2 Mutation identification

RNA sequencing (RNAseq) Libraries were constructed with the TruSeq RNA Sample Preparation Kit (Illumina). Sequencing was performed using an Illumina HiSeq 2000 with 200 cycles paired end runs. Small-scale mutations (SNP and indels) were identified from RNAseq data using CASAVA 1.8.2 or km (https://bitbucket.org/iric-soft/km) approaches according to the previously reported pipeline (1). Briefly, mutations outside of the coding region were excluded, and only nonsynonymous variants (SNP or Indel) were considered. Variants identified in normal controls (representing polymorphisms or sequencing artifacts) were filtered out. Known single nucleotide polymorphisms (SNP) (dbSNP, version137) were also removed, except for those in known leukemia "hotspots". Variants reported have ≥8 variant reads, ≥ 20 total reads and a quality score ≥ 20.

3.10.3 Mutation validation

Identified mutations were validated and their germinal status controlled by PCR and Sanger sequencing of patient normal DNA (oligo sets available in Supplementary Table 1). Eventual cross-contamination of normal DNA by leukemic cells were controlled by screening somatic mutations (with Variant Allele Frequency (VAF) >30%) already characterized in the corresponding patients (oligo sets available in Supplementary Table 2). Since mutated RUNX1 proteins with truncated

RUNT domain are unstable and rapidly degraded (2,3), we considered that mutations leading to a truncated RUNT domain would confer loss-of-function with haploinsufficient phenotype. On the other hand, frameshift mutations found in the C-terminal domain have been reported to create elongated isoforms of RUNX1 with functional RUNT domain and intact DNA binding activity, but with dysfunctional transcriptional regulatory domains. These isoforms are believed to act as dominant negatives isoforms of RUNX1 (4). Germline variants were annotated according to recently published rules for RUNX1 (5) and are specified in Supplementary Table 6.

3.10.4 Low-pass whole genome sequencing for CNV identification

Tumor or normal gDNAs were sequenced on HiSeq4000 (paired-end 100). Alignment to the GRCh38 human genome was done using the BWA aligner (6), PCR duplicates were marked using Picard (7) and applied GATK (V4.1.0) (8) base quality score recalibration. A targeted mean depth coverage ~5X was reached for each sample. Identification of regions of genomic gains and losses was done using FREE-Copy number caller (FREEC) (9). The optimization of algorithm parameters (e.g. sliding window size) was conducted using known alterations as reference.

3.10.5 Analysis of polymorphic markers to infer kinship

Variants were called from RNA-sequencing reads using FreeBayes with a cut-off of 5X on coverage (all variants under 5X of coverage were discarded). Identified small variants such SNPs and indels were used to determine the number of variants in common between the index case and each sample in our cohort.

3.10.6 Statistical analyses

Statistical analyses were performed using the R software (version 3.4.0). Survival analysis was performed with Kaplan-Meier method and log-rank test. Fisher's exact test was used for the analysis of contingency tables. Global analysis of differentially expressed (DE) genes was carried out using the R package DEseq2 (version 1.18.1) with default settings (10) and P values were adjusted for multiple hypotheses testing by the Benjamini-Hochberg method.

3.11 Supplemental Figures and Tables

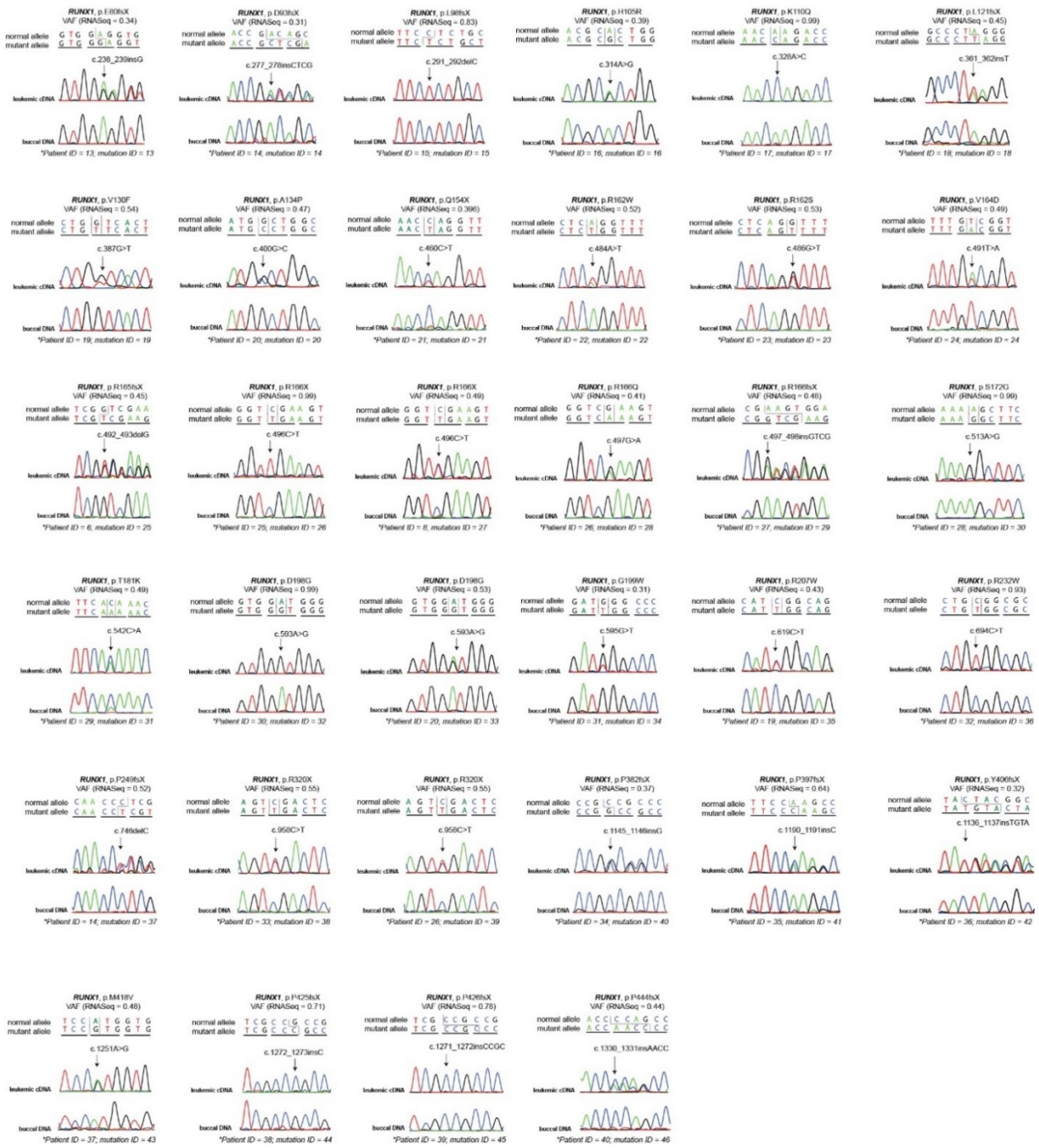

Figure S3.1: Validation of somatic status of *RUNX1* mutations in leukemic cDNA and normal DNA of AML patients

Sequencing chromatograms of leukemic cDNA/normal DNA pairs covering mutation sites for *RUNX1*. Arrow indicates the position of mutation. Description of a sequence change was done based on reference sequence NP_001745.2.

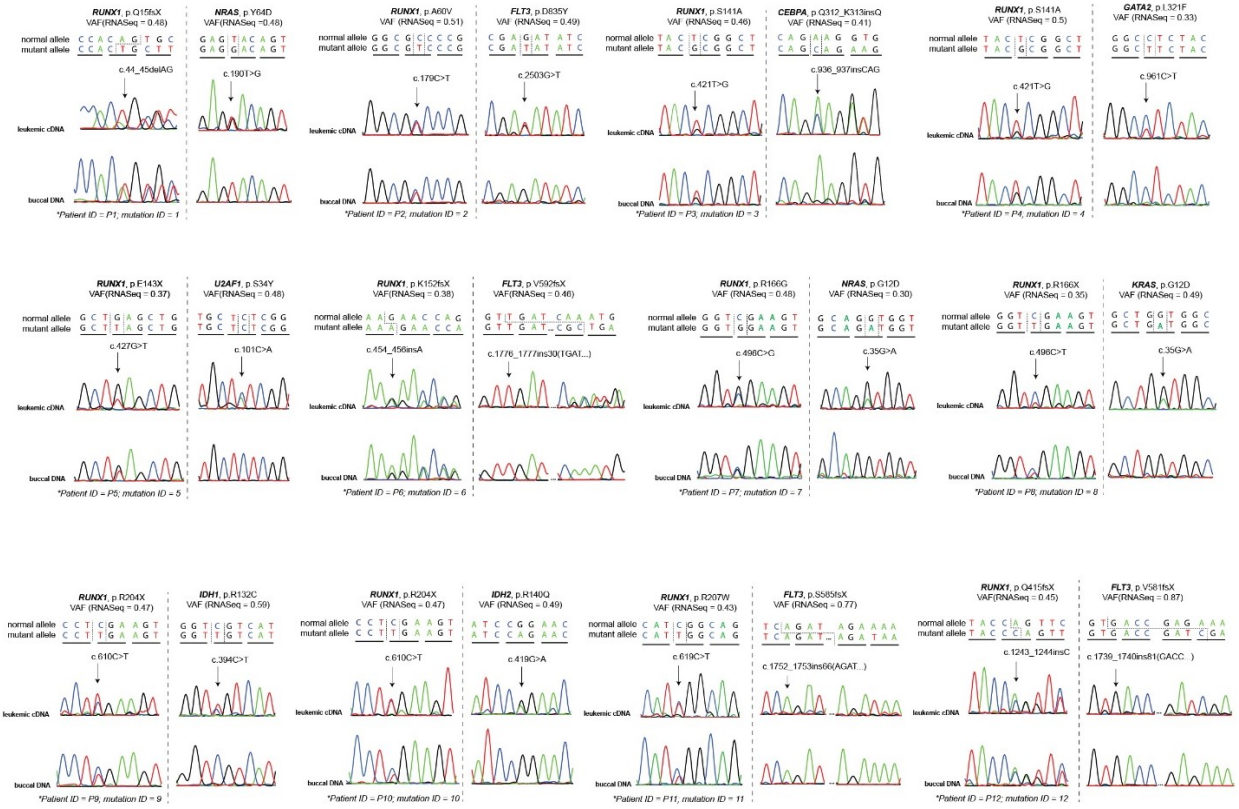

Figure S3.2: Confirmation of germline status of *RUNX1* mutations in leukemic cDNA and normal DNA of AML patients

Sequencing chromatograms of leukemic cDNA/normal DNA pairs covering mutation sites for *RUNX1* and control oncogene (e.g. *NRAS*, *FLT3*, etc.). Arrow indicates the position of mutation.

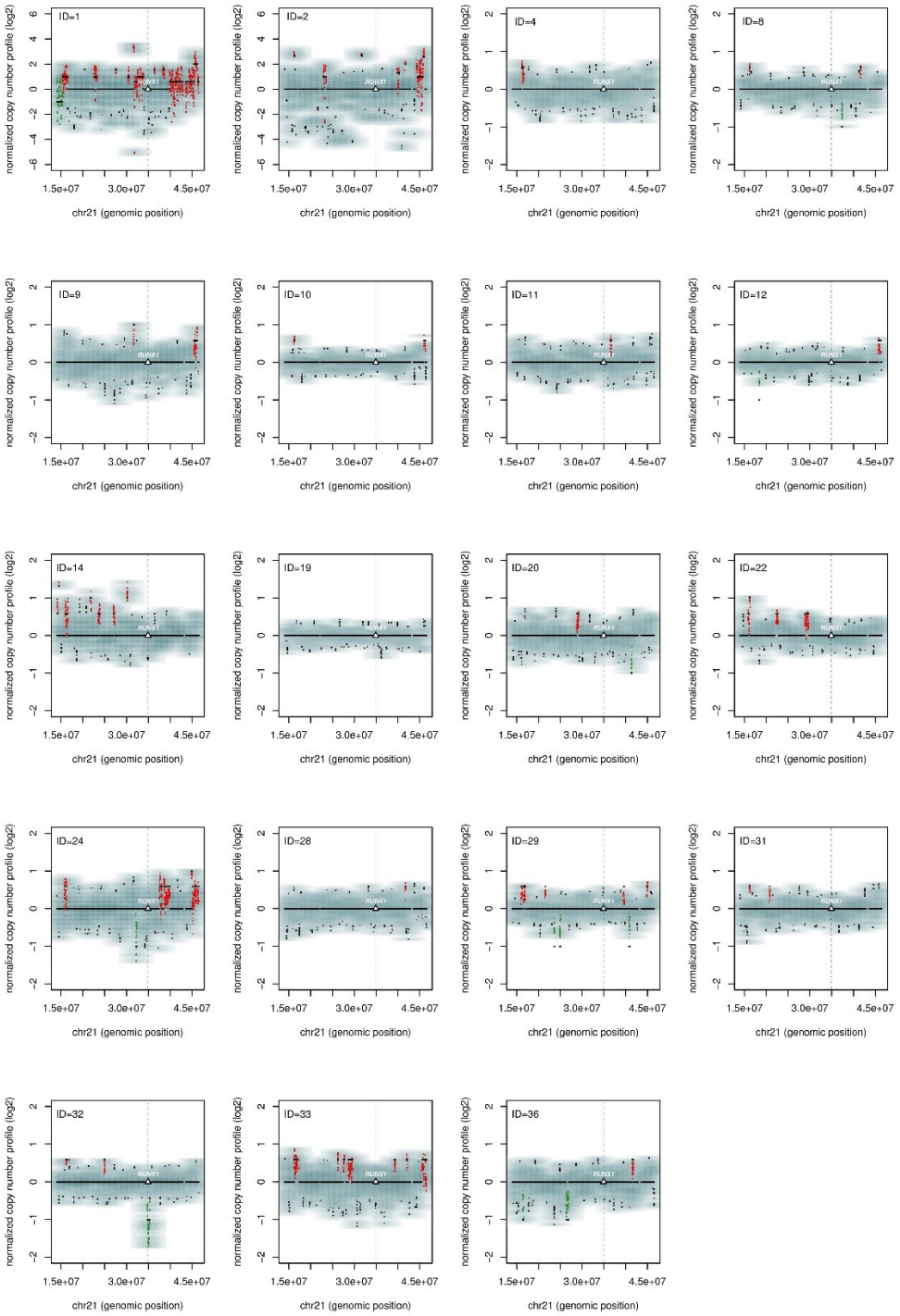

Figure S3.3: Normalized copy number profiles of chromosome 21

Grey density cloud depicts diploid areas. Predicted copy numbers are shown in black. Red and green dots depict copy number gain and loss of copies, respectively. Sample IDs are indicated at the top left corner of each plot. Sample 32 presented a loss of copy event (chr21:34775000-35506999) surrounding the RUNX1 gene. Whole genome sequencing was performed for specimens for which DNA material was still available (n=19).

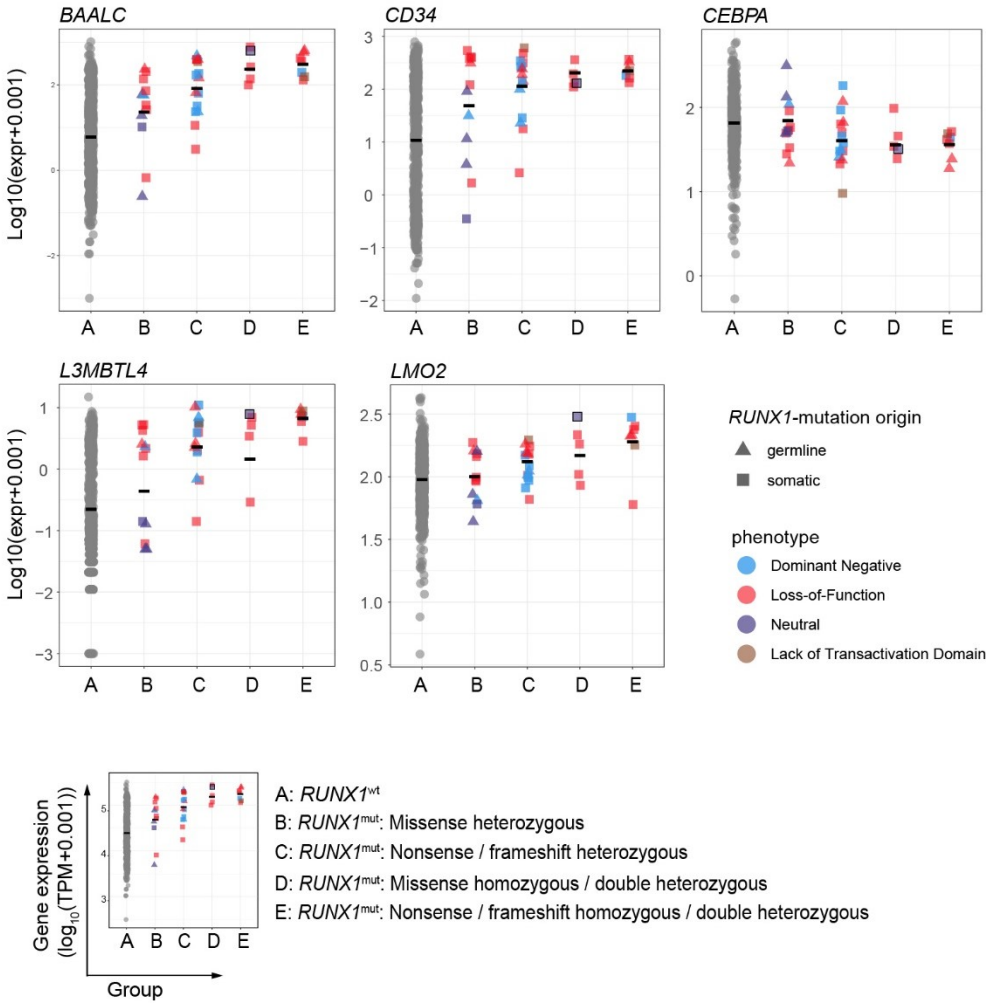

Figure S3.4: Expression of transcripts associated with *RUNX1*^{mut} signature

Specimens are classified as germline (triangle), somatic (square) or unknown (circle). Color codes show predicted functional consequences on RUNX1 function. Specimen with loss of *RUNX1* copy is highlighted with black borders. Genes were selected from *RUNX1*^{mut} signature described in (8).

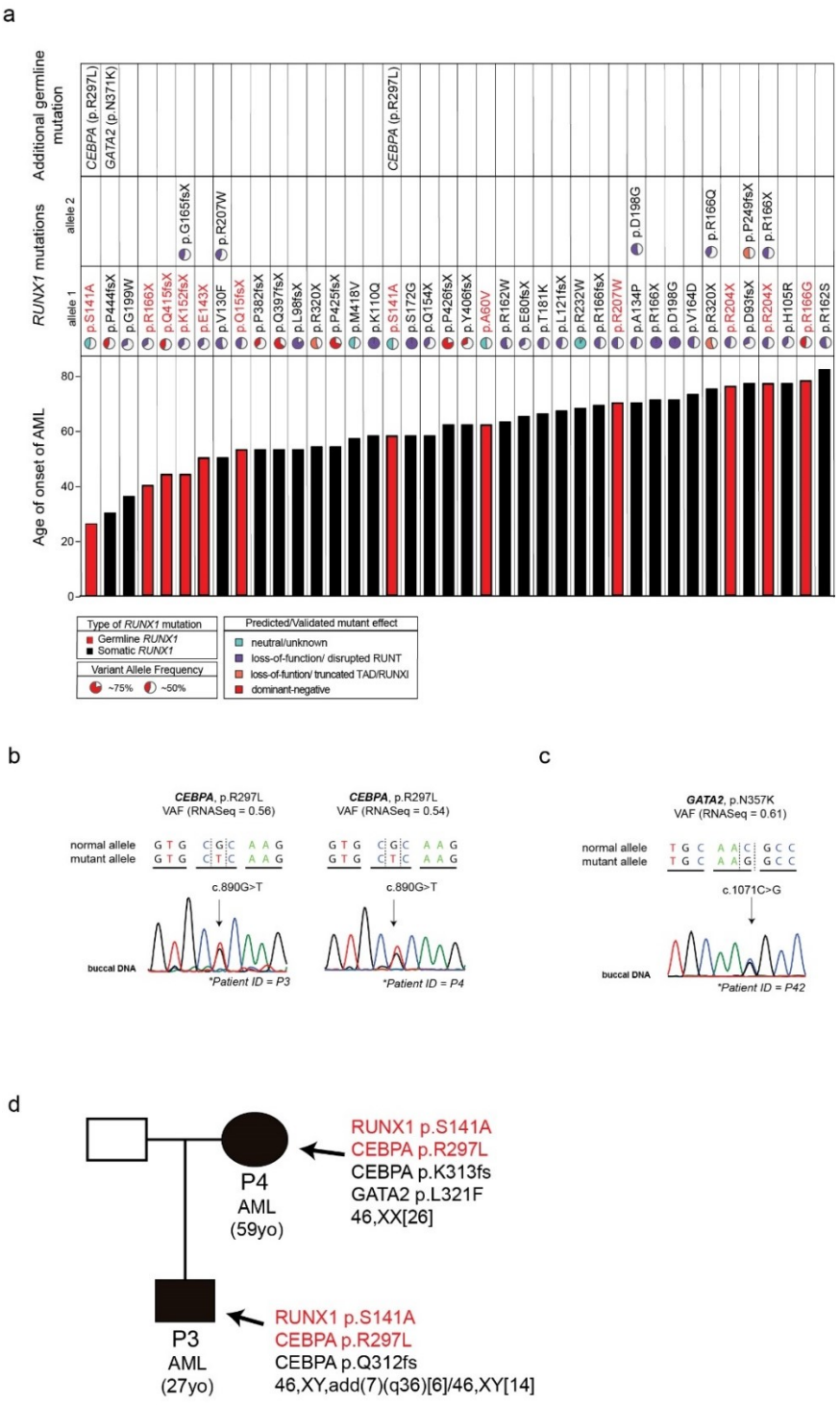

Figure S3.5: Additional germline mutations found in the *RUNX1*-mutated cohort

(a) Additional germline mutations found in the *RUNX1*-mutated cohort and correlation with AML onset. (b) Sequencing chromatograms of normal DNA covering mutation sites for *CEBPA*. (c) Sequencing chromatogram of normal DNA covering mutation sites for *GATA2*. (d) Pedigree chart of mother-child pair identified in our study.

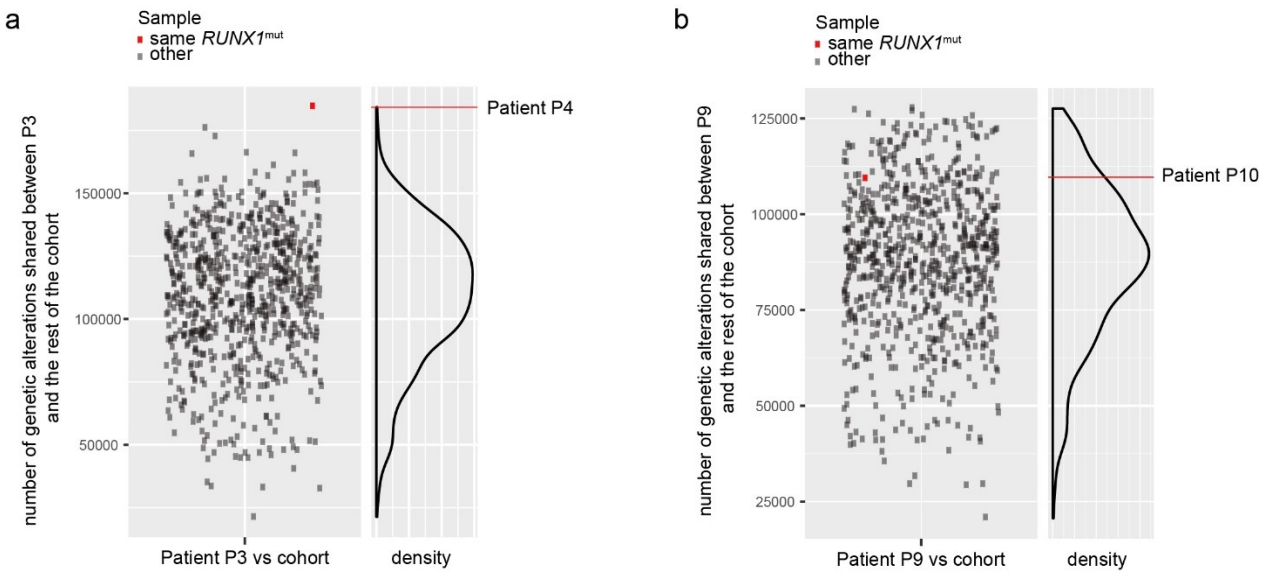

Figure S3.6: Pairwise comparison of variants between index case (a) P3 or (b) P9 and each specimen in the Leucegene cohort

Squares show number of variants in common between index case and each specimen. Red square and red line highlight patients carrying same *RUNX1* mutation as index case.

a

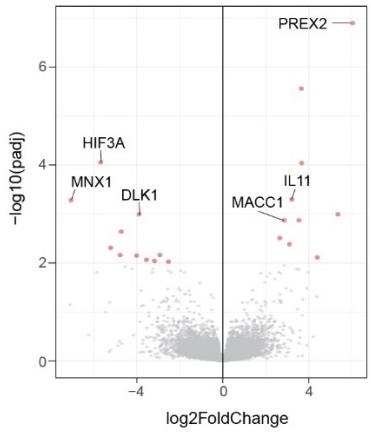

b

Top 500 genes downregulated in germline *RUNX1*

GO Term	GO Processes	Number of genes	FDR q-value
GO:0032502	developmental process	99	3.89E-05
GO:0009653	anatomical structure morphogenesis	43	6.56E-05
GO:0023052	signaling	27	1.04E-04
GO:0007155	cell adhesion	29	3.65E-03

Top 500 genes upregulated in germline *RUNX1*

GO Term	GO Processes	Number of genes	FDR q-value
GO:0031548	regulation of BDNF receptor signaling pathway	2	5.90E-01
GO:0007416	synapse assembly	5	7.88E-01
GO:0048731	regulation of collateral sprouting	3	8.08E-01
GO:0032502	developmental process	47	9.41E-01

c

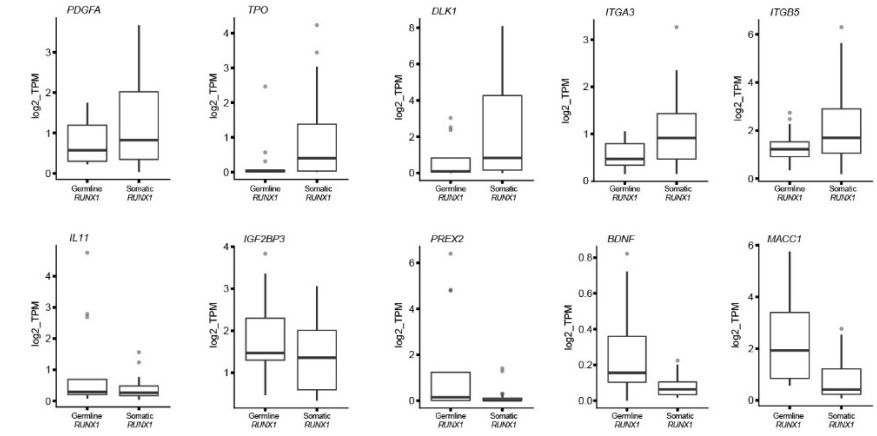

Figure S3.7: Transcriptomic analysis of germline and somatic *RUNX1*-mutated cohorts

(a) Volcano plot shows comparative analysis of expressed genes in germline *RUNX1* AMLs compared with somatic *RUNX1* AMLs. Twenty-one differentially expressed genes are highlighted in red (log2FoldChange>2; FDR<0.01). Wilcoxon rank-sum test (Mann-Whitney), and the false discovery rate method was applied for global gene analysis. (b) Gene Ontology analysis (GO) of top differentially expressed genes. (c) Box plots of the expression levels in germline and somatic *RUNX1* AMLs of genes involved in GO processes revealed by GO analysis.

Table S3.1: Oligo sets used for PCR and Sanger sequencing of individual mutations in cDNA from leukemic cells

Position of mutations are indicated using NM_001754.

NM_001754	Position	*Oligos targeting leukemic cDNA*		*Oligos targeting normal DNA*	
		Primer Forward	Primer Reverse	Primer Forward	Primer Reverse
p.Q15fsX	chr21:36421151	GTGCATTTTCAGGAGGAAGC	AGCACGGAGCAGAGGAAGT	TCGCTCCGAAGGTAAAAGAA	GGCAAGGGACAGCAAAATAA
p.A60V	chr21:36259312	GATGCGTATCCCCGTAGATG	GCGGTAGCATTTCTCAGCTC	TAGGAGCTGTTTGCAGGGTC	TGGGGACACCCTGATGTTTT
p.E80fsX	chr21:36259252	GATGCGTATCCCCGTAGATG	GCGGTAGCATTTCTCAGCTC	TAGGAGCTGTTTGCAGGGTC	TGGGGACACCCTGATGTTTT
p.D93fsX	chr21:36259213	GATGCGTATCCCCGTAGATG	GCGGTAGCATTTCTCAGCTC	TAGGAGCTGTTTGCAGGGTC	TGGGGACACCCTGATGTTTT
p.L98fsX	chr21:36259198	GATGCGTATCCCCGTAGATG	GCGGTAGCATTTCTCAGCTC	TAGGAGCTGTTTGCAGGGTC	TGGGGACACCCTGATGTTTT
p.H105R	chr21:36259177	ACTTCCTCTGCTCCGTGCTG	CCGACAAACCTGAGGTCATT	GTTGCTAGGAGCCCATCCTG	CAAGCTAGGAAGACCGACCC
p.K110Q	chr21:36259163	ACTTCCTCTGCTCCGTGCTG	CCGACAAACCTGAGGTCATT	TAGGAGCTGTTTGCAGGGTC	TGGGGACACCCTGATGTTTT
p.L121fsX	chr21:36252999	ACTTCCTCTGCTCCGTGCTG	CCGACAAACCTGAGGTCATT	TCATTGCTATTCCTCTGCAACC	AGACAGACCGAGTTTCTAGGGA
p.V130F	chr21:36252974	AAGACCCTGCCCATCGCTT	GACTGATCGTAGGACCACGG	TCATTGCTATTCCTCTGCAACC	AGACAGACCGAGTTTCTAGGGA
p.A134P	chr21:36252962	AAGACCCTGCCCATCGCTT	GACTGATCGTAGGACCACGG	TCATTGCTATTCCTCTGCAACC	AGACAGACCGAGTTTCTAGGGA
p.S141A	chr21:36252941	AAGACCCTGCCCATCGCTT	GACTGATCGTAGGACCACGG	TCATTGCTATTCCTCTGCAACC	AGACAGACCGAGTTTCTAGGGA
p.E143X	chr21:36252935	AAGACCCTGCCCATCGCTT	GACTGATCGTAGGACCACGG	TCATTGCTATTCCTCTGCAACC	AGACAGACCGAGTTTCTAGGGA
p.K152fsX	chr21:36252906	AAGACCCTGCCCATCGCTT	GACTGATCGTAGGACCACGG	TCATTGCTATTCCTCTGCAACC	AGACAGACCGAGTTTCTAGGGA
p.Q154X	chr21:36252902	AAGACCCTGCCCATCGCTT	GACTGATCGTAGGACCACGG	TCATTGCTATTCCTCTGCAACC	AGACAGACCGAGTTTCTAGGGA
p.R162W	chr21:36252878	AAGACCCTGCCCATCGCTT	GACTGATCGTAGGACCACGG	TCATTGCTATTCCTCTGCAACC	AGACAGACCGAGTTTCTAGGGA
p.R162S	chr21:36252876	AAGACCCTGCCCATCGCTT	GACTGATCGTAGGACCACGG	TCATTGCTATTCCTCTGCAACC	AGACAGACCGAGTTTCTAGGGA
p.V164D	chr21:36252871	AAGACCCTGCCCATCGCTT	GACTGATCGTAGGACCACGG	TCATTGCTATTCCTCTGCAACC	AGACAGACCGAGTTTCTAGGGA
p.G165fsX	chr21:36252867	AAGACCCTGCCCATCGCTT	GACTGATCGTAGGACCACGG	TCATTGCTATTCCTCTGCAACC	AGACAGACCGAGTTTCTAGGGA
p.R166G	chr21:36252866	AAGACCCTGCCCATCGCTT	GACTGATCGTAGGACCACGG	TCATTGCTATTCCTCTGCAACC	AGACAGACCGAGTTTCTAGGGA
p.R166X	chr21:36252866	AAGACCCTGCCCATCGCTT	GACTGATCGTAGGACCACGG	TCATTGCTATTCCTCTGCAACC	AGACAGACCGAGTTTCTAGGGA
p.R166Q	chr21:36252865	AAGACCCTGCCCATCGCTT	GACTGATCGTAGGACCACGG	TCATTGCTATTCCTCTGCAACC	AGACAGACCGAGTTTCTAGGGA
p.R166fsX	chr21:36252864	AAGACCCTGCCCATCGCTT	GACTGATCGTAGGACCACGG	TCATTGCTATTCCTCTGCAACC	AGACAGACCGAGTTTCTAGGGA
p.S172G	chr21:36231870	AAGACCCTGCCCATCGCTT	GACTGATCGTAGGACCACGG	AAGACCCTGCCCATCGCTT	GACTGATCGTAGGACCACGG
p.T181K	chr21:36231842	AAGACCCTGCCCATCGCTT	GACTGATCGTAGGACCACGG	AAGACCCTGCCCATCGCTT	GACTGATCGTAGGACCACGG
p.D198G	chr21:36231791	AAGACCCTGCCCATCGCTT	GACTGATCGTAGGACCACGG	GGGAACCAGAAGTGGAGAGC	CTTTACGGGGGCCTGACATC
p.G199W	chr21:36231789	AAGACCCTGCCCATCGCTT	GACTGATCGTAGGACCACGG	GGGAACCAGAAGTGGAGAGC	CTTTACGGGGGCCTGACATC
p.R204X	chr21:36231774	AAGACCCTGCCCATCGCTT	GACTGATCGTAGGACCACGG	GGGAACCAGAAGTGGAGAGC	CTTTACGGGGGCCTGACATC
p.R207W	chr21:36206893	AAGACCCTGCCCATCGCTT	GACTGATCGTAGGACCACGG	AGGACAGTGGCCCCAAATTC	TGAGCATCAAGGGGAAACCC
p.R232W	chr21:36206818	AAGACCCTGCCCATCGCTT	GACTGATCGTAGGACCACGG	AGGACAGTGGCCCCAAATTC	TGAGCATCAAGGGGAAACCC
p.P249fsX	chr21:36206765	AAGACCCTGCCCATCGCTT	GACTGATCGTAGGACCACGG	AGGACAGTGGCCCCAAATTC	TGAGCATCAAGGGGAAACCC
p.R320X	chr21:36171607	CTGGGATCCATTGCCTCTCC	GTGAAGGCGCCTGGATAGTG	CAGATCCAACCATCCCCACC	AAGCCACTTCTGCCTTCACA
p.P382fsX	chr21:36164728	CAGGCGCCTTCACCTACTC	CCCACCATGGAGAACTGGTA	ACTTCCGCTCCGTTCTCTTG	GACCTACAGCGAGATCCTGG
p.Q397fsX	chr21:36164685	CAGGCGCCTTCACCTACTC	CCCACCATGGAGAACTGGTA	ACTTCCGCTCCGTTCTCTTG	GACCTACAGCGAGATCCTGG
p.Y406fsX	chr21:36164657	CAGGCGCCTTCACCTACTC	CCCACCATGGAGAACTGGTA	ACTTCCGCTCCGTTCTCTTG	GACCTACAGCGAGATCCTGG
p.Q415fsX	chr21:36164631	CAGGCGCCTTCACCTACTC	CCCACCATGGAGAACTGGTA	ACTTCCGCTCCGTTCTCTTG	GACCTACAGCGAGATCCTGG
p.M418V	chr21:36164623	CGGCTCCTACCAGTTCTCC	CCTCAGTAGGGCCTCCACA	ACTTCCGCTCCGTTCTCTTG	GACCTACAGCGAGATCCTGG
p.P425fsX	chr21:36164600	CGGCTCCTACCAGTTCTCC	CCTCAGTAGGGCCTCCACA	ACTTCCGCTCCGTTCTCTTG	GACCTACAGCGAGATCCTGG
p.P426fsX	chr21:36164597	CGGCTCCTACCAGTTCTCC	CCTCAGTAGGGCCTCCACA	ACTTCCGCTCCGTTCTCTTG	GACCTACAGCGAGATCCTGG
p.P444fsX	chr21:36164544	CGGCTCCTACCAGTTCTCC	CCTCAGTAGGGCCTCCACA	ACTTCCGCTCCGTTCTCTTG	GACCTACAGCGAGATCCTGG

Table S3.2: Oligo sets used for PCR and Sanger sequencing of individual mutations in control genes from leukemic cells DNA

VAF: variant allele frequency

Somatic mutations in other genes	Position	*Oligos targeting leukemic cDNA*		*Oligos targeting normal DNA*	
		Primer Forward	Primer Reverse	Primer Forward	Primer Reverse
NRAS - p.Y64D	chr1:115256521	GACTGATTACGTAGCGGGCG	TAACTCTTGGCCAGTTCGTGG	AGCATTGCATTCCCTGTGGT	CGCCTGTCCTCATGTATTGGT
FLT3 - p.D835Y	chr13:28592642	GGCTGGAAGAAGAGGAGGAC	GGAATGCCAGGGTAAGGATT	AGAACTGCAGCCACCATAGC	CCTGAAGCTGCAGAAAAACC
CEBPA - p.Q312-	chr19:33792384	CTCGGTGCCGCCGGCCT	AACCACTCCCTGGGTCCCCGC	CTCGGTGCCGCCGGCCT	AACCACTCCCTGGGTCCCCGC
GATA2 - p.L321F	chr3:128202759	GCGTCAAGTACCAGGTGTCA	AAGGTGGTGGTTGTCGTCTG	CGTTTCCATCCCTCCTGGTG	AGAGAGACGACCCCAACTGA
U2AF1 - p.S34Y	chr21:44524456	GACTGATTACGTAGCGGGCG	TAACTCTTGGCCAGTTCGTGG	GGCTTCCTGCTAGAGCTGAG	TCCGACAAGTGAGAGACAGGA
FLT3 - p.V592fsX	chr13:28608281	CAATTCCCTTGGCACATCTT	TTTCCAAAAGCACCTGATCC	TCTTTTGTTGCAGGCCCCTT	GACGGCAACCTGGATTGAGA
NRAS p.G12D	chr1:115258747	GACTGATTACGTAGCGGGCG	TAACTCTTGGCCAGTTCGTGG	GGCTTCCTGCTAGAGCTGAG	TCCGACAAGTGAGAGACAGGA
KRAS - p.G12D	chr12:25398284	GGAGAGAGGCCTGCTGAAAATGA	TTGCACTGTACTCCTCTTGACC	AAGCGTCGATGGAGGAGTTT	TGGACCCTGACATACTCCCA
IDH1 - p.R132C	chr2:209113113	GACCAAGTCACCAAGGATGC	TATACATCCCCATGGCAACA	GTGGCACGGTCTTCAGAGAA	GGGATCCTATTGTGCAGCCA
IDH2 - p.R140Q	chr15:90631934	CAGAGCCCACACATTTGCAC	TGTGGCCTTGTACTGCAGAG	CAGAGCCCACACATTTGCAC	TGTGGCCTTGTACTGCAGAG
FLT3 - p.S585fsX	chr13:28608302	CAATTCCCTTGGCACATCTT	TTTCCAAAAGCACCTGATCC	CCCTTCCCTTTCATCCAAGA	TCCATAAGCTGTTGCGTTCA
FLT3 - p.V581fsX	chr13:28608314	CAATTCCCTTGGCACATCTT	TTTCCAAAAGCACCTGATCC	TCTTTTGTTGCAGGCCCCTT	GACGGCAACCTGGATTGAGA

Table S3.3: *RUNX1* variant frequencies in the normal population

VAF: variant allele frequency. NGS: Next-generation Sequencing (RNA-seq). AF: allele frequency

Specimens	NM_001754	VAF by NGS	gnomAD AF Total	1000 Genomes AF
1	p.L56S	0.45	1.48E-02	1.04E-02
2	p.L56S	0.482	1.48E-02	1.04E-02
3	p.L56S	0.669	1.48E-02	1.04E-02
4	p.L56S	0.561	1.48E-02	1.04E-02
5	p.L56S	0.32	1.48E-02	1.04E-02
6	p.L56S	0.416	1.48E-02	1.04E-02
7	p.L56S	0.344	1.48E-02	1.04E-02
8	p.L56S	0.425	1.48E-02	1.04E-02
9	p.L56S	0.451	1.48E-02	1.04E-02
10	p.L56S	0.463	1.48E-02	1.04E-02
11	p.L56S	0.26	1.48E-02	1.04E-02
12	p.L56S	0.472	1.48E-02	1.04E-02
13	p.L56S	1	1.48E-02	1.04E-02
14	p.L56S	0.496	1.48E-02	1.04E-02
15	p.L56S	0.525	1.48E-02	1.04E-02
16	p.L56S	0.294	1.48E-02	1.04E-02
17	p.L56S	0.443	1.48E-02	1.04E-02
18	p.L56S	0.431	1.48E-02	1.04E-02
19	p.L56S	0.435	1.48E-02	1.04E-02
20	p.A60V	0.511	7.03E-05	NA
21	p.S141A	0.459	7.22E-06	NA
22	p.S141A	0.497	7.22E-06	NA
23	p.M418V	0.484	1.65E-05	2.00E-04

Table S3.4: *RUNX1* variants excluded from study

VAF: variant allele frequency; NGS: Next-generation Sequencing (RNA-seq).

Specimens	NM_001754	VAF by NGS	Validation	Karyotype
1	p.K110Q	0.986	inconclusive (no DNA)	44~48,XX,add(1)(p3?2),del(5)(q13),del(6)(p23),+8,add(18)(p11.3),+21[cp22]
2	p.T196fsX	0.34	inconclusive (no DNA)	47,XY,+8[7]/46,XY[13]
3	p.R169fsX	0.117	inconclusive (VAF too low)	46,XY[20]
4	p.T128fsX	0.098	inconclusive (VAF too low)	47,XY,+8[18]/48,XY,+8,+8[3]/46,XY[1]
5	p.D198G	0.521	inconclusive (false pos)	47,XX,+8[19]/46,XX[1]
6	p.Q185R	0.475	inconclusive (false pos)	46,XX,del(5)(q13q33)[24]
7	p.S318fsX	0.403	inconclusive (false pos)	46,XX[25]
8	p.R346fsX	0.41	inconclusive (false pos)	47,XY,+13[2]/48,XY,+13,+22[16]/46,XY[3]

Table S3.5: Karyotype of *RUNX1*-mutated specimens of the Leucegene cohort included in this study

Patient ID	Karyotype
P1	45,X,add(X)(q13),-7,-22,+mar[cp19]/46,XX[1]
P2	46,XY,del(15)(q13q15)[7]/47,idem,+8[14]
P3	46,XY,add(7)(q36)[6]/46,XY[14]
P4	46,XX[26]
P5	47,XX,+8[20]/46,XX[1]
P6	46,XX[20]
P7	47,XX,+8[20]
P8	46,XX,t(3;12)(q26.2;p13)[2]/45,XX,t(3;12)(q26.2;p13),-7[20]
P9	46,XY[19]/92,idemx2[4]
P10	47,XY,+13[3]/46,XY[30]
P11	51~52,XY,+6,+10,+13,+16,+21,+22[cp3]/46,XY[18]
P12	46,XY[19]
P13	47,XY,i(8)(q10),+i(8)(q10),del(12)(p11.2)[20]
P14	48,XY,+13,+19[20]/46,XY[4]
P15	47,XX,+8[21]_HSCT(female_donor).
P16	45,XX,-7[20]
P17	47,XX,+21[6]/46,XX,?del(9)(q21q22)[6]/46,XX[9]
P18	46,XY[20]
P19	44~47,XX,-6,del(7)(q22),der(12)t(12;17)(p13;q21),-17,-20,-22,+1~5mar[cp20]
P20	47,XY,+13[16]/46,XY[5]
P21	46,XX,ider(7)(q10)del(7)(q22)[21]
P22	46,XY,t(4;12)(q12;p13)[21]
P23	44,XX,-5,-7,del(16)(q22),-17,add(18)(q2?1),+mar[20]
P24	46,XY[22]
P25	46,XY,del(20)(q11.2)[19]/46,XY[1]
P26	47,XY,+13[15]/47,XY,+8[2]/46,XY[6]
P27	49,XY,t(4;13)(q31;q32),add(6)(q21),del(7)(q32),+8,+del(8)(q21q21),-20,-20,-21,+mar1,+mar2,+mar3,+mar4[21]
P28	46,XY[20]
P29	46,XY,del(7)(p11.2),del(7)(q11.2),t(11;15)(q23;q1?5),add(17)(p1?3)[21]
P30	45,XY,-7[3]/46,XY[18]
P31	45,XY,add(16)(p13.1),-17[20]
P32	46,XY[21]
P33	46,XY,inv(7)(q22q36)[20]
P34	47,XX,+13[6]/46,XX[18]
P35	47,XX,+21[15]/46,XX,i(21)(q10)[2]/46,XX[3]
P36	52,XX,+5,+5,+6,+8,+15,+20[2]/46,XX[18]
P37	48,X,idic(Y)(q10)X3[5]/46,XY[25]
P38	46,XY[20]
P39	47,XY,+13[13]/49,XY,+9,+13,+13[7]/46,XY[1]
P40	47,XX,+8[21]

Table S3.6: *RUNX1* mutations identified in the Leucegene cohort

Position of mutations are indicated using NM_001754.

Mutation	NM_001754	NM_001754	Germinal status	Described in MDS/AML	Described in RUNX1-FPD	Functional impact on RUNX1	gnomAD AF Total	1000 Genomes AF	ClinVar clinical significance	MM-VCEP ACMG/AMP criteria code			
										Very strong criteria	Strong criteria	Moderate criteria	Supporting criteria
1	p.Q15fsX	c.44_45delAG	germline			Truncated RUNT	NA	NA	Uncertain significance			PM2, PVS1_moderate	PS4_supporting
2	p.A60V	c.179C>T	germline	Carnicer MJ et al., *Leukemia* (2002)	Lorente NP, *thesis* (2018)		7.40E-05	NA	Uncertain significance				
3	p.S141A	c.421T>G	germline		RUNX1db	Normal TA (Zhang L et al., *J Biol Chem*. (2003))	7.22E-06	NA	Uncertain significance				PP3, BS3_supporting, PS4_supporting
4	p.S141A	c.421T>G	germline		RUNX1db	Normal TA (Zhang L et al., *J Biol Chem*. (2003))	7.22E-06	NA	Uncertain significance				PP3, BS3_supporting, PS4_supporting
5	p.E143X	c.427G>T	germline			Truncated RUNT	NA	NA	Pathogenic	PVS1		PM2	PS4_supporting
6	p.K152fsX	c.454_456insA	germline	Ernst T et al., *Haematol.* (2010)		Truncated RUNT	NA	NA	Pathogenic	PVS1		PM2	PS4_supporting
7	p.R166G	c.496C>G	germline	Imai Y et al., *Blood* (2000)		Loss-of-function/Dominant-negative (Imai Y et al., *Blood* (2000))	NA	NA	Pathogenic	PM5		PM2	PP3, PS4_supporting
8	p.R166X	c.496C>T	germline	Preudhomme C et al., *Blood* (2000)	Bluteau D et al., *Blood* (2011)	Truncated RUNT	NA	NA	Pathogenic	PVS1	PS4	PM2	PP1
9	p.R204X	c.610C>T	germline	Osato M et al., *Blood* (1999)	Song W-J et al., *Nat Genet.* (1999)	Loss-of-function (Osato M et al., *Blood* (1999))	NA	NA	Pathogenic	PVS1	PS4	PM2	PP1
10	p.R204X	c.610C>T	germline	Osato M et al., *Blood* (1999)	Song W-J et al., *Nat Genet.* (1999)	Loss-of-function (Osato M et al., *Blood* (1999))	NA	NA	Pathogenic	PVS1	PS4	PM2	PP1
11	p.R207W	c.619C>T	germline	You E et al., *Am J Clin Pathol* (2017)			NA	NA	Uncertain significance			PM2	PP3, PS4_supporting
12	p.Q415fsX	c.1243_1244insC	germline			Elongated RUNX1 isoform	NA	NA	Likely Pathogenic		PVS1_strong	PM2	PS4_supporting
13	p.E80fsX	c.238_239insG	somatic	Chen CY et al., *Br J Haematol.* (2007)		Truncated RUNT							
14	p.D93fsX	c.277_278insCTCG	somatic			Truncated RUNT							
15	p.L98fsX	c.291_292delC	somatic	Harada H et al., *Blood* (2003)		Loss-of-funtion (Harada H et al., *Blood* (2003))							
16	p.H105R	c.314A>G	somatic										
17	p.K110Q	c.328A>C	somatic	Scharenberg C et al., *Haematol.* (2017)	RUNX1db								
18	p.L121fsX	c.361_362insT	somatic	Garg M et al., *Blood* (2015)		Truncated RUNT							
19	p.V130F	c.387G>T	somatic										
20	p.A134P	c.400G>C	somatic		Walker LC et al., *Br J Haematol.* (2002)	Loss-of-function (Matheny CJ et al., *The EMBO Journal* (2007))							
21	p.Q154X	c.460C>T	somatic	Beer PA et al., *Blood* (2010)		Truncated RUNT							
22	p.R162W	c.484A>T	somatic										
23	p.R162S	c.486G>T	somatic	Papaemmanuil E et al., *Blood* (2013)									
24	p.V164D	c.491T>A	somatic	Skokowa J et al., *Blood* (2014)									
25	p.G165fsX	c.492_493delG	somatic			Truncated RUNT							
26	p.R166X	c.496C>T	somatic	Preudhomme C et al., *Blood* (2000)	Bluteau D et al., *Blood* (2011)	Truncated RUNT							
27	p.R166X	c.496C>T	somatic	Preudhomme C et al., *Blood* (2000)	Bluteau D et al., *Blood* (2011)	Truncated RUNT							
28	p.R166Q	c.497G>A	somatic		Song W-J et al., *Nat Genet.* (1999)								
29	p.R166fsX	c.497_498insGTCG	somatic			Truncated RUNT							
30	p.S172G	c.513A>G	somatic		RUNX1db								
31	p.T181K	c.542C>A	somatic										
32	p.D198G	c.593A>G	somatic	Preudhomme C et al., *Blood* (2000)	RUNX1db								
33	p.D198G	c.593A>G	somatic	Preudhomme C et al., *Blood* (2000)	RUNX1db								
34	p.G199W	c.595G>T	somatic	Imagawa J et al., *Blood* (2010)									
35	p.R207W	c.619C>T	somatic	You E et al., *Am J Clin Pathol* (2017)									
36	p.R232W	c.694C>T	somatic	Gaidzik VI et al., *J Clin Oncol.* (2011)									
37	p.P249fsX	c.746delC	somatic	Palomo L et al., *Oncotarget* (2016)									
38	p.R320X	c.958C>T	somatic	Ernst T et al., *Haematol* (2010)	Owen CJ et al., *Blood* (2008)								
39	p.R320X	c.958C>T	somatic	Ernst T et al., *Haematol* (2010)	Owen CJ et al., *Blood* (2008)								
40	p.P382fsX	c.1145_1146insG	somatic			Elongated RUNX1 isoform							
41	p.Q397fsX	c.1190_1191insC	somatic	Papaemmanuil E et al., *NEJM* (2016)		Elongated RUNX1 isoform							
42	p.Y406fsX	c.1136_1137insTGTA	somatic			Elongated RUNX1 isoform							
43	p.M418V	c.1251A>G	somatic										
44	p.P425fsX	c.1272_1273insC	somatic			Elongated RUNX1 isoform							
45	p.P426fsX	c.1271_1272insCCGC	somatic			Elongated RUNX1 isoform							
46	p.P444fsX	c.1330_1331insAACC	somatic			Elongated RUNX1 isoform							

PVS1 = Null variant in a gene where LOF is a known mechanism of disease; PM1 = Located in a mutational hotspot and/or critical and well-established functional domain without BEN variation; PM2 = Absent from control subjects; PM4 = Protein length changes due to in-frame deletions/insertions in a nonrepeat region or stop-loss variants; PM5 = Missense change at AA residue where a different missense change determined to be PATH has been seen before; PP1 = Cosegregation with disease in multiple affected family members; PP3= Multiple lines of computational evidence support a deleterious effect on the gene or gene product; PS4 = The prevalence of the variant in affected individuals is significantly increased compared with the prevalence in controls

Table S3.7: *RUNX1* variants identified in this study and respective predictive values of pathogenicity from SIFT, Polyphen, VEST, CHASM, and REVEL

Protein sequence change	SIFT	Polyphen	VEST score	CHASM score	REVEL
A60V	0.2	0.007	0.20	0.75	0.284
H105R	0	0.943	0.91	0.75	0.942
K110Q	0	0.995	0.68	0.78	0.957
V130F	0	1	0.93	0.70	0.937
A134P	0	1	0.99	0.89	0.945
S141A	0.02	0.442	0.75	0.61	0.851
R162W	0	1	0.97	0.57	0.927
R162S	0	1	0.98	0.94	0.818
V164D	0	0.999	0.95	0.81	0.985
R166G	0	0.997	0.96	0.90	0.914
R166Q	0	0.988	0.99	0.71	0.962
S172G	0	0.345	0.80	0.72	0.939
T181K	0	0.026	0.87	0.85	0.959
D198G	0	0.996	0.94	0.93	0.951
G199W	0	1	0.90	0.85	0.971
R207W	0.01	0.989	0.72	0.42	0.811
R232W	0.02	0.999	0.85	0.53	0.796
M418V	0.02	0.014	0.35	0.55	0.14

Table S3.8: List of top 100 genes ranked by most significant differentially expressed in transcriptomic comparison of germline (n=12) vs somatic (n=28) *RUNX1*-mutated AML specimens

Due to size constraints, this table is not complete in the present document.
A preview of the table is shown.
File is available as an Excel file online at https://ashpublications.org/blood/article-abstract/135/21/1882/452491/High-frequency-of-germline-RUNX1-mutations-in?redirectedFrom=fulltext#supplementary-data

GeneSymbol	EnsemblID	Mean (TPM)	log2_FoldChange Germline vs Somatic	pvalue	adjpvalue (FDR)
PREX2	ENSG00000046889	293.17	6.04	3.71E-12	1.27E-07
HHIP	ENSG00000164161	81.45	3.66	1.62E-10	2.75762E-06
HIF3A	ENSG00000124440	94.51	-5.68	7.77E-09	8.8276E-05
IL12A-AS1	ENSG00000244040	553.77	3.67	1.07E-08	9.1346E-05
IL11	ENSG00000095752	71.03	3.21	7.40E-08	0.000504399
MNX1	ENSG00000130675	160.40	-7.06	9.20E-08	0.000522687
BMP6P1	ENSG00000236323	6.59	5.36	2.21E-07	0.001014426
AC106865.1	ENSG00000250771	291.52	-3.90	2.38E-07	0.001014426
NPTX1	ENSG00000171246	49.70	3.54	3.96E-07	0.001348669
MACC1	ENSG00000183742	698.11	2.86	3.86E-07	0.001348669
DLK1	ENSG00000185559	2008.78	-4.72	7.38E-07	0.002287774
AC020656.2	ENSG00000274979	61.50	2.65	1.09E-06	0.003100392
LINC01222	ENSG00000233410	11.08	3.11	1.58E-06	0.004131717
CDH20	ENSG00000101542	34.96	-5.22	2.01E-06	0.004888947
CCND1	ENSG00000110092	872.16	-2.93	3.24E-06	0.006890874
HS3ST4	ENSG00000182601	33.72	-4.78	3.18E-06	0.006890874
MAB21L1	ENSG00000180660	18.28	-4.01	3.51E-06	0.007043888
KRT79	ENSG00000185640	11.82	4.40	4.07E-06	0.007708128
SASH1	ENSG00000111961	532.74	-3.55	4.79E-06	0.00860002
FAM20A	ENSG00000108950	477.04	-3.18	5.35E-06	0.009121387
LINC00494	ENSG00000235621	40.24	-2.53	5.78E-06	0.009385643
DPEP1	ENSG00000015413	120.38	2.86	7.24E-06	0.011213333
AGR2	ENSG00000106541	408.16	-4.55	8.08E-06	0.011977185
ATP6V0A4	ENSG00000105929	5.94	3.44	9.68E-06	0.013189752
TACC2	ENSG00000138162	50.24	-4.22	9.33E-06	0.013189752
SFTPA1	ENSG00000122852	11.30	-3.25	1.01E-05	0.013273917
NKAIN2	ENSG00000188580	90.44	3.53	1.08E-05	0.013570097
HS3ST1	ENSG00000002587	153.51	-2.53	1.18E-05	0.014333776
SOCS3	ENSG00000184557	9022.03	-1.96	1.22E-05	0.014333776
HNRNPA1P62	ENSG00000259228	18.59	2.61	1.36E-05	0.015469316
EGR1	ENSG00000120738	57594.51	-1.79	1.59E-05	0.015575845
LPAR3	ENSG00000171517	46.56	-3.29	1.60E-05	0.015575845
ZNF560	ENSG00000198028	24.12	-5.86	1.51E-05	0.015575845
SPATA31C1	ENSG00000230246	8.09	3.97	1.58E-05	0.015575845
MIR200CHG	ENSG00000257084	2.95	-2.41	1.43E-05	0.015575845
BDNF	ENSG00000176697	16.23	1.77	1.72E-05	0.016286614
AL121956.1	ENSG00000233365	3.16	2.19	1.82E-05	0.016286614
HHIP-AS1	ENSG00000248890	96.86	2.69	1.78E-05	0.016286614
ARHGEF34P	ENSG00000204959	36.59	2.06	2.15E-05	0.018807876

Table S3.9: Validated variants found in *RUNX1*-mutated patients from a list of 80 leukemia-associated genes

Due to size constraints, this table is not complete in the present document.
A preview of the table is shown.
File is available as an Excel file online https://ashpublications.org/blood/article-abstract/135/21/1882/452491/High-frequency-of-germline-RUNX1-mutations-in?redirectedFrom=fulltext#supplementary-data

Patient ID	Gene	Mutation	VAF	Comments
P1	SRSF2	P95L	0.5151	
	NRAS	Y64D	0.4776	Somatic
	RUNX1	Q15-	0.4771	Germline
	TET2	A991-	0.4379	
	STAG2	L566-	0.1411	
P2	STAG2	Y1044-	0.766	
	RUNX1	A60V	0.511	Germline
	FLT3	D835Y	0.4908	Somatic
	NPM1	W290-	0.478	
	NPM1	W290-	0.4097	
	NRAS	G12D	0.0607	
P3	CEBPA	R297L	0.563	Germline
	RUNX1	S141A	0.4587	Germline
	CEBPA	Q312-	0.4118	Somatic
P4	CEBPA	R297L	0.5447	Germline
	RUNX1	S141A	0.4974	Germline
	CEBPA	K313-	0.4159	Somatic
	GATA2	L321F	0.3349	Somatic
P5	BCOR	R1146*	0.9605	
	U2AF1	S34Y	0.4866	Somatic
	RUNX1	E143*	0.3709	Germline
	NRAS	G12S	0.1652	
	NRAS	Q61P	0.0788	
P6	PHF6	R116*	0.8265	
	STAG2	R69*	0.7013	
	U2AF1	Q157P	0.5168	
	WT1	P390-	0.4872	
	FLT3	V592-	0.4622	Somatic
	RUNX1	G165-	0.4488	Somatic
	RUNX1	K152-	0.3836	Germline
	ASXL1	G643-	0.189	
P7	TET2	R1366C	0.6932	
	CEBPA	G123*	0.5227	
	EZH2	E745K	0.5008	
	RUNX1	R166G	0.4762	Germline
	EZH2	R63*	0.3305	
	NRAS	G12D	0.3007	Somatic
	TET2	C1263Y	0.2	
P8	KRAS	G12D	0.4923	Somatic
	RUNX1	R166*	0.3489	Germline
	ASXL1	G643-	0.3439	

3.12 Supplemental References

1. Lavallée V-P, Gendron P, Lemieux S, D'Angelo G, Hébert J, Sauvageau G. EVI1-rearranged acute myeloid leukemias are characterized by distinct molecular alterations. *Blood.* 2015;125(1):140-143.
2. Imai Y, Kurokawa M, Izutsu K, et al. Mutations of the AML1 gene in myelodysplastic syndrome and their functional implications in leukemogenesis. *Blood.* 2000;96(9):3154-3160.
3. Matheny C, Speck M, Cushing P, et al. Disease mutations in RUNX1 and RUNX2 create nonfunctional, dominant-negative, or hypomorphic alleles. *EMBO J.* 2007;26(4):1163-1175.
4. Kuo M-C, Liang D-C, Huang C-F, et al. RUNX1 mutations are frequent in chronic myelomonocytic leukemia and mutations at the C-terminal region might predict acute myeloid leukemia transformation. *Leukemia*. 2009;23(8):1426–1431.
5. Luo X, Feurstein S, Mohan S, et al. ClinGen Myeloid Malignancy Variant Curation Expert Panel recommendations for germline RUNX1 variants. Blood Adv. 2019;3:2962–2979.
6. Li H. and Durbin R. Fast and accurate long-read alignment with Burrows-Wheeler Transform. *Bioinformatics*. 2010;26(5):589-95.
7. "Picard Toolkit" GitHub Repository, Broad Institute. http://broadinstitute.github.io/picard/ Accessed on December 3, 2019.
8. McKenna A, Hanna M, Banks E, et al. The Genome Analysis Toolkit: a MapReduce framework for analyzing next-generation DNA sequencing data. *Genome Res*. 2010;20(9):1297-303.
9. Boeva V, Popova T, Bleakley K, et al. Control-FREEC: a tool for assessing copy number and allelic content using next generation sequencing data. *Bioinformatics*. 2012;28(3):423-5.
10. Love MI, Huber W, and Anders S. Moderated estimation of fold change and dispersion for RNA-seq data with DESeq2. *Genome Biol*. 2014;15(12):550.

Chapter 4: A Genome-Wide Approach Identifies PLZF as a Key Modulator of Glucocorticoid Sensitivity in Human AML

Laura Simon[1], Azadeh Hajmirza[1], Jean-François Spinella[1], Tara MacRae[1], Bernhard Lehnertz[1], Jalila Chagraoui[1], Nadine Mayotte[1], Thierry Bertomeu[2], Jasmin Coulombe-Huntington[2], Geneviève Boucher[1], Albert Feghaly[1], Marie-Eve Bordeleau[1], Sébastien Lemieux[1,3], Mike Tyers[2], Josée Hébert[1,4,5,6] and Guy Sauvageau[1,4,6]*.

[1] The Leucegene Project at Institute for Research in Immunology and Cancer (IRIC), University of Montreal. [2] Department of Medicine, Institute for Research in Immunology and Cancer (IRIC), University of Montreal. [3] Department of Biochemistry, University of Montreal. [4] Division of Hematology-Oncology, Maisonneuve-Rosemont Hospital. [5] Leukemia Cell Bank of Quebec, Maisonneuve-Rosemont Hospital. [6] Department of Medicine, Faculty of Medicine, University of Montreal, Montreal, QC, Canada.

* Corresponding author

Corresponding authors' information:

Guy Sauvageau

Institute for Research in Immunology and Cancer (IRIC), P.O. Box 6128, Downtown Station, Montreal, QC, Canada, H3C 3J7.
E-mail: guy.sauvageau@umontreal.ca
Phone: (514) 343-7134
Fax: (514) 343-5839

Running title: **PLZF modulates glucocorticoid sensitivity in AML**

Keywords: Acute Myeloid Leukemia; Glucocorticoids; GC-resistance; chemogenomics; CRISPR-Cas9.

The manuscript presented in this chapter is ready to be submitted for publication

4.1 Author contributions

L.S. and G.S. designed the experiments and wrote the manuscript. L.S., T.M., and B.L. performed CRISPR-Cas9 screens. L.S. and A.H. conducted functional experiments and screen validations. J.-F.S. performed bioinformatic analyses of CRISPR-Cas9 screen and of GC-induced transcriptome and generated the corresponding figures. T.B., J.-F.S., J.C., A.H., T.M., B.L., N.M. and M.-E.B. contributed to experiment design, data analysis, and figure editing. N.M. and J.C. assisted with clone generation. G.B., A.F., and S.L. assisted with data analysis. B.L. and T.M., constructed lentivirus vectors used in this study. T.B. and J.C.-H. generated CRISPR-Cas9 pooled lentivirus library. M.-E.B., M.T., J.H. and G.S spearheaded the study.

Contributions:

Data and figure generation for Figures 4.1, 4.3(a),(c),(d),(e),(f), S4.1(a),(b),(d),(e), S4.2, S4.3, S4.6, S4.7, S4.8, and S4.9 were generated by Laura Simon (100%).

Data in Figures 4.2, S4.4, S4.5 were generated by Laura Simon (50%), Tara MacRae (25%) and Bernhard Lehnertz (25%).

Figures 4.2(a), S4.1(c), S4.4(c), and S4.5(a),(d) were generated by Jean-François Spinella.

Figure S4.4(b) was generated by Bernhard Lehnertz.

Data in Figure 4.3(b) was generated by Laura Simon and Azadeh Hajmirza.

4.2 Abstract

Given that Glucocorticoids (GC) remain the cornerstone of acute lymphoblastic leukemia therapeutics, we wanted to explore why only a subset of acute myeloid leukemia (AML) are sensitive to these compounds. Our group recently showed that a small number of human AML, often with RUNX mutations or rearrangements, are specifically sensitive to GC. To better characterize GC-sensitivity in AML and extend their applicability to this disease, we used a combination of descriptive and functional genomics complemented with a series of genetically engineered models. We now report a list of genes activated and suppressed in dexamethasone sensitive and resistant cells which indicate that GC-induced differentiation of AML cells might be a mechanism at play in the antiproliferative response to these drugs. Most critically, we identify the transcriptional repressor PLZF (*ZBTB16*) as the top ranked specific modulator of GC response in sensitive and resistant AML cells. These new findings provide insights into GC mechanism of action and position PLZF as an important factor promoting resistance to glucocorticoids in AML.

4.3 Introduction

It is estimated that the glucocorticoid receptor (GR) can regulate up to 10-20% of the genes in the human genome (1). A cell's response to glucocorticoids (GC) depends on the GR activity and its interaction with numerous co-factors, from molecular chaperones to chromatin, and such interactions will guide cell fate (2). In the absence of a ligand, GR is predominantly found in the cytoplasm and complexed with accessory proteins such as HSP90, HSP70, p23, and immunophilins that assist with ligand binding and nuclear translocation (1). Once in the nucleus, the GR acts as a transcription factor (TF) that can activate (trans-activation) or repress (trans-repression) gene expression either by directly binding DNA sequences known as Glucocorticoid Response Elements (GRE) or by modulating the function of other TFs (tethering) (3).

Due to their potent lymphocytopenic potential, GC have been exploited for the treatment of hematological malignancies, especially those originating from the lymphoid lineage. Indeed, GC induce apoptosis in T-cell Acute Lymphoblastic Leukemia (ALL) by regulating the 'BCL2-rheostat' (4) and in B-cell ALL by antagonizing B cell receptor (BCR) signaling and the mTOR pathway (5).

Myeloid lineage malignancies such as acute myeloid leukemia (AML) and myelodysplasia are generally much less sensitive to GC (6–9). For example, resistance to GC in AML has been associated with the loss of one copy of the glucocorticoid receptor *NR3C1*, as found in del(5q) specimens, and with activating mutations of the tyrosine-kinase receptor *FLT3*.

We have recently shown that a small subset of human AML, especially those carrying null or dominant negative mutations in *RUNX1*, are exquisitely sensitive to GC with IC50 for dexamethasone in the low nanomolar range (6). We also found that a good proportion of AML with t(8;21) chromosomal translocations, which involve the *RUNX1* gene, are also highly sensitive to GC treatment. In this context, it was shown that GC target the t(8;21)/*RUNX1-RUNX1T1* product to proteasomal degradation (10). Besides this observation and the induction by GC of premature monocytic differentiation of $CD34^+$ cells in vitro (7), little is known about the mechanism of action of GC in myeloid diseases. Understanding the genetic predisposition and mechanisms of resistance to GC in AML is an attractive field as it could contribute to the repurposing of GC for this disease, possibly making it as effective as in lymphoblastic leukemias.

In this study, we used transcriptomic and functional genomic approaches to dissect the GC response in AML cells and identified several processes involved in GR biology and activity that significantly

modulate GC-response in these cells. The most prominent hit conferring GC-resistance was PLZF, a transcriptional repressor involved in myeloid differentiation. Accordingly, downregulation of PLZF led to increased sensitivity to GC in two cell lines tested to date. Conversely, we show evidence that forced overexpression of PLZF prior to GC-treatment significantly reduces sensitivity to these compounds, positioning PLZF as an important regulator of GC response. Our results show the power of functional genomics in revealing mechanisms of drug resistance and contribute to a deeper understanding of GC activity in AML.

4.4 Methods

4.4.1 AML cell lines

AML cell lines were purchased from the DSMZ German collection of Microorganisms and cell culture (Leibniz Institute) and the ATCC. Cell lines were obtained from January to October 2015, and no authentication test was done by the authors. Cells were cultured according to manufacturer's instructions.

4.4.2 GC-induced transcriptome

AML cell lines OCI-AML5 and OCI-AML3 were used for drug treatment and transcriptome analysis. OCI-AML3 constitutively expressing shRNA against *NR3C1* (GR) was also analyzed to evaluate the extent of GR-independent gene expression upon GC treatment. Cell lines were seeded at $0.5x10^6$ cells/mL and split 1:2 after 24h. Cells were incubated with dexamethasone (100 nM) or DMSO (control) for 6h, 24h, and 48h. This concentration of dexamethasone is sufficient to inhibit proliferation of OCI-AML3 cells but not OCI-AML5. RNA isolation was done using TRIzol reagent (Thermo Fisher Scientific catalog number 15596026) and chloroform phase separation, followed by precipitation with isopropanol. A clean-up step was performed using RNeasy mini kit (QIAGEN). A minimum of 150 ng of RNA was used for stranded cDNA library preparation (polyA tail capture), according to Illumina protocols, and sequencing was performed using an Illumina NovaSeq 6000 instrument.

4.4.3 RNA-sequencing analysis

RNA-seq reads were aligned to the Genome Reference Consortium Human Build 38 patch release 84 (GRCh38.84) using STAR aligner v.2.5.1 (11) and counted with the RNA-Seq by Expectation Maximization (RSEM) software v1.2.28 (12). Differential expression analyses were performed using the Limma-Voom R/Bioconductor software package (13). We selected differentially expressed genes based on significance (adj.P.value $\leq .05$), their mean expression values in at least 1 of the comparison groups (≥ 1 TPM), and a minimum 1.5-fold expression difference. Heat maps were generated using Morpheus software (Broad Institute). The R package WGCNA was used to perform a weighted correlation network analysis with normalized expression data (TPM) as input. Co-expression similarities were obtained by calculating Pearson's correlations between genes. Adjacencies were computed by raising co-expression similarities to a power $\beta=12$ (soft

thresholding). β was chosen as the lowest integer allowing the resulting network to exhibit an approximate scale-free topology (as advised in the original method) (14). Correlations between eigengenes (first principal component of each module) and time of exposure to dexamethasone were computed and significance assigned to each association.

4.4.4 Virus production and transduction

Lentivirus was produced in HEK-293T cells by co-transfection of the lentiviral vector with the VSV-G envelope and PAX2 packaging plasmids using jetPRIME transfection reagent (Polyplus). AML cell lines were infected with lentiviruses in media supplemented with 10 µg/mL polybrene and spin infection was done at 1,500xg for 2 hours. Infected cells were washed after 24 hours and selected in appropriate antibiotic if required. When needed, infected cells were sorted using a BD Aria II cell sorter and knockdown efficiency was determined by quantitative RT-PCR and western botting using standard methods.

4.4.5 Knockdown experiments

Lentiviral vectors carrying shRNAs targeting the *NR3C1* gene (GR) and *ZBTB16* (PLZF) were generated by cloning appropriate shRNA sequences as described in (6) into MNDU vectors comprising miR-E sequences and GFP. Control vector (shNT) contained shRNA targeting renilla luciferase.

4.5.6 Generation of SAM cells and gene activation with dCas9-VP64

SAM cells were obtained by transducing OCI-AML3 cell line with lentiviruses containing lenti-dCAS-VP64_Blast (Addgene #61425) and lenti-MPHv2 (Addgene #89308 = MS2-P65-HSF1-Hygro) plasmids. Cells were cultured for 7 days in the presence of selection agent Blasticidin (10 µg/mL) and Hygromycin (300 µg/mL), as described by (15,16). For targeting of *ZBTB16* (PLZF), the sgRNA sequence (TGTGGGCAGGGAGCCGGGCT) was cloned into lenti-sgRNA(MS2)-zeo plasmid (Addgene #61427) as described in (15). OCI-AML3-SAM cells were subsequently infected with lentivirus carrying sgRNA vector and selected with 200 µg/mL of Zeocin for 7 days. Empty vector was used as a control. Gene activation efficiency was determined by western blotting.

4.4.7 Generation of Cas9-expressing clones

OCI-AML5 and OCI-AML1 were transduced with the lentiviral doxycycline-inducible FLAG-Cas9 vector (pCW-Cas9, Addgene #50661) (17). Infected cells were selected in puromycin-supplemented media (2 µg/mL) for 4 days. Cells were then submitted to colony-forming assay in semi-solid media containing IMDM, Methylcellulose (1.04%), FCS heat-inactivated (20%), Deionized BSA (1%), Glutamine (2 mM), Holo-transferrin (200 µg/mL), β-mercaptoethanol (10-4M), SCF (100 ng/mL), IL-3 (10 ng/mL), GM-CSF (10 ng/mL), Epo (3 U/mL), IL-6 (10 ng/mL), Tpo (50 ng/mL) and Puromycin (2 µg/mL). Clones were picked after ~10 days of incubation, transferred to suspension media and allowed to grow. Intracellular levels of Cas9 in the presence or absence of 2µg/mL doxycycline were measured for several clonal populations by flow cytometry and western blotting. A single clonal population was selected for both cell lines based on uniform expression of Cas9 upon induction.

4.4.8 Validation of Cas9 activity

Endonuclease activity of Cas9 was assessed by transducing clones with a lentiviral sgRNA construct targeting the surface molecules *PTPRC* (CD45) and *PROCR* (EPCR). Vectors were constructed by cloning appropriate sgRNA sequences into pLKO5.sg.EFS.tRFP657 backbone (Addgene #57824) (18). Levels of membrane proteins were measured after 7 days of culture in the presence or absence of doxycycline. UM171 (STEMCELL Technology) was added 24 hours before flow cytometry analysis to induce EPCR expression (19).

4.4.9 sgRNA library transduction and chemogenomic screening

To generate AML knock-out libraries, we used the EKO 278K whole-genome sgRNA lentivirus pooled library provided by our collaborators. Library sgRNA design and production are detailed in (20). Lentiviral supernatant was titrated in order to achieve multiplicity of infection (MOI) lower than 0.5 to ensure that the majority of cells harbor one sgRNA, thus minimizing the false-positive discovery rate. Genomic DNA was extracted from 100,000 infected cells using the prepGEM DNA extraction kit (ZyGEM). Multiplicity of infection (MOI) was evaluated by Q-PCR of the blasticidin resistance gene, comparing the freshly infected library's DNA to a control DNA of known copy number. To achieve a good library representation for chemogenomic screening, we used a minimum of $140x10^6$ infected cells, which corresponds to 500 cells per sgRNA for the 278,754

different sgRNAs. In all screens, $720x10^6$ cells were transduced with lentiviral pooled library in a spinner flask in media supplemented with 10 µg/mL protamine sulfate. After 24 hours, cells were washed and then selected with blasticidin for 6 days. A representation of the library ($140x10^6$ cells) was harvested for genomic DNA extraction to establish sgRNA frequencies in the library pool prior to Cas9 induction. For chemogenomic screening, $140x10^6$ cells were expanded in a spinner flask in the presence of 2 µg/mL doxycycline for 7 days to induce Cas9 expression and gene knock-out. Subsequently, $140x10^6$ cells were cultured in media containing 0.1 µM or 1 µM dexamethasone for up to 20 days at a cell density of 300,000 cells/ml. Untreated control ($140x10^6$ cells) was grown in 0.01% DMSO for up to 20 days. Cells were counted every two days, harvested for genomic DNA and $140x10^6$ cells were split in fresh media supplemented with compound or DMSO, maintaining the same cell density. gDNA was isolated from cultures at D-7 (pre-doxycycline), D0 (pre-drug treatment), D14, and D20 of drug treatment.

4.4.10 Library amplification and NGS analysis

For experimental controls (D-7 pre-doxycycline, D0 before treatment, D14 DMSO and D20 DMSO) gDNA was extracted from 70 million cells (~250 cells per 278K sgRNAs), whereas for treated conditions (Dex 0.1 µM and Dex 1µM D14) gDNA was obtained from 28 million cells (100 cells per 278K sgRNAs). Cells were incubated overnight in lysis buffer with Proteinase K. RNA was degraded by incubation with RNAse A (Thermo Fisher) and pre-chilled 7.5 M ammonium acetate was added to precipitate proteins. gDNA was then isolated from solution with isopropanol, washed with ethanol 75% and resuspended in 1x TE buffer. ~460µg of gDNA was used to recover sgRNA sequences by large-scale PCR (PCR1). A second PCR reaction (PCR2) added Illumina sequencing adapters and 6 bp indexing primers. Detailed protocol is described in (20). Gel-purified amplicons were sequenced on a HiSeq 2000 in a 35 bp single read configuration with an average target coverage of 100 reads per sgRNA. Resulting reads were trimmed using Trim Galore (https://www.bioinformatics.babraham.ac.uk/projects/trim_galore/) and aligned to the sgRNA sequences using Bowtie aligner v2.3.3 (21). Synthetic rescue/positive selection and synthetic lethality/negative selection beta scores, as well as statistical significance, were determined using the MAGeCK-VISPR-MLE method (22).

4.5 Results

4.5.1 Dexamethasone-induced transcriptional response in sensitive and resistant cells

To gain insight into the mechanism of action of glucocorticoids in AML, we compared the transcriptome of the GC-sensitive OCI-AML3 and GC-resistant OCI-AML5 cell lines in response to dexamethasone over the course of 48h. GC-unresponsive OCI-AML3 in which GR is knocked-down (GR^{KD}) was used to control for off target events (**Figure 4.1(A-B)**). Differential expression analysis showed no significant change in gene expression induced by dexamethasone in GR^{KD} cell line (using a cutoff of FC>1.5 and adj.P.value<0.05; **Figure 4.1(B)**). However, we observed a progressive increase in the number of genes significantly repressed upon dexamethasone treatment in both OCI-AML3 and OCI-AML5 cell lines. In contrast, GC-induced gene expression showed different patterns between the two cell lines, with a progressive increase in the number of upregulated genes in the GC-sensitive cell line, whereas the GC-resistant cell line showed no change in the number of genes upregulated throughout time of exposure (**Figure 4.1(B)**). From 6h to 48h of treatment, upregulated genes in OCI-AML3 showed increase of +564 transcripts, for a total of 749, whereas in OCI-AML5 there was a reduction of -10 transcripts, for a total of 119. Even though activation of well-established GR targets such as *MMP-7*, *TSC22D3*, *FKBP5*, *DUSP1* and *NFKBIA* was similar for both cell lines, appearance of GR-specific transcripts was maximal at 6 hrs in OCI-AML5 compared to 48 hrs in OCI-AML3 (**Figure S4.1(A)**). This observation suggests that while GR is activated in the GC-resistant cell line, it fails to induce the expression of hundreds of genes that are only observed in the GC-sensitive cell line. As evidence suggests that chromatin accessibility and presence of pioneer factors may facilitate GR recruitment to binding loci and transcriptional activation (23,24), the observed outcome of GC-induced gene expression could reflect differences in the chromatin state between the two cell lines. Moreover, the complete nature of glucocorticoid action depends upon the activity of several transcription factors that may interact with the GR and that, alongside the chromatin state, confer GR cell specificity (25). In fact, the magnitude in the expression of numerous myeloid transcription factors was markedly different between GC-resistant and GC-sensitive cell lines, including for TFs known to act as co-activators of GR, such as CEBP and STAT family (**Figure S4.1(B)**). Transcript levels of RUNX1, another TF thought to interfere with GR activity, was ~2.4-fold higher in the GC-resistant cell line OCI-AML5 compared to GC-sensitive OCI-AML3 (**Figure S4.1(B)**). Inactivation of *RUNX1* in AML cells by mutations or shRNA knockdown has been shown to increase GC sensitivity, partially by

upregulation of the GR gene *NR3C1* (6). In line with this, OCI-AML3 showed slightly higher (~1.3 fold) *NR3C1* expression compared to OCI-AML5. Overall, it is likely that the dynamic expression of transcriptional co-regulators and multiple signal transduction pathways contribute to the major difference observed between OCI-AML3 and OCI-AML5 in the magnitude of the dexamethasone-induced response.

4.5.2 Dexamethasone induces expression of differentiation and activation markers

Weighted Gene Co-expression Network Analysis (WGCNA) was used to identify modules of dexamethasone-responsive genes in GC-sensitive OCI-AML3. Fifty-three gene modules were readily identified, with the majority (n=32) showing a negative correlation with treatment time and 21 presenting a positive correlation (blue and red shades respectively, **Figure S4.1(C)**). As revealed by GO term analysis, the top two modules which ranked co-first as the most significantly associated with upregulation by dexamethasone treatment (purple and yellow modules; r= 0.95; p-value = 0.0001), were both highly enriched for genes involved in leukocyte/myeloid cell activation (**Figure S4.1(D)**). Of note, another upregulated module (green module; r=0.79; p-value = 0.01) showed an enrichment for TGF-β signaling and signal transduction pathways. On the other end of the spectrum, for one of the most inversely correlated modules with time of exposure (blue module; r = -0.84; p-value = 0.004; **Figure S4.1(E)**), the strongest GO term enrichment was obtained for nitrogen compound metabolic process and RNA processing/splicing (blue module; r= -0.84; p-value = 0.004; **Figure S4.1(E)**).

In order to gain clues about the potential implication of differentially expressed genes (DEG), we compared dex induced expression levels between GC-resistant and GC-sensitive cell lines. Remarkably, the most differentially upregulated genes in OCI-AML3 are associated with myeloid differentiation. Several gene candidates are known markers of activated macrophages/macrophage polarization, transcriptional events that resemble the well described effects of glucocorticoids in normal monocytes towards an M2 macrophage polarization (26). Expression analysis of glucocorticoid-stimulated monocytes has shown the induction of complement component 1 subunit A (*C1QA*), thrombospondin 1 (*THBS1*), *IL1R2*, and *CD163* (27), genes which are strongly upregulated in OCI-AML3 alone. We also observed that numerous transcription factors involved in M2 macrophage polarization (26) are induced in OCI-AML3 but not in OCI-AML5, namely *STAT6*, *KLF4*, *PPARG* and *CEBPB* (**Figure 4.1(C)**). Among the top DEGs in the transcriptome of

the GC-sensitive cell line, the scavenger receptor *CD163*, a known GR target previously described to be induced through monocytic/macrophage differentiation of AML cells (28), showed a major induction at 48h of dex treatment (48h DMSO=3.7 vs 48h DEX=872.9 TPM; **Figure S4.2(A)**). We confirmed the upregulation of the receptor at the cell surface of OCI-AML3 by flow cytometry, which showed maximum induction after treatment with 10nM of dexamethasone for 48h. As expected, the addition of the GR antagonist RU486 (mifepristone) completely abrogated the dexamethasone-induced upregulation of CD163 (**Figure S4.2(B)**). We observed that CD163 was solely upregulated in the GC-sensitive AML cell lines tested, however expression levels were much higher in OCI-AML3 than NOMO-1, suggesting that this marker might be cell-type specific (**Figure S4.2(C)**).

4.5.3 Genome-wide CRISPR-Cas9 screen identifies modulators of GC response

To identify modulators of GC-response in AML, we carried out a genome-wide CRISPR-Cas9 screen in the absence or presence of dex (2 doses: 0.1 μM and 1 μM). Cas9-inducible clones were generated from 2 AML cell lines, OCI-AML5 and OCI-AML1 (**Figure S4.3**), which showed resistance to several glucocorticoids (6). In the genome-wide CRISPR-Cas9 screen, we targeted ~20,000 protein coding genes with an average of 10 sgRNAs per gene using the EKO lentivirus pooled library (20). Cell proliferation was monitored for up to 20 days in the presence or absence of compound (**Figure S4.4(A)**). Cumulative population doublings showed that dex treatment inhibited growth of OCI-AML5-Cas9 cells to a greater extent than OCI-AML1-Cas9, leading to a 3-fold decrease in the number of population doublings in cells treated with 1 μM dex compared to DMSO at 14 days of treatment (D14) (**Figure S4.4(B)**). We used next generation sequencing (NGS) data from D14 of treatment to determine chemogenomic interaction by comparing the average sgRNA counts in DMSO and treated conditions relative to D0 of treatment. Using this approach, we identified several genes that significantly modulate GC-response (**Figure 4.2(A)**). As expected, the GR gene (*NR3C1*), the molecular target of dex essential for its activity, was ranked as the top positive selection gene in OCI-AML1 and OCI-AML5 (**Figure 4.2(A)**; **Figure S4.5**). In each cell line, we identified ~300 genes that showed a lethal interaction with dex (negative selection; $p<0.01$) and ~400 genes that showed a rescue interaction with dex (positive selection; $p<0.01$) (**Figure 4.2(B-C)**). According to GO term enrichment analysis, the top 500 most significant genes that were positively selected in the screen (rescue) were associated to processes

such as regulation of cell cycle, DNA repair, RNA processing/splicing, and nucleic acid metabolic process (**Figure 4.2(B)**). On the other hand, the top 500 most significant negatively selected genes (lethal) were associated with processes that included chromatin organization, regulation of hemopoiesis, and megakaryocyte differentiation. In OCI-AML5, however, the strongest enrichment for negative selection genes observed was for mitochondrial respiratory chain complex I assembly, which was not observed in OCI-AML1 (**Figure 4.2(C)**). This is consistent with our recent study indicating differential effects of ETC1 inhibition by mubritinib in human AMLs (29). Most other top candidate genes were cell line specific, e.g. acetyltransferase EP300 was significantly depleted in OCI-AML1 and the deubiquitinase OTUD5 was significantly depleted in OCI-AML5 (**Figure 4.2(A)**), highlighting intrinsic genetic characteristics that predispose cells to GC response. The gene list in the intersect between the two cell lines showed that approximately 10-15% of the top ranked genes were shared (**Figure 4.2(B-C)**, right panels and **Figure S4.5(A-C)** and **(D-F)**).

4.5.4 Specific GR co-regulators affect sensitivity to dex

While exploring the list of top ranked genes, we observed that specific co-regulators of GR activity affect GC response. Components of the chaperone HSP90-GR complex influence the maturation and nuclear translocation of GR. In the screen, knockout (KO) of *STIP-1* (HOP), which has been shown to play important roles in the maturation of GR (30), rescued the toxicity induced by dex Similarly, *FKBPL* showed rescue interaction with dex in both cell lines. FKBPL stimulates interaction with dynein and translocation of GR to the nucleus via the microtubuli system, increasing GR's transcriptional activity (31). Once in the nucleus, GR relies on the activity of pioneer factors and chromatin remodeling enzymes that modulate GR-induction of transcriptional regulation. Depletion of Krüppel-like transcription factor ZBP-89 (*ZNF148*), a sequence-specific regulator that plays key roles in cellular growth and differentiation, significantly protected both lines against dex toxicity in our assays (**Figure 4.2(A)**). It's been shown that although on its own it behaves as a modest activator, ZBP-89 potently synergizes with heterologous activators including the GR (32) in the activation of target genes. Another important GR coregulator, GRIP1 (*NCOA2*), was ranked among top synthetic rescue genes (**Figure 4.2(A**) and **Figure S4.5(A-B)** and **(D-E)**). GRIP1 can act both as a GR corepressor that facilitates the downregulation of pro-inflammatory genes (33) and as a GR coactivator promoting the expression of anti-inflammatory

genes (34). Importantly, GRIP1 activity as coactivator of GC responsive elements is controlled by CDK9 phosphorylation (34), whose KO also rescued GC toxicity in the screen. These observations suggest that transactivation of targets genes by the GR might be important for the antiproliferative response of GC, corroborating the results of GC-induced transcriptome that showed a marked increase in the number of upregulated genes in the GC-sensitive line compared to GC-resistant line.

4.5.5 Loss of leukemia-associated genes increase GC-sensitivity

Several genes that are altered in AML showed lethal interaction with dexamethasone, indicating that inactivation of such genes could influence response to GC. Transcription factors that control the self-renewal and differentiation of myeloid progenitors such as GATA-2, RUNX1 and PLZF (*ZBTB16*) were significantly depleted in treated conditions. GATA-2 regulates a wide variety of genes involved in cell cycle and myeloid differentiation (35). GR is known to interfere with GATA proteins; while not yet characterized, it is possible that GATA-2 and GR collaborate in target gene modulation. Similarly, we speculate that RUNX1 can also interfere with GR activity by negatively regulating GR gene activation or by competing with GR for transcriptional co-activators. RUNX motifs are indeed significantly enriched at GR-bound regions in human myeloid cells, and RUNX enrichment fluctuates according to the cell's differentiation stage (36). Importantly, RUNX1 physical interaction with GR has been demonstrated in AML cells (37), reinforcing the idea that RUNX1 might act as a negative regulator of GR activity.

ZBTB16 codes for the promyelocytic leukemia zinc factor (PLZF) and was ranked number 1 and 11 in the OCI-AML1 and the OCI-AML5 screens, respectively. PLZF is a transcription factor belonging to the Krüppel-like zinc finger family first identified in a translocation with the RARA locus in a patient with Acute Promyelocytic Leukemia (38). PLZF is normally expressed in early myeloid cells where it represses the promoters of genes involved in both differentiation and cell proliferation (39,40). PLZF mediates its silencing effect, at least in part, by associating with the essential components of the mSin3-HDAC-SMRT corepressor complex (41). Sin3A depletion was among top negative selection genes in the OCI-AML5 screen. Additionally, acetylation of PLZF by EP300, a leukemia-associated gene that was in the top negative selection list if genes in the OCI-AML1 screen, is essential for its transcriptional repressor activity (42). Taken together, this

data suggests that PLZF could have an important role in the GC response of these 2 resistant AML cell lines.

4.5.6 PLZF as a major determinant of GC resistance

By comparing the steady-state transcriptome of GC-sensitive OCI-AML3 and GC-resistant OCI-AML5, we found that *ZBTB16* (PLZF coding gene) was upregulated in OCI-AML5 (**Figure 4.3(A)**). Next, we determined PLZF levels in whole-protein extracts from several AML cell lines by western blotting and observed that PLZF protein levels on its own could not discriminate between the GC-sensitive and GC-resistant lines (**Figure 4.3(B)**).

To further investigate the role of PLZF in the GC-response, we infected the PLZF-positive GC-resistant OCI-AML5 and OCI-AML1 cell lines with 2 different shRNAs targeting PLZF or targeting luciferase as a control and confirmed the knockdown of PLZF in both lines (**Figure 4.3(C)**). Dexamethasone or Flumetasone (another GC) treatment of infected cells showed that $PLZF^{KD}$ specifically confers sensitivity to GC in both cell lines compared to shControl (**Figure 4.3(C)**; **Figure S4.6(A)**). Interestingly, significantly lower IC_{50} values for Dexamethasone and Flumethasone were observed for $PLZF^{KD}$ cells compared to shControl, whereas IC_{50} values for other types of drugs, such as Cytarabine and 6-thioguanine were not affected by $PLZF^{KD}$ (**Figure 4.3(D); Figure S4.6(B)**). Despite nearly undetectable levels of PLZF transcripts and protein in untreated OCI-AML3 cells at steady-state, we observed that expression of PLZF was strongly induced upon dex treatment (**Figure S4.7(A)**) in a GR-activity-dependent manner (**Figure S4.7(B)**). PLZF has been shown to be upregulated by glucocorticoids in different tissues (43) and can physically interact with GR and repress the transcriptional activation of GREs (44). It is possible, however, that high levels of PLZF at the moment of GR activation could block activation of GR target genes, dampening GR signaling towards differentiation in AML cells. To test this hypothesis, we used the Synergistic Activation Mediator (SAM) system to induce endogenous overexpression of PLZF ($PLZF^{OE}$) in the PLZF-low GC-sensitive OCI-AML3 cell line (OCI-AML3-SAM) prior to GC treatment (**Figure 4.3(E)**). $PLZF^{OE}$ strongly reduced (>2-3 log) the sensitivity of OCI-AML3-SAM cells to glucocorticoids (dexamethasone, flumethasone and hydrocortisone) while maintaining the response to other classes of drugs (cytarabine, 6-thioguanine and All-trans retinoic acid) (Figure 4.3(E) and (F); Figure S4.8).

4.6 Discussion

Despite extensive clinical use of glucocorticoids, there are still substantial gaps in our understanding of glucocorticoid-mediated effects and key cellular targets in particular cell types or disease states (45), such as AML. GR control of gene expression is determined by either direct GR binding to DNA or tethering to another TF thus negatively or positively interfering with the expression of the TF's target genes. Thus, the ability of the GR to modulate cell survival depends on the activity of numerous factors, which are intrinsic to the cell type and/or differentiation state. To understand GR modulation in AML cells, we compared the GC-induced transcriptomic response of a GC-resistant cell line (OCI-AML5) and a GC-sensitive one (OCI-AML3). While the number of genes downregulated upon dex treatment was similar at all time points analyzed, the number of genes significantly upregulated in the GC-sensitive OCI-AML3 line was more than 6 times higher than in GC-resistant OCI-AML5 line at 48 hours of dex exposure. We also observed that gene induction was time-dependent and progressively increased in the sensitive line, whereas it remained essentially unchanged over time of dex exposure in the resistant line. These results suggest that GC-sensitivity in these cell lines may rely on the activation of gene transcription, which is likely coordinated by several transcription factors and chromatin modifiers expressed at basal level or activated/repressed upon dex treatment.

Even though several genes are ubiquitously regulated by GR in both the resistant and sensitive cell lines, numerous DEGs upregulated by dexamethasone exclusively in the GC-sensitive cell line are associated with leukocyte and macrophage activation towards M2 alternative phenotype. It has been shown that GC induce the differentiation of AML cells and primary human monocytes (7,27). It is unknown, however, why GR fails to activate the differentiation program in the GC-resistant cell line. Recent data has shown that ubiquitous target gene regulation is more likely to occur through GR occupancy of promoter sites, whereas GR association with distal enhancers confers cell type-specific regulation by GR since these distal sites are predominantly accessible in a cell type-specific manner (46). Epigenomic analysis demonstrated that GC-induced differentiation of primary human monocytes into macrophages strongly impacts histone acetylation marks at enhancers, which coincides with gene activation and recruitment of acetyltransferases by GR (36,47). Our data suggests that GC-induced differentiation could contribute to the antiproliferative effect observed in AML cells. However, the role of chromatin accessibility in guiding GR action remains to be elucidated.

By performing a genome-wide CRISPR-Cas9 chemogenomic screen, we were able to assess the influence of virtually all protein-coding genes on the response to GC in two GC-resistant AML cell lines. Most importantly, our strategy allowed the identification of genes that antagonize the GC-induced antiproliferative response in AML cells and can be associated with mechanisms of resistance. Among top candidates which KO showed lethal interaction with dex, PLZF has been shown to influence GC sensitivity in ALL cells (48), but its role in the GC response of AML cells has never been described. Multiple layers of regulation affect PLZF function, such as post-translational modifications and ability to interact with co-factors. Posttranslational modifications such as acetylation and sumoylation are required for PLZF transcriptional repressor activity. EP300, which acetylates PLZF, was among top negative selection genes in the OCI-AML1 screen, suggesting their cooperation in antagonizing GC-response. Moreover, cytokines and growth factors that stimulate myeloid differentiation or immunomodulatory reactions have been shown to modulate PLZF activity. For example, inactivation of PLZF can be achieved through nuclear export induced by IL-3 and ATRA (49), or degradation by the ubiquitin-proteasome pathway. PLZF degradation is enabled by complex formation with CUL3 (50), which in turn has shown a rescue phenotype in both CRISPR-Cas9 screens.

We postulate that PLZF could block the transcriptional activity of GR in AML cells by direct binding to GR at the DNA interface and impairing gene activation by GR, similarly to what has been previously described (44). Alternatively, PLZF could act by modulating the chromatin accessibility in AML cells, thus impeding GR from binding at specific sites. In murine myeloid progenitors, PLZF binds to enhancers reducing their chromatin accessibility culminating in a restrictive effect on gene expression (51). Either way, it appears that PLZF levels prior to GC treatment determines GC-sensitivity for a proportion of AML cell lines. SKNO-1, a cell line expressing the AML associated fusion protein RUNX1-RUNX1T1 that results from the chromosomal translocation t(8;21), expresses high levels of PLZF at steady-state (Figure 4.3(B)); nonetheless, it shows high sensitivity to GC. RUNX1-RUNX1T1 can exclude PLZF from the nuclear matrix and reduce its ability to bind to its cognate DNA-binding site, blocking transcriptional repression by PLZF (39). Moreover, sensitivity of t(8;21) leukemic cells has been attributed to GC-induced proteasome degradation of the fusion protein RUNX1-RUNX1T1 (10), which triggers the apoptosis. On the other hand, the antiproliferative response of t(8;21)-negative and PLZF-low cells, such as OCI-AML3 and NOMO-1, might result from GC-induced

transcriptional activation of effector genes, as suggested by the transcriptomic analysis of OCI-AML3. In support of this, we observed that treatment with the inhibitor of protein synthesis cycloheximide significantly reduced sensitivity to dexamethasone in OCI-AML3 and NOMO-1 cells, whereas it didn't affect the response of t(8;21)-positive cells SKNO-1 and Kasumi-1 (**Figure S4.9**). Altogether, these observations emphasize the multifactorial, cell type–dependent effects of this class of drugs.

In summary, our findings provide a mechanistic understanding of GC action and revealed PLZF as an important regulator of GC sensitivity in AML cells. Identifying mechanisms of resistance is a crucial initial step towards the development of combinatorial therapies that potentiate the desirable effects of GC and reverse GC-resistance. Additional studies will enable the deconvolution of PLZF-GR interaction and provide greater insight towards the understanding of the actions of glucocorticoids in different subsets of human AML.

4.7 Figures

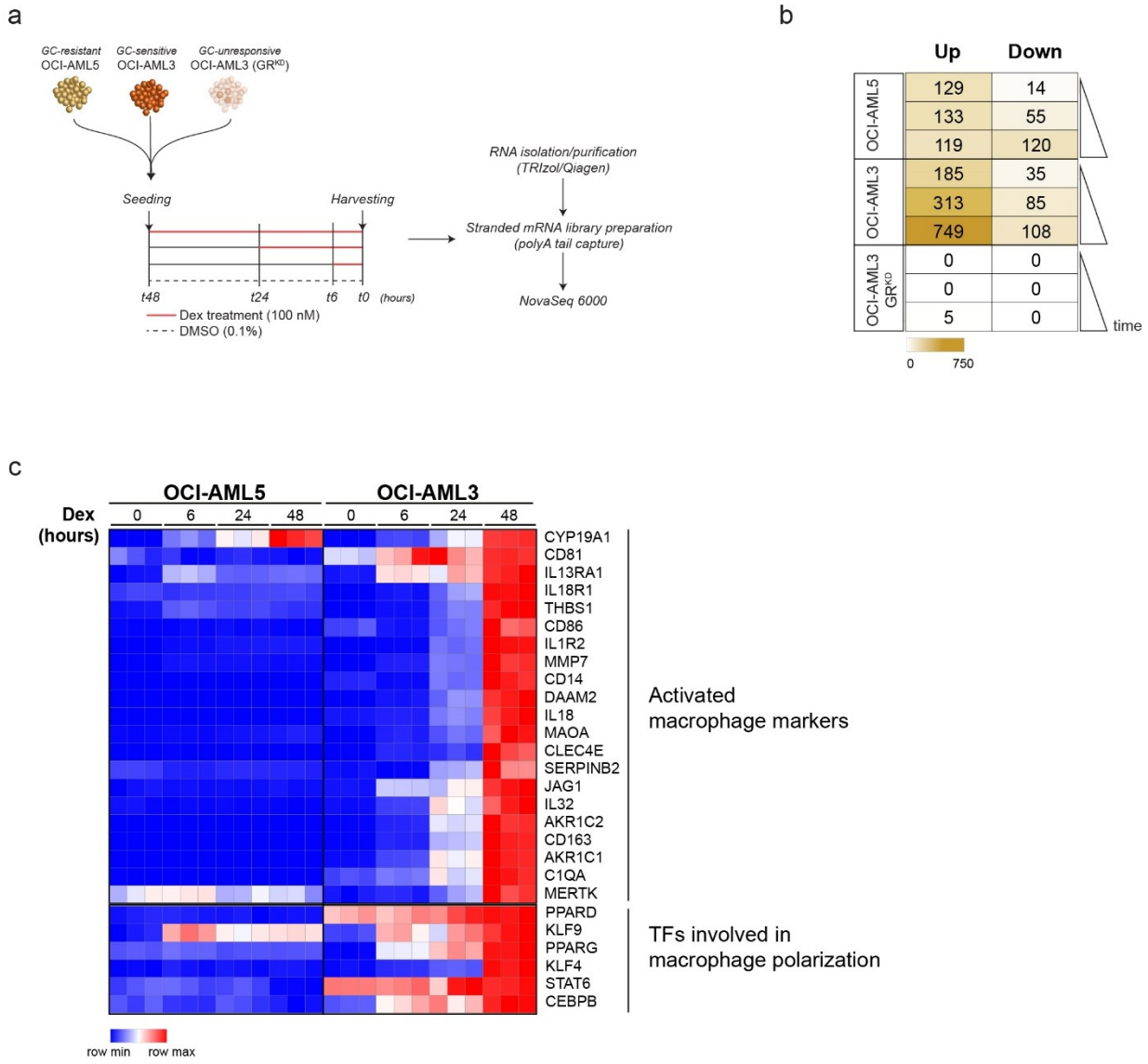

Figure 4.1: Differential analysis of GC-induced transcriptome of GC-resistant and GC-sensitive cell lines

A) Layout of *in vitro* dexamethasone treatment for transcriptome analysis. **B)** Number of genes upregulated (Up) and downregulated (Down) following 6, 24 and 48h of dexamethasone treatment (100 nM) in GC-resistant OCI-AML5 and GC-sensitive OCI-AML3 (cut-off FC>1.5 and adj.P.value<0.05). OCI-AML3 GR^{KD} expresses shRNA against GR gene (*NR3C1*). **C)** Heatmap representation of gene expression values of selected macrophage activation/polarization associated genes in response to dexamethasone treatment in OCI-AML5 and OCI-AML3 cell lines. TPM values in the heat map are mapped to colors using the minimum and maximum of each row independently.

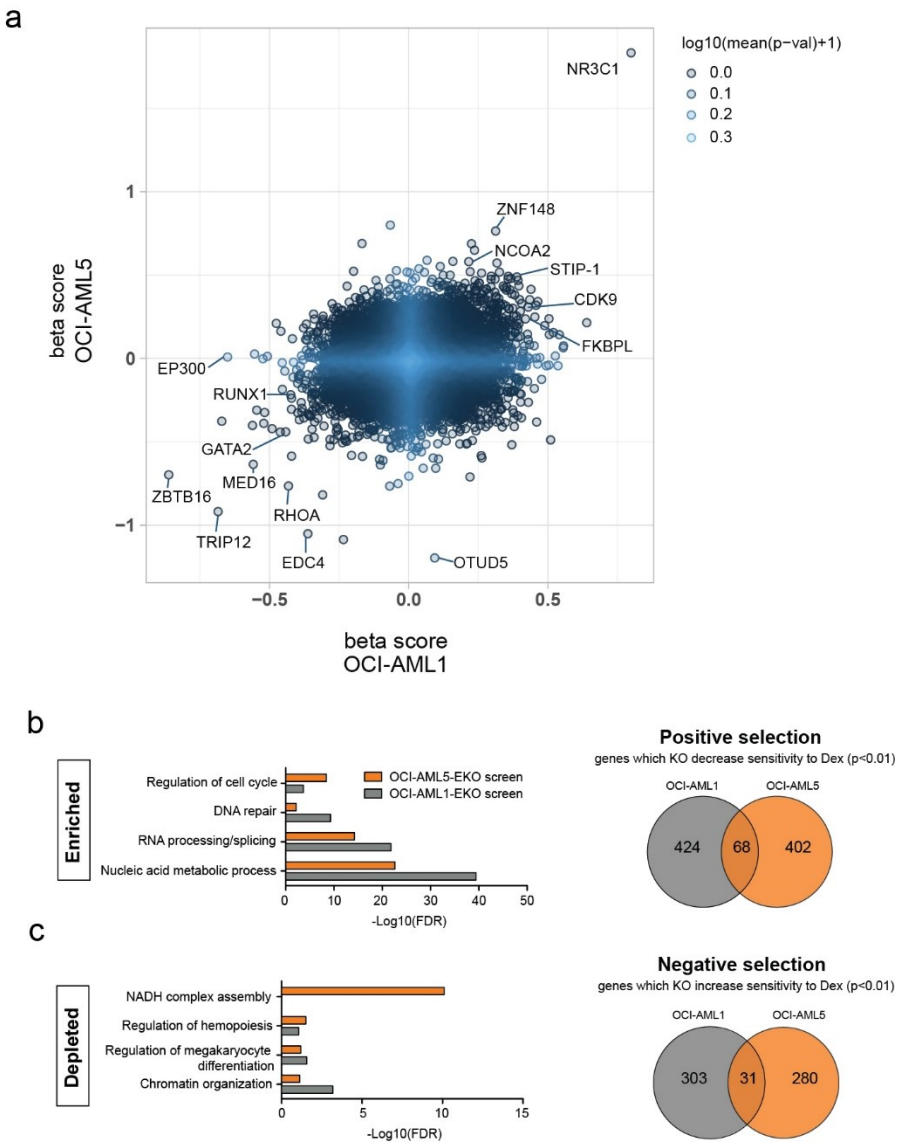

Figure 4.2: Genome-wide CRISPR-Cas9 screen of dexamethasone response in AML cell lines

A) Scatter plot showing MAGeCK beta scores of CRISPR knockout OCI-AML5 (y-axis) and OCI-AML1 (x-axis) exposed to dexamethasone (1000nM) for 14 days. Positive values show synthetic rescue interactions and negative values show synthetic lethal interactions. **B)** *Left* GO terms enriched among genes whose KO conferred rescue interaction with dexamethasone in OCI-AML5 and OCI-AML1 screens *Right* Venn diagram depicting overlap of candidate genes that rescued dexamethasone toxicity (p<0.01) and **C)** *Left* GO terms enriched among genes whose KO conferred lethal interaction with dexamethasone in OCI-AML5 and OCI-AML1 screens *Right* Venn diagram depicting overlap of candidate genes that increased dexamethasone toxicity (p<0.01).

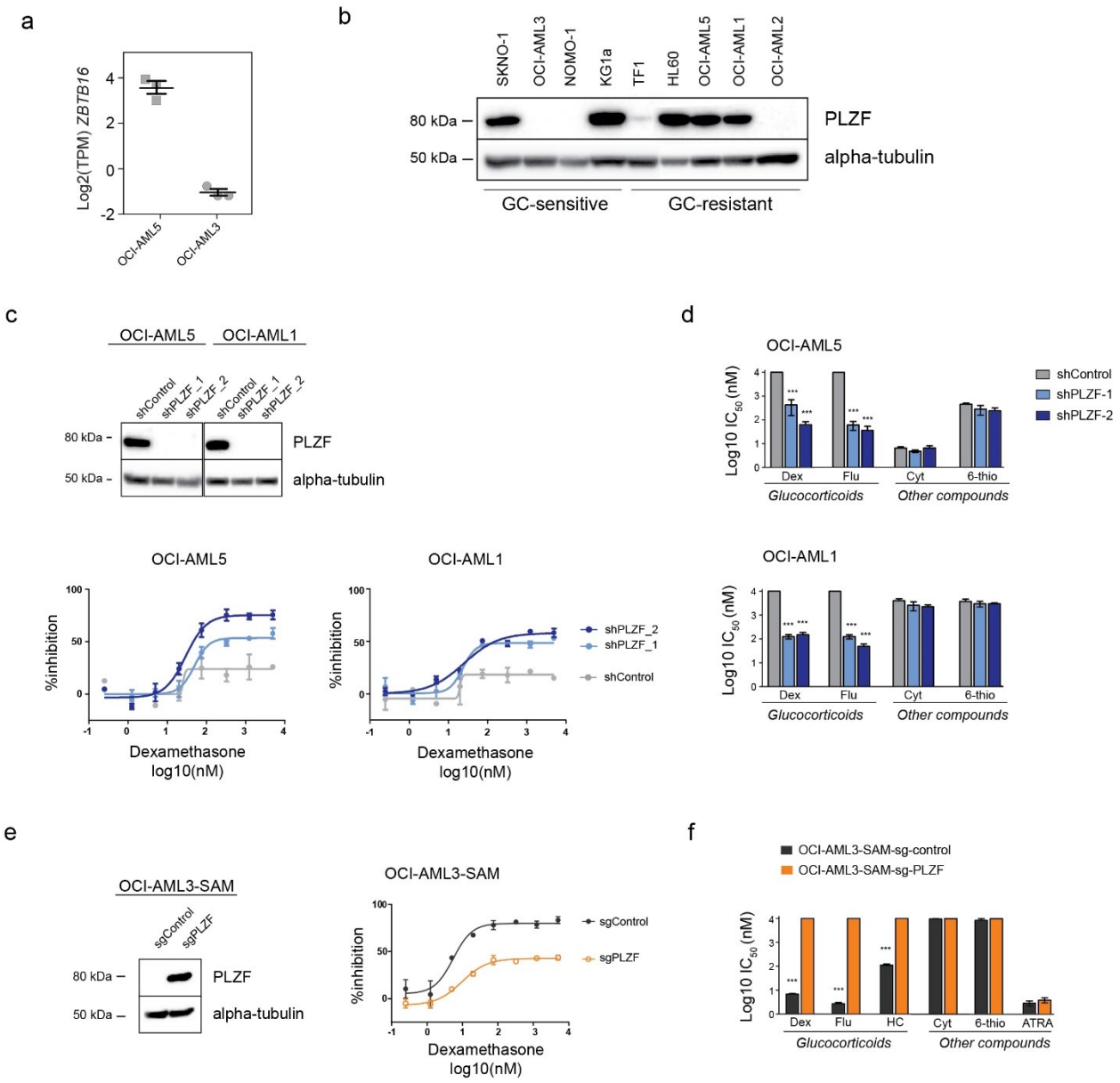

Figure 4.3: PLZF confers GC-resistance in AML cell lines

A) Expression levels of PLZF transcript (*ZBTB16*) in GC-resistant OCI-AML5 and GC-sensitive OCI-AML3 cell lines. **B)** Western blotting analysis of PLZF in whole protein extracts from AML cell lines. Alpha-tubulin was used as loading control **C)** *Top* PLZF knockdown efficiency determined by western blotting of whole protein extracts from AML cells infected with shControl (Luciferase) or shPLZF-1 and -2. Alpha-tubulin was used as loading control. *Bottom* Dose-response curves for dexamethasone treatment (7 days) of cells expressing shControl or shPLZF. Results from 3 independent experiments are shown as mean±SEM **D)** IC_{50} values for glucocorticoids (dexamethasone and flumethasone) and other compounds (cytarabine and 6-

thioguanine) in OCI-AML5 and OCI-AML1 cells expressing shPLZF or shControl (Luciferase). Results from 3 independent experiments are shown with SEM. p values were determined by two-tailed unpaired t-test. ***p<0.001. **E)** *Left* PLZF overexpression efficiency determined by western blotting of whole protein extracts from OCI-AML3-SAM cells infected with sgControl (empty vector) or sgPLZF. Alpha-tubulin was used as loading control. *Right* Dose-response curves for dexamethasone treatment (7 days) of cells expressing sgControl or sgPLZF. Results from 3 independent experiments are shown as mean±SEM **F)** IC_{50} values for glucocorticoids (dexamethasone, flumethasone and hydrocortisone) and other compounds (cytarabine, 6-thioguanine and All-trans retinoic acid) in OCI-AML3-SAM cells overexpressing PLZF (sgPLZF) or sgControl (empty vector). Results from 3 independent experiments are shown with SEM. p values were determined by two-tailed unpaired t-test. ***p<0.001.

4.8 Acknowledgments

We thank members of the Tyers lab at IRIC for sharing helpful advice, reagents and lab space for conducting genome-wide CRISPR-Cas9 screening. The research was supported by the Leukemia and Lymphoma Society and the Babich Family Foundation Runx1 Research Program (grant #6553-18), by the Government of Canada through Genome Canada and the Ministère de l'Économie et de l'Innovation du Québec through Génome Québec (grant #13528). J Hébert is recipient of the Industrielle-Alliance research chair in leukemia at Université de Montréal. L Simon received graduate scholarships from the Cole Foundation and the FRQS. JF Spinella is supported by a postdoctoral fellowship from the Canadian Institutes of Health Research (#158159).

Disclosure of Conflicts of Interest: No conflict of interest for any of the authors.

4.9 References

1. Oakley RH, Cidlowski JA. Cellular Processing of the Glucocorticoid Receptor Gene and Protein: New Mechanisms for Generating Tissue-specific Actions of Glucocorticoids. Journal of Biological Chemistry. 2011;286(5):3177–84.
2. Duma D, Jewell CM, Cidlowski JA. Multiple glucocorticoid receptor isoforms and mechanisms of post-translational modification. J Steroid Biochem Mol Biology. 2006;102(1–5):11–21.
3. Timmermans S, Souffriau J, Libert C. A General Introduction to Glucocorticoid Biology. Front Immunol. 2019;10:1545.
4. Ploner C, Rainer J, Niederegger H, Eduardoff M, Villunger A, Geley S, et al. The BCL2 rheostat in glucocorticoid-induced apoptosis of acute lymphoblastic leukemia. Leukemia. 2008;22(2):370–7.
5. Kruth KA, Fang M, Shelton DN, Abu-Halawa O, Mahling R, Yang H, et al. Suppression of B-cell development genes is key to glucocorticoid efficacy in treatment of acute lymphoblastic leukemia. Blood. 2017;129(22):3000–8.
6. Simon L, Lavallée V-P, Bordeleau M-E, Krosl J, Baccelli I, Boucher G, et al. Chemogenomic Landscape of RUNX1-mutated AML Reveals Importance of RUNX1 Allele Dosage in Genetics and Glucocorticoid Sensitivity. Clin Cancer Res. 2017;23(22):6969–81.
7. Laverdière I, Boileau M, Neumann AL, Frison H, Mitchell A, Ng SWK, et al. Leukemic stem cell signatures identify novel therapeutics targeting acute myeloid leukemia. Blood Cancer J. 2018;8(6):52.
8. Bertoli S, Picard M, Bérard E, Griessinger E, Larrue C, Mouchel P-L, et al. Dexamethasone in hyperleukocytic acute myeloid leukemia. Haematologica. 2018;103(6):haematol.2017.184267.
9. Malani D, Murumägi A, Yadav B, Kontro M, Eldfors S, Kumar A, et al. Enhanced sensitivity to glucocorticoids in cytarabine-resistant AML. Leukemia. 2017;31(5):1187–95.
10. Corsello SM, Roti G, Ross KN, Chow KT, Galinsky I, DeAngelo DJ, et al. Identification of AML1-ETO modulators by chemical genomics. Blood. 2009;113(24):6193–205.
11. Dobin A, Davis CA, Schlesinger F, Drenkow J, Zaleski C, Jha S, et al. STAR: ultrafast universal RNA-seq aligner. Bioinformatics. 2013;29(1):15–21.
12. Li B, Dewey CN. RSEM: accurate transcript quantification from RNA-Seq data with or without a reference genome. BMC Bioinformatics. 2011;12(1):323.
13. Ritchie ME, Phipson B, Wu D, Hu Y, Law CW, Shi W, et al. limma powers differential expression analyses for RNA-sequencing and microarray studies. Nucleic Acids Research. 2015;43(7):e47–e47.
14. Langfelder P, Horvath S. WGCNA: an R package for weighted correlation network analysis. BMC Bioinformatics. 2008;9(1):559.
15. Konermann S, Brigham MD, Trevino AE, Joung J, Abudayyeh OO, Barcena C, et al. Genome-scale transcriptional activation by an engineered CRISPR-Cas9 complex. Nature. 2015;517(7536):583–8.
16. Joung J, Konermann S, Gootenberg JS, Abudayyeh OO, Platt RJ, Brigham MD, et al. Genome-scale CRISPR-Cas9 knockout and transcriptional activation screening. Nat Protoc. 2017;12(4):828–63.
17. Wang T, Wei JJ, Sabatini DM, Lander ES. Genetic Screens in Human Cells Using the CRISPR-Cas9 System. Science. 2013;343(6166):80–4.
18. Heckl D, Kowalczyk MS, Yudovich D, Belizaire R, Puram RV, McConkey ME, et al. Generation of mouse models of myeloid malignancy with combinatorial genetic lesions using CRISPR-Cas9 genome editing. Nat Biotechnol. 2014;32(9):941–6.
19. Fares I, Chagraoui J, Gareau Y, Gingras S, Ruel R, Mayotte N, et al. Pyrimidoindole derivatives are agonists of human hematopoietic stem cell self-renewal. Science. 2014;345(6203):1509–12.
20. Bertomeu T. A High-Resolution Genome-Wide CRISPR/Cas9 Viability Screen Reveals Structural Features and Contextual Diversity of the Human Cell-Essential Proteome. n.d.;
21. Langmead B, Trapnell C, Pop M, Salzberg SL. Ultrafast and memory-efficient alignment of short DNA sequences to the human genome. Genome Biology. 2009;10(3):R25.
22. Li W, Köster J, Xu H, Chen C-H, Xiao T, Liu JS, et al. Quality control, modeling, and visualization of CRISPR screens with MAGeCK-VISPR. Genome Biology. 2015;16(1):281.
23. Burd CJ, Archer TK. Burd and Trevor, 2013 - Chromatin architecture defines the GC response.pdf. Mol Cell Endocrinol. 2013;380(1–2):25–31.
24. Hoffman JA, Trotter KW, Ward JM, Archer TK. BRG1 governs glucocorticoid receptor interactions with chromatin and pioneer factors across the genome. Elife. 2018;7:e35073.
25. Mayran A, Drouin J. Pioneer transcription factors shape the epigenetic landscape. J Biol Chem. 2018;293(36):13795–804.

26. Wang N, Liang H, Zen K. Molecular Mechanisms That Influence the Macrophage M1–M2 Polarization Balance. Frontiers in Immunology. 2014;5:614.
27. Ehrchen J, Steinmüller L, Barczyk K, Tenbrock K, Nacken W, Eisenacher M, et al. Glucocorticoids induce differentiation of a specifically activated, anti-inflammatory subtype of human monocytes. Blood. 2007;109(3):1265–74.
28. Bächli EB, Schaer DJ, Walter RB, Fehr J, Schoedon G. Functional expression of the CD163 scavenger receptor on acute myeloid leukemia cells of monocytic lineage. Journal of leukocyte biology. 2005;79(2):312–8.
29. Baccelli I, Gareau Y, Lehnertz B, Gingras S, Spinella J, Corneau S, et al. Mubritinib Targets the Electron Transport Chain Complex I and Reveals the Landscape of OXPHOS Dependency in Acute Myeloid Leukemia. Cancer Cell. 2019;36(1):84-99.e8.
30. Pratt WB, Toft DO. Regulation of Signaling Protein Function and Trafficking by the hsp90/hsp70-Based Chaperone Machinery. Exp Biol Med. 2003;228(2):111–33.
31. McKeen HD, McAlpine K, Valentine A, Quinn DJ, McClelland K, Byrne C, et al. A Novel FK506-Like Binding Protein Interacts with the Glucocorticoid Receptor and Regulates Steroid Receptor Signaling. Endocrinology. 2008;149(11):5724–34.
32. Chupreta S, Brevig H, Bai L, Merchant JL, Iñiguez-Lluhí JA. Sumoylation-dependent Control of Homotypic and Heterotypic Synergy by the Krüppel-type Zinc Finger Protein ZBP-89. Journal of Biological Chemistry. 2007;282(50):36155–66.
33. Chinenov Y, Gupte R, Dobrovolna J, Flammer JR, Liu B, Michelassi FE, et al. Role of transcriptional coregulator GRIP1 in the anti-inflammatory actions of glucocorticoids. Proceedings of the National Academy of Sciences. 2012;109(29):11776–81.
34. Rollins DA, Kharlyngdoh JB, Coppo M, Tharmalingam B, Mimouna S, Guo Z, et al. Glucocorticoid-induced phosphorylation by CDK9 modulates the coactivator functions of transcriptional cofactor GRIP1 in macrophages. Nat Commun. 2017;8(1):1739.
35. Huang Z, Dore LC, Li Z, Orkin SH, Feng G, Lin S, et al. GATA-2 Reinforces Megakaryocyte Development in the Absence of GATA-1 ▿ †. Mol Cell Biol. 2009;29(18):5168–80.
36. Wang C, Nanni L, Novakovic B, Megchelenbrink W, Kuznetsova T, Stunnenberg HG, et al. Extensive epigenomic integration of the glucocorticoid response in primary human monocytes and in vitro derived macrophages. Sci Rep-uk. 2019;9(1):2772.
37. Simon L, Lavallee V, Bordeleau M, Lehnertz B, MacRae T, Chagraoui J, et al. Chemogenomic Approach Unveils the Increased Susceptibility of RUNX1-Mutated AML to Glucocorticoids. Blood. 2018;132(Supplement 1):4675–4675.
38. Chen Z, Brand NJ, Chen A, Chen SJ, Tong JH, Wang ZY, et al. Fusion between a novel Krüppel-like zinc finger gene and the retinoic acid receptor-alpha locus due to a variant t(11;17) translocation associated with acute promyelocytic leukaemia. Embo J. 1993;12(3):1161–7.
39. Melnick A, Carlile GW, McConnell MJ, Polinger A, Hiebert SW, Licht JD. AML-1/ETO fusion protein is a dominant negative inhibitor of transcriptional repression by the promyelocytic leukemia zinc finger protein. Blood. 2000;96(12):3939–47.
40. Girard N, Tremblay M, Humbert M, Grondin B, Haman A, Labrecque J, et al. RARα-PLZF oncogene inhibits C/EBPα function in myeloid cells. Proc National Acad Sci. 2013;110(33):13522–7.
41. David G, Alland L, Hong S-H, Wong C-W, DePinho RA, Dejean A. Histone deacetylase associated with mSin3A mediates repression by the acute promyelocytic leukemia-associated PLZF protein. Oncogene. 1998;16(19):2549–56.
42. Guidez F, Howell L, Isalan M, Cebrat M, Alani RM, Ivins S, et al. Histone Acetyltransferase Activity of p300 Is Required for Transcriptional Repression by the Promyelocytic Leukemia Zinc Finger Protein. Mol Cell Biol. 2005;25(13):5552–66.
43. Suliman BA, Xu D, Williams BRG. The Promyelocytic Leukemia Zinc Finger Protein: Two Decades of Molecular Oncology. Frontiers Oncol. 2012;2:74.
44. Martin PJ, Delmotte M-H, Formstecher P, Lefebvre P. PLZF is a negative regulator of retinoic acid receptor transcriptional activity. Nuclear Receptor. 2003;1(1):6.
45. Franco LM, Gadkari M, Howe KN, Sun J, Kardava L, Kumar P, et al. Immune regulation by glucocorticoids can be linked to cell type–dependent transcriptional responses. J Exp Med. 2019;216(2):384–406.
46. Love MI, Huska MR, Jurk M, Schöpflin R, Starick SR, Schwahn K, et al. Role of the chromatin landscape and sequence in determining cell type-specific genomic glucocorticoid receptor binding and gene regulation. Nucleic Acids Res. 2017;45(4):1805–19.

47. Johnson T, Chereji R, Stavreva D, Morris S, Hager G, Clark D. Conventional and pioneer modes of glucocorticoid receptor interaction with enhancer chromatin in vivo. Nucleic Acids Res. 2017;46(1):gkx1044-.
48. Wasim M, Carlet M, Mansha M, Greil R, Ploner C, Trockenbacher A, et al. PLZF/ZBTB16, a glucocorticoid response gene in acute lymphoblastic leukemia, interferes with glucocorticoid-induced apoptosis. The Journal of steroid biochemistry and molecular biology. 2010;120(4–5):218–27.
49. Doulatov S, Notta F, Rice KL, Howell L, Zelent A, Licht JD, et al. PLZF is a regulator of homeostatic and cytokine-induced myeloid development. Gene Dev. 2009;23(17):2076–87.
50. Ismail MS, Martin SR, Ball NJ, Taylor IA, Howell S, Wilkinson DG, et al. Btbd6-dependent Plzf recruitment to Cul3 E3 ligase complexes through BTB domain heterodimerization. Biorxiv. 2019;575910.
51. Poplineau M, Vernerey J, Platet N, N'guyen L, Hérault L, Esposito M, et al. PLZF limits enhancer activity during hematopoietic progenitor aging. Nucleic Acids Res. 2019;47(9):4509–20.

4.10 Supplemental Figures and Tables

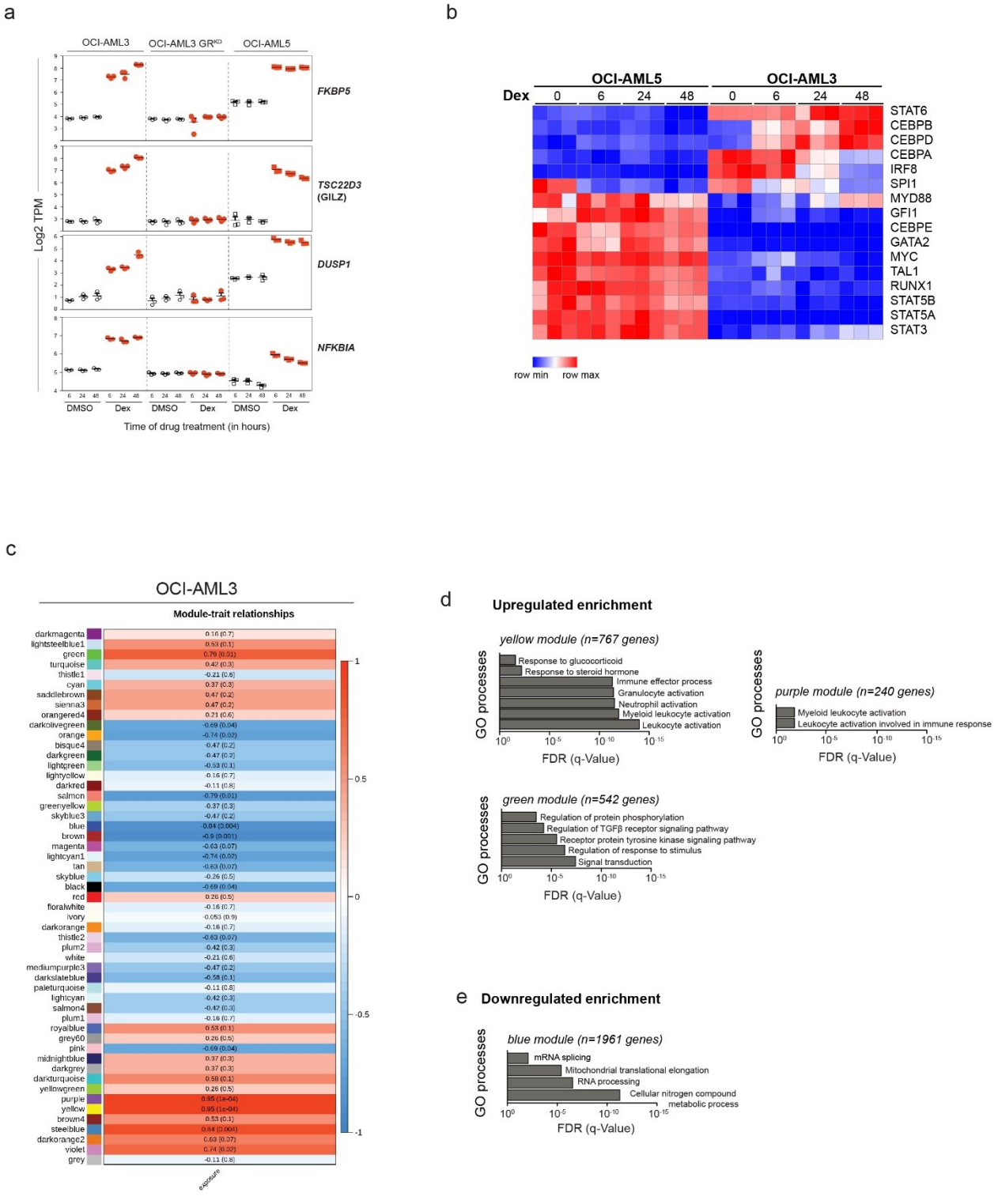

Figure S4.1: GC-induced transcriptome of GC-resistant OCI-AML5 and GC-sensitive OCI-AML3 cell lines

A) Pattern of expression of GR target genes. **B)** Heatmap representation of gene expression values of transcription factors involved in myeloid development and differentiation in response to dexamethasone treatment in OCI-AML5 and OCI-AML3 cell lines. TPM values in the heat map are mapped to colors using the minimum and maximum of each row independently. **C)** Correlation of module eigengenes to time of exposure to dexamethasone. Each row corresponds to a module eigengene. The values in the cells are presented as "Pearson r (p value)" and color-coded by direction and degree of the correlation (red = positive correlation, genes are upregulated over time of exposure; blue = negative correlation, genes are downregulated over time of exposure). **D)** Pathway analysis using gene ontology (GO) showing the top pathways enriched in the gene-sets of the yellow, purple and green modules, top positively correlated modules. **E)** Pathway analysis using gene ontology (GO) showing the top pathways enriched in the gene-sets of the blue module, top negatively correlated module.

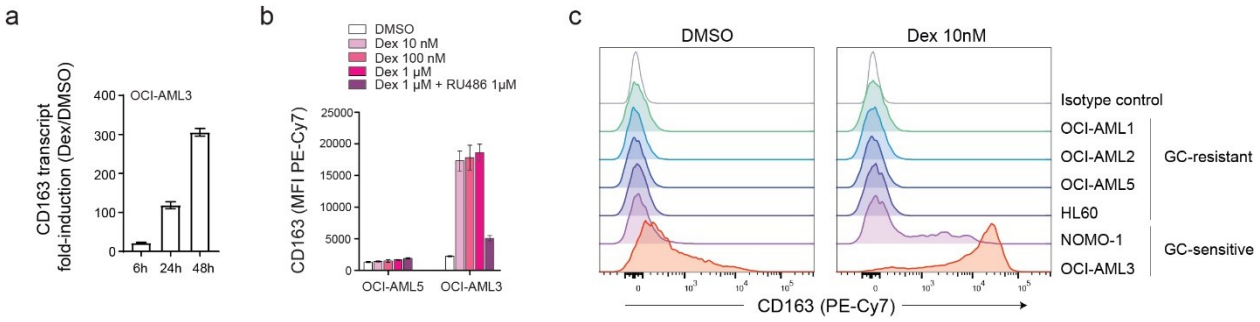

Figure S4.2: Validation of GC-induced CD163 expression

A) Fold-change in CD163 transcript levels (TPM) in OCI-AML3 cells cultured for 6, 24 or 48h in the presence of dexamethasone or DMSO. **B)** Flow cytometry-based analysis of CD163 surface expression in OCI-AML5 and OCI-AML3 exposed to DMSO, dexamethasone (10nM, 100nM, 1µM) or combination of dexamethasone (1µM) + RU486 (1µM) for 48 hours. Data show mean±SEM of mean fluorescent intensity (MFI) of 3 independent experiments. **C)** Representative histogram overlay of flow cytometry-based analysis of CD163 surface expression in multiple AML cells lines exposed to DMSO or dexamethasone (10nM) for 48 hours.

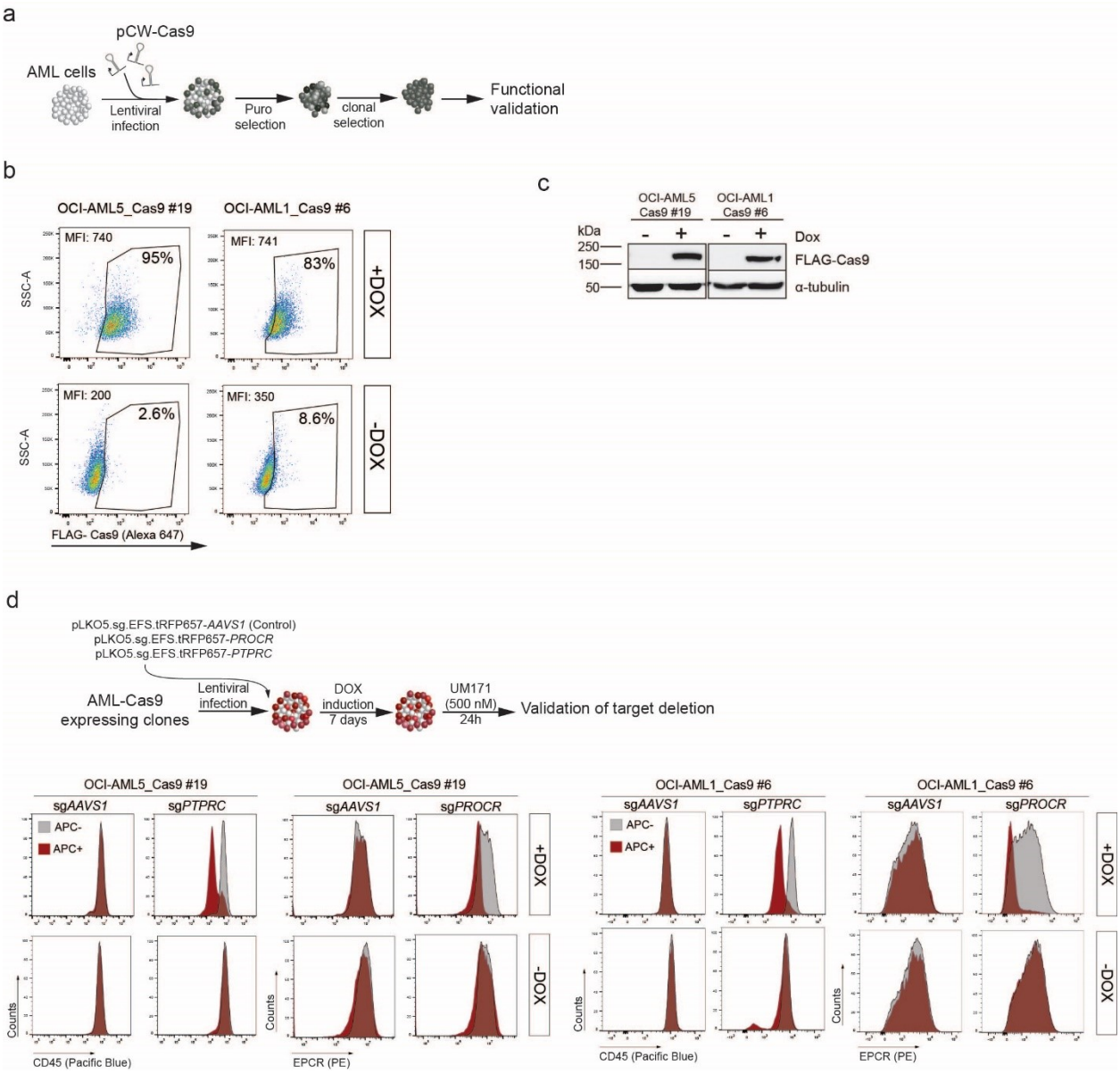

Figure S4.3: Generation of Cas9-expressing AML clones

A) Diagram depicting generation of AML Cas9-expressing clones. Cells were infected with lentivirus carrying the pCW-Cas9 vector and selected in puromycin-containing media for 7 days. Resistant cells were plated in colony-forming assay in semi-solid media at 100 cells/mL dilution and clones were picked after ~10 days. Clones were expanded in liquid culture for validation of Cas9 expression and activity. **B)** Flow cytometry-based analysis of intracellular staining of FLAG-Cas9 in OCI-AML5-Cas9 (#19) and OCI-AML1-Cas9 (#6) clones cultured for 4 days in the presence or absence of doxycycline (DOX). Anti-FLAG antibody was used for detection of FLAG-Cas9. Results show gated Cas9-expressing population and MFI for ungated single cell population.

C) Western blotting analysis of FLAG-Cas9 in whole protein extracts of OCI-AML5-Cas9 (#19) and OCI-AML1-Cas9 (#6) clones cultured in the presence or absence of doxycycline (Dox) for 4 days. α-tubulin was used as loading control. **D)** *Top* Diagram depicting functional validation of Cas9 activity. Lentivirus carrying sgControl targeting AAVS1 (sg.EFS.tRFP657-AAVS1) or sgPROCR targeting EPCR (sg.EFS.tRFP657-PROCR) or sgPTPRC targeting CD45 (sg.EFS.tRFP657-PTPRC) were used to infect AML-Cas9 expressing clones. Clones were cultured in the presence or absence of DOX for 7 days for induction of Cas9 expression and target deletion. Clones were exposed to UM171 (500nM) for 24 hours to induce surface expression of EPCR. *Bottom* Flow cytometry-based analysis of surface expression of CD45 and EPCR. Representative histograms show overlay of uninfected APC- (grey) and infected APC+ (red) gated subsets.

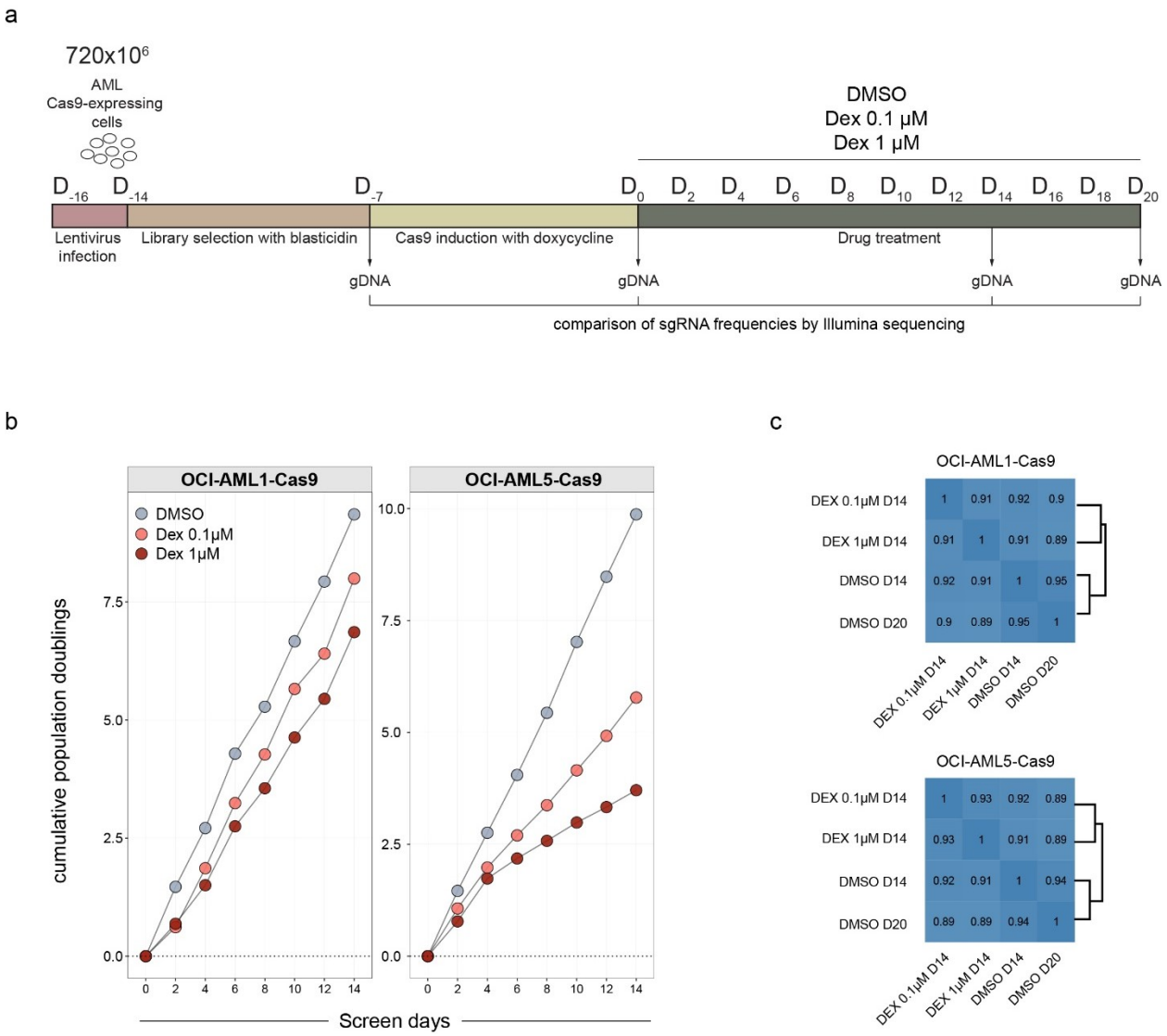

Figure S4.4: CRISPR-Cas9 screen overview

A) Diagram depicting experimental outline of whole-genome CRISPR-Cas9 screen of OCI-AML5-Cas9 and OCI-AML1-Cas9 clones exposed to DMSO or dexamethasone (0.1µM and 1µM) for up to 20 days. **B)** Cumulative cell population doubling in OCI-AML1-Cas9 and OCI-AML5-Cas9 screens. **C)** Pairwise Pearson correlations of sample log read counts in OCI-AML1-Cas9 and OCI-AML5-Cas9 screens.

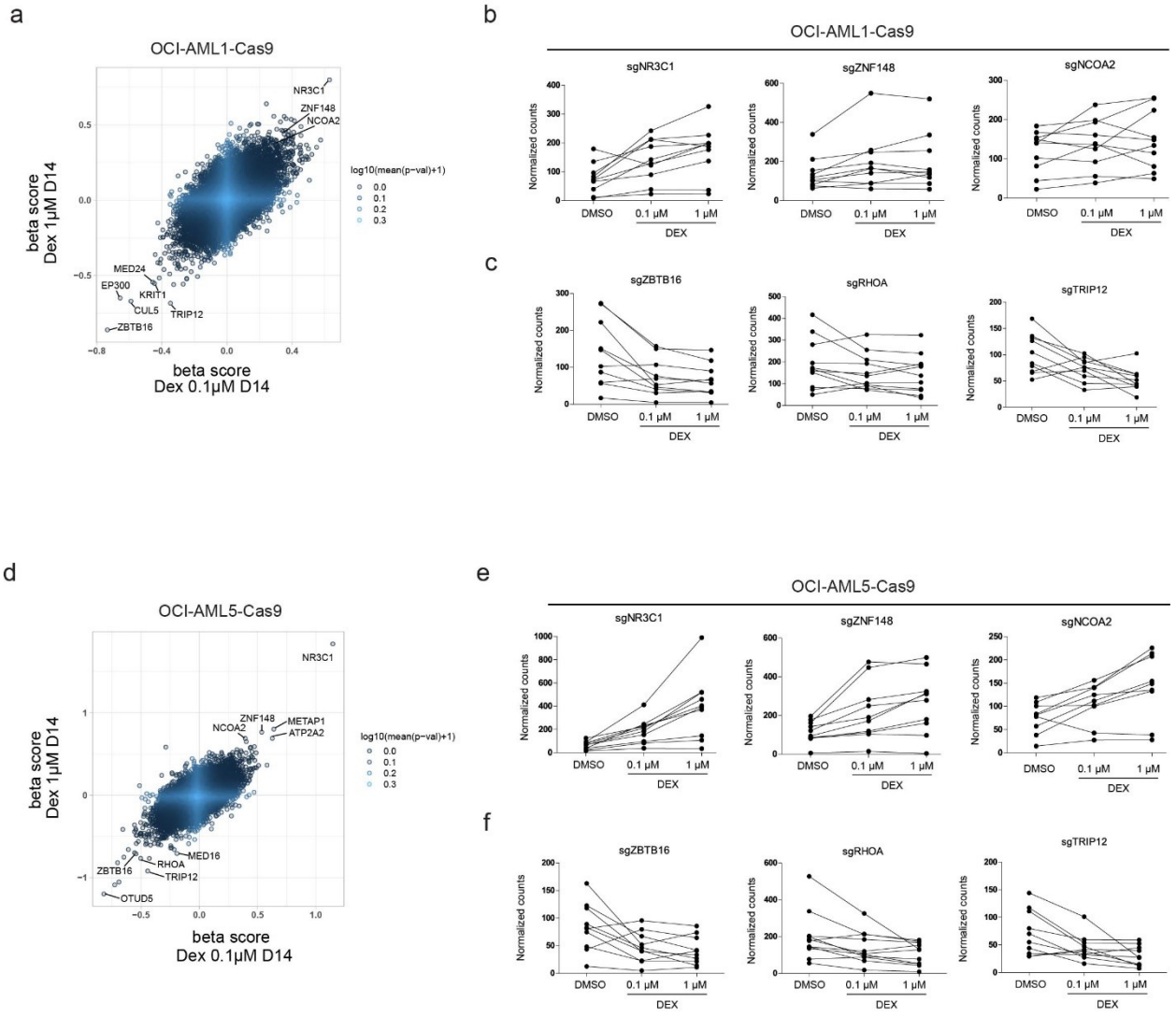

Figure S4.5: Candidate genes identified in both screens and sgRNA count evolution

A) Scatter plot showing MAGeCK outputs beta scores of CRISPR knockout in OCI-AML1-Cas9 exposed to 1µM (displayed on the y-axis) and 0.1µM (x-axis) of dexamethasone for 14 days. **B)** Normalized counts for individual sgRNAs targeting top synthetic rescue and **C)** synthetic lethal interaction genes. **D)** Scatter plot showing MAGeCK outputs beta scores of CRISPR knockout in OCI-AML5-Cas9 exposed to 1µM (displayed on the y-axis) and 0.1µM (x-axis) of dexamethasone for 14 days. **E)** Normalized counts for individual sgRNAs targeting top synthetic rescue and **F)** synthetic lethal interaction genes.

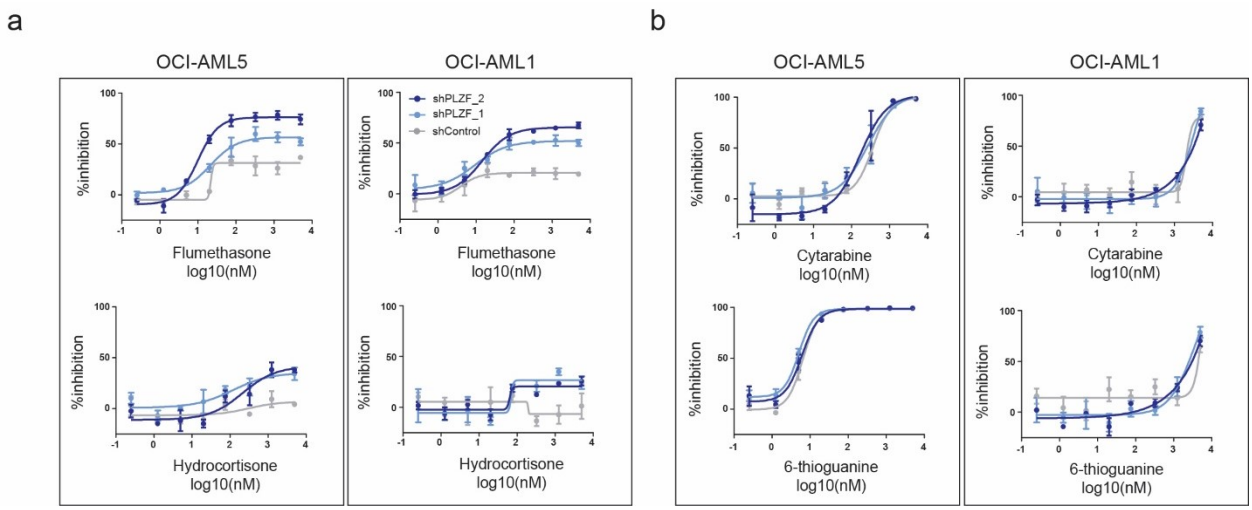

Figure S4.6: PLZF^{KD} cells' response to GC and other compounds

A) Dose-response curves for glucocorticoids flumethasone and hydrocortisone of OCI-AML5 and OCI-AML1 cells expressing shControl or shPLZF. Drug treatments were carried out for 7 days. Results from 3 independent experiments are shown as mean±SEM. **B)** Dose-response curves for cytarabine and 6-thioguanine of OCI-AML5 and OCI-AML1 cells expressing shControl or shPLZF. Drug treatments were carried out for 7 days. Results from 3 independent experiments are shown as mean±SEM.

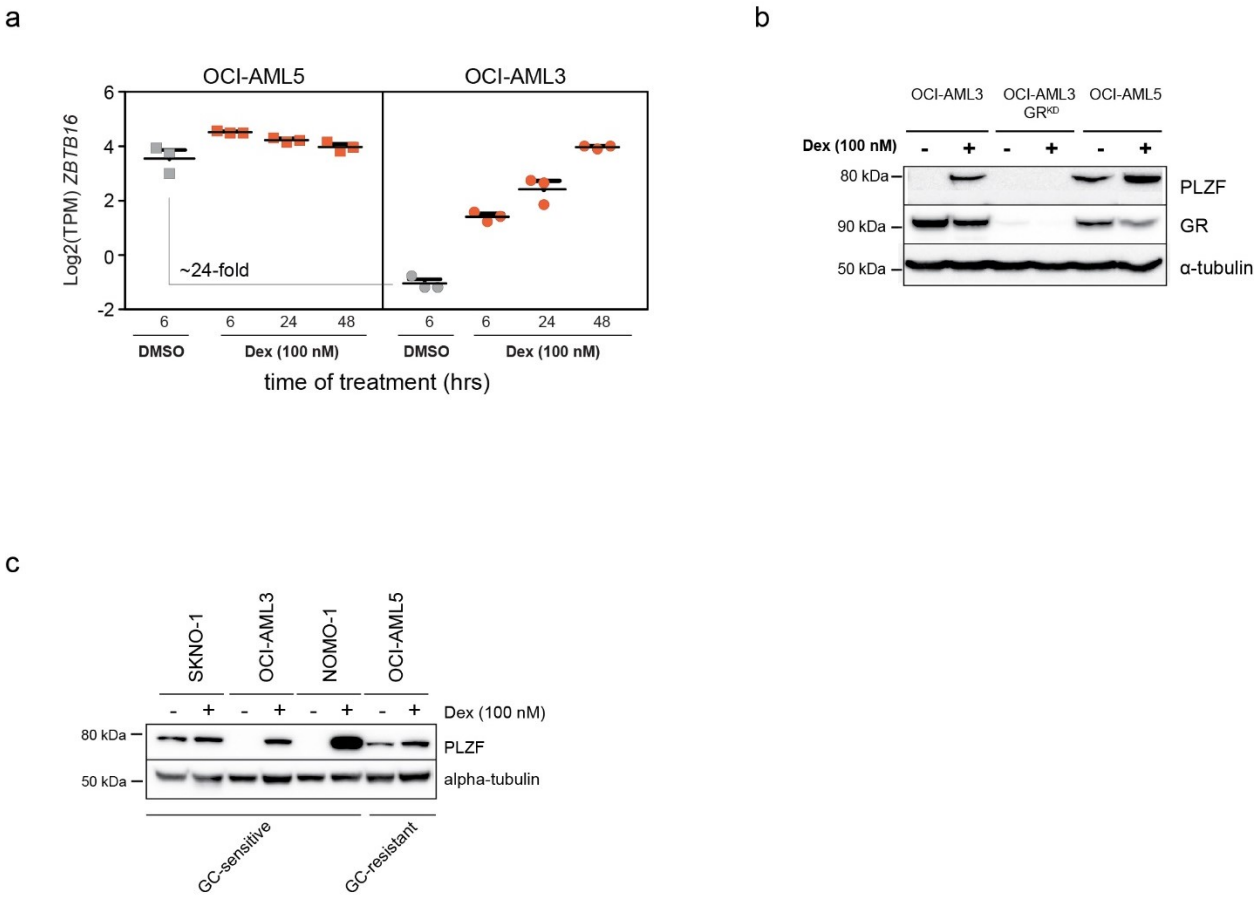

Figure S4.7: PLZF expression levels in AML cell lines

A) *ZBTB16* transcript expression (TPM) in OCI-AML5 and OCI-AML3 cells exposed to DMSO for 6 hours or dexamethasone for 6, 24 or 48 hours. **B)** Western blotting analysis of PLZF and GR expression in whole protein extract from OCI-AML3, OCI-AML3 GR^{KD}, and OCI-AML5 cell lines treated with DMSO or dexamethasone (100nM) for 24 hours. OCI-AML3 GR^{KD} express shRNA against the GR gene, *NR3C1.* α-tubulin was used as loading control. **C)** Western blotting analysis of PLZF expression in whole protein extract from AML cell lines treated with DMSO or dexamethasone (100nM) for 48 hours. α-tubulin was used as loading control.

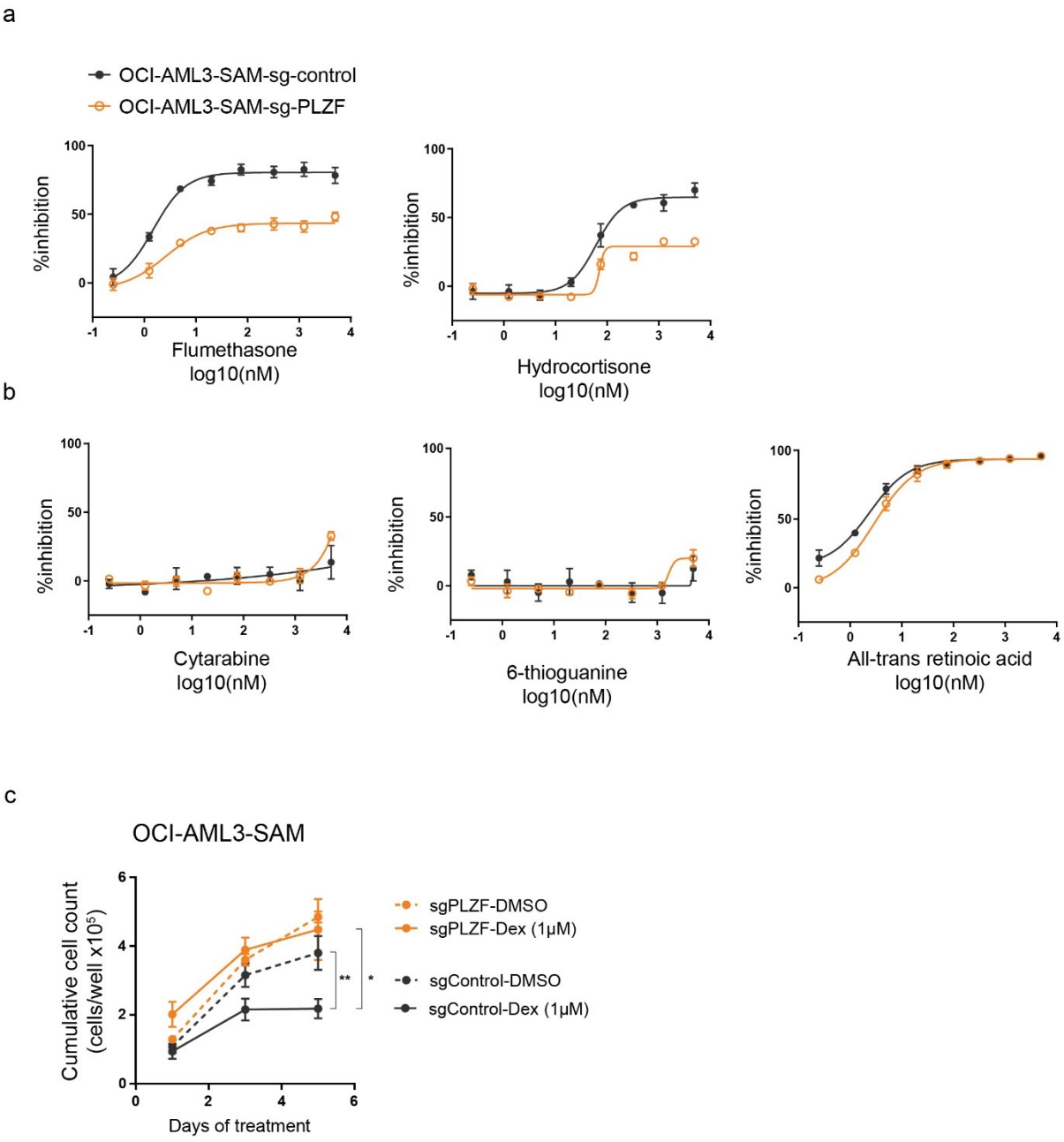

Figure S4.8: PLZF^{OE} cells' response to GC and other compounds

A) Dose-response curves for glucocorticoids flumethasone and hydrocortisone of OCI-AML3-SAM expressing sgControl (empty vector) or sgPLZF (overexpression guide vector). Drug treatments were carried out for 7 days. Results from 3 independent experiments are shown as mean±SEM. **B)** Dose-response curves for cytarabine, 6-thioguanine and All-trans retinoic acid of OCI-AML3-SAM expressing sgControl (empty vector) or sgPLZF (overexpression guide vector). Drug treatments were carried out for 7 days. Results from 3 independent experiments are shown as

mean±SEM. **C)** Cumulative cell counts on the course of 5 days of culture in the presence of DMSO or dexamethasone (Dex, 1µM). Results from 3 independent experiments are shown as mean±SEM.

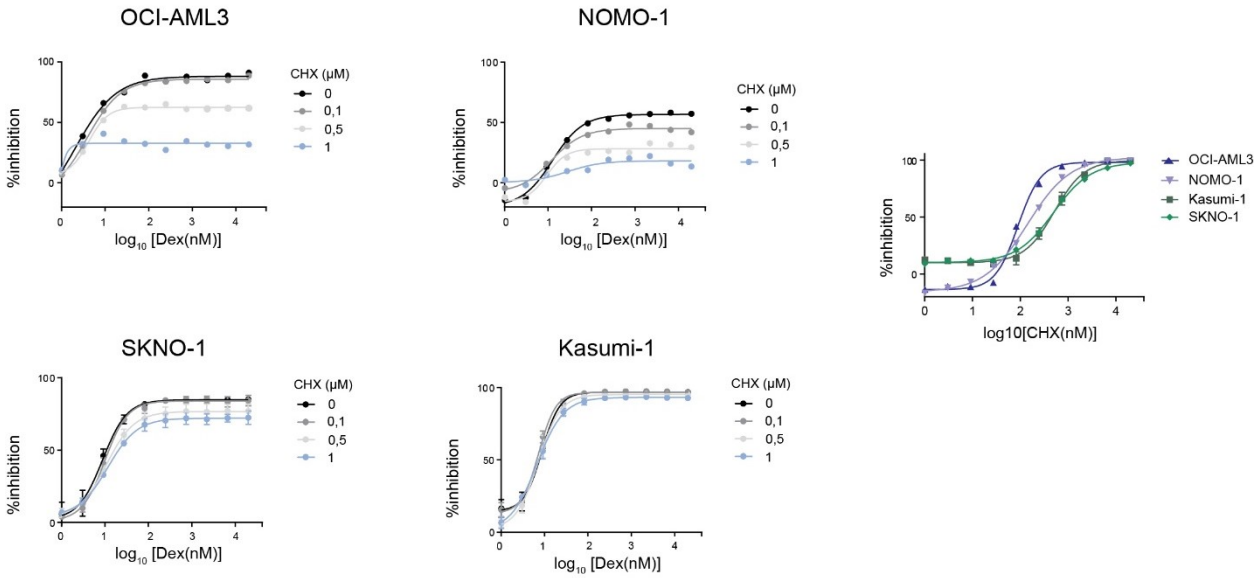

Figure S4.9: Effect of protein synthesis inhibition in the response to GC

Left Dose-response curves for dexamethasone in the presence of increasing concentrations of cycloheximide (CHX) in AML cell lines OCI-AML3, NOMO-1, SKNO-1, and Kasumi-1. *Right* Dose-response curves for CHX alone. Drug treatments were carried out for 5 days.

Chapter 5. Discussion

The master transcription factor RUNX1 is essential for the emergence of primitive hematopoietic stem cells and, during adult hematopoiesis, it exerts important functions in the definitive differentiation of myeloid, megakaryocytic and lymphocytic lineage progenitors. Therefore, abnormalities in RUNX1 are linked to numerous hematological disorders such as AML. The results presented in this thesis aimed at increasing our understanding of the molecular characteristics of AML with mutated *RUNX1* and provide rationale for the development of more efficient therapeutic strategies for patients suffering from this disease. Chemical interrogation of primary AML specimens revealed that *RUNX1* mutations predispose to increased sensitivity to glucocorticoids *in vitro*, unveiling a new role for RUNX1 in the glucocorticoid signaling. We further explored how other factors influence the response of AML cells to glucocorticoids and the potential connection with RUNX1 in determining glucocorticoid sensitivity.

5.1 *RUNX1*^{mut} AML: clinical and molecular characteristics

In chapters 2 and 3 of this thesis, we presented clinical and molecular characterization of AML specimens carrying *RUNX1* mutations from the Leucegene cohort. By further subdividing *RUNX1*^{mut} patients according to the type of *RUNX1* mutation (missense vs nonsense/frameshift) and allelic burden (heterozygous vs homozygous), we observed that a large proportion of *RUNX1*-mutated patients (29.7%) lacked a *RUNX1* wild-type allele (*RUNX1*$^{-/-}$). Those samples were characterized by mutations with VAF>75% (homozygous or LOH) or double heterozygous mutations, which were predicted to result in very low RUNX1 activity. Similarly, in a larger cohort of 147 *RUNX1*-mutated AML patients, 8.6% of patients had 2 different heterozygous mutations and another 17.9% patients showed absence of the wild-type allele (Schnittger et al., 2011). *RUNX1*^{mut} specimens were associated with older age at AML diagnosis, FAB M0 morphology, intermediate-risk cytogenetics with abnormal karyotype and poor patient survival compared to *RUNX1*^{wt} specimens, in accordance with published characteristics (Gaidzik et al., 2016; Rose et al., 2017). Importantly, there was a strong enrichment for AML-M0 in the samples with no remaining *RUNX1* wild-type allele (*RUNX1*$^{-/-}$), compared to samples carrying *RUNX1* heterozygous mutations (*RUNX1*$^{-/+}$), which has been described as an important characteristic of AML patients with biallelic *RUNX1* mutations (Osato, 2004).

Systematic analysis of 97 gene mutations and fusions confirmed most mutations in other genes previously reported for this subgroup, such as mutations in splicing factors (*SRSF2*, *SF3B1*, *U2AF1*), epigenetic modifiers (*ASXL1*, *EZH2, IDH2*), and *STAG2*, *PHF6*, *BCOR*, and inverse correlation with *NPM1, FLT3* mutations and CBF-rearrangements (Gaidzik et al., 2016; Gaidzik et al., 2011; Papaemmanuil et al., 2016). Interestingly, *RUNX1* dosage also showed association with co-occurring mutations and chromosome aberrations. Biallelic *RUNX1* mutations were associated with +13 and higher frequency of *ASXL1* mutations, characteristics that were confirmed in an independent cohort of 467 *RUNX1*-mutated AML patients (Stengel et al., 2018). Moreover, specimens carrying frameshift/nonsense *RUNX1* mutations were strongly enriched for both *ASXL1* and *SRSF2* mutations. Of interest, patients with $RUNX1^{mut}$/$ASXL1^{mut}$ or $RUNX1^{mut}$/$SRSF2^{mut}$ show particularly poor prognosis among $RUNX1^{mut}$ AML patients (Gaidzik et al., 2016). These findings highlight that even within this AML subgroup, considerable heterogeneity exists due to *RUNX1* dosage and cooperating mutations.

Given the causative role of *RUNX1* mutations in RUNX1-FPD, germline testing is recommended for any individual presenting a deleterious mutation in *RUNX1* found at MDS/AML diagnosis (Arber et al., 2016). Our efforts to fully characterize the $RUNX1^{mut}$ cohort included the validation of somatic and germline status, which is presented in chapter 3, and revealed that 30% of our patients carried germline *RUNX1* mutations. Even though the true prevalence of germline *RUNX1* mutations remains to be determined, the high incidence of AML cases in the Leucegene cohort carrying germline *RUNX1* mutations reinforces the notion that these entities are underappreciated (Team, 2016). In the small collection of *RUNX1*-mutated AML analyzed in chapter 3, germline *CEBPA* and germline *GATA2* mutations were also identified. In familial AML/MDS patients, germline mutations were reported at a frequency of 12% for *RUNX1*, 8% for *CEBPA*, and 8% for *GATA2* (Rio-Machin et al., 2020). A recent study that described 10 *RUNX1* familial cases also found germline mutations of clinical interest in *ASXL1*, *CEBPA*, *GATA2*, *JAK2* and *IDH1* (Brown et al., 2020), suggesting that many other germline events might contribute to the establishment of a predisposition state for leukemia.

Subgroup comparison between somatic and germline *RUNX1* mutated AML showed no significant clinical and molecular differences. Germline *RUNX1* patients showed a tendency to develop leukemia at a younger age (median = 56.5 yo for germline vs 63.5 yo for somatic *RUNX1* AML patients). The median age of onset of AML in our cohort is higher than that

described for RUNX1-FPD patients (33 yo) (Godley, 2014), however, extensive heterogeneity in penetrance and age of onset is observed within RUNX1-FPD families (Brown et al., 2020). Nonetheless, a great proportion of germline *RUNX1* patients (33.3%) developed AML under the age of 50, stressing the importance of germline testing in patients diagnosed with acute leukemia at a younger age who carry *RUNX1* mutations.

5.2 *RUNX1* mutations and development of cancer: different roles of germline and somatic events

The notion of *RUNX1* as a tumor suppressor gene is supported by its role in RUNX1-FPD. Studies with *Runx1*$^{+/-}$ heterozygous mice showed that loss of a normal *RUNX1* allele (haploinsufficiency) results in a significant decrease in either the number of HSCs or their capacity to expand and differentiate during development (Sun and Downing, 2004), leading to the hypothesis that the function of *RUNX1* is dose-dependent and that haploinsufficiency may contribute by itself to leukemogenesis. However, many authors have suggested that the type of *RUNX1* mutation influence leukemogenesis. Various indels or point mutations result in grossly truncated proteins or affect the C-terminal TAD, frequently resulting in abnormal subcellular localization and functional defects (Blyth et al., 2005; Christiansen et al., 2004; Harada, 2004). In addition, some missense mutations appear to have a higher penetrance and potential for leukemogenesis in familial disorder, corroborating the idea that considering *RUNX1* mutations as loss-of-function is very simplistic (Osato, 2004). Understanding the mechanism underlying disease progression in germline *RUNX1* carriers is of major interest to the field. Proposed mechanisms include haploinsufficiency for tumor suppression, dominant-negative effects on normal RUNX1 function, acquisition of a *de novo* mutation in the nonmutated germline allele, and acquisition of cooperating mutations (Nickels et al., 2013).

In MDS and AML, somatic *RUNX1* mutations are more frequently found as subclonal events rather than the founding clone and are believed to be acquired later in the leukemogenesis process (Haferlach et al., 2014; Papaemmanuil et al., 2013). On the other hand, in individuals carrying germline *RUNX1* mutations, they act as the initiating event and acquisition of somatic events is required for progression to MDS or leukemia and most likely contribute to the heterogeneity observed within families (Brown et al., 2020). While the role of *RUNX1*^{mut} as an initiating event in RUNX1-FPD remains to be fully elucidated, it's been shown that clonal hematopoiesis occurs

in 67% of asymptomatic *RUNX1* carriers under the age of 50, which is rarely present in healthy individuals (<1%), suggesting that clonal hematopoiesis frequently precedes development of overt MDS/AML in these carriers (Churpek et al., 2015). Evidence suggests that germline *RUNX1* mutations in RUNX1-FPD may have a mutator effect that could promote leukemogenesis through acquired chromosome changes or point mutations (Minelli et al., 2004). In our series, a similar number of mutations and chromosome abnormalities was detected in patients carrying germline or somatic *RUNX1* mutations. Even though acquisition of a secondary mutation in *RUNX1* is frequently observed in patients that develop AML (Antony-Debré et al., 2015), that was observed in only 2 of the 12 germline *RUNX1* patients in our series. In the study published by Latger-Cannard et al. (Latger-Cannard et al., 2016), 28.5% of RUNX1-FPD patients that developed AML had a second alteration of *RUNX1.* Brown et al. reported that 40% of RUNX1-FPD patients with progression to myeloid malignancy had a secondary acquired *RUNX1* mutation while only 17% of somatic *RUNX1*-mutated AML patients presented a secondary acquired *RUNX1* mutation (Brown et al., 2020). Conversely, we observed secondary acquired *RUNX1* mutation at a rate of 16.6% for germline *RUNX1* and 32.1% for somatic *RUNX1* (**Figure 3.2**). In our collection, *NRAS* and *FLT3* mutations were the most frequent acquired events in germline *RUNX1*, and we observed a trend for higher frequency of acquired *NRAS* mutations in germline *RUNX1* specimens than somatic *RUNX1* specimens. Hyperactivation of RAS signaling pathway in MDS/AML has been previously associated with *RUNX1* mutations (Niimi et al., 2006). Due to sample size limitation, these results require further validation in larger cohorts. Technical limitations in the use of bulk RNA-Seq for sample characterization prevent us from better understanding clonal architecture in these patients. Prospective studies should include multisampling analyses by single-cell RNA-Seq initiated before the diagnosis of MDS/AML, which would generate data on tumor evolution and contribution of cooccurring mutations thus leading to optimized timing of treatment intervention.

5.3 Importance of diagnosing AML with germline *RUNX1*

Due to significant heterogeneity in age of presentation and clinical course, RUNX1-FPD is frequently undetected until patients present with malignant transformation and the lack of proper germline tissue for genetic testing often leads to underdiagnosis of a leukemia predisposition

syndrome (Tang et al., 2019). While the availability of fibroblasts offers a gold standard approach to discriminate germline from somatic changes, this was not practical in our series. Germline material for genetic testing was obtained from buccal swab or saliva collected at the time of AML diagnosis. Despite the risk of sample contamination with blood carrying leukemic blasts, our pipeline included strict rules for mutation calling and confirmation of somatic non-*RUNX1* mutations, allowing us to confirm sample purity and identify *RUNX1* mutations of germline origin.

Identifying individuals affected by a leukemia predisposition syndrome is important because they require a unique approach in clinical management. This is highlighted in the latest 2016 update of the WHO classification of hematopoietic neoplasms that includes myeloid neoplasm with genetic predisposition as new provisional diagnostic entities (Arber et al., 2016). Importantly, patients suffering from AML with *RUNX1* mutations display poor overall survival and are candidates to receive HSCT. In cases where allogeneic stem cell transplantation with related donor is envisioned, genetic analysis is imperative to avoid the use of HSCs from an asymptomatic *RUNX1* mutation carrier. Inadvertent use of HSCs from donors carrying RUNX1 germline mutation may result in poor engraftment and/or donor-derived MDS/acute leukemia (Team, 2016).

In chapter 3 we showed evidence that 12 individuals previously diagnosed with AML carried germline *RUNX1* mutations, two of them who belonged to the same family. Unfortunately, family history and/or antecedent episodes of thrombopenia/bleeding disorders were not documented for these patients. Since *de novo* familial mutations in *RUNX1* are rare, we believe that we have identified 11 RUNX1-FPD families in the province of Quebec, Canada, which were unaware of their condition. Only 2 germline mutations were recurrent in more than one patient. For one pair (P3 and P4), we could confirm that they were related (mother and son). For the other pair (P9 and P10), analysis of genetic markers could not differentiate them from random unrelated pairs. Based on the results shown in **Figure S3.6**, we can assume that patients P9 and P10 are unlikely to be first-degree relatives, but we could not determine their kinship or rule out distant relationship. If a germline *RUNX1* mutation and potential underlying predisposition syndrome is identified, referral to genetic counselling is highly recommended. Genetic counseling includes obtaining and analyzing a multigenerational medical family history and may impact the proband's own treatment as well as help identify family members at risk and plan for

future screening or preventive strategies (Niemeyer and Mecucci, 2017). It is recommended that all mutation carriers undergo a baseline blood count with annual checkups, and a bone marrow biopsy in the event of significant changes in peripheral blood counts. Screening for somatic mutations typically observed in MDS/AML can provide useful information regarding disease evolution (Godley and Shimamura, 2017; Tang et al., 2019).

Because RUNX1-FPD displays strong anticipation (the phenomenon in which members of younger generations present with disease at earlier ages than those of previous generations), it is critical to provide close clinical follow-up for members of the youngest generations in the family (Nickels et al., 2013). This is exemplified in the family identified in chapter 3, a mother and son pair carrying *RUNX1* and *CEBPA* germline mutations presented with AML at very different ages. Even though mother and son had the same germline mutation load, the mother developed AML at age 59, while her son developed AML at age 27 (**Figure S3.5**).

5.4 *RUNX1* allele dosage influences transcriptional signature and drug response in *RUNX1*^{mut} AML

In entities such as *RUNX1*^{mut} AML, dissection of transcriptional signature is a valuable tool given that abnormal RUNX1 function is likely to cause disruptions in target gene expression. In chapter 2, we presented comparative transcriptomic analysis of *RUNX1*^{mut} and *RUNX1*^{wt} AML specimens, which revealed a list of genes differentially expressed between the two groups. Interestingly, and in agreement with other reports (Mendler et al., 2012), in *RUNX1*^{mut} specimens several genes normally expressed in early hematopoietic progenitors, such as *CD34*, *PROM1*, *BAALC*, *LMO2*, *FOXO1*, *DNTT* were upregulated, while several genes involved in myelopoiesis and granulocytic differentiation such as *CEBPA*, *AZU1* were downregulated (**Figure S2.1**). These findings are in line with the observation that *RUNX1*^{mut} specimens display an undifferentiated phenotype (enriched for FAB-M0) and provide evidence for stemness-related genes that are regulated by RUNX1. More interestingly, we observed that RUNX1 dosage influences the transcriptional signature of *RUNX1*^{mut} AML. The levels of expression of the most specific transcripts of the *RUNX1*^{mut} gene expression profile showed strong correlation with the type of mutation and allelic burden in *RUNX1*. These analyses improve the dissection of this genetic subgroup and reinforce its heterogenic character. Among top differentially expressed genes with known functional role in AML, *HMAG2* is a novel prognostic marker in AML (Marquis et al.,

2018) and is upregulated in *RUNX1*^{mut} AML, which may contribute to the poor outcome of *RUNX1*^{mut} patients. Additionally, *NR3C1*, the gene coding for the Glucocorticoid Receptor (GR), showed high correlation with our model, suggesting that its expression is determined by *RUNX1* allele dosage in primary *RUNX1*^{mut} AML specimens. It is known that GC sensitivity in AML cells is associated with increased expression of *NR3C1* (Malani et al., 2017), however, a role for RUNX1 in the modulation of *NR3C1* levels or GC sensitivity in AML has never been reported. Conversely, RUNX1 overexpression in fibroblasts and lymphoid cells leads to downregulation of *NR3C1* and increased resistance to GCs (Wotton et al., 2008). Evidence shows a binding site occupied by RUNX1 in the promoter region of *NR3C1* in hematopoietic progenitors and AML cell lines (Chacon et al., 2014), thus indicating that RUNX1 can directly control GR expression and inactivation of RUNX1 could lead to abnormal expression of *NR3C1*. In accordance with this, we showed that RUNX1 silencing results in upregulation of *NR3C1* in AML cell lines (**Figure 2.6d**).

These observations provided mechanistic insights for the *RUNX1*^{mut} subgroup sensitivity to GC. Chemical screening of primary AML specimens was conducted in an improved culture condition developed by our group that supports AML LSC activity (Pabst et al., 2014). Our strategy facilitates the identification of chemogenomic interactions targeting the founding clone, and it has unveiled numerous tumor vulnerabilities within the Leucegene cohort (Baccelli et al., 2017, 2019; Bisaillon et al., 2019; Lavallée et al., 2015, 2016). In this work, we described the effect of RUNX1 dosage in the response to GC. Primary AML specimens carrying *RUNX1* frameshift/nonsense mutations (*RUNX1*$^{fs/ns}$) showed increased sensitivity to GC when compared to samples harboring RUNX1 missense mutations (*RUNX1*^{mis}). Moreover, frameshift mutations that disrupt C-terminal TAD while leaving the DNA-binding domain intact were enriched among GC sensitive specimens. These mutations are believed to act as dominant-negative since the mutant RUNX1 can occupy its target sites and block occupancy and transactivation by full length RUNX proteins (Bellissimo and Speck, 2017). We also show that AML cell lines are susceptible to the modulation of RUNX1 dosage as RUNX1 silencing dramatically increased the sensitivity of various AML cell lines to GC. Similarly, residual RUNX1 activity in primary AML specimens carrying heterozygous mutations or hypomorphic alleles could contribute to the resistance of these specimens to GC. Moreover, cooperating mutations can influence GC-sensitivity in *RUNX1*^{mut} subgroup. Chemical screening showed that specimens carrying *SRSF2* and *CEBPA*-

biallelic mutations were more sensitive to GC than the rest of the cohort. Interestingly, primary AML samples expressing the highest levels of *NR3C1* were enriched for specimens harboring *SRSF2* and *RUNX1* mutations (**Figure S2.7**), further suggesting the importance of GR levels in GC-sensitivity.

5.5 Therapeutic use of GC for AML treatment

Glucocorticoids are the mainstay of ALL treatment; however, clinical studies have shown that most AML patients are resistant to GC therapy. Nonetheless, due to their extensive use in the clinics, GCs could be rapidly repurposed for the treatment of AML patients. Considering that *RUNX1* sequencing is now included in the initial prognostic assessment of AML patients, our study supports the rationale to evaluate the addition of GC therapy for a subset of patients who are refractory to conventional chemotherapy, specially those carrying $RUNX1^{fs/ns}$ mutations. Importantly, data collected from studies in ALL patients show a positive correlation between *in vitro* and *in vivo* sensitivity to GC (Bostrom et al., 2003; Inaba and Pui, 2010; Kaspers et al., 1998), corroborating the idea that patient selection for receiving GC treatment could be done on the basis of our chemogenomic screen; yet clinical trials are required to determine the nature of these interventions. Based on preclinical data from our study and others showing GC activity in AML (Bertoli et al., 2018; Laverdière et al., 2018), a Phase II clinical trial has begun in 2018 to assess the impact of adding dexamethasone to both induction and consolidation therapy in older patients with *de novo* or therapy-related AML (clinicalTrials.gov, NCT03609060) and is expected to end in 2025.

The use of GC as targeted therapy for $RUNX1^{mut}$ AML would require the establishment of a companion diagnostic (CDx) test to validate *RUNX1* status. Although *RUNX1* mutations could predict GC response in our primary specimen collection *in vitro*, considerable heterogeneity was observed, highlighting the influence of additional factors in the response to GC. For example, *FLT3* mutations and del(5q) are common features in AML and have been linked to GC resistance (Chougule et al., 2019; Emadali et al., 2016; Malani et al., 2017). On the other hand, inactivation mutations in *CEBPA* and *SRSF2* were also associated with GC sensitivity (**Figure 2.5**). These observations provide additional markers for GC response and opportunity to evaluate their impact in preclinical studies and clinical trials. Cooccurrence of *RUNX1* and *SRSF2* are frequently

observed in AML patients, which is associated with particularly poor prognosis (Gaidzik et al., 2016). Future development of CDxs must consider the detection of biomarkers of resistance and toxicity that are complementary to CDxs predicting therapeutic drug efficacy (Hofman and Barlesi, 2019). In this context, comprehensive CDxs that match a favorable genotype, such as *RUNX1*$^{fs/ns}$/*SRSF2*^{mut}/*FLT3*^{wt}, would be informative for decision-making for therapeutic use of GC in AML.

5.6 GC-induced transcriptional signature in AML

Modulation of gene expression is an important component of GC response thus by comparing the GC-induced transcriptome of a GC-resistant cell line (OCI-AML5) and a GC-sensitive cell line (OCI-AML3) we identified important differences between the cell lines' response downstream of GR activation. We observed that the number of upregulated genes in the GC-sensitive OCI-AML3 line progressively increased from 6h to 48h of dex exposure. At 48h, the number of upregulated genes in OCI-AML3 were 6 times greater than in GC-resistant OCI-AML5 line. In GC-sensitive AML cell line, the transcriptional signature showed increase in expression of genes associated with leukocyte activation/differentiation. Several top upregulated DEGs are known markers of macrophage activation towards M2 alternative phenotype. These findings go in line with studies that showed that GC treatment induces differentiation of normal monocytes (Ehrchen et al., 2007; Wang et al., 2014) and AML LSCs towards monocytic maturation (Laverdière et al., 2018).

Even though side effects arising from chronic use of GC are linked to transactivation by GR, our results indicate that induced expression of a subset of genes is important for the therapeutic response in AML cells. Upregulation of genes can occur through direct binding of the GR to GREs (transactivation) or through gene activation by other TFs that are in part regulated by GR. Additional experiments are required to further understand the mechanism by which GR influences the expression of these genes in OCI-AML3. The search for dissociated compounds that could separate between transactivation and transrepression by the GR led to development of series of compounds with the ability to preferentially induce one or the other activity. GR agonist RU782 exhibits transrepression but has limited transactivation activity (~20% of dexamethasone's TA), which is related to a reduction in the ability of GR to recruit transcriptional coactivators to GRE-containing promoter (Dezitter et al., 2014). Structurally, the 17α-hydroxyl group (17α-OH) of dex

was shown to be anchored by the G642 residue in GR and constitutes an essential contact for transactivation (Lind et al., 2000). In the RU782 agonist, the 17α-OH function is lacking, preventing any contact with G642. We evaluated the activity of dex (+/- 17α-OH) and RU782 (+/- 17α-OH) in AML cell lines and primary AML specimens to assess the impact of dissociated compounds in the GC-sensitivity. While RU782 is significantly less potent in inhibiting AML cell proliferation, RU782-OH analog on which we appended a 17α-OH group, markedly enhanced the ability of the analog to inhibit leukemia cell survival (**Figure 5.1**). These results suggest that transactivation mechanisms and, at the molecular level this particular structural element, play an important role in GC-mediated AML cell death, but do not rule out potential involvement of the transrepression mechanism. Moreover, desoximethasone, a dexamethasone analog which lacks the 17α-OH, strongly inhibits survival of leukemia-derived cell lines and all dexamethasone-sensitive primary AML cells indicating that anti-leukemia action of GC involves more complex molecular mechanisms.

a

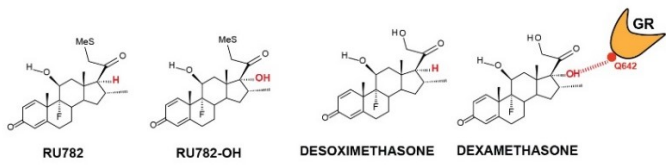

b

	Cell line				
Compound	SKNO-1 IC_{50} (nM)	Kasumi-1 IC_{50} (nM)	KG1a IC_{50} (nM)	Nomo-1 IC_{50} (nM)	OCI-AML3 IC_{50} (nM)
RU782	1,270	10,000	360	10,000	1,440
RU782-OH	33	171	85	10,000	13
Dexamethasone	4	7	4	127	4
Desoximethasone	4	9	21	210	4

c

AML#	Dex IC_{50} (nM)	Desoxi IC_{50} (nM)
04H001	33	48
08H087	15	18
04H055	43	42
11H046	37	39
12H151	10,000	10,000
10H136	10,000	10,000
11H138	5,400	3,700
11H170	10,000	10,000

Figure 5.1: Transactivation ability alone is not sufficient for anti-leukemia effect of GC
(a) Structures of the tested glucocorticoids. Red color identifies the presence or absence of αOH group at position C17 reported to be required for the transactivation function of dexamethasone. **(b)** IC_{50} values in AML cell lines determined for glucocorticoids characterized by dissociation of transrepressive and transactivation function. **(c)** IC_{50} values in primary AML specimens determined for dexamethasone (Dex) and desoximethasone (Desoxi).

5.7 Use of CRISPR-Cas9 technology to identify glucocorticoid-resistance genes

Glucocorticoid receptors have been reported to interact with a number of cell-restricted and ubiquitous transcriptional regulators. Functional genomic studies utilizing genome-wide CRISPR-Cas9 technology have been used to characterize GC mechanism of action and mechanisms of resistance (Poulard et al., 2019). Considering that GR regulates a vastly different set of genes in different cell types, we generated knock-out (KO) libraries using CRISPR-Cas9 in AML cell lines that show resistance to GC, in order to identify genes associated with GC-resistance. Our strategy also allowed the detection of genes involved in GC-induced cell death (synthetic rescue), which included the GR itself, molecular chaperones that support GR translocation to the nucleus, and transcriptional co-activators. Numerous genes were identified as GC-resistance genes (synthetic lethal). Transcription factors that control the self-renewal and differentiation of myeloid progenitors such as GATA-2, RUNX1 and PLZF (*ZBTB16*) were significantly depleted in treated conditions, providing evidence that these TFs antagonize GC-induced anti-leukemia effect. Similar to the effects observed for RUNX1 presented in chapter 2, PLZF also showed dosage effect in the response of AML cell lines to GCs (**Figure 4.3**). In normal hematopoiesis, PLZF acts to maintain immature myeloid progenitors in a primed state, so that when it is inactivated proliferation and maturation can rapidly occur to satisfy the demand for mature cells (Dick and Doulatov, 2009).

We postulate that PLZF could block the transcriptional activity of GR in AML cells by direct binding to GR at the DNA interface and impairing gene activation by GR, similarly to what has been previously described (Martin et al., 2003). Alternatively, PLZF could act by modulating the chromatin accessibility in AML cells, thus impeding GR from binding at specific sites and inducing differentiation. Moreover, analyses of GR bound and unbound regions revealed that GR bound sites are enriched for promoter-distal regions in sites that are accessible prior to hormone treatment (John et al., 2011; Love et al., 2017). In GC-resistant cells that express $PLZF^{high}$, GR sites might not be accessible prior to hormone treatment, resulting in a blunt response to GC and decreased antiproliferative effects. This hypothesis is in agreement with the observation that overexpression of PLZF in GC-sensitive and $PLZF^{low}$ OCI-AML3 cell line prior to hormone treatment provoked GC-resistance (**Figure 4.3**).

Additional experiments are required to determine how PLZF protects AML cells against GC-induced antiproliferative effect. The cooperation between PLZF and RUNX1 is also being investigated. RUNX1 was shown to be essential to induce PLZF expression in NK cells by direct

interaction with an enhancer of the *ZBTB16* locus (Mao et al., 2017). Combination of knock-down/overexpression strategies and functional chromatin analyses will provide insights into the mechanism at play and additional target genes controlled by these factors.

5.8 RUNX1 interaction with GR signalling

In chapter 2 and 4 we provide evidence that RUNX1 antagonizes the antiproliferative response to GC in AML cells. Although RUNX1 was shown to directly modulate GR gene expression, levels of GR in primary AML specimens and AML cell lines could only partially explain sensitivity to GC-treatment. Given the important roles of RUNX1 in transcriptional and chromatin regulation, we postulated that RUNX1 could interact with GR and interfere with GR modulation of target genes. Recently, two independent studies have demonstrated that RUNX1 and GR physically interact in AML cell lines (Lu et al., 2018; Simon et al., 2018). Co-immunoprecipitation assays (co-IP) revealed that RUNX1 and GR interact *in vivo* in the presence of dex in the GC-resistant cell line OCI-AML5 but not in the GC-sensitive cell line OCI-AML3 (**Figure 5.2**), indicating that RUNX1 interaction with GR might influence response to GC through modulation of target gene expression. Sub-cellular fractionation confirmed that the interaction occurs in the chromatin-bound fraction only, not in the cytoplasm. This was expected since RUNX1 wild-type protein is primarily found in the nucleus, tightly bound to the chromatin. To test the effect of *RUNX1* mutations in the RUNX1-GR interaction, we transfected HEK293T cells with overexpression plasmids carrying FLAG-tagged RUNX1-RUNX1T1, RUNX1c, and truncated proteins RUNX1c-Δ398, Δ318, and Δ204. Co-IP showed that only wild-type RUNX1c protein could pull down GR, indicating that the domain for interaction between RUNX1 and GR could be mapped to the TAD region in RUNX1. Similarly, RUNX1-RUNXT1, fusion protein that lacks the TAD, was not immunoprecipitated with GR. This observation goes in line with the data from another study, which mapped the interaction region to amino acids 321 to 391 within the RUNX1c TAD (Lu et al., 2018).

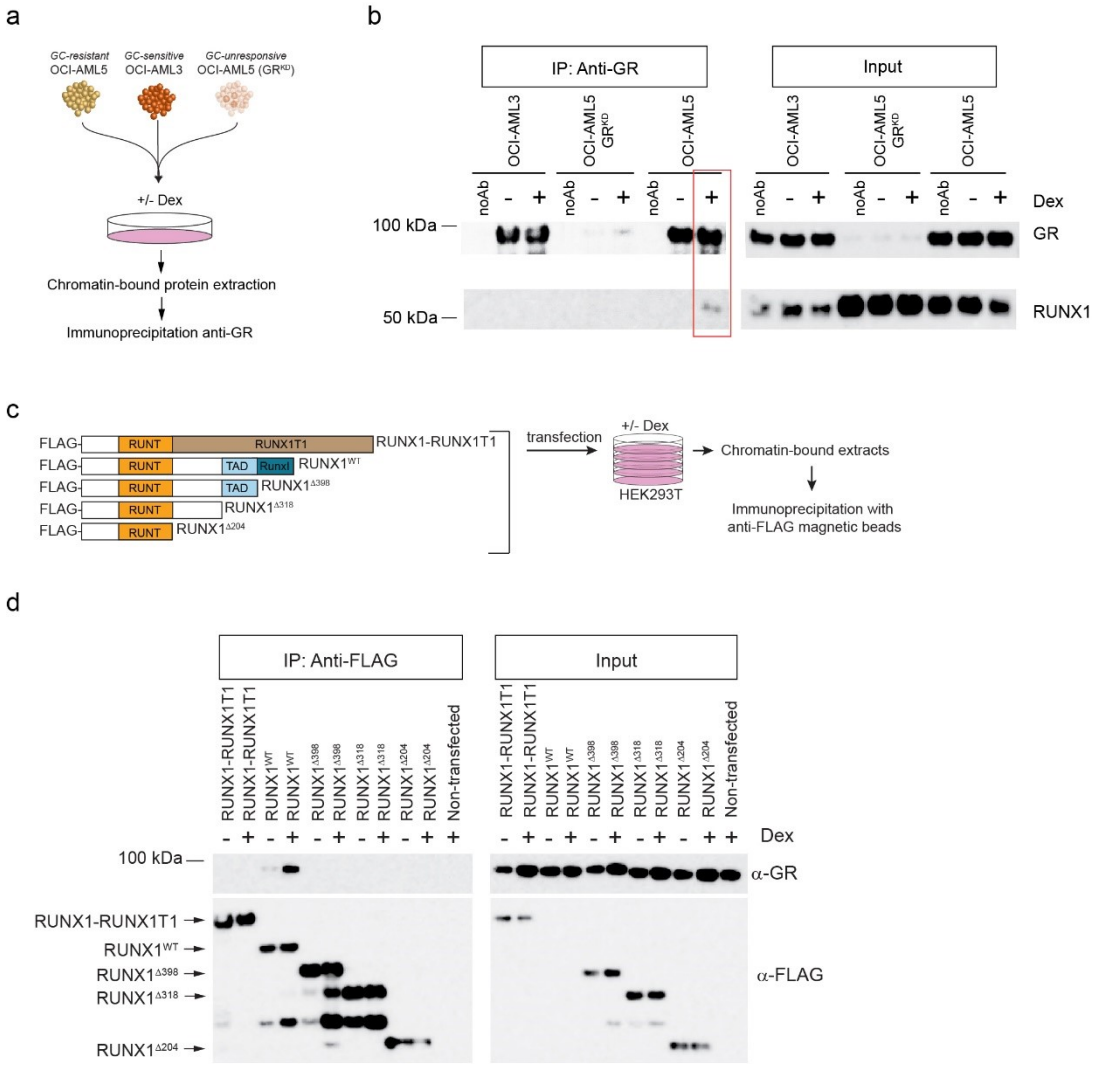

Figure 5.2: GR and RUNX1 physically interact in the presence of dex

(a) Immunoprecipitation of GR from chromatin-bound extracts of OCI-AML5 cells, OCI-AML5 sh*NR3C1* cells (GR^{KD}) and OCI-AML3 cells treated with Dexamethasone (Dex)or vehicle. **(b)** Co-immunoprecipitation of RUNX1 with GR was assessed by western blotting of the eluted fraction. **(c)** Overexpression of FLAG-tagged RUNX1 mutants in HEK293T cells followed by immunoprecipitation of FLAG-tagged RUNX1 from chromatin-bound extracts. **(d)** Co-immunoprecipitation of GR with RUNX1 was assessed by western blotting of the eluted fraction.

Additionally, we wanted to assess the potential of *RUNX1* missense mutations in disrupting the interaction with GR. Matheny et al., have demonstrated that disease-associated mutations in *RUNX1* can disrupt the DNA-binding, CBFB binding or both, depending on the residue that is

mutated (Matheny et al., 2007). We generated FLAG-tagged RUNX1c carrying point mutations found in the Leucegene cohort that are predicted to affect RUNX1 interactions differently (**Figure 5.3**). We then assessed their ability to bind CBFB and GR in co-IP assays. As demonstrated in biochemical studies, mutations in residues A134, R162 and D198 impair the association of RUNX1 with CBFB (Matheny et al., 2007), whereas mutations in residues R162, R166 and D198 disrupt DNA binding (Tahirov et al., 2001). As shown in **Figure 5.3**, all RUNX1 mutant proteins were immunoprecipitated from the chromatin-bound fraction of transfected HEK293T cells. Physical interaction with CBFB was decreased for RUNX1 mutants A134P, R162S and to a lesser extent D198N, when compared to RUNX1 wild-type, in agreement with published data (Matheny et al., 2007). However, all mutants retained the ability to co-IP GR in the chromatin-bound fraction. In comparison to RUNX1 wild-type, mutants R162S, R166G and D198N showed reduced interaction with GR, with R166G and D198N showing the lowest levels of GR co-immunoprecipitated. Collectively, our results suggest that both RUNX1 DNA-binding ability and interaction with co-factors though an intact TAD are important factors for the RUNX1-GR association at the chromatin level. On the other hand, RUNX1 ability to bind GR seems to be independent from the ability to bind CBFB, as illustrated by mutant A134P that can co-IP GR despite weak interaction with CBFB. Analysis of the chromatin landscape in ALL cells showed that, in the presence of dex, GR-bound enhancers are also enriched for RUNX1 binding sites, which is compatible with RUNX1 serving as a pioneering and/or tethering factor for GR (Wu et al., 2015). Additional experiments are needed to further investigate the mechanism by which RUNX1 interferes with GR response in AML.

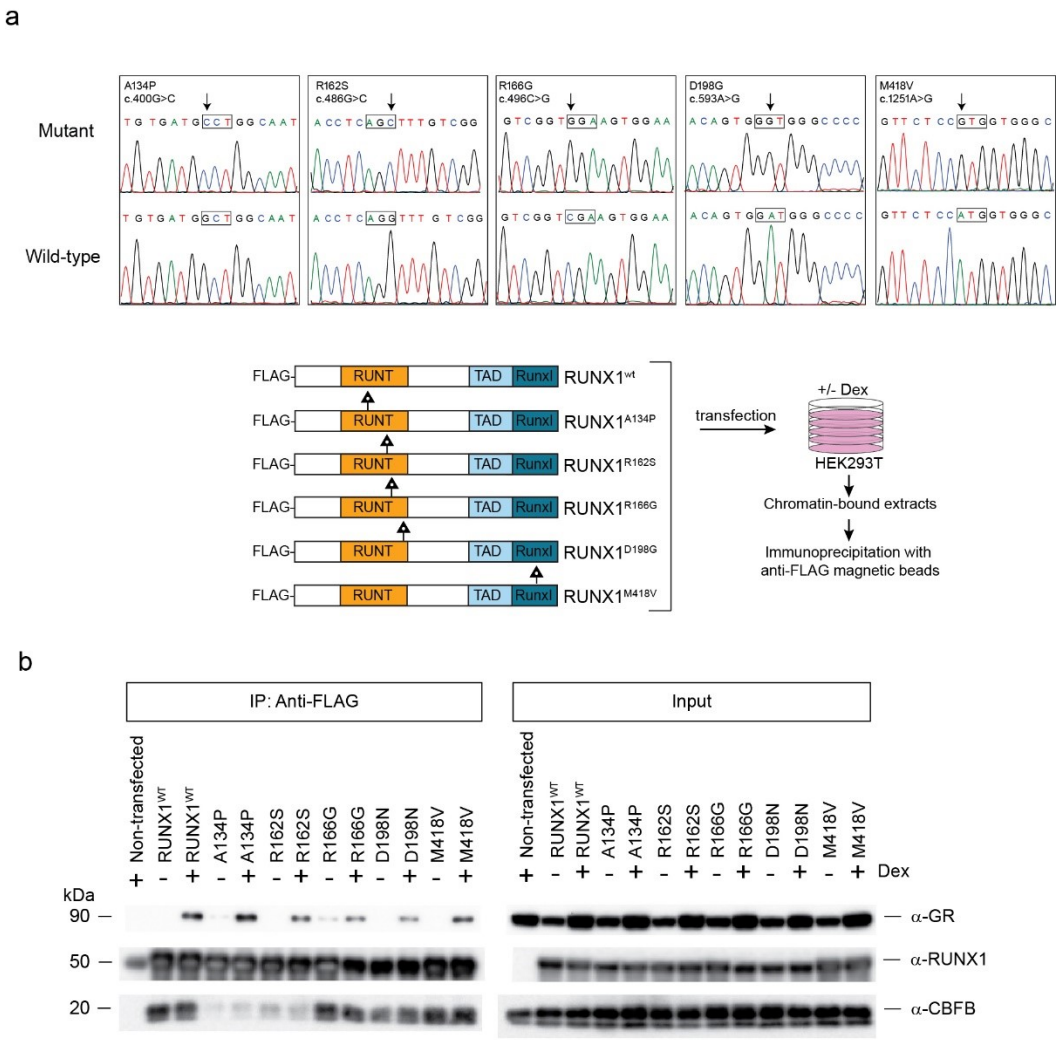

c

	Interaction RUNX1-GR	Interaction RUNX1-DNA	Interaction RUNX1-CBFB
RUNX1^{wt}	+++	+++	+++
A134P	+++	++	+
R162S	++	+	+
R166G	+	+	+++
D198N	+	+	++
M418V	++	?	+++

d

Patient ID	*RUNX1* mutation	Dex (IC_{50})	Variants identified in each specimen
08H022	R162S	10000.0	Complex, del(5q), *TP53*
08H088	R166G	10.0	Trisomy/tetrasomy 8, *CEBPA* , *NRAS* , *RUNX1* , *TET2* , *EZH2*
12H151	D198G / A134P	10000.0	Intermediate abnormal karyotype, *NF1* , *ASXL1* , *RUNX1* , *TET2* , *JAK2* , *PHF6*
06H048	D198G	10000.0	Trisomy/tetrasomy 8, *DNMT3A, ETV6, KMT2A, NRAS, RUNX1, U2AF1, MLL.PTD*
04H096	D198G / D198G	189.3	Monosomy 7/ 7q-
13H139	M418V	35.3	Intermediate abnormal karyotype, *FLT3*^{low}, *SRSF2* , *RUNX1, IDH1, NPM1*

Figure 5.3: *RUNX1* missense mutations influence interaction with GR

(a) Site-directed mutagenesis for overexpression of FLAG-tagged RUNX1 mutant proteins in HEK293T cells and immunoprecipitation of FLAG-tagged proteins from chromatin-bound

fraction after treatment with Dexamethasone (Dex) or vehicle. **(b)** Co-immunoprecipitation of RUNX1 with GR and CBFB was assessed by western blotting of the eluted fraction. **(c)** Summary of mutant RUNX1 interaction with GR, DNA (based on literature reports), and CBFB. **(d)** Specimens from the Leucegene expressing mutant RUNX1 and their *in vitro* response to dex.

5.9 Modulation of RUNX1 activity for therapeutic purposes

Strategies to either block abnormal activities of CBF proteins or restore RUNX1 function are warranted in the clinical setting. Although transcription factors represent a challenging class of proteins for the development of small molecule inhibitors, growing evidence suggests that dimeric transcription factors can be potently and selectively inhibited by small molecules that inhibit protein–protein interactions or protein–DNA interactions (Berg, 2008). Physical interactions between RUNX1 fusion proteins (RUNX1–RUNX1T1 and ETV6–RUNX1) and CBFB, and between the CBFB fusion protein (CBFB–SMMHC) and RUNX1 result in dominant inhibition of RUNX1 function and is critical for the oncogenic potential of the fusion proteins and the pathogenesis of CBF leukemias (Speck and Gilliland, 2002). Therefore, several groups have developed strategies to block RUNX1–CBFB interaction (Gorczynski et al., 2007; Illendula et al., 2015; Illendula et al., 2016). Compound Ro5-3335 was demonstrated to bind to RUNX1 and CBFB, inhibit their functions, and to be a potent inhibitor of CBF leukemia (Cunningham et al., 2012). Ro5-3335 treatment also showed particularly high toxicity towards MLL-AF9 leukemia cells, reproducing the effects of shRNA knock-down of *RUNX1*, which is believed to result from the growth dependency of MLL-AF9 cells on RUNX1 activity (Goyama et al., 2013). Therefore, we postulated that treatment combination of RUNX1 small molecule inhibitor and GC would synergize to induce AML cell death, especially in cell lines that showed increased sensitivity to GC upon *RUNX1* downregulation (chapter 2). However, despite Ro5-3335 ability to inhibit AML cell proliferation at high dose (25μM), it did not show sensitizing effects in the response to GC (**Figure 5.4**). Another group reported that Ro5-3335 showed no effect on CBFB-Runt domain binding in their FRET assay and no interaction was detected with either CBFB or the RUNX1 Runt domain by NMR. Instead, Ro5-3335 was observed to inhibit SMARCA2 and WDR9(2) bromodomains, which could have an indirect effect on RUNX1 activity (Illendula et al., 2016).

a

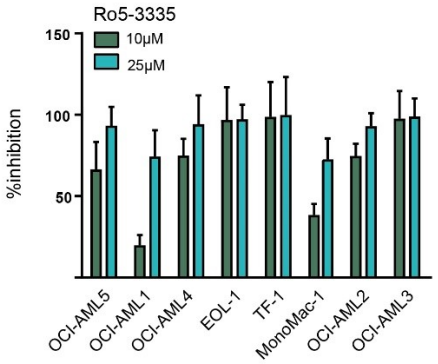

b

	IC_{50} Dex (nM)	IC_{50} Dex (+10µM Ro5-3335) (nM)
OCI-AML5	>10,000	>10,000
OCI-AML1	>10,000	>10,000
OCI-AML4	>10,000	>10,000
EOL-1	>10,000	>10,000
TF-1	>10,000	>10,000
MonoMac-1	>10,000	>10,000
OCI-AML2	>10,000	>10,000
OCI-AML3	9.1	15.4

Figure 5.4: RUNX1 small molecule inhibitor Ro5-3335 did not synergize with GC treatment
(a) AML cell lines growth inhibition upon treatment with 10µM and 25µM Ro5-3335 for 7 days in culture compared to DMSO controls. **(b)** IC_{50} values (in nM) for Dexamethasone (Dex) in AML cell lines that received vehicle or 10µM Ro5-3335.

While gain-of-function of CBF fusion proteins is associated with leukemogenesis, platelet disorder and predisposition to neoplasms are resulting from inherited *RUNX1* haploinsufficiency. Thus, many groups have explored different approaches aiming at restoring normal RUNX1 levels, including pharmacological enhancement of wild type RUNX1 transcriptional activity or small molecule-inhibition of the degradation of the wild type RUNX1 protein through the ubiquitin-proteasome pathway (Connelly et al., 2014; Leong et al., 2015). These strategies are being evaluate at the pre-clinical level and offer an opportunity to stop malignant progression in RUNX1-FPD patients, which is much desired for patients at high risk of developing AML.

5.11 Conclusions

We performed the molecular characterization of *RUNX1*^{mut} AML patients from the Leucegene cohort and showed the profound impact of *RUNX1* allele dosage on gene expression profile and on the association with cooperating mutations, revealing the complexity and heterogeneity of this AML subgroup. Using rigorous criteria, we could identify a high incidence of 30% germline *RUNX1* mutations in *RUNX1*^{mut} AML. These observations reinforce the importance of genetic testing and retrieval of a robust family history of first- and second-degree relatives in suspected

familial predisposition syndromes. As indicated by our study, this is extremely important in the context of AML with *RUNX1* mutations in younger patients (<50 years of age).

Chemical interrogation of primary AML specimens showed that *RUNX1* allele dosage can predispose AML cells to GC sensitivity or resistance, thereby opening opportunities for preclinical testing which may lead to drug repurposing and improved disease characterization. *RUNX1*^{mut} specimens show increased expression of *NR3C1*, the Glucocorticoid Receptor gene, which is believed to contribute to the increased sensitivity to GC. We also show that AML cell lines are susceptible to the modulation of *RUNX1* dosage as *RUNX1* silencing dramatically increased the sensitivity of various AML cell lines to GC. Mutations in *SRSF2* and *CEBPA*-biallelic also showed association with GC sensitivity, implying that additional factors are involved in predisposing cells to GC.

Analysis of GC-induced transcriptome in AML cell lines revealed that GC-sensitivity may rely on the activation of gene transcription and induction of leukocyte activation/differentiation, with strong induction of genes involved in macrophage activation towards M2c alternative phenotype. Chemogenomic screening using a genome-wide CRISPR library revealed that PLZF, a TF involved in myeloid differentiation, is an important regulator of GC-sensitivity. Identifying mechanisms of resistance is a crucial initial step towards the development of combinatorial therapies that potentiate the desirable effects of GC and reverse GC-resistance. Additional studies will enable the deconvolution of GR target gene regulation and provide greater insight into the actions of GC in different subsets of human AML.

5.12 References

Antony-Debré, I., Duployez, N., Bucci, M., Geffroy, S., Micol, J.-B., Renneville, A., … Preudhomme, C. (2015). Somatic mutations associated with leukemic progression of familial platelet disorder with predisposition to acute myeloid leukemia. *Leukemia*, *30*(4), 999-1002. doi:10.1038/leu.2015.236

Arber, D. A., Orazi, A., Hasserjian, R., Thiele, J., Borowitz, M. J., Beau, M. M. L., … Vardiman, J. W. (2016). The 2016 revision to the World Health Organization classification of myeloid neoplasms and acute leukemia. *Blood*, *127*(20), 2391-2405. doi:10.1182/blood-2016-03-643544

Baccelli, I., Gareau, Y., Lehnertz, B., Gingras, S., Spinella, J., Corneau, S., … Sauvageau, G. (2019). Mubritinib Targets the Electron Transport Chain Complex I and Reveals the Landscape of OXPHOS Dependency in Acute Myeloid Leukemia. *Cancer Cell*, *36*(1), 84-99.e8. doi:10.1016/j.ccell.2019.06.003

Baccelli, I., Krosl, J., Boucher, G., Boivin, I., Lavallée, V.-P., Hébert, J., … Sauvageau, G. (2017). A novel approach for the identification of efficient combination therapies in primary human acute myeloid leukemia specimens. *Blood cancer journal*, *7*(2), e529. doi:10.1038/bcj.2017.10

Bellissimo, D. C. and Speck, N. A. (2017). RUNX1 Mutations in Inherited and Sporadic Leukemia. *Frontiers in Cell and Developmental Biology*, *5*, 111. doi:10.3389/fcell.2017.00111

Berg, T. (2008). Inhibition of transcription factors with small organic molecules. *Current Opinion in Chemical Biology*, *12*(4), 464-471. doi:10.1016/j.cbpa.2008.07.023

Bertoli, S., Picard, M., Bérard, E., Griessinger, E., Larrue, C., Mouchel, P.-L., … Récher, C. (2018). Dexamethasone in hyperleukocytic acute myeloid leukemia. *Haematologica*, *103*(6), haematol.2017.184267. doi:10.3324/haematol.2017.184267

Bisaillon, R., Moison, C., Thiollier, C., Krosl, J., Bordeleau, M., Lehnertz, B., … Sauvageau, G. (2019). Genetic characterization of ABT-199 sensitivity in human AML. *Leukemia*, *34*(1), 63-74. doi:10.1038/s41375-019-0485-x

Blyth, K., Cameron, E. R. and Neil, J. C. (2005). The runx genes: gain or loss of function in cancer. *Nature Reviews Cancer*, *5*(5), 376-387. doi:10.1038/nrc1607

Bostrom, B. C., Sensel, M. R., Sather, H. N., Gaynon, P. S., La, M. K., Johnston, K., … Trigg, M. E. (2003). Dexamethasone versus prednisone and daily oral versus weekly intravenous mercaptopurine for patients with standard-risk acute lymphoblastic leukemia: a report from the Children's Cancer Group. *Blood*, *101*(10), 3809-3817. doi:10.1182/blood-2002-08-2454

Brown, A. L., Arts, P., Carmichael, C. L., Babic, M., Dobbins, J., Chong, C.-E., … Scott, H. S. (2020). RUNX1-mutated families show phenotype heterogeneity and a somatic mutation profile unique to germline predisposed AML. *Blood Advances*, *4*(6), 1131-1144. doi:10.1182/bloodadvances.2019000901

Chacon, D., Beck, D., Perera, D., Wong, J. W. H. and Pimanda, J. E. (2014). BloodChIP: a database of comparative genome-wide transcription factor binding profiles in human blood cells. *Nucleic Acids Research*, *42*(D1), D172-D177. doi:10.1093/nar/gkt1036

Chougule, R., Shah, K., Moharram, S., Vallon-Christersson, J. and Kazi, J. (2019). Glucocorticoid-resistant B cell acute lymphoblastic leukemia displays receptor tyrosine kinase activation. *npj Genomic Medicine*, *4*(1), 7. doi:10.1038/s41525-019-0082-y

Christiansen, D. H., Andersen, M. K. and Pedersen-Bjergaard, J. (2004). Mutations of AML1 are common in therapy-related myelodysplasia following therapy with alkylating agents and are significantly associated with deletion or loss of chromosome arm 7q and with subsequent leukemic transformation. *Blood*, *104*(5), 1474-1481. doi:10.1182/blood-2004-02-0754

Churpek, J. E., Pyrtel, K., Kanchi, K.-L., Shao, J., Koboldt, D., Miller, C. A., … Graubert, T. A. (2015). Genomic analysis of germ line and somatic variants in familial myelodysplasia/acute myeloid leukemia. *Blood*, *126*(22), 2484-90. doi:10.1182/blood-2015-04-641100

Connelly, J., Kwon, E., Gao, Y., Trivedi, N., Elkahloun, A., Horwitz, M., … Liu, P. (2014). Targeted correction of RUNX1 mutation in FPD patient-specific induced pluripotent stem cells rescues megakaryopoietic defects. *Blood*, *124*(12), 1926-1930. doi:10.1182/blood-2014-01-550525

Cunningham, L., Finckbeiner, S., Hyde, K. R., Southall, N., Marugan, J., Yedavalli, V. R., … Liu, P. (2012). Identification of benzodiazepine Ro5-3335 as an inhibitor of CBF leukemia through quantitative high throughput screen against RUNX1–CBFβ interaction. *Proceedings of the National Academy of Sciences*, *109*(36), 14592-14597. doi:10.1073/pnas.1200037109

Dezitter, X., Fagart, J., Taront, S., Fay, M., Masselot, B., Hétuin, D., … Idziorek, T. (2014). A Structural Explanation of the Effects of Dissociated Glucocorticoids on Glucocorticoid Receptor Transactivation. *Molecular Pharmacology*, *85*(2), 226-236. doi:10.1124/mol.113.085860

Dick, J. and Doulatov, S. (2009). The Role of PLZF in Human Myeloid Development. *Annals of the New York Academy of Sciences*, *1176*(1), 150-153. doi:10.1111/j.1749-6632.2009.04965.x
Ehrchen, J., Steinmüller, L., Barczyk, K., Tenbrock, K., Nacken, W., Eisenacher, M., … Roth, J. (2007). Glucocorticoids induce differentiation of a specifically activated, anti-inflammatory subtype of human monocytes. *Blood*, *109*(3), 1265-1274. doi:10.1182/blood-2006-02-001115
Emadali, A., Hoghoughi, N., Duley, S., Hajmirza, A., Verhoeyen, E., Cosset, F., … Callanan, M. (2016). Haploinsufficiency for NR3C1, the gene encoding the glucocorticoid receptor, in blastic plasmacytoid dendritic cell neoplasms. *Blood*, *127*(24), 3040-3053. doi:10.1182/blood-2015-09-671040
Gaidzik, V. I., Bullinger, L., Schlenk, R. F., Zimmermann, A. S., Röck, J., Paschka, P., … Döhner, K. (2011). RUNX1 Mutations in Acute Myeloid Leukemia: Results From a Comprehensive Genetic and Clinical Analysis From the AML Study Group. *Journal of Clinical Oncology*, *29*(10), 1364-1372. doi:10.1200/JCO.2010.30.7926
Gaidzik, V., Teleanu, V., Papaemmanuil, E., Weber, D., Paschka, P., Hahn, J., … Döhner, H. (2016). RUNX1 mutations in acute myeloid leukemia are associated with distinct clinico-pathologic and genetic features. *Leukemia*. doi:10.1038/leu.2016.126
Godley, L. A. (2014). Inherited predisposition to acute myeloid leukemia. *Seminars in hematology*, *51*(4), 306-21. doi:10.1053/j.seminhematol.2014.08.001
Godley, L. A. and Shimamura, A. (2017). Genetic predisposition to hematologic malignancies: management and surveillance. *Blood*, *130*(4), 424-432. doi:10.1182/blood-2017-02-735290
Gorczynski, M., Grembecka, J., Zhou, Y., Kong, Y., Roudaia, L., Douvas, M., … Bushweller, J. (2007). Allosteric Inhibition of the Protein-Protein Interaction between the Leukemia-Associated Proteins Runx1 and CBFβ. *Chemistry & Biology*, *14*(10), 1186-1197. doi:10.1016/j.chembiol.2007.09.006
Goyama, S., Schibler, J., Cunningham, L., Zhang, Y., Rao, Y., Nishimoto, N., … Mulloy, J. C. (2013). Transcription factor RUNX1 promotes survival of acute myeloid leukemia cells. *The Journal of clinical investigation*, *123*(9), 3876-88. doi:10.1172/JCI68557
Haferlach, T., Nagata, Y., Grossmann, V., Okuno, Y., Bacher, U., Nagae, G., … Ogawa, S. (2014). Landscape of genetic lesions in 944 patients with myelodysplastic syndromes. *Leukemia*, *28*(2), 241-247. doi:10.1038/leu.2013.336
Harada, H. (2004). High incidence of somatic mutations in the AML1/RUNX1 gene in myelodysplastic syndrome and low blast percentage myeloid leukemia with myelodysplasia. *Blood*, *103*(6), 2316-2324. doi:10.1182/blood-2003-09-3074
Hofman, P. and Barlesi, F. (2019). Companion diagnostic tests for treatment of lung cancer patients: what are the current and future challenges? *Expert Review of Molecular Diagnostics*, *19*(5), 429-438. doi:10.1080/14737159.2019.1611426
Illendula, A, Pulikkan, J., Zong, H., Grembecka, J., Xue, L., Sen, S., … Bushweller, J. (2015). A small-molecule inhibitor of the aberrant transcription factor CBFβ-SMMHC delays leukemia in mice. *Science*, *347*(6223), 779-784. doi:10.1126/science.aaa0314
Illendula, Anuradha, Gilmour, J., Grembecka, J., Tirumala, V. S. S., Boulton, A., Kuntimaddi, A., … Bushweller, J. H. (2016). Small Molecule Inhibitor of CBFβ-RUNX Binding for RUNX Transcription Factor Driven Cancers. *EBioMedicine*, *8*(Semin. Cell Dev. Biol. 11 2000), 117-131. doi:10.1016/j.ebiom.2016.04.032
Inaba, H. and Pui, C. (2010). Glucocorticoid use in acute lymphoblastic leukaemia. *The Lancet Oncology*, *11*(11), 1096-1106. doi:10.1016/s1470-2045(10)70114-5
John, S., Sabo, P. J., Thurman, R. E., Sung, M.-H., Biddie, S. C., Johnson, T. A., … Stamatoyannopoulos, J. A. (2011). Chromatin accessibility pre-determines glucocorticoid receptor binding patterns. *Nature Genetics*, *43*(3), 264-268. doi:10.1038/ng.759
Kaspers, G., Zantwijk, C., VanWering, E., Berg, A. and Veerman, A. (1998). Prednisolone Resistance in Childhood Acute Lymphoblastic Leukemia: Vitro-Vivo Correlations and Cross-Resistance to Other Drugs. *Blood*, *92*(1), 259-266. doi:10.1182/blood.v92.1.259.413k21_259_266
Latger-Cannard, V., Philippe, C., Bouquet, A., Baccini, V., Alessi, M.-C., Ankri, A., … Favier, R. (2016). Haematological spectrum and genotype-phenotype correlations in nine unrelated families with RUNX1 mutations from the French network on inherited platelet disorders. *Orphanet Journal of Rare Diseases*, *11*(1), 49. doi:10.1186/s13023-016-0432-0
Lavallée, V.-P., Baccelli, I., Krosl, J., Wilhelm, B., Barabé, F., Gendron, P., … Sauvageau, G. (2015). The transcriptomic landscape and directed chemical interrogation of MLL-rearranged acute myeloid leukemias. *Nature Genetics*, *47*(9), 1030-1037. doi:10.1038/ng.3371

Lavallée, V.-P., Krosl, J., Lemieux, S., Boucher, G., Gendron, P., Pabst, C., … Sauvageau, G. (2016). Chemogenomic interrogation of CEBPA mutated AML reveals recurrent CSF3R mutations and subgroup sensitivity to JAK inhibitors. *Blood*, *127*(24), 3054-61. doi:10.1182/blood-2016-03-705053

Laverdière, I., Boileau, M., Neumann, A. L., Frison, H., Mitchell, A., Ng, S. W. K., … Eppert, K. (2018). Leukemic stem cell signatures identify novel therapeutics targeting acute myeloid leukemia. *Blood Cancer Journal*, *8*(6), 52. doi:10.1038/s41408-018-0087-2

Leong, W., Guo, H., Ma, O., Huang, H., Cantor, A. and Friedman, A. (2015). Runx1 Phosphorylation by Src Increases Trans-activation via Augmented Stability, Reduced Histone Deacetylase (HDAC) Binding, and Increased DNA Affinity, and Activated Runx1 Favors Granulopoiesis. *Journal of Biological Chemistry*, *291*(2), 826-836. doi:10.1074/jbc.m115.674234

Lind, U., Greenidge, P., Gillner, M., Koehler, K., Wright, A. and Carlstedt-Duke, J. (2000). Functional Probing of the Human Glucocorticoid Receptor Steroid-interacting Surface by Site-directed Mutagenesis: Gln-642 PLAYS AN IMPORTANT ROLE IN STEROID RECOGNITION AND BINDING. *Journal of Biological Chemistry*, *275*(25), 19041-19049. doi:10.1074/jbc.m000228200

Love, M. I., Huska, M. R., Jurk, M., Schöpflin, R., Starick, S. R., Schwahn, K., … Meijsing, S. H. (2017). Role of the chromatin landscape and sequence in determining cell type-specific genomic glucocorticoid receptor binding and gene regulation. *Nucleic Acids Research*, *45*(4), 1805-1819. doi:10.1093/nar/gkw1163

Lu, L., Wen, Y., Yao, Y., Chen, F., Wang, G., Wu, F., … Song, Y. (2018). Glucocorticoids Inhibit Oncogenic RUNX1-ETO in Acute Myeloid Leukemia with Chromosome Translocation t(8;21). *Theranostics*, *8*(8), 2189-2201. doi:10.7150/thno.22800

Malani, D., Murumägi, A., Yadav, B., Kontro, M., Eldfors, S., Kumar, A., … Kallioniemi, O. (2017). Enhanced sensitivity to glucocorticoids in cytarabine-resistant AML. *Leukemia*, *31*(5), 1187-1195. doi:10.1038/leu.2016.314

Mao, A., Ishizuka, I., Kasal, D., Mandal, M. and Bendelac, A. (2017). A shared Runx1-bound Zbtb16 enhancer directs innate and innate-like lymphoid lineage development. *Nature Communications*, *8*(1), 863. doi:10.1038/s41467-017-00882-0

Marquis, M., Beaubois, C., Lavallée, V.-P., Abrahamowicz, M., Danieli, C., Lemieux, S., … Hébert, J. (2018). High expression of HMGA2 independently predicts poor clinical outcomes in acute myeloid leukemia. *Blood Cancer Journal*, *8*(8), 68. doi:10.1038/s41408-018-0103-6

Martin, P. J., Delmotte, M.-H., Formstecher, P. and Lefebvre, P. (2003). PLZF is a negative regulator of retinoic acid receptor transcriptional activity. *Nuclear Receptor*, *1*(1), 6. doi:10.1186/1478-1336-1-6

Matheny, C. J., Speck, M. E., Cushing, P. R., Zhou, Y., Corpora, T., Regan, M., … Speck, N. A. (2007). Disease mutations in RUNX1 and RUNX2 create nonfunctional, dominant-negative, or hypomorphic alleles. *The EMBO Journal*, *26*(4), 1163-1175. doi:10.1038/sj.emboj.7601568

Mendler, J. H., Maharry, K., Radmacher, M. D., Mrózek, K., Becker, H., Metzeler, K. H., … Bloomfield, C. D. (2012). RUNX1 Mutations Are Associated With Poor Outcome in Younger and Older Patients With Cytogenetically Normal Acute Myeloid Leukemia and With Distinct Gene and MicroRNA Expression Signatures. *Journal of Clinical Oncology*, *30*(25), 3109-3118. doi:10.1200/JCO.2011.40.6652

Minelli, A., Maserati, E., Rossi, G., Bernardo, M. E., Stefano, P. D., Cecchini, M. P., … Pasquali, F. (2004). Familial platelet disorder with propensity to acute myelogenous leukemia: Genetic heterogeneity and progression to leukemia via acquisition of clonal chromosome anomalies. *Genes, Chromosomes and Cancer*, *40*(3), 165-171. doi:10.1002/gcc.20030

Nickels, E. M., Soodalter, J., Churpek, J. E. and Godley, L. A. (2013). Recognizing familial myeloid leukemia in adults. *Therapeutic Advances in Hematology*, *4*(4), 254-269. doi:10.1177/2040620713487399

Niemeyer, C. M. and Mecucci, C. (2017). Practical considerations for diagnosis and management of patients and carriers. *Seminars in Hematology*, *54*(2), 69-74. doi:10.1053/j.seminhematol.2017.04.002

Niimi, H., Harada, H., Harada, Y., Ding, Y., Imagawa, J., Inaba, T., … Kimura, A. (2006). Hyperactivation of the RAS signaling pathway in myelodysplastic syndrome with AML1/RUNX1 point mutations. *Leukemia*, *20*(4), 635-644. doi:10.1038/sj.leu.2404136

Osato, M. (2004). Point mutations in the RUNX1/AML1 gene: another actor in RUNX leukemia. *Oncogene*, *23*(24), 4284-96. doi:10.1038/sj.onc.1207779

Pabst, C., Krosl, J., Fares, I., Boucher, G., Ruel, R., Marinier, A., … Sauvageau, G. (2014). Identification of small molecules that support human leukemia stem cell activity ex vivo. *Nature methods*, *11*(4), 436-42. doi:10.1038/nmeth.2847

Papaemmanuil, E., Gerstung, M., Bullinger, L., Gaidzik, V. I., Paschka, P., Roberts, N. D., … Campbell, P. J. (2016). Genomic Classification and Prognosis in Acute Myeloid Leukemia. *The New England Journal of Medicine*, *374*(23), 2209-2221. doi:10.1056/NEJMoa1516192

Papaemmanuil, E., Gerstung, M., Malcovati, L., Tauro, S., Gundem, G., Loo, P. V., … Consortium, C. M. D. W. G. of the I. C. G. (2013). Clinical and biological implications of driver mutations in myelodysplastic syndromes. *Blood*, *122*(22), 3616-27; quiz 3699. doi:10.1182/blood-2013-08-518886

Poulard, C., Kim, H. N., Fang, M., Kruth, K., Gagnieux, C., Gerke, D. S., … Pufall, M. A. (2019). Relapse-associated AURKB blunts the glucocorticoid sensitivity of B cell acute lymphoblastic leukemia. *Proceedings of the National Academy of Sciences*, *116*(8), 201816254. doi:10.1073/pnas.1816254116

Rio-Machin, A., Vulliamy, T., Hug, N., Walne, A., Tawana, K., Cardoso, S., … Dokal, I. (2020). Rio-Machin, 2020 - The complex genetic landscape of familial MDS and AML reveals pathogenic germline variants.pdf. *Nature Communications*, *11*(1), 1044. doi:10.1038/s41467-020-14829-5

Rose, D., Haferlach, T., Schnittger, S., Perglerová, K., Kern, W. and Haferlach, C. (2017). Subtype-specific patterns of molecular mutations in acute myeloid leukemia. *Leukemia*, *31*(1), 11-17. doi:10.1038/leu.2016.163

Schnittger, S., Dicker, F., Kern, W., Wendland, N., Sundermann, J., Alpermann, T., … Haferlach, T. (2011). RUNX1 mutations are frequent in de novo AML with noncomplex karyotype and confer an unfavorable prognosis. *Blood*, *117*(8), 2348-2357. doi:10.1182/blood-2009-11-255976

Simon, L., Lavallee, V., Bordeleau, M., Lehnertz, B., MacRae, T., Chagraoui, J., … Sauvageau, G. (2018). Chemogenomic Approach Unveils the Increased Susceptibility of RUNX1-Mutated AML to Glucocorticoids. *Blood*, *132*(Supplement 1), 4675-4675. doi:10.1182/blood-2018-99-111030

Speck, N. A. and Gilliland, G. D. (2002). Core-binding factors in haematopoiesis and leukaemia. *Nature reviews. Cancer*, *2*(7), 502-13. doi:10.1038/nrc840

Stengel, A., Kern, W., Meggendorfer, M., Nadarajah, N., Perglerovà, K., Haferlach, T. and Haferlach, C. (2018). Number of RUNX1 mutations, wild-type allele loss and additional mutations impact on prognosis in adult RUNX1-mutated AML. *Leukemia*, *32*(2), 295-302. doi:10.1038/leu.2017.239

Sun, W. and Downing, J. (2004). Haploinsufficiency of AML1 results in a decrease in the number of LTR-HSCs while simultaneously inducing an increase in more mature progenitors. *Blood*, *104*(12), 3565-3572. doi:10.1182/blood-2003-12-4349

Tahirov, T., Inoue-Bungo, T., Morii, H., Fujikawa, A., Sasaki, M., Kimura, K., … Ogata, K. (2001). Structural analyses of DNA recognition by the AML1/Runx-1 Runt domain and its allosteric control by CBFbeta. *Cell*, *104*(5), 755-67. doi:10.1016/S0092-8674(01)00271-9

Tang, C., Rabbolini, D. J., Morel-Kopp, M.-C., Connor, D. E., Crispin, P., Ward, C. M. and Stevenson, W. S. (2019). The clinical heterogeneity of RUNX1 associated familial platelet disorder with predisposition to myeloid malignancy - A case series and review of the literature. *Research and practice in thrombosis and haemostasis*, *4*(1), 106-110. doi:10.1002/rth2.12282

Team, T. U. of C. H. M. C. R. (2016). How I diagnose and manage individuals at risk for inherited myeloid malignancies. *Blood*, *128*(14), 1800-1813. doi:10.1182/blood-2016-05-670240

Wang, N., Liang, H. and Zen, K. (2014). Molecular Mechanisms That Influence the Macrophage M1–M2 Polarization Balance. *Frontiers in Immunology*, *5*, 614. doi:10.3389/fimmu.2014.00614

Wotton, S., Terry, A., Kilbey, A., Jenkins, A., Herzyk, P., Cameron, E. and Neil, J. (2008). Gene array analysis reveals a common Runx transcriptional programme controlling cell adhesion and survival. *Oncogene*, *27*(44), 5856-66. doi:10.1038/onc.2008.195

Wu, J. N., Pinello, L., Yissachar, E., Wischhusen, J. W., Yuan, G.-C. and Roberts, C. W. (2015). Functionally distinct patterns of nucleosome remodeling at enhancers in glucocorticoid-treated acute lymphoblastic leukemia. *Epigenetics & Chromatin*, *8*(1), 1-17. doi:10.1186/s13072-015-0046-0